Elliptic Fibrations for F-Theory Geometric Engineering

Kuentzler, Moritz

Awarding institution:
King's College London

KING'S COLLEGE LONDON

Elliptic Fibrations for F-Theory Geometric Engineering

by

Moritz Küntzler

A thesis submitted for the
degree of Doctor of Philosophy

in the
Department of Mathematics
School of Natural and Mathematical Sciences

September 2014

Abstract

Elliptic Fibrations for F-Theory Geometric Engineering

String phenomenology aims to explain the physics of the universe in the context of string theory, the leading candidate to unify gravitational and quantum physics. A main ingredient in constructing such models is compactifying the ten-dimensional theory on a six-dimensional manifold, so that one is left with the four non-compact dimensions modelling space-time. Performing this step allows one to reformulate many physical phenomena as properties of the geometry of the compactification manifold, and to find generic constraints on physical models using methods from algebraic geometry. One such phenomenon in nature are gauge theories, both abelian and non-abelian. In this thesis, we undertake a systematic investigation of the interplay of the two in compactifications of F-theory.

In F-theory, the relevant compactification spaces are elliptically fibered Calabi-Yau manifolds. They are particularly well-suited to the study of gauge symmetries in string phenomenology, since they both allow the existence of exceptional gauge symmetries such as E_6 as well as the localization of gauge degrees of freedom on subloci of the compactification manifold. Specifically, non-abelian gauge theories are encoded as singularities of the elliptic fibration, and the rational sections of the fibration specify the abelian part of the gauge group. Using tools from algebraic geometry, we study singularities of elliptic fibrations with a group of rational sections of rank 1, i.e. with a single abelian gauge factor.

In the first part of the thesis, we refine the spectral cover formalism, which is a way to study local properties of the subloci of the compactification manifold on which gauge degrees of freedom are localized in F-theory. We do so by introducing the spectral divisor. The spectral divisor allows one to construct gauge fluxes in F-theory in a purely local description. We exemplify this construction for an elliptic fibration with associated gauge group E_6.

In the second part of the thesis, we use Tate's algorithm to obtain a comprehensive classification of singular fibers and an explicit list of possible realizations of F-theory compactifications with both an abelian and non-abelian gauge symmetries. This list is complete for low-rank gauge symmetries, which are most relevant for building models of the universe, and thus allows to completely classify all F-theory models with a single abelian gauge factor. In particular, this list includes phenomenologically interesting fibrations not considered in the literature before.

Acknowledgements

I am greatly indebted to Sakura Schäfer-Nameki for her supervision throughout my Ph.D. student years. Her enthusiasm about getting to the core of things, her tenacity in attacking a problem until a solution emerges, and her permanent willigness to share her time and whiteboard in innumerable discussions have improved this work in countless ways in both scope and quality.

I would also like to thank my fellow student Craig Lawrie, for the collaborative smoothing of many rough edges in our research projects during a multiplicity of enlightening debates, and for the proofreading of large parts of this thesis. I am also grateful towards Andreas Braun and Jenny Wong for our numerous group discussions on F-theory, geometry, and phenomenology and for spotting more errors in the various drafts of this text.

My thanks go to the maths department at King's College London and especially to Paul, Mike, Jan, Mike, Jakob, Nick, Pascal, Jun, Sam, Barbara, Silvia, and Saška for making my three years here social and enjoyable. I would also like to thank Oliver, Alex, and Andreas for proofreading parts of the thesis.

Finally, I would like to express my deep gratitude towards my family and Cosima, for their perpetual support in navigating the calms and storms of research in theoretical physics.

Contents

List of Tables

List of Figures

Chapter 1

Introduction

The central theme of string phenomenology is the search for string theoretic settings encompassing both particle physics and cosmology models in accordance with all physical observations. Not only are gravitational and gauge interactions unified in this way, one also constrains the space of feasible models by requiring them to be realizable in string theory.

Models of currently observable physics are built in two areas: quantum field theory and general relativity. General relativity is the framework to explain gravitational interactions and the large-scale structure of the universe, whereas quantum field theory, and more specifically the Standard Model of Particle Physics, addresses the structure of matter at small scales and the electromagnetic, weak, and strong interactions.

As such, the Standard Model of Particle Physics is one of the most successful theories of physics to date, and its predictions, notably the existence of massive gauge bosons, have been tested and confirmed to high precision [4]. However, the Standard Model suffers from a few shortcomings. Among them are the lack of a description of gravity, the large disparity between the electroweak energy scale of about 1 TeV and the Planck scale $E_P \approx 1.22 \times 10^{19}\,\mathrm{GeV}$ — known as the Hierarchy problem and related to the very small value of the mass of the Higgs boson around 125 GeV [5, 6] — and the fact that its dynamics depend on 19 different parameters, whose numerical values need to be found experimentally.

There have been many attempts to address some or all of these issues in field theory. Among the most appealing solutions to the hierarchy problem is supersymmetry. Furthermore, the three forces in the Standard Model can be combined into a single unified

force within Grand Unified Theories, which also reduces the number of free parameters in the Standard Model.

The arguably most promising candidate at unifying quantum field theories and gravity is string theory [7–12]. This fact arises from two central properties of string theory. The first one is that after quantization of string theory, the massless spectrum of string theory contains a symmetric 2-tensor, which behaves like the graviton of a quantized version of general relativity. Secondly, string theory contains the basic building blocks of the Standard Model, e.g. non-abelian gauge theories, chiral charged matter in replicated generations, and Yukawa couplings.

The underlying assumption behind string theory model building is therefore that string theory gives an accurate description of nature at energies as high as the Planck energy E_P, and that all physical models at smaller energy scales, such as the electroweak scale or the GUT scale 10^{16} GeV, arise as effective theories in the low-energy sector of string theory. In this way, embeddability into a string theory model becomes a criterion with which one can constrain the space of feasible field theoretic constructions.

It turns out that there is a large number of ways in which models of string theory at low energies can be engineered. Central in this procedure is the process of compactification, where one assumes that six of the ten spacetime dimensions of string theory parametrize a compact manifold which one is free to specify as an input. Crucially, the geometry of this manifold describes many physical properties of the remaining four non-compact dimensions. Studying string compactifications thus allows one to reformulate physical questions into geometric ones, and to use powerful tools of algebraic geometry to address them.

In turn, if one finds a classification of geometric objects with certain properties, one is often able to translate it into a complete set of physical attributes present in string compactifications, and thereby to give restrictions on the low-energy models which can be realized in string theory. In this way, one is able to study entire classes of string phenomenology models *systematically* by learning about the geometry of sufficiently generic compactification manifolds. To apply this general idea in concrete settings is the goal of this thesis.

In the remainder of this introduction we give more detail on the Standard Model and its shortcomings, and explain supersymmetry and Grand Unified Theories as field-theoretic solutions to some of these. We motivate the study of string theory and its phenomenology as an attractive area to find general constraints to field theory models, and F-theory as a

particularly fruitful subfield of it. We close with an overview over the rest of the thesis. Throughout this thesis, we use natural units in which $c = \hbar = 1$.

1.1 The Standard Model and its limitations

The Standard Model of Particle Physics [4, 13] is, together with the ΛCDM model of cosmology [14], one of the two fundamental models describing our current knowledge about the physics of the universe. Its predictions have been tested at a wide range of energies, notably with the discovery of a Higgs boson at CERN in 2012 [5, 6], and to unrivalled precision [4, 15].

The Standard Model (SM) is a quantum field theory, and among its specifying data are its gauge group G_{SM}, its matter content — that is, the non-abelian representations and $U(1)$ charges of its fermion and scalar fields — and its Yukawa couplings. The gauge group is given by

$$G_{\mathrm{SM}} = SU(3) \times SU(2) \times U(1)_Y \tag{1.1.1}$$

with vector gauge bosons

$$(g, W, B) = \left((\mathbf{8}, \mathbf{1})_0 , (\mathbf{1}, \mathbf{3})_0 , (\mathbf{1}, \mathbf{1})_0\right) , \tag{1.1.2}$$

and the representations of any of the three generations of quark and lepton fermions are

$$(Q, u^c, d^c, L, e^c) = \left((\mathbf{3}, \mathbf{2})_{1/6} , \left(\overline{\mathbf{3}}, \mathbf{1}\right)_{-2/3} , \left(\overline{\mathbf{3}}, \mathbf{1}\right)_{1/3} , \left(\mathbf{1}, \overline{\mathbf{2}}\right)_{-1/2} , (\mathbf{1}, \mathbf{1})_1\right) . \tag{1.1.3}$$

On top of these, there is the scalar Higgs boson

$$H = (\mathbf{1}, \mathbf{2})_{-1/2} . \tag{1.1.4}$$

Since H transforms as an $SU(2)$-doublet, one can decompose it into its component complex scalar fields

$$H = \begin{pmatrix} \phi_1 \\ \phi_2 \end{pmatrix} \tag{1.1.5}$$

The scalar potential of the Higgs field then reads

$$V(H) = -\mu^2 \left(\bar{\phi}_1 \phi_1 + \bar{\phi}_2 \phi_2\right) + \lambda \left(\bar{\phi}_1 \phi_1 + \bar{\phi}_2 \phi_2\right)^2 , \tag{1.1.6}$$

and it induces a vacuum expectation value (vev) for H, spontaneously breaking the electroweak symmetry group $SU(2) \times U(1)_Y \subset G_{\text{SM}}$ to the electromagnetic $U(1)_{EM}$. One can make an $SU(2) \times U(1)$ transformation to turn any vev of H into the form

$$\langle \phi_1 \rangle = 0\,, \qquad \langle \phi_2 \rangle = v/\sqrt{2} \tag{1.1.7}$$

for real v, with $v^2 = \mu^2/2\lambda \approx 170\,\text{GeV}$ set by experiment. Simultaneously, v generates masses for the quarks and leptons via Yukawa couplings Y in the Standard Model Lagrangian,

$$\mathcal{L}_{SM} \supset Y_u Q u^c \phi^* + Y_d Q d^c \phi + Y_l L e^c \phi + \text{h.c.}\,, \tag{1.1.8}$$

where Y_u, Y_d and Y_l are 3×3-matrices in the generation space spanned by (1.1.3).

The Standard Model as sketched above largely describes all of the currently available data of particle physics. However, there are some fundamental problems in the Standard Model, hinting towards its incompleteness as a fundamental description of nature:

- The Standard Model does not describe *gravity*. In fact, there is no known way to augment quantum field theory with a theory of gravitational interactions.
- In order for electroweak symmetry breaking to work, the mass m_H of the Higgs particle has to be roughly at the electroweak scale. However, m_H is subject to quantum loop corrections, which are about 18 orders of magnitude larger than m_H itself. To keep the Higgs mass at the electroweak scale, one has to consider an extreme fine-tuning of about 1 part in 10^{26}. This issue originates in the relative smallness of the electroweak scale itself and is known as the *hierarchy problem*.
- There is a large *number of free parameters* in the Standard Model. Apart from the ad hoc choices of gauge group and particle content, there are 19 free parameters (for instance the Yukawa matrix entries in (1.1.8) and the λ and μ of (1.1.6)), whose numerical values need to be given as an input into the model, rather than being a prediction of it.
- More specifically, the form of the *Higgs potential* $V(\phi)$ is an input into the Standard Model as well, and at present we do not understand its origin, which is of fundamental importance to electroweak symmetry breaking.
- The Standard Model predicts neutrinos to be massless particles. However, there is evidence for *neutrino masses* from neutrino oscillation experiments [16].
- Observations of rotational velocities of galaxies [17] and of gravitational lensing [18] have shown that only about 4% of the total energy content of the universe consists

of the particles described in the Standard Model. A large fraction of matter, about 27% of the total energy, only interacts gravitationally with Standard Model fields. The Standard Model does not provide any description of such *Dark Matter*.

- It also does not explain the remaining 68% of the universe's energy content, which have been denoted *Dark Energy*, and for which there is evidence from e.g. type Ia supernovae [19] and the cosmic microwave background [20, 21].

- Finally, one regularly observes a striking *imbalance of fundamental scales*, leading to the question of apparent fine-tunings. Besides the smallness of $M_{\text{EW}}/M_{\text{Planck}} \approx 10^{-17}$, which was already mentioned, there is also the almost vanishing cosmological constant at $\Lambda \approx 10^{-120} M_{\text{Planck}}^4$, and the hierarchy in the Yukawa couplings of the Standard Model, with $M_{\text{electron}}/M_{\text{top}} \approx 10^{-6}$.

To each of these problems, there exist proposed solutions. In the next sections, we consider some of them: Supersymmetry, which solves the hierarchy and the dark matter problems, and Grand Unified Theories, which confront the number of free SM parameters and can also incorporate supersymmetry. We then argue that string theory is a promising candidate to unify quantum field theory and general relativity, solving the gravity problem of the Standard Model, and furthermore provides one with a promising framework to address all other problems on the list.

1.2 Supersymmetry and the MSSM

In this section, we discuss in more detail the hierarchy problem of the Standard Model, show how supersymmetry yields a solution to it, and give an overview over the Minimal Supersymmetric Standard Model. Far more detailed treatments of supersymmetry can be found e.g. in [22–24].

As we have stated, the hierarchy problem of the Standard Model is the fact that the mass of the Higgs boson obtains quantum corrections from loops involving virtual SM fermions, with the top quark giving the dominant contribution. Such a loop is shown on the left of figure 1.1. They have a quadratic divergence, and impose a correction to the Higgs mass of the form (see e.g. [23] for a full computation of the top loop and the two scalar loops mentioned below)

$$m_H^2 = m_{H,\text{tree}}^2 + \delta m_H^2 \,, \qquad \delta m_H^2 \sim -\int^{\Lambda^2} \mathrm{d}k^2 \sim -\Lambda^2 \,, \tag{1.2.1}$$

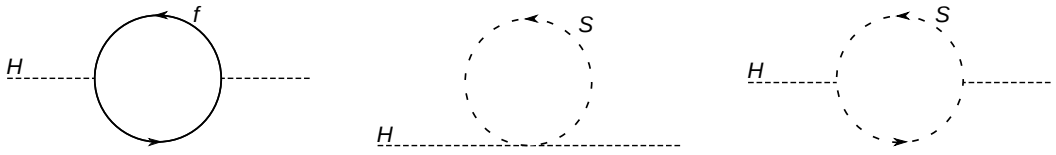

FIGURE 1.1: Contributions to the Higgs mass term from fermion loops (left) and scalar loops via the quartic (middle) and trilinear (right) coupling.

with the cutoff energy scale Λ, where the Standard Model ceases to be an effective theory of nature. If one assumes the existence of a finite theory of quantum gravity at the Planck scale, one has $\Lambda^2 \sim M^2_{\text{Planck}}$, and finds a correction on the scale of $\left(10^{18}\,\text{GeV}\right)^2$, which has to almost entirely cancel with the tree-level term to produce the renormalized squared Higgs mass of about $(125\,\text{GeV})^2$. In the Standard Model, the only way to do so is to impose an extreme fine-tuning on $m^2_{H,\text{tree}}$. Therefore, one assumes that there exists new physics beyond the Standard Model that effectively reduces the cutoff scale Λ to about 1 TeV and stabilizes the Higgs mass above it by canceling the loop corrections. The leading proposal to do so is Supersymmetry, or SUSY.

The observation underlying the SUSY solution to the hierarchy problem comes from introducing new scalar particles into the Standard Model, one (complex) scalar per fermion and one fermion per scalar and vector, transforming in the same representations as the SM fermions and with the same masses. The extra scalars induce additional loop corrections to the Higgs mass terms, as depicted in the middle and right panels of figure 1.1. It turns out that the new loops *exactly* cancel the Λ^2-divergences from the SM fermion loops in (1.2.1). Furthermore, all divergent corrections from two- or higher-loop diagrams are also cancelled.

Supersymmetry realizes these additional particles by proposing a new symmetry algebra that extends the Poincaré algebra $\mathcal{P}$ of spacetime symmetry [25]. Specifically, the SUSY algebra contains new complex, anticommuting spinors Q and their conjugates $Q^\dagger$ with

$$\{Q_\alpha, Q_\beta\} = \{Q^\dagger_{\dot\alpha}, Q^\dagger_{\dot\beta}\} = 0 \tag{1.2.2}$$

whose anticommutators with each other give the translation generator P_μ of the Poincaré algebra:

$$\left\{Q_\alpha, Q^\dagger_{\dot\alpha}\right\} = 2\sigma^\mu_{\alpha\dot\alpha} P_\mu\,, \tag{1.2.3}$$

with $\sigma^\mu = \left(\mathbf{1}, \sigma^i\right)$ and the Pauli matrices σ^i. Further, the new generators commute with translations:

$$[P_\mu, Q_\alpha] = \left[P_\mu, Q^\dagger_{\dot\alpha}\right] = 0\,. \tag{1.2.4}$$

Note that this algebra is invariant under multipliying Q by some phase e^{ia}, hence there will generally be a set of $U(1)$ charges, called the R-charge, that does not commute with Q and $Q^\dagger$:

$$[Q_\alpha, R] = Q_\alpha \,, \qquad \left[Q^\dagger_{\dot\alpha}, R\right] = -Q^\dagger_{\dot\alpha} \,, \tag{1.2.5}$$

and one denotes the corresponding symmetry group as $U(1)_R$.

The representations of this new SUSY algebra extend the scalar, spinor and vector multiplets of $\mathcal{P}$ to so-called supermultiplets, each of which contains both bosons and fermions. Particles belonging to the same supermultiplet are called superpartners, and they possess the same mass and transform in identical gauge representations, as one requires in order to solve the hierarchy problem.

There is a minimal embedding of the Standard Model into a supersymmetric formulation, called the Minimal Supersymmetric Standard Model or MSSM. In the MSSM, every Standard Model fermion and vector boson multiplet is replaced by its associated supermultiplet. Instead of a single Higgs scalar, there are two supermultiplets H_u and H_d transforming as

$$(H_u, H_d) = \left((\mathbf{1},\mathbf{2})_{1/2} \,, (\mathbf{1},\mathbf{2})_{-1/2}\right) \tag{1.2.6}$$

under $G_{\text{MSSM}} = G_{\text{SM}}$. The interactions between particles in a supersymmetric model are governed by its holomorphic superpotential, which in the case of the MSSM reads

$$W_{\text{MSSM}} = Y_u Q u^c H_u - Y_d Q d^c H_d - Y_l L e^c H_d + \mu H_u H_d \,, \tag{1.2.7}$$

and re-encodes the Yukawa and Higgs self-interaction sectors of the Standard Model in its Yukawa and μ-terms, respectively. The holomorphicity of W_{MSSM} also provides the reason for the additional Higgs supermultiplet – if there is only one charged Higgs boson, one cannot generate a holomorphic mass for it. Furthermore, the superpotential is protected from loop corrections due to the non-renormalization theorem of supersymmetric theories (proven e.g. in [22]).

In principle, one can construct additional allowed terms in the MSSM superpotential with no equivalent in the SM, concretely

$$W_{\text{extra}} = aLH_u + bQLd^c + cu^c d^c d^c + dLLe^c \,. \tag{1.2.8}$$

These terms induce proton decay at a rate that would have been experimentally observed,

and must therefore be forbidden in W_{MSSM}. One way to do so is by invoking the R-symmetry obtained from the SUSY algebra, with R-charge assignments

$$R_{(Q,u^c,d^c,L,e^c)} = 1\,, \qquad R_{(H_u,H_d)} = 0\,. \tag{1.2.9}$$

The only terms in $W_{\text{MSSM}}+W_{\text{extra}}$ consistent with these charges are the Yukawa couplings. To generate the (phenomenologically relevant) μ-term, one has to spontaneously break the R-symmetry to its $\mathbb{Z}_2$ R-parity subgroup.

Since we do not observe e.g. a scalar superpartner of the electron with a mass of 511 keV, or of any other SM particle for that matter, supersymmetry cannot be an unbroken symmetry of nature. It can be shown that spontaneous supersymmetry breaking cannot occur in the MSSM itself [26], since this would always lead to a light scalar $SU(3)$-triplet, which is not observed in nature. This is a consequence of the mass sum rule, which states that even after breaking supersymmetry, the masses of the bosonic and fermionic particles of a supermultiplet, weighted by their degrees of freedom, sum up to the same value.

One therefore has to augment the MSSM with mechanisms to spontaneously break supersymmetry, for instance as in the O'Raifeartaigh [27] or Fayet-Illiopoulos [28] models, in a 'hidden' sector of the theory and to transmit the breaking to the MSSM fields. Assuming that the hidden sector contains a superfield S with vacuum expectation value $\langle S\rangle$ and that there exist non-renormalizable couplings of S to the MSSM fields, one obtains a large set $\mathcal{L}_{\text{soft}}$ of so-called soft supersymmetry breaking terms, that is, terms that when added to the MSSM Lagrangian do not spoil the cancellation of the Higgs mass loop terms, and therefore do not affect the solution to the hierarchy problem.[1] These include mass terms for all SM field superpartners and both Higgs doublets, with 105 parameters [30].

Thus, soft supersymmetry breaking seems to introduce a huge number of new variables into the theory. There is however experimental evidence (e.g. from flavour-changing neutral currents [31]) that strongly restricts most of the new parameters, and there are also phenomenological mechanisms for mediating supersymmetry breaking [32–34] which lead to a much more constrained picture. Furthermore, SUSY breaking requires the presence of an R-symmetry, and spontaneously breaking the latter is a sufficient condition for the breaking former in generic settings [35].

It turns out that $\mathcal{L}_{\text{MSSM}} + \mathcal{L}_{\text{soft}}$ also breaks electroweak symmetry radiatively, rendering the need for a non-trivial Higgs potential obsolete. Furthermore, the superpartner which

[1] Supersymmetry breaking at a scale that is higher than the electroweak scale reintroduces some fine-tuning, albeit on a much smaller level than the one required to solve the hierarchy problem. This issue is called the little hierarchy problem or LEP paradox [29].

has the lightest mass after supersymmetry breaking is a stable particle that only interacts with the SM particles gravitationally (any other interaction would violate R-parity), and is therefore a suitable dark matter candidate.

1.3 Grand Unified Theories

Another fundamental building block of particle physics beyond the Standard Model are Grand Unified Theories, or GUTs. In this section, we discuss their relevance and some of their properties relevant to this thesis. Much more can be said about GUTs, and an introductory review is [36]. For Lie groups and Lie algebras, we use notation as presented in [37, 38].

The central observation underlying the idea of GUTs [39, 40] is that the Standard Model gauge group G_{SM} from (1.1.1) is a maximal subgroup of $SU(5)$. That is, there exists exactly one element up to scaling in $su(5)$, the Lie algebra of $SU(5)$, which commutes with the $su(3) \oplus su(2)$ subalgebra of $su(5)$. This element generates the $U(1)_Y$ in G_{SM}.

The decomposition of the adjoint **24** representation of $SU(5)$, in which the $SU(5)$ gauge bosons transform, is given by

$$\mathbf{24} \to (\mathbf{8},\mathbf{1})_0 + (\mathbf{1},\mathbf{3})_0 + (\mathbf{1},\mathbf{1})_0 + \left(\mathbf{3},\overline{\mathbf{2}}\right)_{-5} + \left(\overline{\mathbf{3}},\mathbf{2}\right)_5 \,. \tag{1.3.1}$$

The first three terms are precisely the required gauge bosons of $SU(3)$, $SU(2)$, and $U(1)$ of G_{SM}, respectively. The last two terms however do not appear in the Standard Model spectrum. The gauge bosons to which these representations correspond to are typically denoted X- and Y-bosons. The existence of such bosons at the electroweak scale would induce proton decay at a magnitude that has been experimentally ruled out. In fact, the mass of X and Y bosons has to be roughly at the GUT scale of 10^{16} GeV.

Furthermore, decomposing the antifundamental $\overline{\mathbf{5}}$ and antisymmetric **10** representations of $SU(5)$ in terms of representations of $SU(3) \times SU(2) \times U(1)$, one finds

$$\begin{aligned} \overline{\mathbf{5}} &\to \left(\overline{\mathbf{3}},\mathbf{1}\right)_2 + \left(\mathbf{1},\overline{\mathbf{2}}\right)_{-3} \,, \\ \mathbf{10} &\to (\mathbf{3},\mathbf{2})_1 + \left(\overline{\mathbf{3}},\mathbf{1}\right)_{-4} + (\mathbf{1},\mathbf{1})_6 \,. \end{aligned} \tag{1.3.2}$$

Therefore, after rescaling the $U(1)$ charges by a factor of 6, the two representations $\overline{\mathbf{5}}$ and **10** replicate *exactly* one generation of Standard Model fermions (cf. (1.1.3)).

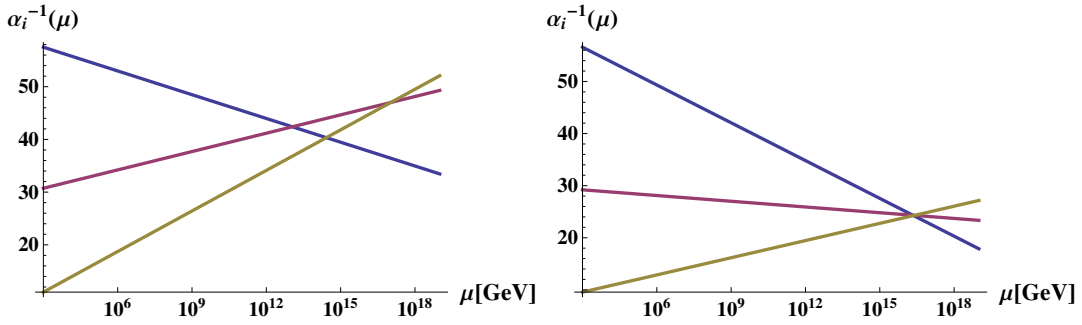

FIGURE 1.2: Renormalization group flows of the coupling constants of the Standard Model (left) and the Minimal Supersymmetric Standard Model (right). Underlying data from [3].

The exact replication of the Standard Model fermion representations does however not work as well for the Higgs bosons. While the Standard Model Higgs doublet originates from the fundamental **5** representation of $SU(5)$ with correct $U(1)_Y$ charge, the decomposition

$$\mathbf{5} \to (\mathbf{3}, \mathbf{1})_{-2} + (\mathbf{1}, \mathbf{2})_3 \tag{1.3.3}$$

includes an additional $SU(3)$-triplet that does not appear in the spectrum of the Standard Model. Again, in order to prevent proton decay, all components of the Higgs triplet are required to have a mass at the GUT scale, while the Higgs doublet contains a light field which has a mass of only 125 GeV. This issue is known as the doublet-triplet-splitting problem of GUTs. If an $SU(5)$-GUT is realized in nature, one expects the presence of a mechanism to confront doublet-triplet-splitting.

If the three factors of the Standard Model gauge group unify at about 10^{16} GeV, one expects the same for their respective coupling constants. In other words, the renormalization group flows of the three coupling constants of G_{SM} [40] should all intersect at a single point for an energy of about 10^{16} GeV. This is not the case for G_{SM}, cf. figure 1.2. However, one can construct a supersymmetric version of a GUT which extends the MSSM in a way essentially analogous to the non-supersymmetric case: One adds superpartners to the Standard Model fermion fields, and requires an additional fundamental **5** and anti-fundamental $\overline{\mathbf{5}}$ supermultiplet of $SU(5)$ to be present, in order to account for the two Higgs doublets H_u and H_d of the MSSM. SUSY GUTs not only combine the phenomenological advantages of Supersymmetry and Grand Unified Theories, they also exhibit the desired gauge coupling unification at 10^{16} GeV, see again figure 1.2. This observation motivates the numerical value of the GUT scale.

After the breaking of a SUSY GUT and minimization of its scalar potential, the Higgs vacuum expectation value v_H yields different contributions to the masses

$$\mu_t H_u^t H_d^t \qquad \text{and} \qquad \mu_d H_u^d H_d^d \tag{1.3.4}$$

of the Higgs triplets and Higgs doublets, and one again requires fine-tuning to achieve $m_{\text{EW}} \sim \mu_d \ll \mu_t \sim m_{\text{GUT}}$. This is the SUSY version of the doublet-triplet splitting problem. This problem is somewhat related to the μ-problem of supersymmetric theories, which is the observation that in order for radiative electroweak symmetry breaking to work, the μ-term

$$\mu H_u H_d \subset W_{\text{MSSM}} \tag{1.3.5}$$

has to be at about the electroweak scale, which is unnaturally small for a theory that is defined at the GUT scale.

One way to address the μ-problem in supersymmetric GUTs is to postulate the existence of an additional local $U(1)$-symmetry beyond the $U(1)_Y$ of G_{MSSM}. Under this additional symmetry, which is often denoted as a Peccei-Quinn or PQ-symmetry [41, 42], the two Higgs fields are required not to carry exactly opposite charges:

$$PQ(H_u) + PQ(H_d) \neq 0\,. \tag{1.3.6}$$

Such a symmetry forbids the μ-term for the Higgs fields. This term will therefore be absent until the $U(1)_{PQ}$ is broken at a convenient scale. More importantly, a PQ-symmetry forbids certain proton decay operators which would otherwise appear in GUT models, such as the dimension-five operator

$$\mathcal{O} \sim \frac{1}{\Lambda} Q^3 L\,. \tag{1.3.7}$$

In an unbroken $SU(5)$ GUT, a PQ-symmetry also forbids the μ-term for the Higgs triplets. However, this need not be true after breaking $SU(5)$ to the Standard Model gauge group, and there indeed exist GUT-breaking mechanisms that lift the masses of both the Higgs triplets and the X- and Y-bosons to the GUT scale. We will allude to one such mechanism present in GUT embeddings within string theory in section 3.6.

With $U(1)_R$ and $U(1)_{PQ}$, we have now seen two examples of abelian gauge symmetries that were important in the construction of extensions of the Standard Model. In field theory, one is not restricted in any way in one's choice of $U(1)$ charges. One might hope that such constraints are obtainable from an embedding into a UV-complete theory, such

as string theory. This turns out to be the case for F-theory constructions, as we will see in chapter 5.

1.4 The Case for String Theory as a Fundamental Description of Nature

Supersymmetry and Grand Unified Theories solve some, but not all of the shortcomings of the Standard Model – in fact, one of the biggest of all issues, namely the absence of gravity in the SM, is not even addressed. It is therefore clear that, even if SUSY or GUTs are realized in nature, new physics is still required to unify all fundamental forces. The leading candidate for such new physics is string theory. This section seeks to justify that statement.

Let us note that there are many other good reasons for studying string theory, such as the AdS/CFT correspondence [43,44] with applications e.g. in condensed matter physics [45], or the interplay between string theory and mathematics in areas like mirror symmetry [46] or monstrous moonshine [47,48]. Nonetheless, in this thesis, our primary interest will be in the application of string theory as a candidate fundamental description of nature.

The single new assertion in string theory compared to quantum mechanics and general relativity is that *the fundamental objects of nature are* 1*-dimensional strings instead of pointlike particles.* Combined with the covariance principle from general relativity and the quantization procedure of quantum mechanics, one obtains a theory that naturally realizes non-abelian gauge interactions and gravity. More specifically, the low-energy spectrum[2] of the quantized closed string contains a symmetric 2-tensor with an Einstein-Hilbert Lagrangian, which can be identified with a quantized graviton.

Furthermore, any string theory necessarily also includes higher-dimensional objects called branes (roughly, hyperplanes on which open strings can have their endpoints), and it turns out, after quantizing the open string, that their low-energy theories are precisely Yang-Mills gauge theories. Chiral matter and Yukawa couplings can arise within string theory as well, e.g. from intersections between branes. Furthermore, any string theory that includes spacetime fermions (and is thus of any phenomenological interest) automatically contains supersymmetry as one of its fundamental components.

[2] One typically assumes that the energy scale of string theory is near the Planck scale, as expected for any theory of quantum gravity. In this setting, the vast majority of currently observable physics has to arise in the low-energy or massless spectrum of string theory.

In this way, string theory has all the building blocks required to reconstruct both the Standard Model of Particle Physics and the ΛCDM model of cosmology in a string theoretic setting. It does, however, go further than that: In string theoretic settings, many if not all of the Standard Model shortcomings of section 1.1 can be addressed.

As we have argued, string theory automatically takes care of the unification of gravity and gauge theories. Many of the other issues of the Standard Model can be confronted by simply re-using known solutions embedded in string theory: For instance, since string theory is formulated intrinsically supersymmetric, one can try to find a setting which spontaneously breaks supersymmetry at energies as low as the TeV scale, and by doing so reproduces the SUSY solution to the hierarchy, Higgs potential, and dark matter problems. It is also possible (and not much harder than direct embeddings of the Standard Model) to construct Grand Unified Theories in string theoretic settings, thereby addressing the SM parameter issue and gauge coupling unification.

Apart from embedding known field-theory solutions into string theoretic settings, there are also new, genuinely string-theoretic answers to some problems of the Standard Model. For instance, the imbalance of fundamental scales observed in the Standard Model and between the SM and the ΛCDM model of cosmology can addressed in a way similar to the warped extra dimension scenarios [49, 50] through the concept of compactification, discussed in more detail in section 1.5. Furthermore, compactified string vacua have an absolute scalar potential behaving essentially as a cosmological constant. If one dynamically engineers the vacuum expectation value of the scalar potential to be small and positive, one can address the dark energy problem [51–53]. Finally, string theory not only contains answers to the principal shortcomings of the Standard Model of Particle Physics, but also to the problems of ΛCDM, for instance by embedding models of cosmological inflation [54, 55] into string theory vacua [56, 57].

In summary, string theory seems to possess sufficient richness to be able to solve each currently known problem of our current fundamental theories. However, this does not mean that all is done: The challenge lies in combining all the ingredients into a single string theoretic model that solves all problems of the SM and ΛCDM while staying self-consistent and not introducing unwanted side-effects like unobserved particles. Another less ambitious aim would be to find restrictions on field theoretic models by requiring their embeddability in a string theory compactification.

Making progress towards this goal is the subject of string phenomenology, the field in which this thesis is situated. The next section aims to explain some basic concepts of string phenomenology.

1.5 String Phenomenology Concepts

String phenomenology aims to explain the physics of the universe in the context of string theory. As argued in the preceding section, it assumes that string theory gives a precise description of the universe at energy scales up to the Planck scale, and intends to unify models of lower-energy physics, such as SUSY, GUTs, or models of cosmological inflation [54, 55, 57], into a single description in string theory.

A defining feature of model building in string phenomenology is the fact that (super-)string theory is well-defined exactly in ten spacetime dimensions, whereas there are only four observed dimensions of spacetime. This seems to be a problem at first sight, but there is a way out: six of the nine spatial dimensions required by string theory might parametrize a compact manifold whose finite size is too small to be observable at currently measurable energy scales. This idea of compactification was first proposed in the 1920s [58, 59], and has been reanimated from 1983 onwards [49, 60–62]. Not only does compactification solve the apparent disparity of spacetime dimensions, it also turns out that the geometry of the compactification manifold determines much of the physics in the remaining four non-compact dimensions. In fact, the reformulation of physical questions into geometric constraints on the compactification is both a driving force of and a main challenge for string phenomenology.

Apart from the compactification manifold, a second choice to be made in any string phenomenology model is the type of low-energy string theory used as framework, with prominent choices being type IIA/IIB, and $E_8 \times E_8$ heterotic string theory. In type IIA/IIB string theory models, reviewed e.g. in [63], the non-abelian gauge degrees of freedom are localized on branes, which trace out a subspace of the compactification manifold. This locality enables a modular approach to model building, where one can study the gauge physics largely independent of global properties of the compactification. On the other hand, phenomenological models in heterotic string theory (see e.g. [64] for a review) allow for the presence of exceptional gauge groups. Such gauge groups have their own desirable consequences, for instance the easy implementation of a large top Yukawa coupling in GUT models.

There is a framework that unifies the advantages of type IIA/IIB and heterotic compactifications, at the expense of leaving the regime of perturbative string theory. This framework is called F-theory [65], and throughout this thesis, we will work in F-theory. In section 1.6, we motivate F-theory as a non-perturbative generalization of type IIB string theory, and in chapter 3 we define it on a more technical level.

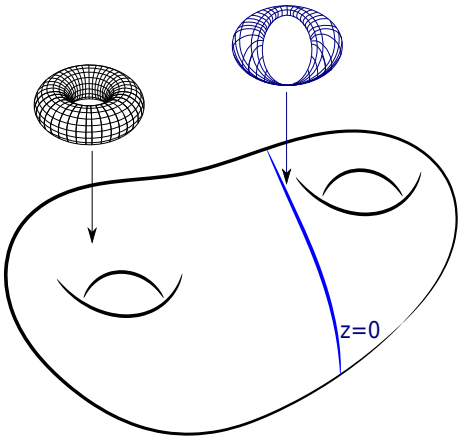

FIGURE 1.3: An elliptic fibration becoming singular over a locus described by the vanishing of a local coordinate z.

1.6 Why F-Theory?

As we have seen, the underlying idea behind the study of compactified string theory models rests on the fact that they provide a framework to embed low-energy models into a UV-complete theory, which allows one to translate physically motivated constraints into geometric questions, and in reverse to use results from geometry to restrict the space of allowed physical models.

An area in which this approach has been very successful is F-theory. F-theory is easiest understood as a non-perturbative generalization of vacua of type IIB string theory, where the (physical) string coupling constant is modelled by the (geometric) complex structure of an elliptic fibration over the compactification manifold. Loci where the fibration becomes singular indicate diverging string coupling, and thus correspond to the locations of 7-branes. Crucially, F-theory thus provides the localization of gauge degrees of freedom on subloci of the compactification, enabling a modular approach to the construction of phenomenological models. On the other hand, F-theory allows for the construction of exceptional gauge symmetries, making it comparatively easy to embed low-energy models into F-theory vacua.

In order to describe F-theory models, one makes heavy use of the algebraic geometry of elliptic fibrations. One of its main results is a classification of singularities of elliptic fibrations, along with a set of normal forms describing fibrations with a given singularity type. This translates into a classification of non-abelian gauge groups hosted on the brane localized on the singular locus, as well as providing a collection of representations for charged matter and Yukawa couplings of the low-energy gauge theory on the brane.

Using results about elliptic fibrations to answer physical questions in F-theory compactifications can be substantially extended beyond these examples, for instance in the systematic construction of abelian gauge symmetries, as we will see in chapter 5, or of G-flux in chapter 4. In fact, this philosophy underpins much of F-theory model building, as one can analyze many physical features of F-theory compactifications in isolation due to their modularity, and then harness the simplification coming from doing so by being able to comprehensively survey the range of possibilities for these features in F-theory. In a second step, one is then able to recombine the various ingredients — gauge groups, matter curves, Yukawa couplings, fluxes, etc. — into complete models. After having introduced the individual pieces of F-theory in chapter 3, we will do exactly this for an $SU(5)$ GUT model in F-theory in section 3.6.

To a certain extent, the interplay between low-energy models and their embeddings is even present within F-theory itself. Since gauge degrees of freedom are localized on subloci of the compactification manifold, one can zoom into a purely local description of an F-theory model on such a sublocus and extract physical information from it. This might then again be supplemented or constrained by features arising from global properties of the model. One such procedure is the spectral cover formalism, which we will extend and constrast with global constructions in chapter 4.

Chapter 3 introduces F-theory in more detail, and shows how physical properties such as abelian gauge symmetries are tied to the geometry of an F-theory compactification. In order to properly define and reason about F-theory compactifications, one therefore needs to know about some algebraic geometry, especially on T^2- or elliptic fibrations. Chapter 2 establishes the relevant geometric groundwork.

1.7 Outline of the Thesis

This introduction provided the phenomenological context for this thesis and attempted to motivate the study of compactified string theories as a promising way to address fundamental shortcomings of the Standard Model. The rest of this thesis is organized as follows.

- In chapter 2, we undertake a more detailed exposition of the mathematics of elliptic fibrations. This allows us to give a self-contained formal introduction into F-theory in chapter 3.

- Chapter 4 presents an extension of the spectral cover formalism which studies local properties of subloci of the compactification manifold on which gauge degrees of freedom are present in F-theory. This extension, called the spectral divisor, allows one to construct gauge fluxes in a purely local setting. The construction is exemplified on an elliptic fibration with gauge group E_6. The exposition follows the associated publication [66].

- In chapter 5, we systematically classify singularities of elliptic fibrations with an additional rational section using Tate's algorithm following [67]. The classification provides us with a list of possible F-theory compactifications with both one abelian and (possibly several) non-abelian gauge symmetries. This list is complete for the low-rank gauge symmetries, and includes fibrations of phenomenological relevance that have not been considered in the literature before.

We give concluding remarks and an outline of open research questions building on the work presented here in chapter 6.

Chapter 2

The Geometry of Elliptic Fibrations

In chapter 1 we motivated the study of string theory, and more specifically F-theory, as a promising framework to realize UV-completions of the Standard Model. In this chapter, we explain the algebraic geometry of elliptic fibrations relevant to reasoning about F-theory. This will allow us in chapter 3 to give a self-contained overview over F-theory and its ingredients relevant to engineering models in string phenomenology.

We have argued that a central object in string model building is the compactification manifold, and that its geometrical attributes translate into the physics of the string model. A very desirable physical property for such a model is the presence of supersymmetry at low energies, not only for the phenomenological advantages of SUSY we have described in sections 1.2 and 1.3, but also since one can study such vacua in a controlled way.

The SUSY requirement indeed translates into a geometric property of the compactification manifold: four-dimensional F-theory vacua with $\mathcal{N} = 1$ supersymmetry are obtained by compactification on a Calabi-Yau fourfold Y, i.e. a complex Kähler fourfold with vanishing Ricci curvature, and following a theorem conjectured by Calabi and proven by Yau, this is equivalent to the manifold having vanishing first Chern class [68]. The condition originates from the fact that compactifications of M-theory on Calabi-Yau fourfolds lead to three-dimensional $\mathcal{N} = 2$ SUSY [69] and the duality between M- and F-theory which we will discuss in section 3.2.

Furthermore, Y itself is an elliptic fibration over a complex and Kähler base threefold B [65]:

$$\begin{array}{ccc} T^2 & \hookrightarrow & Y \\ & & \downarrow \pi \\ & & B \end{array}$$

and the elliptic fibrations of interest for us are endowed with at least one holomorphic section, i.e. one holomorphic map $\sigma : B \to Y$ such that $\pi \circ \sigma = \mathrm{id}$, with π being the projection from the total space Y to the base space B. We will see that non-abelian gauge groups in F-theory correspond to singular fibers over subloci of B, and abelian gauge factors correspond to additional rational sections.

In this section, we present the algebraic geometry of elliptic fibrations necessary to the aspects of F-theory models we are interested in. We show how elliptic curves and fibrations can be embedded as hypersurfaces in weighted projective spaces, and define the Mordell-Weil group of their rational sections. In order to study singular elliptic fibrations, we explain resolutions of algebraic varieties via blow-ups, and intersections of divisors of resolved varieties. The section closes with the classification of singular elliptic fibrations of Kodaira and Néron, and their construction following Tate's Algorithm. Having gained some knowledge about singular elliptic fibrations, we are then in a position to discuss compactifications of F-theory on a technical level.[1]

2.1 Normal Forms for Elliptic Curves

Before turning to the description of elliptic fibrations, let us look at the simpler setup of elliptic curves. Our first goal is to construct the Weierstraß equation for such curves, following [71,72]. That is, we aim to show that any elliptic curve $(\mathbb{E}, P)$ – i.e. any projective non-singular curve of genus 1 with a specified point P – can be written as a hypersurface embedded in $\mathbb{P}_{[1,2,3]}$ with projective coordinates w, x, and y, described by the Weierstraß equation

$$P_W : \qquad y^2 = x^3 + fxw^4 + gw^6 \,. \tag{2.1.1}$$

We will then generalize this construction to elliptic fibrations, and show that these fibrations are Calabi-Yau manifolds. This allows us to obtain results about generic elliptic fibrations and their associated F-theory models by explicitly studying Weierstraß forms.

[1] In this chapter, knowledge of classical algebraic geometry, including projective varieties, line bundles and divisors on them, their (co-)homology, and Chern classes, is assumed. These subjects are for instance presented in [46, 70].

Used heavily in the construction of the Weierstraß form is the [73]

Riemann-Roch theorem: Let C be a non-singular projective algebraic curve of genus g, $\mathcal{L}$ be a line bundle on C and let the space of sections of $\mathcal{L}$ be denoted with $H^0(C,\mathcal{L})$ and have dimension $h^0(C,\mathcal{L})$. Also let K be the canonical bundle on C. Then,

$$h^0(C,\mathcal{L}) - h^0(C,\mathcal{L}^{-1}\otimes K) = \deg(\mathcal{L}) + 1 - g\,. \tag{2.1.2}$$

Moreover, if $\deg(\mathcal{L}) \geq 2g-1$, then $h^0(C,\mathcal{L}^{-1}\otimes K) = 0$.

Now consider an elliptic curve $(\mathbb{E},P)$ over a field K. Since it has genus 1, the Riemann-Roch theorem for line bundles $\mathcal{L}$ of degree at least 1 reduces to the statement that $h^0(\mathbb{E},\mathcal{L}) = \deg(\mathcal{L})$. For brevity, we will usually write just $\mathbb{E}$ to refer to the elliptic curve, with the presence of the point always being understood.

Let $\mathcal{L}$ be the line bundle $\mathcal{L} = \mathcal{O}(P)$. Then, $H^0(\mathcal{L})$ is spanned by a single section, which we will call w. There are two sections generating $H^0(2\mathcal{L})$: w^2 and a new one, which we will denote by x. Continuing in this fashion, the three sections of $H^0(3\mathcal{L})$ are w^3, wx, and a new section y. The four sections of $H^0(4\mathcal{L})$ are then w^4, w^2x, wy, and x^2, and the five sections of $H^0(5\mathcal{L})$ are w^5, w^3x, wx^2, w^2y, and xy.

Naively, one can construct seven independent sections spanning $H^0(6\mathcal{L})$: y^2, x^3, wxy, w^2x^2, w^3y, w^4x, and w^6. But the Riemann-Roch theorem tells us there should only be six. The seven sections therefore have to be related

$$A_1y^2 + \tilde{a}_1wxy + \tilde{a}_3yw^3 = A_2x^3 + \tilde{a}_2w^2x^2 + \tilde{a}_4w^4x + \tilde{a}_6w^6\,, \tag{2.1.3}$$

with generic coefficients $\tilde{a}_1$, $\tilde{a}_2$, $\tilde{a}_3$, $\tilde{a}_4$, $\tilde{a}_6$, A_1, $A_2 \in K$. One can show that $A_1\,, A_2 \neq 0$. One can then replace x by $-A_1A_2x$, y by $A_1A_2^2y$, and divide by $A_1^3A_2^4$ to obtain the equation

$$y^2 + a_1wxy + a_3yw^3 = x^3 + a_2w^2x^2 + a_4w^4x + a_6w^6\,, \tag{2.1.4}$$

where the y^2- and x^3- coefficients are identical to 1, and with new, still generic coefficients a_i. Since we are only interested in elliptic curves over fields K whose characteristic is neither 2 nor 3, we can furthermore complete the square in y and the cube in x to get rid of the terms with coefficients a_1, a_2, and a_3.

An elliptic curve with a rational point can thus be described as a sextic hypersurface in the weighted projective space $\mathbb{P}_{[1,2,3]}$ given by the Weierstraß equation

$$P_W: \qquad y^2 - x^3 - fxw^4 - gw^6 = 0\,, \tag{2.1.5}$$

where w, x and y are the homogeneous projective coordinates of $\mathbb{P}_{[1,2,3]}$ and f and g are parameters in K determining the shape of the elliptic curve. Furthermore, the elliptic curve constructed in this way over $K = \mathbb{C}$ is a Calabi-Yau onefold, since its first Chern class vanishes. We will prove this last statement explicitly for the more general case of elliptic fibrations below.

Since the point P must be located at the vanishing locus of the only section of $H^0(\mathcal{L})$, that is at $w = 0$, it is now given by the equation

$$y^2 = x^3 \,. \tag{2.1.6}$$

Using the scaling relation of $\mathbb{P}_{[1,2,3]}$, one finds that P has coordinates $[0:1:1]$.

Note that there are other ways to parametrize elliptic curves, such as quartic hypersurfaces in $\mathbb{P}_{[1,1,2]}$ and cubic hypersurfaces in $\mathbb{P}^2$. These are important for realizing F-theory models with abelian gauge factors, and we discuss them in section 2.2. However, any elliptic curve with a section can always be brought to Weierstraß form (2.1.5).

Our main interest in F-theory is however not in elliptic curves, but in elliptic fibrations over a complex three-dimensional base manifold B with a holomorphic section. In order to describe such fibrations, one promotes the constants f and g in (2.1.5) to sections of suitable line bundles over B, and replaces P with the section.[2]

One way of constructing the Weierstraß form for such elliptically fibered fourfolds is to first replace the above $\mathbb{P}_{[1,2,3]}$ by an auxiliary fivefold X which is a $\mathbb{P}^2$-fibration over B given by

$$X = \mathbb{P}\left(\mathcal{O} \oplus K_B^{-2} \oplus K_B^{-3}\right) \,, \tag{2.1.7}$$

where K_B is the canonical bundle of B. The divisors in X are pullbacks of divisors in B under the projection $\pi_X : X \to B$ and a new divisor σ coming from the hyperplane of the $\mathbb{P}^2$ fiber. We parametrize the fiber using the projective coordinates $[w : x : y]$ which then have classes

$$[w] = \sigma \,, \qquad [x] = \sigma + 2c_1 \,, \qquad [y] = \sigma + 3c_1 \,, \tag{2.1.8}$$

where $c_1 = \pi_X^*(c_1(B))$ denotes the pullback of the first Chern class of B under π_X and σ is a new divisor inherited from the hyperplane class of the $\mathbb{P}^2$ fiber. This allows to

[2] More precisely speaking, start with a base threefold B with a ring of sections R. Now construct the fractions of the ring elements, that is equivalence classes of pairs a, $b \in R$ with $b \neq 0$ where $(a, b) \sim (c, d)$ if $ad = bc$. These objects form a field K, called the fraction field associated to R. One defines an elliptic fibration over B as an elliptic curve over K. Since f and g are defined to be elements of R (and are therefore in K), they are now sections of line bundles over B.

generalize (2.1.5): Y is given as the zero locus of the Weierstraß form

$$Y: \qquad y^2w - x^3 - fxw^2 - gw^3 = 0\,, \tag{2.1.9}$$

with f and g being sections of $\mathcal{O}(4c_1)$ and $\mathcal{O}(6c_1)$, respectively. This equation is in the class $[Y] = 3\sigma + 6c_1$. One can immediately check that the fourfold defined in this way is Calabi-Yau: The total Chern class of X is given by

$$\begin{aligned} c(X) &= c(B)\cdot(1+\sigma)\cdot(1+\sigma+2c_1)\cdot(1+\sigma+3c_1) \\ &= 1 + 3\sigma + 6c_1 + \cdots\,. \end{aligned} \tag{2.1.10}$$

Here, the dots denote forms of higher rank. The total Chern class of Y follows by adjunction:

$$c(Y) = \frac{c(X)}{1+3\sigma+6c_1}\bigg|_{Y_4} = (1+3\sigma+6c_1) - (3\sigma+6c_1) + \cdots = 1 + 0 + \cdots\,. \tag{2.1.11}$$

Indeed, the first Chern class of Y vanishes and Y is Calabi-Yau. By letting the base B consist of a single point, this also shows that elliptic curves – that is, elliptic fibrations over a point – are Calabi-Yau onefolds, as was claimed earlier.

2.2 The Mordell-Weil Group

In F-theory, abelian gauge degrees of freedom are geometrically described by the Mordell-Weil group of the elliptic fibration one compactifies on, as we describe in section 3.4. In this section, we define the Mordell-Weil group. Constructing elliptic fibrations with non-trivial Mordell-Weil groups is difficult when using the Weierstraß form. We then show that there is another normal form for elliptic fibrations which realizes rank 1 Mordell-Weil group, given as a quartic hypersurface in the weighted projective space $\mathbb{P}_{[1,1,2]}$ with defining equation

$$y^2 + b_0yx^2 + b_1ywx + b_2yw^2 = c_0w^4 + c_1w^3x + c_2w^2x^2 + c_3wx^3\,. \tag{2.2.1}$$

This form allows us in chapter 5 to systematically study elliptic fibrations with rank 1 Mordell-Weil group, and thus to comprehensively classify F-theory compactifications with one additional abelian gauge factor.

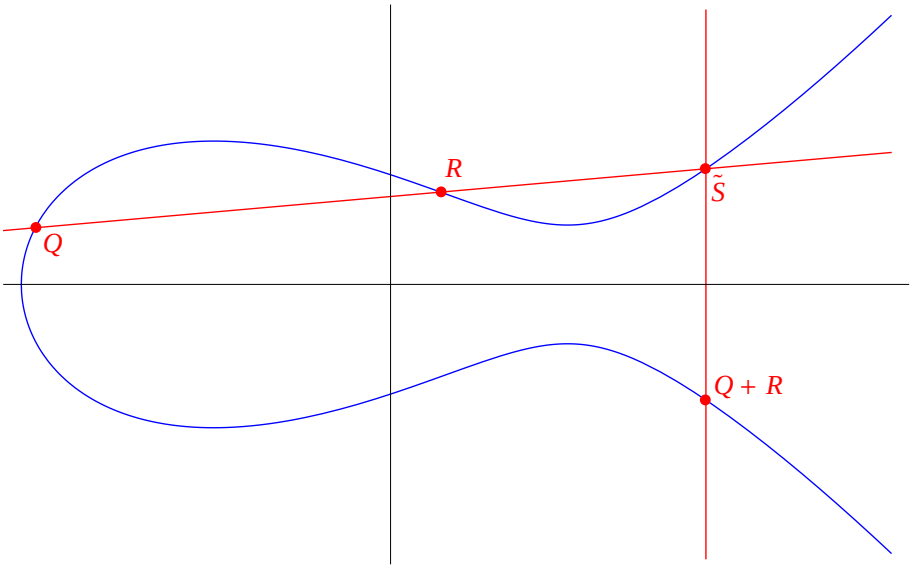

FIGURE 2.1: The Group Law on an Elliptic Curve

One can define an operation that gives a group structure to the points on an elliptic curve: Intuitively, if Q and R are two points on the elliptic curve, then there is a unique third point $\tilde{S}$ which is the intersection of the elliptic curve with a line going through Q and R. Further, there is a unique vertical line λ going through $\tilde{S}$. The other intersection of this line with the elliptic curve is the sum $Q \boxplus R$ of Q and R in the elliptic curve. This construction is depicted in figure 2.1.

More precisely, let the two points $Q = (1, x_Q, y_Q)$ and $R = (1, x_R, y_R)$ be on the elliptic curve in the $w = 1$ patch of $\mathbb{P}_{[1,2,3]}$. Then, their sum $S = Q \boxplus R = (1, x_S, y_S)$ is defined such that $(1, x_S, -y_S)$ is the third intersection of the elliptic curve with the line going through Q and R.

The sum $Q \boxplus Q$ is defined by taking the other intersection point of the elliptic curve with the line tangent to the curve at Q. The single point of the elliptic curve that is not in the $w = 1$ patch is the rational point P, and we define $P \boxplus Q = Q$ for all points Q.

Furthermore, the rational points of the elliptic curve — that is, the solutions of its Weierstraß equation with K-rational coefficients — form a subgroup under $\boxplus$, and one can show [74–76] the

Mordell-Weil theorem: Let $\mathbb{E}$ be an elliptic curve defined over some field K. Then, the group $\mathbb{E}(K)$ of rational points on $\mathbb{E}$ together with the operation $\boxplus$ is a finitely generated abelian group.

According to the fundamental theorem of finitely generated abelian groups [77], any such group A can be written as

$$A = \mathbb{Z} \oplus \cdots \oplus \mathbb{Z} \oplus A_T \,, \tag{2.2.2}$$

where A_T is the torsion subgroup of finite order. If $\sigma_1, \ldots, \sigma_r$ are a minimal set of rational points spanning the non-torsion part of the Mordell-Weil group, then r is defined to be the Mordell-Weil rank of the elliptic curve.

To generalize the notion of the Mordell-Weil group to elliptic fibrations, recall that an elliptic fibration is an elliptic curve over the ring of sections of line bundles on the base B. The rational points of this curve thus consist of solutions to its Weierstraß equation whose coefficients are K-rational in the quotient field of the ring of sections.

Therefore, the rational sections of an elliptic fibration are the rational points of the elliptic curve over the sections of B. Another way of thinking of rational sections is to find them fiberwise, since they must map to the rational points of each generic fiber in a continuous way. These two definitions agree [78]. Also note that the holomorphic section σ is a rational section (since given by the point $[0:1:1]$ in the generic fiber), but rational sections need not be holomorphic.

According to the Mordell-Weil theorem, the rational sections of an elliptic fibration therefore form a finitely generated abelian group. This group is also called the Mordell-Weil group of the elliptic fibration.

As the marked point of the Weierstraß model plays the role of the origin under $\boxplus$, it does not generate any non-trivial part of the Mordell-Weil group. To obtain a Mordell-Weil group of rank 1, we therefore need fibers which are elliptic curves with a second rational point. Such elliptic curves can be constructed as quartic hypersurfaces in $\mathbb{P}_{[1,1,2]}$, again using the Riemann-Roch theorem in a way similar to the one we employed in section 2.1 to find the Weierstraß form:

Start with an elliptic curve over a field K with two rational points P and Q, and consider sections of the line bundle $\mathcal{L} = \mathcal{O}(P+Q)$. Since $\mathcal{L}$ is a degree two line bundle, $H^0(\mathcal{L})$ is generated by two sections, and we will call them w and x. $H^0(2\mathcal{L})$ is spanned by four sections, three of which are w^2, wx, and x^2, and the fourth we will call y. $H^0(3\mathcal{L})$ has the six sections w^3, w^2x, wx^2, x^3, wy, and xy. Finally, there are nine sections generating $H^0(4\mathcal{L})$: y^2, yx^2, yxw, yw^2, x^4, x^3w, x^2w^2, xw^3, and w^4. But there should only be eight. One therefore has the relation (again arguing that the y^2-coefficient is a unit in the

underlying ring, and finding new coordinates to scale it to 1):

$$y^2 + b_0 y x^2 + b_1 y w x + b_2 y w^2 = c_0 w^4 + c_1 w^3 x + c_2 w^2 x^2 + c_3 w x^3 + c_4 x^4 \,. \tag{2.2.3}$$

Similar to before, we can now consider w, x and y as homogeneous coordinates of $\mathbb{P}_{[1,1,2]}$ with weights 1, 1, and 2 respectively. Let us further pick the sections w and x of $H^0(\mathcal{L})$ such that w vanishes exactly at P and Q. The relation above then is, for $w = 0$, given by

$$y^2 + b_0 y x^2 = c_4 x^4 \,. \tag{2.2.4}$$

Since P and Q are rational points in the field K, this quadratic equation in y must factor, which happens if and only if its discriminant $b_0^2 + 4c_4$ is a perfect square. That is, there must be a section $\tilde{b}_0 \in R$ such that $b_0^2 + 4c_4 = \tilde{b}_0^2$. If this is the case, the coordinate shift $y \to y + (\tilde{b}_0/2)x^2$ eliminates the c_4-term from the main relation, and we are left with the equation

$$y^2 + b_0 y x^2 + b_1 y w x + b_2 y w^2 = c_0 w^4 + c_1 w^3 x + c_2 w^2 x^2 + c_3 w x^3 \tag{2.2.5}$$

for a generic elliptic curve with rank 1 Mordell-Weil group. Its two rational points are located at $[0:1:0]$ and $[0:1:-b_0]$. A similar construction also exists — and is given for instance in [79, 80] — for elliptic curves with Mordell-Weil rank 2. Such curves can be represented as cubic polynomials in $\mathbb{P}^2$.

Like the curves embedded as sextics in $\mathbb{P}_{[1,2,3]}$, one can promote the elliptic curves realized as quartics in $\mathbb{P}_{[1,1,2]}$ to elliptic fibrations, by an appropriate embedding into an ambient space X. We will discuss this embedding in detail in section 5.1.7.

2.3 Singular Elliptic Fibrations and their Resolutions

As we shall see, 7-branes in F-theory and the non-abelian gauge theories they host are realized as loci where the complex structure of the elliptic fiber, and with it the string coupling constant, degenerates. These are given by the singular loci of the elliptic fibration. In this section, we develop the notion of singular loci of algebraic varieties and techniques to study them. These will allow us in the next section to completely classify singularities of elliptic fibrations, as well as construct normal forms for them. In section 3.2, we will then map this classification into a classification of non-abelian gauge groups of their associated F-theory models.

A singular point of an algebraic variety V is a point at which the tangent space of V degenerates. Specifically for a hypersurface $F(x, y, z, \dots) = 0$, the singular points are those where all partial derivatives of F vanish.

For an elliptic curve described by a Weierstraß equation P_W, the tangent space degenerations are given when $\mathrm{d}P_W = 0$. First, consider the coordinate patch of $\mathbb{P}_{[1,2,3]}$ where w does not vanish, and use the scaling relation to set $w = 1$. The remaining coordinates are x and y, and they are not related by a scaling relation anymore. For brevity, we will call this the $w = 1$ patch, and define the $x = 1$ patch and the $y = 1$ patch analogously. Here, $P_W = \mathrm{d}P_W = 0$ reads

$$\begin{aligned} \partial_y P_W &= 2y = 0 \\ P_W = x^3 + fx + g &= (x-a)(x-b)(x-c) = 0 \\ \partial_x P_W &= (x-a)(x-b) + (x-a)(x-c) + (x-b)(x-c) = 0\,, \end{aligned} \tag{2.3.1}$$

with a, b and c defined in the second line as the roots of $P_W = 0$. The three equations of 2.3.1 are all fulfilled when two or three of the roots coincide, i.e. whenever $(a-b)(a-c)(b-c) = 0$. This happens if and only if the discriminant Δ vanishes:

$$\Delta = 4f^3 + 27g^2 = 0\,. \tag{2.3.2}$$

One can perform a similar analysis for the other two coordinate patches $x = 1$ and $y = 1$: Note that the only locus in $\mathbb{P}_{[1,2,3]}$ that is not contained within the $w = 1$ coordinate patch is the locus where $w = 0$. The Weierstraß equation (2.1.5) here reduces to $y^2 = x^3$. Since either x or y have to be non-vanishing on the $w = 0$ locus, the Weierstraß equation is only fulfilled at the point $[0:1:1]$. Here however one has $\partial_y P_W = 2y = 1$, and the elliptic curve cannot be singular. All singularities of the curve are therefore located within the $w = 1$ coordinate patch.

Generalizing to elliptic fibrations, the parameters f and g are sections of line bundles on the base manifold B, and their values depend on the points of B. The same then goes for Δ, via (2.3.2): the discriminant here is promoted to be a section of some line bundle as well, and it will take on different values over different base loci. For example, in the Weierstraß model described in section 2.1 with $f \in H^0\left(\mathcal{O}(4c_1)\right)$ and $g \in \left(\mathcal{O}(6c_1)\right)$, one has $\Delta = \mathcal{O}(12c_1)$. Such a section generically vanishes over a codimension 1 sublocus of B. Over this sublocus, the elliptic fibration is singular. It is not clear at this point what the fibers of an elliptic fibration on $\Delta = 0$ are – if they are not a nonsingular elliptic curve, what are they then? Can singular elliptic fibers be classified, and how?

To answer this question, one introduces the notion of resolving singularities. A resolution of an algebraic variety X consists of a new non-singular space $\tilde{X}$, the resolved space, together with a proper[3] birational[4] map $\pi : \tilde{X} \to X$ that satisfies two properties: π is surjective and π is bijective for all points outside of the singular sublocus $Z \subset X$. Furthermore, if $c_1(\tilde{X}) = c_1(X)$, the resolution is denoted as crepant.

One can often construct crepant resolutions of singular varieties by first embedding the singular variety into a larger ambient variety W — as we have already done for elliptic fibrations — and then repeatedly performing so-called *blow-ups* on certain subvarieties of W, thus obtaining a new ambient variety $\tilde{W}$ of which $\tilde{X}$ is a subspace. Note that the blow-ups need not necessarily occur (only) at the singular subvarieties of X.

A standard example of a blow-up is given by blowing up $\mathbb{P}^2$ in a point: Let $\mathbb{P}^2$ be parametrized by homogeneous coordinates $[w : x : y]$, and let Z be the single point $[0 : 1 : 0]$. That is, Z is described by the two polynomials $w = 0$ and $y = 0$. This locus is blown up by introducing a new space that consists of the already present $\mathbb{P}^2$, a new coordinate ζ, a new $\mathbb{P}^1$ with homogeneous projective coordinates $\tilde{w}$ and $\tilde{y}$, and the coordinate relations

$$w = \zeta\tilde{w}\,, \qquad y = \zeta\tilde{y}\,. \tag{2.3.3}$$

Since $\tilde{w}$ and $\tilde{y}$ cannot vanish together, the locus Z is now described precisely by $\zeta = 0$. Away from Z, there is a 1-to-1 mapping between the old coordinates w, x, y, and the new coordinates $\tilde{w}$, x, $\tilde{y}$, and ζ, due to the relations above. In other words, if $\zeta \neq 0$, the relations fix a single point on the new $\mathbb{P}^1$ for every point on $\mathbb{P}^2 \backslash Z$. However, on Z, one has $\zeta = 0$, and the relations are automatically fulfilled. Therefore, every point on Z is the image of the whole new $\mathbb{P}^1$ under the blow-up map π. In fact, $\zeta = 0$ is a new divisor of the resolved algebraic variety, independent of the divisor σ associated to the hyperplane bundle $\mathcal{O}(H)$ of $\mathbb{P}^2$. Such a divisor E has negative self-intersection and therefore is an exceptional divisor. Furthermore, the divisor classes of the new coordinates are $[\tilde{w}] = [\tilde{y}] = \sigma - E$, and the total Chern class of $\tilde{X}$ is given by

$$c(\tilde{X}) = (1 + [\tilde{w}])\,(1 + [x])\,(1 + [\tilde{y}])\,(1 + [\zeta]) = 1 + 3\sigma - 2E + \cdots\,, \tag{2.3.4}$$

with the dots denoting higher-rank forms, and therefore differs from the Chern class of X.

[3] Roughly speaking, a proper morphism is a map with compact inverse images of compact sets. This criterion is required to exclude trivial solutions, such as letting $\tilde{X}$ be the subvariety of non-singular points of X.

[4] To algebraic varieties are birationally equivalent if they have open subsets in their Zariski topology which are isomorphic. The isomorphism is called a birational map.

One also can blow up points on an elliptic curve or fibration $\mathbb{E}$ embedded in an ambient space X, and usually does so by blowing up a sublocus Z in the ambient space which contains the points. The elliptic curve in the resolved space away from the blow-up locus is simply given as the preimage of the elliptic curve in the unresolved space under the blow-up map π – recall that π is bijective away from Z. There are two ways of defining the elliptic curve in the resolved space of Z, namely the total transform and the proper transform. The total transform again is the preimage of Z under the blow-up locus, and therefore contains the entire exceptional divisor. The proper transform is the closure of $\pi^{-1}(\mathbb{E}\backslash Z)$ in $\tilde{X}$, and its normal bundle in $\tilde{X}$ generically differs from the normal bundle of $\mathbb{E}$ in X. Note that the procedure described in this paragraph generalizes to arbitrary algebraic varieties, not just elliptic curves.

As a simple example, consider the cubic hypersurface

$$Y: \qquad y^3 + xw^2 = 0 \tag{2.3.5}$$

in $\mathbb{P}^2$ with homogeneous coordinates w, x, and y as above. Note that the divisor class of Y is 3σ, since its terms are sections of $\mathcal{O}(3H)$. Now blow up the point $[0:1:0]$, also as above. Naively replacing w and y by their new coordinates yields

$$Y_{\text{tot}}: \qquad \tilde{y}^3\zeta^3 + x\tilde{w}^2\zeta^2 = \zeta^2\left(\tilde{y}^3\zeta + x\tilde{w}^2\right) = 0\,. \tag{2.3.6}$$

This object is called the total transform of Y. One observes that Y_{tot} is reducible, and furthermore that its class is identical to the class of Y. Its first Chern class is now non-vanishing:

$$c(Y_{\text{tot}}) = \frac{c(\tilde{X})}{1+[Y_{\text{tot}}]}\bigg|_{Y_{\text{tot}}} = (1+3\sigma-2E) - (1+3\sigma) + \cdots = 1 - 2E + \cdots\,, \tag{2.3.7}$$

and the hypersurface defined by Y_{tot} therefore is not Calabi-Yau. In other words, blowing up Y into Y_{tot} is not crepant.

In order to find a crepant resolution which results in another Calabi-Yau hypersurface, one has to take the proper transform $\tilde{Y}$, which is identified with the non-trivial irreducible component of Y_{tot}:

$$\tilde{Y}: \qquad \tilde{y}^3\zeta + x\tilde{w}^2 = 0\,. \tag{2.3.8}$$

From the relations between the untilded and the tilded coordinates, one finds $[\tilde{w}] = [w] - [\zeta] = \sigma - E$ and $[\tilde{y}] = [y] - [\zeta] = \sigma - E$, with E the exceptional divisor $\zeta = 0$. The

class of $\tilde{Y}$ is different from the class of Y:

$$[\tilde{Y}] = 3\sigma - 2E = [Y] - 2E\,. \tag{2.3.9}$$

One can check that the resolution defined in this way is crepant, since

$$c(\tilde{Y}) = \frac{c(\tilde{X})}{1+[\tilde{Y}]}\bigg|_{\tilde{Y}} = (1+3\sigma-2E) - (3\sigma-2E) + \cdots = 1 + \cdots\,, \tag{2.3.10}$$

and therefore

$$c_1(\tilde{Y}) = c_1(Y) = 0\,. \tag{2.3.11}$$

Taking the proper instead of the total transform preserves the first Chern class — and thus the Calabi-Yau property — of an algebraic variety also in general.

This example also shows how one can desingularize algebraic varieties by performing sequences of blow-ups. Before the blow-up, our toy algebraic variety (2.3.5) is singular at $[0:1:0]$, since its w- and y-derivatives at this point vanish. However, after performing the blow-up, (2.3.8) is regular everywhere: $\tilde{Y}$ intersects the divisor $\zeta = 0$ over the formerly singular locus in the two points $\tilde{w} = 0$ and $\tilde{y} = 0$. Both these points are in the inhomogeneous coordinate patch $x = 1$ of the original $\mathbb{P}^2$, and they are also in the patch $\tilde{y} = 1$ and $\tilde{w} = 1$ of the new exceptional $\mathbb{P}^1$, respectively. Thus, for $\tilde{w} = 0$ the $\tilde{w}$-derivative is non-vanishing, and for $\tilde{y} = 0$ the $\tilde{y}$-derivative is non-vanishing.

Another example resolution, where a space containing a singular elliptic curve is blown up at the point where the curve is singular, is shown in figure 2.2. Note that the resolved space maps surjectively onto the unresolved space, and away from the blow-up locus, the mapping indeed is bijective. Also, the blow-up did introduce a new exceptional divisor at $\pi^{-1}(Z)$, as expected from the general case. The total transform of the singular curve is given by the union of the red and blue lines in the resolved space, whereas the proper transform includes only the red line.

One is often interested in computing intersections between divisors of algebraic varieties, for instance in the classification of the singular fibers in section 2.4. Such calculations can be done by using two technical results. The first is

Bézout's theorem in weighted projective space: [81, 82] Let $a = 0$ and $b = 0$ be two curves in weighted projective space $\mathbb{P}_{[w_1,w_2,w_3]}$, with hyperplane class σ and $[a] = A\sigma$, $[b] = B\sigma$. The intersection number between a and b is then given by

$$\frac{A \cdot B}{w_1 w_2 w_3}\,. \tag{2.3.12}$$

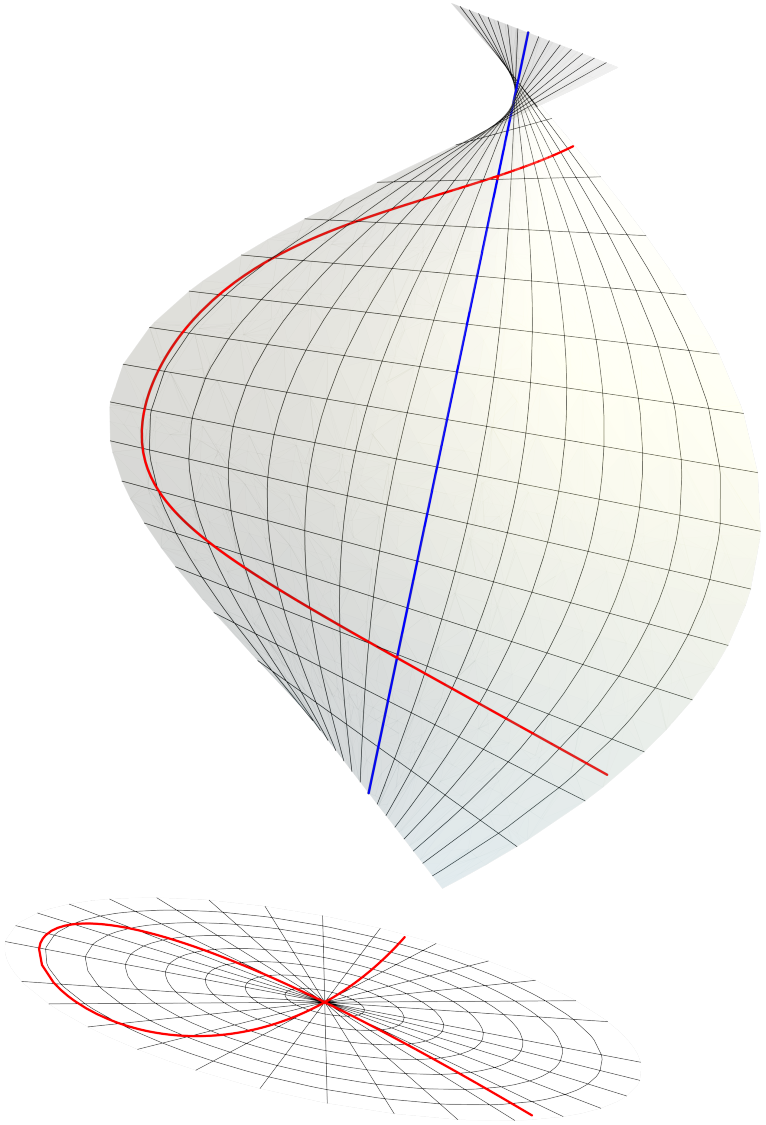

FIGURE 2.2: An elliptic curve (red) in $\mathbb{R}^2$ with a singularity. Above it, a resolution of $\mathbb{R}^2$ at the singular locus of the curve, the proper transform of the elliptic curve (red), and the new exceptional divisor introduced after resolution (blue).

The second fact relevant for intersection computations allows us to take care of the exceptional divisors introduced by resolutions, by using their

projective relations: Since the homogeneous coordinates of some (possibly weighted) projective space cannot vanish simultaneously, their divisor classes have intersection number zero. Specifically, the exceptional $\mathbb{P}^d$s with exceptional divisor E introduced by blowing up have coordinates which are sections of line bundles of the form $\mathcal{O}(D-E)$. Setting the product of their divisor classes to zero yields a relation of the form

$$E^d = \sum_{k=0}^{d-1} D^{d-k} E^k \,, \tag{2.3.13}$$

which we can use to replace any power of E greater than E^{d-1} by a collection of terms with lower powers of E.

However, any term of the form $D \cdot E^k$ with $0 < k < d$ has to vanish, since the exceptional divisor does not intersect any subvariety of the total space X with codimension greater than $n - d$. Combining these two facts allows us to reduce all intersections involving powers of E to either zero, or to intersections not involving E.

Applying Bézout's theorem to the elliptic fibrations in chapters 4 and 5, we find that intersections in the total space of the $\mathbb{P}^2$-embedding of Weierstraß forms for chapter 4 are only non-vanishing if they are of the form

$$\sigma^2 \cdot D_1 \cdot D_2 \cdot D_3 \,, \tag{2.3.14}$$

with D_i being divisors of B, and their value is given by the intersection $D_1 \cdot_B D_2 \cdot_B D_3$ in the base B. The same holds for the intersections of the $\mathbb{P}_{[1,1,2]}$-embedding used in chapter 5. However, in the latter case, all results have to be divided by a factor of two coming from the weight product in $\mathbb{P}_{[1,1,2]}$ via (2.3.12).

In practice, calculating resolutions and intersections of elliptic fibrations can be automated, and many results in this thesis have been computed using `Smooth` [83], a Mathematica package currently in development for precisely this purpose.

2.4 The Kodaira-Néron Classification of Singular Fibers and Tate's Algorithm

We are now able to describe the classifaction of singular fibers of an elliptic fibration. The classification was first given by Kodaira and Néron [84–86] for elliptic surfaces, that is, elliptic fibrations over a one-dimensional base. Up to a few subtleties, it generalizes codimension 1 for elliptic fibrations over higher-dimensional base manifolds.

One starts with an elliptic fibration in Weierstraß form

$$y^2 = x^3 + fx + g \tag{2.4.1}$$

and a codimension 1 sublocus S on the base manifold over which the fiber is singular, described by the vanishing of some coordinate $z = 0$. A finite sequence of crepant resolutions over S desingularizes the elliptic fibration, and also produces a set of exceptional

$\mathbb{P}^1$s, as seen in the previous section. Kodaira and Néron showed that the intersection matrix of the exceptional divisors, together with the proper transform of $z = 0$, must be negative semidefinite, connected, symmetric, and have no diagonal entries equal to -1.[5] The matrices satisfying this set of conditions are precisely the $\mathbf{0}$ matrix and the Cartan matrices of the affine simply-laced Dynkin diagrams. Correspondingly, the exceptional divisors of the fibration introduced by resolving the singularity are called Cartan divisors in the literature.

The fiber of an elliptic fibration over a singular locus S therefore consists of a set of $\mathbb{P}^1$s intersecting like an ADE-type affine Dynkin diagram. Apart from three special cases, different affine Dynkin diagrams uniquely correspond to different Kodaira fiber types, and the first few fiber types with their intersection structure are shown in table 2.2. The special cases are:

- If the intersection matrix is the $\mathbf{0}$ matrix, the fiber is either a non-singular elliptic curve (with Kodaira type I_0), a curve with a double point (Kodaira type I_1, this is the singular curve of figure 2.2), or a cusp (Kodaira type II).
- If the intersection matrix is the matrix corresponding to the $\tilde{A}_1$ Dynkin diagram, the fiber consists of two components with intersection number 2. The two intersections can either be in two distinct points, corresponding to Kodaira type I_2, or in a single multiplicity two point, with Kodaira type III (cf. table 2.2).
- If the intersection matrix is the matrix corresponding to the $\tilde{A}_2$ Dynkin diagram, the fiber consists of three components with intersections between each pair. The three intersections can either be in three distinct points (Kodaira type I_3) or in a single point (Kodaira type IV, again cf. table 2.2).

It was also shown in [84–86] that the Kodaira type of the fibration over S can be determined by expanding f, g and the discriminant Δ in z,

$$\begin{aligned} f &= \sum_i f_i z^i \\ g &= \sum_i g_i z^i \\ \Delta &= \sum_i \Delta_i z^i \,, \end{aligned} \tag{2.4.2}$$

[5] The last condition comes from demanding the elliptic fibration to be relatively minimal. That is, one asserts that there are no -1-curves in the fibers of $\mathbb{E}$. If there are such curves, one sits in the last, 'non-minimal' row of the Kodaira table 2.1. F-theory models with non-minimal loci involve light strings in their low-energy spectrum [87] and are therefore not very relevant for string phenomenology.

Fiber type	dual diagram	$\mathrm{ord}_S(f)$	$\mathrm{ord}_S(g)$	$\mathrm{ord}_S(\Delta)$
I_0	$\mathbf{0}$	≥ 0	≥ 0	0
I_1	$\mathbf{0}$	0	0	1
$I_{m\geq 2}$	$\tilde{A}_m$	0	0	m
II	$\mathbf{0}$	≥ 1	1	2
III	$\tilde{A}_2$	1	≥ 2	3
IV	$\tilde{A}_3$	≥ 2	2	4
I_0^*	$\tilde{D}_4$	≥ 2	≥ 3	6
$I_{m\geq 1}^*$	$\tilde{D}_{m+4}$	2	3	$m+6$
IV^*	$\tilde{E}_6$	≥ 3	4	8
III^*	$\tilde{E}_7$	3	≥ 5	9
II^*	$\tilde{E}_8$	≥ 4	5	10
non-min	—	≥ 4	≥ 6	≥ 12

TABLE 2.1: Kodaira's classification of singular fibers.

and comparing the vanishing orders of f, g and Δ on S to the entries in table 2.1. Finally, the section σ_0 of the Weierstraß form always intersects the affine curve of the affine Dynkin diagram. We will see a more general version of this fact in section 5.1.3.

While Kodaira and Néron classified the singular fibers, they did not give an explicit way to construct an elliptic surface with a section and a given fiber type, i.e. a way to find sections f and g such that f, g and the discriminant Δ vanish to the desired orders on S. An algorithm to do so was first provided by Tate [88], and later reexamined with a view towards elliptic fibrations over higher-dimensional base varieties and F-theory [1, 89].

Starting with an elliptic fibration with a singularity of a given Kodaira type over a base divisor $z = 0$, the goal of Tate's algorithm is to provide a so-called Tate form that explicitly realizes the fibration. The Tate form can be viewed as an extension of the Weierstraß form, with defining hypersurface equation in the $w = 1$ patch of $\mathbb{P}_{[1,2,3]}$ being

$$y^2 + a_1xy + a_3y = x^3 + a_2x^2 + a_4x + a_6\,. \tag{2.4.3}$$

Tate's algorithm essentially provides a set of vanishing orders i_j of the coefficients a_j of the fibration over the locus $z = 0$. That is, it guarantees that one can always write the a_j as

$$a_j = \sum_{k=i_j}^{\infty} a_{j,k} z^k\,, \tag{2.4.4}$$

where the coefficient sections $a_{j,k}$ do not depend on z and are otherwise generic. In most cases, there is a distinct set of vanishing orders for each Kodaira fiber type, and the vanishing orders are tabularized in table 2.3.

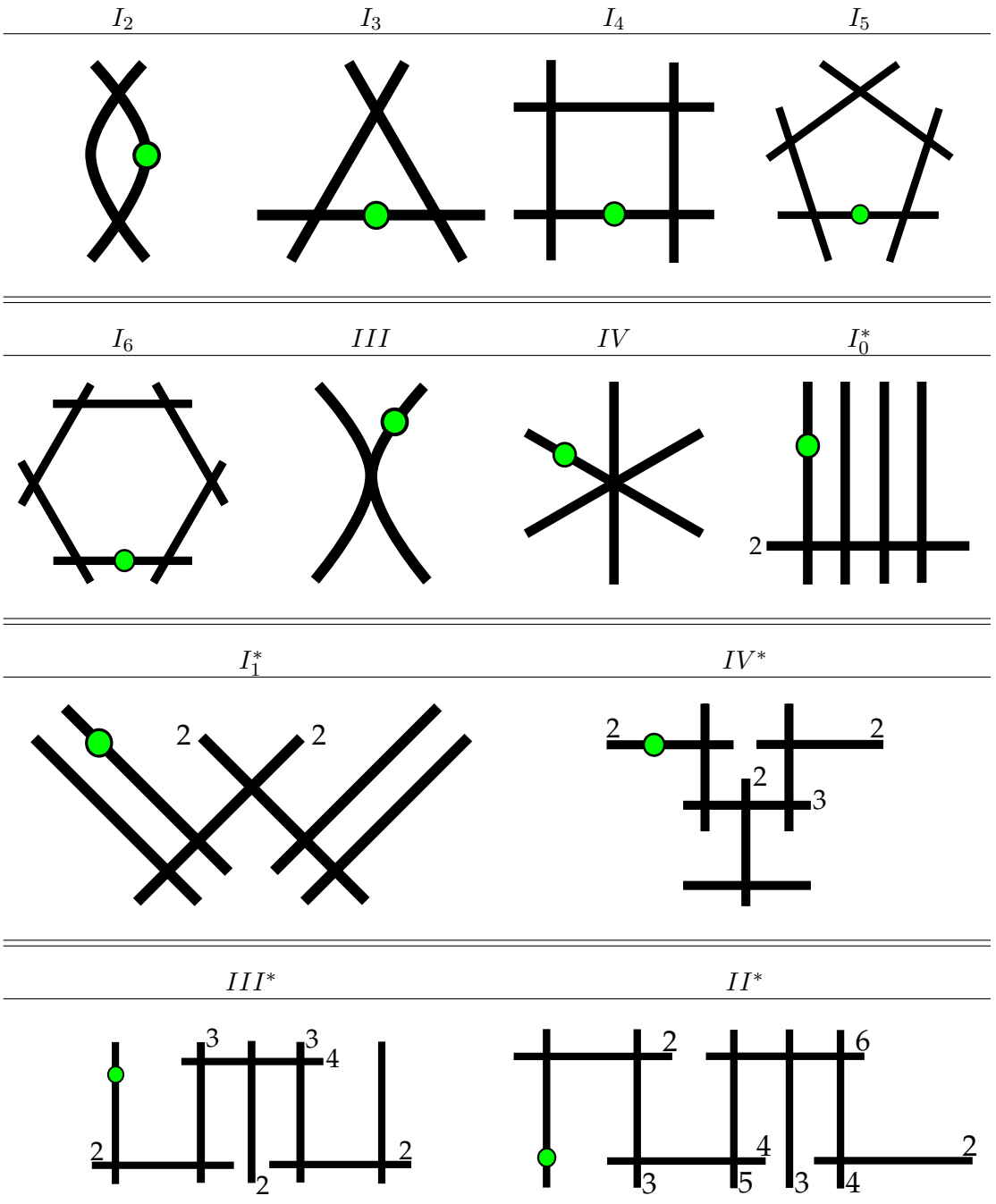

TABLE 2.2: Schematic depictions of the Kodaira fiber types at the beginning of the infinite list of fiber types. Every line represents a $\mathbb{P}^1$ of the singular fiber, and every intersection of lines an intersection of the corresponding $\mathbb{P}^1$s. The intersection patterns reproduce the dual extended Dynkin diagrams of the ADE Lie algebras. The section of the Weierstraß form, shown with a green node, always intersects the affine node of the affine dual Dynkin diagram. Numbers next to the black lines indicate the multiplicity of corresponding fiber components, with no number corresponding to multiplicity 1 curves.

Fiber type	group	a_1	a_2	a_3	a_4	a_6	Δ
I_0	—	0	0	0	0	0	0
I_1	—	0	0	1	1	1	1
I_2	$SU(2)$	0	0	1	1	2	2
I_3^{ns}	$Sp(1)$	0	0	2	2	3	3
I_3^{s}	$SU(3)$	0	1	1	2	3	3
I_{2n}^{ns}	$Sp(n)$	0	0	n	n	$2n$	$2n$
I_{2n}^{s}	$SU(2n)$	0	1	n	n	$2n$	$2n$
I_{2n+1}^{ns}	$Sp(n)$	0	0	n	$n+1$	$2n+1$	$2n+1$
I_{2n+1}^{s}	$SU(2n+1)$	0	1	n	$n+1$	$2n+1$	$2n+1$
II	—	1	1	1	1	1	2
III	$SU(2)$	1	1	1	1	2	3
IV^{ns}	$Sp(1)$	1	1	1	2	2	4
IV^{s}	$SU(3)$	1	1	1	2	3	4
I_0^{*ns}	G_2	1	1	2	2	3	6
I_0^{*ss}	$SO(7)$	1	1	2	2	4	6
I_0^{*s}	$SO(8)^*$	1	1	2	2	4	6
I_1^{*ns}	$SO(9)$	1	1	2	3	4	7
I_1^{*s}	$SO(10)$	1	1	2	3	5	7
I_2^{*ns}	$SO(11)$	1	1	3	3	5	8
I_2^{*s}	$SO(12)^*$	1	1	3	3	5	8
I_{2n-3}^{*ns}	$SO(4n+1)$	1	1	n	$n+1$	$2n$	$2n+3$
I_{2n-3}^{*s}	$SO(4n+2)$	1	1	n	$n+1$	$2n+1$	$2n+3$
I_{2n-2}^{*ns}	$SO(4n+3)$	1	1	$n+1$	$n+1$	$2n+1$	$2n+4$
I_{2n-2}^{*s}	$SO(4n+4)^*$	1	1	$n+1$	$n+1$	$2n+1$	$2n+4$
IV^{*ns}	F_4	1	2	2	3	4	8
IV^{*s}	E_6	1	2	2	3	5	8
III^*	E_7	1	2	3	3	5	9
II^*	E_8	1	2	3	4	5	10
non-min	—	1	2	3	4	6	12

TABLE 2.3: Tate forms for all fiber types of the Kodaira classification. The two gauge groups marked with * pose additional conditions on the sections a_i, cf. (2.4.5) and (2.4.6). Adopted from [1].

The new forms in table 2.3 compared to the Kodaira table 2.1 and their associated non-simply laced gauge groups are due to the additional subtlety arising for elliptic fibrations over higher-dimensional bases mentioned earlier: Consider an elliptic fibration over a base manifold parametrized by z_1 and z_2, with a singular fiber over $z_1 = 0$, and resolve the singularity. As discussed, over any point of z_2 the fibers will intersect like in an affine ADE-type Dynkin diagram. However, if one goes over a non-trivial cycle in z_2 while staying on $z_1 = 0$, the fiber components may undergo monodromy [89]. The monodromy can exchange some of the components according to an outer automorphism of the affine Dynkin diagram, and if this is the case, the Lie group actually corresponding to the singular fiber will be a subgroup of the group described by the diagram. These cases are denoted as *non-split* or *ns* cases in the literature, while the cases where the fiber components are not exchanged are called *split* or *s* cases. The conditions distinguishing between non-split and split cases are also found by Tate's Algorithm and yield the entries in the table.

In the two special cases of I_0^{*s} and I_{2n-2}^{*s}, there are additional conditions on the coefficients in the Tate equation: for I_0^{*s}, one requires that

$$\left.\frac{a_2^2 - 4a_4}{z^4}\right|_{z=0} \tag{2.4.5}$$

is a perfect square in the ring of sections R over which the fibration is defined, that is, that there is a section $\tilde{a} \in R$ whose square equals the expression above. For I_{2n-2}^{*s}, the perfect square condition is

$$\left.\frac{a_4^2 - 4a_2a_6}{z^{2n+2}}\right|_{z=0} . \tag{2.4.6}$$

Furthermore, most of the Kodaira types found in table 2.3 are generic, in that any elliptic fibration of a given Kodaira type can be brought into the form specified in the table entry by coordinate shift. This has been discussed in [1], along with the edge cases where such a coordinate shift is not possible. We will revisit and extend this discussion in section 5.6.

To find the coefficient vanishing orders displayed in the table, one has to run Tate's algorithm. The algorithm systematically enhances the vanishing of the discriminant order by order, and derives constraints on the sections f and g of the Weierstraß equation from these enhancements. It then performs a set of coordinate changes that bring the fibration into Tate form. A detailed discussion can again be found in [1], but in order to provide some intuition, we trace out the first few steps. Start with a Weierstraß equation in the $w = 1$ patch of the ambient space X,

$$y^2 = x^3 + fx + g\,, \tag{2.4.7}$$

and expand the coefficients f and g as a power series in z:

$$f = \sum_i f_i z^i\,, \qquad g = \sum_i g_i z^i\,. \tag{2.4.8}$$

The discriminant of the fibration then reads

$$\Delta = 4f^3 + 27g^2 = \left(4f_0^3 + 27g_0^2\right) + \left(12f_1f_0^2 + 54g_0g_1\right) z + O(z^2)\,. \tag{2.4.9}$$

A necessary condition to have nonzero discriminant vanishing order therefore is the existence of a function u_0 such that

$$f_0 = -\frac{1}{3}u_0^2\,, \qquad g_0 = \frac{2}{27}u_0^3\,. \tag{2.4.10}$$

If this condition is fulfilled, the change of coordinates

$$x \to x + \frac{1}{3}u_0 w \tag{2.4.11}$$

transforms the Weierstraß equation above into

$$y^2 = x^3 + u_0 x^2 + \left(f_1 z + f_2 z^2 + \cdots\right) x + \left(\left(g_1 + \frac{1}{3}u_0 f_1\right) z + \left(g_2 + \frac{1}{3}u_0 f_2\right) z^2 + \cdots\right) . \tag{2.4.12}$$

This is the Tate form from the table for fiber type I_1, with the coefficient sections a_4 and a_6 vanishing to linear order in z. To proceed, one would (for notational simplicity) define $\tilde{g}_j = g_j + \frac{1}{3}u_0 f_j$, and write the equation as

$$y^2 = x^3 + u_0 x^2 + \left(f_1 z + f_2 z^2 + \cdots\right) x + \left(\tilde{g}_1 z + \tilde{g}_2 z^2 + \cdots\right) . \tag{2.4.13}$$

The discriminant of this equation is at leading order given by

$$\Delta = 4u_0^3 \tilde{g}_1 z + O(z^2) , \tag{2.4.14}$$

and if either $u_0 = 0$ or $\tilde{g}_1 = 0$, the vanishing order of the discriminant further enhances and the fiber type changes again. Specifically, for $u_0 = 0$, one obtains a type II fiber, and for $\tilde{g}_1 = 0$, one has an I_2 fiber. Repeating this process for each order of the discriminant power series in z, one obtains all the fiber types listed in table 2.3.

There is a two-fold benefit to Tate's algorithm. One the one hand, it provides one with a standard form for each Kodaira type, allowing for the construction of models with any given singularity structure from these building blocks. On the other hand, these standard forms are very generic, in that — up to a few exceptions, which have been found in [1] and which we will discuss in more detail in section 5.6 — each elliptic fibration with a given Kodaira fiber type can be brought into its associated Tate form at least locally near the singular locus. Therefore, studying Tate forms amounts to studying singular fibrations in general.

In chapter 5, we will apply Tate's algorithm to elliptic fibrations with Mordell-Weil group of rank 1 whose fibers are represented as quartic hypersurfaces in $\mathbb{P}_{[1,1,2]}$. This will allow us to study generic elliptic fibrations with Mordell-Weil rank 1, and in doing so to extract information about generic F-theory compactifications with an additional $U(1)$ gauge factor.

Chapter 3

F-theory and Geometric Engineering

In this chapter, we can now give a more formal introduction into F-theory, with the aim of providing enough context to render the subsequent chapters self-contained.

Following the idea of translating physical objects into geometric ones, we will see how a faithful implementation of 7-branes and their backreaction onto a compactification manifold in type IIB string theory necessarily leads to considering elliptic fibrations over the manifold, and that the locations of 7-branes are described by the singular loci of the fibration. Further, as we will see the Kodaira type of the fibration over a singular locus determines the local non-abelian gauge theory on the brane.

Then, we describe how further enhancements of the singularity in higher codimensions of a singular locus lead to localized matter multiplets transforming in non-trivial representations of the gauge theory on the brane, and to Yukawa couplings between such matter multiplets. We continue with abelian gauge factors in F-theory, which arise from the non-torsion part of the Mordell-Weil group of the elliptic fibration.

The section closes with an exposition of G-flux in F-theory, a discussion of how to use F-theory compactifications to engineer phenomenologically attractive models for particle physics, and a description of the spectral cover construction in the local approach to F-theory model building.[1]

[1] Complementary reviews of F-theory are for instance [90], or, focusing more on a model building context, [91].

3.1 Non-perturbative Type IIB String Theory with 7-Branes

Our first aim is to show how the backreaction of 7-branes onto the geometry of a type IIB compactification manifold naturally motivates the study elliptic fibrations over the manifold. Recall that the low-energy field content of type IIB string theory consists of the dilaton ϕ, the metric tensor g, the Kalb-Ramond 2-form B_2, and the R-R 0-, 2-, and 4-forms C_0, C_2, and C_4. The dilaton and the C_0-form, often called axion, are typically combined into the single axio-dilaton

$$\tau = C_0 + ie^{-\phi}\,. \tag{3.1.1}$$

The bosonic type IIB effective action then is [10]

$$S_{\text{IIB}} = \frac{2\pi}{l_s^8}\int \mathrm{d}^{10}x\sqrt{-g}\left[\mathcal{R} - \frac{\partial_M\tau\partial^M\bar{\tau}}{2\left(\text{Im}\tau\right)^2} - \frac{G_3\cdot\bar{G}_3}{12\text{Im}\tau} - \frac{\tilde{F}_5^2}{4\cdot 5!}\right] \tag{3.1.2}$$

in the Einstein frame (i.e. with canonically normalized Ricci scalar $\mathcal{R}$). We have used $F_{i+1} = \mathrm{d}C_i$, $H_3 = \mathrm{d}B_2$, $G_3 = F_3 - \tau H_3$, and $\tilde{F}_5 = F_5 - \frac{1}{2}C_2\wedge H_3 + \frac{1}{2}B_2\wedge F_3$. The effective action is supplemented by the self-duality condition $\tilde{F}_5 = \star\tilde{F}_5$ of the 5-form field strength, to be imposed on the equations of motion.

In the Einstein frame, the type IIB effective action (3.1.2) possesses an invariance under the $\text{SL}(2,\mathbb{R})$ symmetry

$$\tau \to \frac{a\tau+b}{c\tau+d}\,, \qquad \begin{pmatrix} C_2 \\ B_2 \end{pmatrix} \to \begin{pmatrix} a & b \\ c & d \end{pmatrix}\begin{pmatrix} C_2 \\ B_2 \end{pmatrix}, \qquad \begin{pmatrix} a & b \\ c & d \end{pmatrix} \in \text{SL}(2,\mathbb{R})\,. \tag{3.1.3}$$

Due to $D(-1)$-instanton effects, this classical symmetry is broken to $\text{SL}(2,\mathbb{Z})$ on the quantum level [10].

Gauge degrees of freedom in type IIB string theory compactifications arise from the open string sector, that is from strings ending on D7-branes in the compactification manifold B. Heuristically speaking, a Dp-brane in ten dimensions yields a source term in the other $9-p$ spatial directions. Thus, there should be a Poisson-type equation in the theory:

$$\Delta\Phi(r) \sim \delta(r) \qquad \Rightarrow \qquad \Phi(r) \sim \frac{1}{r^{7-p}}\,. \tag{3.1.4}$$

Therefore, the backreaction from a Dp-brane on the geometry should naively be negligible for sufficiently large r. However, as one can immediately see, this logic does not work for

$p = 7$, which is the case of interest in type IIB. Here, one expects Φ to scale logarithmically with a nowhere vanishing backreaction.

To make this statement more precise, one can find, from the effective actions of D7-branes in type IIB and the IIB effective action itself, that D7-branes act as source terms for the $F_9 = \star F_1$ field in the complex direction z normal to the brane:

$$\mathrm{d} \star F_9 = \delta(z - z_0) \qquad \Rightarrow 1 = \int_{\mathbb{C}} \mathrm{d} \star F_9 = \oint_{S^1} F_1 = \oint_{S^1} \mathrm{d}C_0 \,, \tag{3.1.5}$$

using Stokes' theorem and with S^1 encircling z_0 in the complex plane. The equation (3.1.5) is locally solved by

$$\tau(z) = \tau(z_0) + \frac{1}{2\pi i} \log(z - z_0) + \cdots \,. \tag{3.1.6}$$

Clearly, as one circles z around z_0 and crosses the logarithmic branch cut, the axio-dilaton undergoes a monodromy transformation

$$\tau \to \tau + 1 \,. \tag{3.1.7}$$

While worrying at first sight, this does not pose a problem, since it is precisely the monodromy action of an $\mathrm{SL}(2, \mathbb{Z})$ transformation from (3.1.3)! In fact, arguments similar to this one find the other monodromies of τ when encircling (p, q) 7-branes, that is, generalizations of D7-branes which have p units of C_2-charge and q units of B_2-charge.

The central idea of F-theory [65, 87, 92] is to identify the physical $\mathrm{SL}(2, \mathbb{Z})$ symmetry of the low-energy type IIB action with the geometric $\mathrm{SL}(2, \mathbb{Z})$ symmetry of a complex torus T^2, and thereby to identify the axio-dilaton τ with the complex structure of the T^2. Since complex tori are the only Calabi-Yau onefolds, and we have found in section 2.1 that elliptic curves are Calabi-Yau onefolds, it follows that we can describe complex tori as elliptic curves. The dependency of τ on the points of the compactification manifold B is modelled by making the complex structure of the torus point-dependent as well, or in other words, by fibering the elliptic curve over B.[2]

From now on, we will take τ to be the complex structure of an elliptic curve fibering B, thereby baking the $\mathrm{SL}(2, \mathbb{Z})$-structure encountered above into the geometry. From (3.1.6), τ diverges at the 7-brane positions, and diverging τ indicates a singularity in the fiber. Therefore, 7-branes (and their gauge degrees of freedom) will be located at the singular locus $\Delta = 0$ of the elliptic fibration.

[2] Strictly speaking, one only requires a genus-1 fibration over B to construct models in F-theory, without the existence of a section. Such compactifications have been studied in [93–95].

3.2 Non-abelian Gauge Symmetries from Kodaira fiber types and M/F-Duality

In the preceding section, it was discussed that the positions of 7-branes in an F-theory compactification are given by the singular loci $\Delta = 0$ of the elliptic fibration. In section 2.4, the singular fibers over such loci were classified using Kodaira fiber types (augmented with a split-/non-split distinction). A natural question to ask is whether the fiber types encode any information about the 7-brane physics, and the answer turns out to be positive: A brane sitting on a singularity with Kodaira type from the first column of table 2.3 accommodates a non-abelian gauge theory with non-abelian gauge factor given in the second column of the same table. For example, branes on I_n^s-singularities contain $SU(n)$ gauge theories.

One can understand this correspondence by approaching F-theory not as a generalization of perturbative type IIB string theory as in the previous section, but from its duality to M-theory, first described in [69]. A detailed discussion of M/F-duality can be found e.g. in [96].

The M/F-duality proceeds as follows:

- Start with M-theory compactified on a two-torus, with the complex structure of the torus $T^2 = S^1_A \times S^1_B$ being τ.
- Take the perturbative limit of M-theory to type IIA theory by letting the radius R_A of the circle S^1_A go to zero. In this limit, one has perturbative type IIA theory on S^1_B.
- T-dualize this theory along the other circle S^1_B, and obtain type IIB theory on $\tilde{S}^1_B$, with the circle $\tilde{S}^1_B$ having radius $\tilde{R}_B = \frac{1}{R_B}$. The type IIB string coupling $g_{s,\text{IIB}}$ is now proportional to $\text{Im}(\tau)$.

The duality can be extended to T^2- (or elliptic) fibrations over some base B by performing its steps fiberwise, thus obtaining a type IIB compactification with varying axio-dilaton. This construction effectively realizes the F-theory compactification on the elliptically fibered base B.

The decomposition of the M-theory 3-form potential C_3 in such a T^2-fibration yields the higher-rank type IIB R-R forms [97]. Let a and b be the coordinates along the two circles

S_A and S_B of the T^2 respectively, and reduce C_3 along it:

$$C_3 = \tilde{C}_3 + B_2 \wedge \mathrm{d}a + C_2 \wedge \mathrm{d}b + B_1 \wedge \mathrm{d}a \wedge \mathrm{d}b\,. \tag{3.2.1}$$

After T-dualizing to type IIB, C_2 turns into the R-R 2-form potential of IIB, B_2 is the Kalb-Ramond 2-form, and $\tilde{C}_3$ provides the degrees of freedom of $C_4 = \tilde{C}_3 \wedge \mathrm{d}b$. The transformation properties of C_2 and B_2 in (3.1.3) follow from the geometric transformations of S^1_A and S^1_B under the $\mathrm{SL}(2,\mathbb{Z})$-action of the T^2.

We have seen in section 2.3 that resolving a singularity of an elliptic fibration inserts new $\mathbb{P}^1$s into the geometry, described by the vanishing loci $\zeta_i = 0$ of new coordinates ζ_i introduced by the resolution. Also recall from section 2.4 that the two-cycles $[\zeta_i]$ constituted the nodes of the affine Dynkin diagrams used in Kodaira's classification. As in (3.2.1), one can reduce the M-theory C_3 along those new cycles, and obtains new 1-forms $A_i = \int_{[\zeta_i]} C_3$ living on the 7-brane. Those 1-forms provide the gauge potential degrees of freedom for the factors in the Cartan subalgebra of the brane's gauge group. Furthermore, the $M2$-branes of M-theory can wrap chains of such 2-cycles $S_{ij} = [\zeta_i] \cup [\zeta_{i+1}] \cup \cdots \cup [\zeta_j]$, as long as ζ_k and ζ_{k+1} intersect for $k = i, \ldots, j-1$. The degrees of freedom arising from $M2$-branes along such chains become massless in the singular F-theory limit where the volume of the $\mathbb{P}^1$s vanishes and give the non-Cartan generators of the brane gauge group. Explicitly for 7-branes with $SU(n)$ gauge group, all cycles S_{ij} where $i < j$ are permitted, leading to $n(n-1)/2$ states arising from $M2$-branes wrapping the S_{ij}.

Therefore, one finds the gauge group of a 7-brane in F-theory by determining the Kodaira type of the singular 7-brane locus on B. This can be done by either directly resolving the singularity and computing the intersection matrix of the exceptional $\mathbb{P}^1$s, or by shifting the elliptic fibration into Tate form and applying the results from Tate's Algorithm.

3.3 Matter Representations and Yukawa Couplings

We have seen that the singularity structure of the elliptic fibration in codimension 1, given by its Kodaira type and associated Lie algebra $\mathfrak{g}$, determines the gauge group of the 7-brane on the singular locus. For F-theory compactifications on elliptic surfaces (on which the Kodaira classification is constructed), this would be all there is to say. However, we are interested in elliptic fibrations over 3-dimensional base manifolds. There is additional structure present in higher base codimension, i.e., on loci defined by two or three equations in B. On such loci, the discriminant of the fibration can vanish to higher

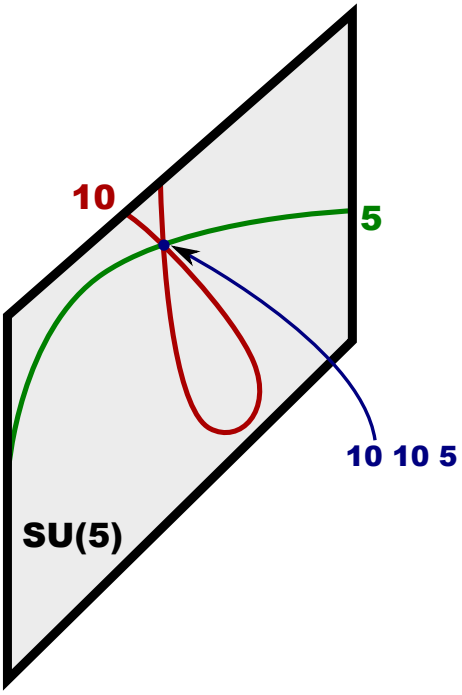

FIGURE 3.1: Gauge Group, Matter curves and a Yukawa coupling of an I_5-singularity at subloci of enhanced Kodaira type.

order, indicating a further enhancement of the singularity. The enhancement signifies the presence of additional localized matter transforming in some representation $\mathbf{R}$ of $\mathfrak{g}$ [98].

Consider the leading and first subleading term in the discriminant expansion on the singular locus S, given again by $z = 0$:

$$\Delta = \Delta_d z^d + \Delta_{d+d'} z^{d+d'} + \mathcal{O}(z^{d+d'+1}) \tag{3.3.1}$$

Over a generic point on $z = 0$, the discriminant vanishes to some order d. However, since Δ_d is a section of a line bundle on B, there will generically be a sublocus of S, with base codimension 2, where $\Delta_d = 0$. There, we expect a 'worsening' of the singularity, as the discriminant vanishes to higher order $d + d'$. Since this argument requires an at least 2-dimensional base manifold, the Kodaira-Néron classification does not say anything about such loci.

Recent work [99] has shown that over codimension 2 loci with singularity enhancement, the fibers can be classified using decorated representation graphs corresponding to a representation $\mathbf{R}$ of the Lie algebra $\mathfrak{g}$ of the codimension 1 singularity. Specifically, some of the exceptional divisors intersecting in the affine Dynkin diagram of $\mathfrak{g}$ in codimension 1 become reducible, and split according to roots of $\mathfrak{g}$ splitting into weights of $\mathbf{R}$ [100–102]. Generically, Δ_d will be reducible, and each irreducible component of it gives rise to a

splitting of fiber curves. In this way, different representations of $\mathfrak{g}$ can be associated to different subloci of S.

In an F-theory compactification, one encounters matter multiplets transforming in $\mathbf{R}$ localized on the curve(s) given by $z = \Delta_d = 0$ in B, which are therefore called matter curves in the literature. In the typical case where Δ_d is reducible, each irreducible component of Δ_d will give rise to a matter curve carrying matter in the representation associated to the splitting fibers. The physical origin of the states comprising the localized matter can again be understood in terms of M/F-duality: reducing the M-theory 3-form and wrapped $M2$-branes along the new curves leads to new massless modes, similar to what we have seen in the previous section. These new modes transform in the representation of $\mathfrak{g}$ associated to the matter curve. Away from the enhancement locus $z = \Delta_d = 0$, these additional states become massive, hence the matter is indeed localized on the matter curves.[3]

There is a good heuristic to determine the representation of a given matter locus, which we illustrate on the non-trivial and phenomenologically relevant example of an I_5-singularity with associated gauge group $SU(5)$. The I_5 Tate form in the $w = 1$ patch of $\mathbb{P}_{[1,2,3]}$ reads

$$y^2 + b_1 xy + b_3 z^2 y = x^3 + b_2 z x^2 + b_4 z^3 x + b_6 z^5 \tag{3.3.2}$$

and has discriminant (up to constant factors, which we always omit)

$$\Delta_{I_5} = b_1^4 P z^5 + O(z^6)\,, \tag{3.3.3}$$

with

$$P = b_2 b_3^2 - b_1 b_3 b_4 + b_1^2 b_6\,. \tag{3.3.4}$$

Therefore, this model contains the two matter curves $z = b_1 = 0$ and $z = P = 0$. From Tate's Algorithm, we know that enhancing the vanishing orders of b_1 would yield an I_1^* singularity with associated Lie group $SO(10)$, whereas tuning the complex structure of the fibration such that $P = 0$ results in an I_6 singularity with Lie group $SU(6)$. Upon decomposing the adjoint representation of $SO(10)$ under the breaking

$$SO(10) \to SU(5) \oplus U(1)\,, \tag{3.3.5}$$

one obtains

$$\mathbf{45} \to \mathbf{24}_0 + \mathbf{10}_4 + \overline{\mathbf{10}}_{-4} + \mathbf{1}_0\,, \tag{3.3.6}$$

[3] While F-theory compactifications contain additional matter states propagating in the bulk of the 7-brane [103], we do not consider them in this thesis.

with the **10** appearing as non-trivial non-adjoint representation, whereas the adjoint of $SU(6)$ decomposes under $SU(6) \to SU(5) \oplus U(1)$ as

$$\mathbf{35} \to \mathbf{24}_0 + \mathbf{5}_6 + \overline{\mathbf{5}}_{-6} + \mathbf{1}_0 \,. \tag{3.3.7}$$

where the **5** appears as non-trivial non-adjoint representation. It is a fact [101] that over $z = b_1 = 0$ one obtains matter transforming in the **10** representation of $SU(5)$, and over $z = P = 0$ one has matter in the **5** representation. This method generalizes to general singularities – the matter representation over a matter curve can be obtained by decomposing the adjoint representation of the Lie group associated to the enhanced singularity.

In codimension 3, there can be a further singularity enhancement at loci given by

$$z = \Delta_d = \Delta_{d+d'} = 0 \,. \tag{3.3.8}$$

Here, the exceptional divisors in the fiber either remain irreducible or one of the reducible components of a divisor in codimension 2 becomes homologous to the sum of two others, which we interpret physically as the existence of a Yukawa coupling between the representations associated to the three homologous divisors [101]. This leads to such points being named Yukawa points in the literature. Again, if the locus $z = \Delta_d = \Delta_{d+d'} = 0$ has multiple different irreducible components, one obtains multiple Yukawa points and, in the F-theory compactification, multiple Yukawa couplings. In the I_5 example from above, one finds two Yukawa points, with Yukawa couplings $\mathbf{10}\,\overline{\mathbf{5}}\,\overline{\mathbf{5}}$ and $\mathbf{10}\,\mathbf{10}\,\mathbf{5}$ (as well as their conjugates $\overline{\mathbf{10}}\,\mathbf{5}\,\mathbf{5}$ and $\overline{\mathbf{10}}\,\overline{\mathbf{10}}\,\overline{\mathbf{5}}$).

3.4 Abelian Gauge Symmetries

As we have seen in chapter 1, abelian gauge symmetries are of high relevance but essentially unconstrained in phenomenology. String theory provides one with the opportunity to embed $U(1)$ symmetries in a UV-complete settings and find restrictions on the sets of allowed charges, and consequently they have been the subject of much study in F-theory. The focus of much work has been on local models in the spectral cover formalism [104–106] and lifts of it to specialized Weierstraß forms [80,107], and on models [2,108–110] obtained from toric geometry methods [111]. In this thesis, we are interested in implementing $U(1)$ symmetries as a property of generic global F-theory compactifications, which allows for a systematic study of them.

In section 3.2, it was shown that non-abelian gauge groups appear in F-theory via the singular loci of the elliptic fibration on which the theory is compactified. Abelian gauge groups, however, do not feature in the Kodaira classification of singular fibers, and they are not bound locally to 7-branes in F-theory. Instead, they arise as a global feature of the compactification.

From analyzing degrees of freedom, [87] observed that the number of $U(1)$ symmetries in an F-theory compactification on an elliptically fibered n-fold is given by the rank of its Mordell-Weil group of rational sections, which was discussed in section 2.2.[4] The physical origin of the abelian gauge fields can again be understood from M/F-duality: each additional section σ_i yields an extra divisor $\sigma_i = 0$ with Poincaré-dual $(1,1)$-form ω_i, along which the C_3-field of M-theory can be reduced,

$$C_3 = \sum_i \omega_i \wedge A_i \,, \tag{3.4.1}$$

providing the extra degrees of freedom A_i.

Apart from the number of abelian gauge symmetries present in a given model, one is of course also interested in the corresponding $U(1)$ charges of matter. More formally, given an elliptic fibration with non-trivial Mordell-Weil group, a singularity with gauge group $\mathfrak{g}$ and a matter curve with representation $\mathbf{R}$ on it, what is the set of $U(1)$ charges of that representation under the abelian gauge symmetries?

To answer this question, one has to consider the Shioda map, which was analyzed in detail in [112]. Essentially, if one has a collection of rational sections $\sigma_1, \ldots, \sigma_r$ generating the Mordell-Weil group, applying the Shioda map to each of them gives a collection of homology classes $s(\sigma_1), \ldots, s(\sigma_r)$. The abelian vector fields A_i of the F-theory compactification are in a sense dual to the $s(\sigma_i)$, in that a matter multiplet coming from a rational curve with homology class C has charge under A_i given by the intersection

$$s(\sigma_i) \cdot C \,. \tag{3.4.2}$$

Specifically, all $s(\sigma_i)$ have intersection number zero with any of the Cartan divisors $D_{-\alpha_i}$ of the resolved fibration, and with any divisor D_H pulled back from the base B:

$$s(\sigma_i) \cdot D_{-\alpha_i} = s(\sigma_i) \cdot \pi^* D_H = 0 \,. \tag{3.4.3}$$

[4] As was also seen in section 2.2, the Mordell-Weil group may also contain a finite torsion subgroup, and there has been recent progress in analyzing its F-theory implications [95]. Throughout this thesis, we assume trivial torsion subgroup.

Therefore, no vector multiplets of any 7-brane gauge groups are charged under the additional $U(1)$s, only hypermultiplets coming from matter curves can be. In practice, these two constraints serve to specify the Shioda map for all intersection computations up to transformations of the $s(\sigma_i)$ preserving charge minimality.

We have also seen in section 2.2 that elliptic fibrations with Mordell-Weil rank 1 can be engineered as quartic hypersurfaces embedded in $\mathbb{P}_{[1,1,2]}$, and F-theory vacua realized in this way thus contain an additional abelian gauge factor. Therefore, a systematic study of F-theory compactifications with a single additional abelian gauge factor can be undertaken by classifying the singularities of such fibrations, not only with respect to their Kodaira fiber types, but also including the structure of the rational sections. This will be the aim of chapter 5.

Another consequence of the definition of the Shioda map is that, by virtue of its non-intersection property with Cartan divisors, the way the extra rational sections themselves intersect the singular fibers in codimensions 1 and 2 determines their image under the Shioda map. One might therefore suspect that the relative location of the rational sections on the singular fibers is sufficient to determine the full $U(1)$ spectrum of the compactification. This turns out to be the case at least for fibrations with Mordell-Weil rank 1, as we will also see in chapter 5.

3.5 G-flux

A key role in F-theory compactifications is played by G-flux. So far, we have only determined the locations of matter curves within the compactification manifold and their associated representations. Another relevant piece of information for phenomenology is the number of generations and antigenerations of matter arising from a given matter curve, or at least the chiral index, which gives the difference between generations and antigenerations. G-flux determines such chiral indices.[5] Furthermore, G-flux encodes information on 3-brane charges in the compactification.

Formally, G-flux is defined as a $(2,2)$ form which integrates non-trivially over holomorphic surfaces and satisfies the quantization condition [115]

$$G + \frac{1}{2}c_2(\tilde{Y}_4) \in H^4\left(\tilde{Y}_4, \mathbb{Z}\right) , \tag{3.5.1}$$

[5] There is also recent progress on methods to compute the absolute number of generations and antigenerations using Chow groups and Deligne cohomology [113, 114].

where $\tilde{Y}_4$ is a resolution of the Calabi-Yau fourfold. Physically, G-flux can be thought of as unifying the type IIB three-form flux $G_3 = F_3 - \tau H_3$ and brane fluxes F, arising from $D7$-brane gauge field strengths.

The chiral index χ of a matter representation $\mathbf{R}$ localized on a matter curve $C_{\mathbf{R}}$ is then given by integrating G over $C_{\mathbf{R}}$ [101, 116]:

$$\chi = \int_{C_{\mathbf{R}}} G\,. \tag{3.5.2}$$

The induced 3-brane charge by G is given by its self-intersection within the resolved Calabi-Yau manifold $\tilde{Y}_4$. That is, the full 3-brane tadpole cancellation condition in F-theory reads [117]

$$\frac{\chi(\tilde{Y}_4)}{24} = N_{D3} + \frac{1}{2}\int_{\tilde{Y}_4} G \cdot G\,, \tag{3.5.3}$$

with $\chi(\tilde{Y}_4)$ being the Euler characteristic, or top Chern class, of the resolved manifold, which can be computed using equation (2.1.11). Note that for singular compactification manifolds with associated gauge groups $SU(5)$, $SO(10)$, and $E_{6/7/8}$, a simple form of $\chi(\tilde{Y}_4)$ has been suggested in [118], and for $SU(5)$ this form was confirmed in [101], providing a nice example of the use of geometrical tools to answer physical questions. In chapter 4, we will confirm the conjecture of [118] in the case of an E_6-type singularity, as well as discuss existing methods and introduce a new one to construct G-flux explicitly in resolved and singular Calabi-Yau fourfolds.

3.6 F-theory for Engineering Phenomenology Models

This section fleshes out some of the ideas of section 1.5. It also justifies the promises made there about the phenomenological attractiveness of F-theory compactifications, by presenting an implementation of the $SU(5)$ GUT model from section 1.3 in F-theory.

First and foremost, an embedding of the $SU(5)$ GUT requires an $SU(5)$ gauge group in the compactification. We have seen that this gauge group can be realized on a 7-brane in F-theory, by considering an elliptic fibration over some base manifold B with a singularity of Kodaira type I_5. If B has more than one complex dimension – and, as GUTs are to model the physics of the universe, B should be complex three-dimensional – one expects this singularity to enhance in codimension two. The two loci over which this happens have been discussed in section 3.3, and the matter multiplets arising over them transform in the fundamental and antifundamental $\mathbf{5}$ and $\overline{\mathbf{5}}$, as well as the antisymmetric $\mathbf{10}/\overline{\mathbf{10}}$

representation of $SU(5)$. These are precisely the representations required to engineer the Standard Model fermions and Higgs bosons.

In order to construct the three generations of quarks and leptons, one has to find a G-flux configuration such that the chiral index of section 3.5 over the **10** matter curve is $\chi_{c_{\mathbf{10}}} = +3$. Also, one needs $\chi_{c_{\mathbf{5}}} = -3$, since the right-handed down-type quarks and the leptons transform in the $\overline{\mathbf{5}}$ representation in an $SU(5)$ GUT.

Recall that the two Yukawa couplings generically arising in an I_5 singularity at codimension three are $\mathbf{10}\,\overline{\mathbf{5}}\,\overline{\mathbf{5}}$ and $\mathbf{10}\,\mathbf{10}\,\mathbf{5}$. After the breaking of $SU(5)$ to G_{SM}, the former can give the down-type Yukawa couplings of the Standard Model, while the latter is suited to replicate the up-type Yukawa couplings, most notably the top Yukawa coupling. Unlike in compactifications of type IIA/IIB string theory, the top Yukawa coupling is presented generically in F-theory models, and does not have to be generated by e.g. instanton effects with small coupling constants. This is rooted in the fact that the singular fiber at the top Yukawa point enhances to Kodaira type IV^* with associated Lie group E_6. Type IIA/IIB compactifications do not contain any exceptional gauge symmetries, and their appearance in F-theory can be understood as a consequence of the theory being genuinely non-perturbative.

Lastly, there are various options to break the $SU(5)$ GUT to the Standard Model gauge group in F-theory. A way of doing so is via hypercharge flux, i.e., gauge flux associated to the generator of the hypercharge $U(1)_Y$ in the $SU(5)$ [103, 119].

It is worth noting again that this construction serves as an example of the reformulation of physical questions, e.g. about the matter or Yukawa content of a theory, into geometric constraints on the compactification manifold, which can be answered using tools from algebraic geometry. Furthermore, all the constraints presented are local, in that they affect a single divisor of the compactification and are otherwise independent of the choice of base manifold. In this way, F-theory preserves the modularity of type IIB constructions, while adding non-perturbative features such as the top Yukawa coupling.

The naive GUT model we have constructed in this section has a few shortcomings. Since the Higgs fields are located on the same **5** curve as the matter fields, the Yukawa point that gives the top Yukawa coupling $\mathbf{10}_M\,\mathbf{10}_M\,\mathbf{5}_H$ also yields the proton-decay inducing operator $\mathbf{10}_M\,\mathbf{10}_M\,\mathbf{5}_M$. We have also so far not dealt with the issue of doublet-triplet-splitting in the Higgs sector.

It is conceivable that both of these problems could be solved at once if one were to consider an F-theory model with additional abelian gauge factors, which also have multiple **5** curves

that are differently charged under the extra $U(1)$s. Given suitable $U(1)$ charges, it might be possible to locate the Standard Model fermion fields and the two Higgs doublets on three different matter curves, in a way that

- the top Yukawa coupling $\mathbf{10}_M\,\mathbf{10}_M\,\mathbf{5}_H$ is allowed by the $U(1)$ charges, whereas $\mathbf{10}_M\,\mathbf{10}_M\,\mathbf{5}_M$ is not,
- and a linear combination of the additional $U(1)$ factors acts as a $U(1)_{PQ}$, thereby addressing the μ-problem.

One might also be able to use the extra $U(1)$s to accommodate more phenomenological constraints, such as the additional absence of proton-decay producing operators of dimension 5 or 6.

It is therefore crucial to gain an understanding of the possible sets of charged matter curves in an F-theory compactification. A systematic study of the matter structure of F-theory models with a single additional abelian gauge factor is the subject of chapter 5, and its associated paper [67]. Two companion papers, currently in progress, will perform a similar analysis for F-theory models with two additional $U(1)$ factors [120], and investigate the phenomenological implications of these compactifications [121].

3.7 The Spectral Cover Construction

Section 3.6 discussed that many physical constraints on an F-theory model depend only on the geometry of the GUT divisor S of the compactification manifold. This observation forms the basis for local F-theory model building [103,122,123]. One approach to construct local models in F-theory is the spectral cover construction [116,124,125], which this section briefly reviews.

The local gauge theory hosted on a 7-brane is the maximally supersymmetric Yang-Mills theory in eight dimensions on the surface S wrapped by the brane. If one is only interested in a local description of the compactification around S, one can consider an ALE-fibration of S instead of an elliptic fibration of B. Since S is compact, one needs to consider a partially twisted version of the $8D$ gauge theory [103] containing a gauge field A and a Higgs field Φ transforming in $K_S \otimes Ad(G)$, where G is the gauge group of the brane. To

ensure $\mathcal{N} = 1$ supersymmetry, one has to satisfy the BPS equations

$$\begin{aligned} F_S^{(0,2)} = F_S^{(2,0)} &= 0 \\ \partial_A \Phi &= 0 \\ \omega \wedge F_S + \frac{i}{2}\left[\Phi, \bar{\Phi}\right] &= 0 \end{aligned} \tag{3.7.1}$$

with ω being the Kähler form on S and F the field strength of A. The first two equations are associated to the vanishing of F-terms in the language of $\mathcal{N} = 1$ supersymmetry, while the third corresponds to a D-term condition, and all three equations are called Hitchin's equations.

One can find solutions to Hitchin's equations by first analyzing the vacuum expectation values of Φ. We assume that they are such that Φ is diagonalizable, which is equivalent to having $\left[\Phi, \bar{\Phi}\right] = 0$.[6]

To construct the spectral cover, one diagonalizes the Higgs field Φ of the Bundle H and obtains its eigenvalues and -vectors – that is, its spectrum. For $G = SU(n)$ (with equivalent constructions existing for all other gauge groups) the Casimirs of Φ are the coefficients of

$$\det\left(s\mathbf{I} - \Phi\right) = 0\,. \tag{3.7.2}$$

where s denotes a coordinate on the canonical bundle K_S. For each point on S, the n roots λ_i of this equation give n points on the fiber of a fibration $K_S \to S$. Taking all those points together, one obtains a surface $\mathcal{C}$ which is an n-cover of S. This surface is the spectral cover for the fundamental representation of $SU(n)$. One can rewrite the spectral cover equation as

$$0 = b_0 s^n + b_1 s^{n-1} + \cdots + b_n\,. \tag{3.7.3}$$

The eigenvalues of a Higgs field in $SU(n)$ add up to zero due to the tracelessness conditions. Comparing (3.7.2) and (3.7.3), one finds that

$$b_1 = \lambda_1 + \cdots + \lambda_n\,, \tag{3.7.4}$$

and can therefore set $b_1 = 0$.

Having obtained the spectral cover $p_C : \mathcal{C} \to S$ from the vacuum expectation values for Φ, one can obtain a vacuum solution of the gauge field A on S by choosing a line bundle

[6] F-theory compactifications with non-diagonalizable Higgs field exist, and have been discussed e.g. in [114, 126–130].

$\mathcal{L}$ on $\mathcal{C}$. The gauge field is reconstructed by using the push-forward

$$A = p_{C*}\left(\mathcal{L}\right) . \tag{3.7.5}$$

Since this needs to be an $SU(n)$ bundle, one requires $\mathcal{L}$ to satisfy

$$c_1\left(p_{C*}\mathcal{L}\right) = 0 . \tag{3.7.6}$$

This construction allows one to determine properties local to the 7-brane, such as matter curves or Yukawa couplings. Furthermore, the construction of G-flux in local spectral cover models is also possible and reviewed in section 4.1.2.

Starting from a global model with an I_5 Tate form (i.e. $G = SU(5)$), the associated $SU(5)$ spectral cover model can also be reconstructed by considering the Tate divisor of the elliptic fibration in Weierstraß form, given by [131]

$$\mathcal{C}_{\text{Tate, } SU(5)} : \qquad y^2 = x^3 \tag{3.7.7}$$

and performing the local limit

$$t = x/y \to 0 \qquad \text{with} \qquad s = z/t \qquad \text{fixed}, \tag{3.7.8}$$

which maps the I_5-type Tate form (3.3.2) to the $SU(5)$ spectral cover model (3.7.3). In chapter 4, we will show that if one refines the definition of the Tate divisor, the local limit also yields correct results for general $G \subset E_8$.

The spectral cover construction thus provides one with a tool to consider models of low-energy models in a local setting within F-theory and a framework for the systematic study of features arising in such models. For instance, a comprehensive survey of abelian gauge symmetries, whose relevance in F-theory model building has been discussed in section 3.6, was undertaken for spectral cover models in [106]. These results are then to be supplemented by global aspects of the F-theory compactification. In the case of a single additional abelian gauge symmetry, the global models are discussed in chapter 5, and the comparison between them and models arising from the spectral cover can be found in appendix B.3.

Chapter 4

G-flux and Spectral Divisors

In section 3.5, we have outlined the phenomenological relevance of G-flux in F-theory model building. There are several ways to construct G, the most straightforward one being in terms of holomorphic surfaces in the resolved Calabi-Yau fourfold. However, as G-flux depends crucially on the singularity structure of the elliptic fibration, it is natural to anticipate a framework that makes more direct use of the singularity structure in the construction of the flux.

Progress on the development of such a framework has been made using various approaches: in local models flux was constructed in the setup of spectral covers [124] starting with [104, 116, 132]. On the other hand the resolution of a general A_4 singularity was proposed in [133] and used to directly construct G-flux in terms of homolorphic surfaces in [101].

Another approach to G-fluxes which makes use of the singularity structure was proposed in the papers [131, 134] and shown to be consistent with the direct construction of the flux in $\tilde{Y}_4$ in [101]. The idea is to construct the fluxes from a special divisor, the *spectral divisor*, in the resolved Tate form [1, 89] of the geometry $\tilde{Y}_4$, which behaves close to the singularity in the same way as the spectral cover of the Higgs bundle in the local model. This proposal was exclusively performed and tested in the context of A_4 singularities.

In this chapter, we point out that this spectral divisor formalism generalizes to all singularity types which allow for a local spectral cover description as explained in [124]. However, to make contact with the local Higgs bundle spectral cover, the Tate form has to be modified. This construction is exemplified in the case of $SU(3)$ covers, which correspond to a singularity of Kodaira type IV^* with associated gauge group E_6, by first resolving the singular Tate form of IV^* (which also serves as another more extensive example of the formalism developed in section 2.3) and then constructing G-flux both

globally in terms of holomorphic surfaces and locally using the spectral divisor formalism. This chapter closely follows its associated publication [66].

4.1 G-flux and Spectral Divisors

4.1.1 Spectral Form of the Singularity

Consider a singular elliptic Calabi-Yau fourfold Y_4 with base threefold B and with a singularity of type G along a surface S, given by $z = 0$ in terms of a local holomorphic coordinate z on B. Recall from section 2.4 that the equation for Y_4 can then be put globally into the Tate form for G [89] (modulo subtleties discussed in [1, 67]):

$$y^2 + a_1 xy + a_3 y = x^3 + a_2 x^2 + a_4 x + a_6 \,, \tag{4.1.1}$$

where the vanishing order in z is determined by the type of the singularity

$$a_i = z^{n_i} b_i \,, \tag{4.1.2}$$

and b_i are sections of $\mathcal{O}(ic_1 - n_i S)$ and $c_1 = c_1(B)$. Consider F-theory on $Y_4 \times \mathbb{R}^{1,3}$, then the physics close to the locus $z = 0$ has a description in terms of an $\mathcal{N} = 1$ supersymmetric gauge theory with gauge group G.

We will restrict our attention to gauge groups G which can be thought to arise from higgsing an underlying E_8 gauge theory by adjoint scalar vevs, and where the data of the gauge theory is geometrically encoded in a spectral cover $\mathcal{C}$ over S [124]. Additional data corresponding to G-flux is encoded in spectral cover fluxes, which are constructed from line bundles over $\mathcal{C}$. This construction has a dual description, in case the CY fourfold has a $K3$ fibered structure, to heterotic compactifications with $H = SU(N)$ or $Sp(N)$ vector bundles, where H is the commutant of G inside E_8. We will restrict our discussion to the case when such a spectral cover (SC) construction is known to exist in the local limit, and denote these groups by type G_{SC}. Concretely, the cases that allow for a SC formulation in the local limit have vanishing orders n_i of the sections a_i and the discriminant Δ for

the elliptic fibration that are summarized in the following table

G_{SC}	H	n_1	n_2	n_3	n_4	n_6	Δ
E_7	$SU(2)$	1	2	3	3	5	8
E_6	$SU(3)$	1	2	2	3	5	8
$SO(10)$	$SU(4)$	1	1	2	3	5	7
$SU(5)$	$SU(5)$	0	1	2	3	5	5
$SO(11)$	$Sp(2)$	1	1	3	3	5	8

(4.1.3)

There are of course other groups that can arise by a higgsing of an E_8 gauge theory. However, the commutant H of G is then not of $SU(N)$ or $Sp(N)$ type, and so the construction of fluxes will not come from a SC (see [124]).

In concrete F-theory constructions, in particular in view of phenomenologically relevant models, we often require $U(1)$ symmetries in addition to the gauge symmetry G. Realizations of these in the spectral cover formalism have been shown to be possible by imposing a factored form for the spectral cover [104–107, 135, 136]. Gauge fluxes in the direction of these $U(1)$s have been constructed from the factored spectral cover. One important question is then, how these local constructions lift to the full Calabi-Yau fourfold Y_4, and its resolution $\tilde{Y}_4$, and how fluxes associated to $U(1)$ symmetries are realized in this context. Progress in this direction has been made in [136, 137], showing that local split spectral covers do not necessarily reproduce the global information correctly, and the extension of the local construction of fluxes to global models with abelian gauge symmetries, such as the ones presented in chapter 5, would be an interesting avenue for future work.

In [101, 131, 134] a proposal was made in terms of spectral divisors, which in a local limit reduce to the spectral cover $\mathcal{C}$ of the Higgs bundle. The construction there was mainly focused on the settting of $G = SU(5)$. We will detail how this proposal for a spectral divisor formalism generalizes for any gauge group G, which allows for a spectral cover construction in the local limit.

Recall that in [131, 134] the Tate divisor was defined as the divisor that in the local limit reduces to the spectral cover, with the property that in the presence of additional $U(1)$ symmetries it maintains the factored form of the spectral cover. In the resolved Tate form $\tilde{Y}$ for $SU(5)$ it can be characterized by the equation

$$\mathcal{C}_{\text{Tate},SU(5)}: \qquad x^3 = y^2\,. \tag{4.1.4}$$

The local limit is defined by taking

$$t = x/y \to 0\,, \qquad \text{while} \qquad s = z/t \quad \text{fixed}\,. \tag{4.1.5}$$

Indeed, the Tate divisor reproduces in this local limit in the case of the $SU(5)$ spectral cover [116], i.e.,

$$\mathcal{C}_{\mathrm{SC},SU(5)}: \qquad b_1 - b_2 s + b_3 s^2 - b_4 s^3 - b_6 s^5 = 0\,. \tag{4.1.6}$$

More generally, the definition of the Tate divisor has to be refined[1].

Applying the characterization in terms of (4.1.4) and the limit (4.1.5) for a general Tate form yields

$$b_1 s^{n_1} t^{n_1+5} - b_2 s^{n_2} t^{n_2+4} + b_3 s^{n_3} t^{n_3+3} - b_4 s^{n_4} t^{n_4+2} - b_6 s^{n_6} t^{n_6} = 0\,. \tag{4.1.7}$$

On the other hand, the spectral cover equations for the groups in (4.1.3) are

G	H	$\mathcal{C}_{\mathrm{SC}}$
E_7	$SU(2)$	$\bar{b}_6 s^2 + \bar{b}_4$
E_6	$SU(3)$	$\bar{b}_6 s^3 + \bar{b}_4 s - \bar{b}_3$
$SO(10)$	$SU(4)$	$\bar{b}_6 s^4 + \bar{b}_4 s^2 - \bar{b}_3 s + \bar{b}_2$
$SU(5)$	$SU(5)$	$\bar{b}_6 s^5 + \bar{b}_4 s^3 - \bar{b}_3 s^2 + \bar{b}_2 s - \bar{b}_1$
$SO(11)$	$Sp(2)$	$\bar{b}_6 s^4 + \bar{b}_4 s^2 + \bar{b}_2$

(4.1.8)

Here the sections $\bar{b}_n = b_n|_S$. Each of these arise from $y^2 = x^3$ in the local limit (4.1.5) as the leading equations in t. However, in order to define the lift into the resolved geometry $\tilde{Y}$ this is not a suitable definition of the spectral divisor. Consider what we will refer to as the *spectral form* of the singular elliptic CY, namely, each of the Tate forms can be put into the following spectral form by shifting the coordinates x and y. This form has also appeared in [107].

For E_7, we can shift successively

$$y \to y - \frac{1}{2}\left(b_1 z x + b_3 z^3\right)\,, \qquad x \to x - \frac{1}{12} z^2 (b_1^2 + 4 b_2) \tag{4.1.9}$$

[1] We will refer to the divisor, which in the local limit results in the spectral cover, maintaining potential factorizations, as *the spectral divisor*. As in general this divisor does not result from the Tate form, we will not use the terminology *Tate divisor*.

so that the equation in the new coordinates takes the form

$$y^2 = x^3 + b'_4 z^3 x + b'_6 z^5 \,, \tag{4.1.10}$$

with new sections b'_n. Note that this equation satisfies the requirements from Kodaira's classification for an E_7 singular fiber at z, i.e. the corresponding Weierstraß form $y^2 = x^3 + fx + g$ satisfies that the degrees of vanishing at z are

$$\deg(f) = 3\,, \qquad \deg(g) \geq 5\,, \qquad \deg(\Delta) = 9\,. \tag{4.1.11}$$

In the form (4.1.10), which we will refer to as the spectral form of the E_7 singularity, we can now define the spectral divisor $\mathcal{C}_{\text{spectral}}$ by $y^2 = x^3$, which under (4.1.5) limits precisely to the spectral cover for the E_7 gauge theory.

For each of the cases in (4.1.3) we can pass from the Tate form to a unique spectral form[2]

$$\begin{aligned} E_6: &\quad y \to y - \frac{1}{2} b_1 z x\,, \qquad x \to x + \frac{1}{12} z^2 (b_1^2 + 4 b_2) \\ SO(10): &\quad y \to y - \frac{1}{2} b_1 z x \\ SO(11): &\quad y \to y - \frac{1}{2} \left(b_1 z x + b_3 z^3 \right)\,. \end{aligned} \tag{4.1.12}$$

For $SU(5)$ the Tate form is conveniently already the spectral form. The resulting spectral forms of the singularities are in summary

G	Spectral form of singularity	
E_7	y^2	$= x^3 + b_4 z^3 x + b_6 z^5$
E_6	$y^2 + b_3 z^2 y$	$= x^3 + b_4 z^3 x + b_6 z^5$
$SO(10)$	$y^2 + b_3 z^2 y$	$= x^3 + b_2 z x^2 + b_4 z^3 x + b_6 z^5$
$SU(5)$	$y^2 + b_1 x y + b_3 z^2 y$	$= x^3 + b_2 z x^2 + b_4 z^3 x + b_6 z^5$
$SO(11)$	y^2	$= x^3 + b_2 z x^2 + b_4 z^3 x + b_6 z^5$

(4.1.13)

In the spectral form of the singularity we can now define the *spectral divisor*, i.e., the divisor which in the local limit (4.1.5) reduces to the spectral cover of the Higgs bundle, and furthermore maintains any factored form of the spectral cover[3], in terms of the

[2] This is unique in the sense that it has the minimal set of non-vanishing sections b_i, which give rise to the required degrees of vanishing in the Kodaira classification for singular elliptic fibers.

[3] To eliminate any confusion in terminology: this is what in the $SU(5)$ case was named Tate divisor, however, for obvious reasons this is not a suitable name since the Tate form is not relevant for this discussion. In [131, 134] spectral divisors were defined as the family of divisors in the resolved fourfold, that limit locally to the spectral cover. The member of this family, which furthermore lifts a factored form of the spectral cover is the most relevant for the purpose of constructing fluxes (in particular $U(1)$ fluxes

equation in the spectral form by

$$\mathcal{C}_{\text{spectral}}: \qquad y^2 = x^3\,. \tag{4.1.14}$$

In the local limit defined as in (4.1.5), it is straightforward to see that the spectral divisor restricts to the SC of the local models.

4.1.2 Local G-flux from Spectral Covers

Before discussing the construction of global flux from the spectral divisor, it is useful to recall the construction in the local model. In the local framework of spectral covers, flux is constructed as follows (see [116] and for a summary appendix D of [101]). Consider

$$\mathcal{C}_{\text{SC}} \cdot \pi^*\Sigma \qquad \text{and} \qquad \mathcal{C}_{\text{SC}} \cdot \sigma_{\text{SC}}\,, \tag{4.1.15}$$

where σ_{SC} is the class of the hyperplane of the $\mathbb{P}^1$-bundle $Z = \mathbb{P}(\mathcal{O} \oplus K_S)$ in which the spectral cover is embedded, and Σ is a curve in S and π the projection map

$$\pi: \quad Z \;\to\; S\,. \tag{4.1.16}$$

The thereby induced covering map of the spectral cover will be denoted by

$$p: \quad \mathcal{C}_{\text{SC}} \;\to\; S\,. \tag{4.1.17}$$

To describe the gauge bundle in a local model, we specify a line bundle L on $\mathcal{C}_{\text{SC}}$ (4.1.8), which via the pushforward gives rise to an H-gauge bundle. For $H = SU(N)$ we require tracelessness, which amounts to

$$c_1(p_*L) = p_*c_1(L) - \frac{1}{2}p_*r = 0\,, \tag{4.1.18}$$

where r denotes the ramification divisor of the covering p and is given by

$$r = (\mathcal{C}_{\text{SC}} - \sigma_{\text{SC}} - \sigma_\infty)\cdot\mathcal{C}_{\text{SC}} = ((N-2)\sigma_{\text{SC}} + \pi^*(\eta - c_1(S)))\cdot\mathcal{C}_{\text{SC}}\,. \tag{4.1.19}$$

corresponding to the factorization of the spectral cover). Since this is the key object to study, it will be refered to as *the spectral divisor*.

We used the standard shorthand $\sigma_\infty = \sigma_{\rm SC} + \pi^* c_1(S)$. The class η is defined via

$$[\mathcal{C}_{\rm SC}] = N\sigma_{\rm SC} + \pi^*\eta\,. \tag{4.1.20}$$

The tracelessness condition (4.1.18), which amounts to requiring that the projection of the spectral flux to S is trivial, leaves only a specific combination of the two types of local spectral fluxes for the $SU(N)$ case (for $SU(5)$ this was obtained in [116], and for split covers in [104, 105])

$$\gamma = \alpha(N\sigma_{\rm SC} - \pi^*(\Sigma_N)) \cdot \mathcal{C}_{\rm SC}\,, \qquad \alpha \in \mathbb{C}\,. \tag{4.1.21}$$

The curve Σ_N is characterized by $b_{N_b} = 0$ in (4.1.8), where $b_{N_b} = 0$ corresponds to the class of the curve $s = 0$ in the SC, i.e.

$$\Sigma_N = (\eta - N_b c_1(S))\,, \tag{4.1.22}$$

with $(N, N_b) \in \{(2,4),(3,3),(4,2),(5,1)\}$. So, the following combination has to be an integral class

$$\frac{r}{2} + \gamma = \left(-1 + N\alpha + \frac{N}{2}\right)\sigma_{\rm SC} + \pi^*\left(\left(\frac{1}{2} - \alpha\right)\eta - \left(\frac{1}{2} - \alpha N_b\right)c_1(S)\right)\,. \tag{4.1.23}$$

For odd N this flux is properly quantized by choosing $\alpha \in \mathbb{Z} + \frac{1}{2}$. However, for N even, such as in the case of $SO(10)$ singularities, the universal flux is not automatically properly quantized, unless there are further assumptions about S (e.g. $c_1(S)$ even).

4.1.3 Global G-flux from Spectral Divisors

The discussion in the last section defines a divisor in the spectral form for the singularities of type $G_{\rm SC}$ which we can now use to carry out the construction of global G-flux, as outlined in [101, 131, 134]. The direct construction using holomorphic surfaces in the resolved geometry can be connected to the construction with the spectral divisor, as was demonstrated for $SU(5)$ in [101], and as we will show for E_6 in the following. The flux constructed in this way is quantized [115] by means of the second Chern class of the resolved geometry

$$G + \frac{1}{2}c_2(\tilde{Y}_4) \in H^4(\tilde{Y}_4, \mathbb{Z})\,. \tag{4.1.24}$$

Let $\tilde{Y}_4$ be the resolution of the singular Calabi-Yau fourfold Y_4, where at least all codimension 1 singularities have been blown up, for instance along the lines of [101, 102, 138]. The resolution is usually done starting with the Tate form of the singular fourfold. However, likewise, we can pass to the spectral form, which is what we will consider.[4] The proper transform of $\mathcal{C}_{\text{spectral}}$ will generically be reducible, with components correponding to exceptional divisors of the blow-ups, and we refer to the spectral divisor in the resolved geometry as the irreducible component of this, after subtraction of various exceptional divisors.

To make contact between the local SC construction and the global G-flux obtained from linear combinations of surfaces, consider the surfaces in the resolved fourfold $\tilde{Y}_4$ obtained from divisors D in B that restrict to curves Σ in S

$$\mathcal{S}_D = \mathcal{C}_{\text{spectral}} \cdot D \qquad \text{and} \qquad \mathcal{S}_{\sigma_{\text{SC}}} \,. \tag{4.1.25}$$

These are the global analogs of (4.1.15). The surface $\mathcal{S}_{\sigma_{\text{SC}}}$ is defined to contain in the local limit the matter curve that is defined in the spectral cover by $\sigma_{\text{SC}} \cdot \mathcal{C}_{\text{SC}}$, which amounts to $s = 0$ inside $\mathcal{C}_{\text{SC}}$ in (4.1.8), i.e. the **10** matter curve $b_1 = 0$ for $SU(5)$, the **27** matter curve $b_3 = 0$ for E_6, etc.

The lift of the universal spectral cover flux (4.1.21) requires the special case when D is

$$\mathcal{S}_{p^*(\eta - N_b c_1(S))} = \mathcal{C}_{\text{spectral}} \cdot p^*(\eta - N_b c_1(S)) \,. \tag{4.1.26}$$

Only a linear combination of these will be the lift of a traceless local flux and does not break the symmetry with respect to the group G, i.e. intersects trivially with the Cartan divisors of the resolved geometry. The ramification divisor lifts to the surface

$$\mathcal{S}_r = (N-2)\mathcal{S}_{\sigma_{\text{SC}}} + \mathcal{S}_{p^*(\eta - c_1(S))} \,. \tag{4.1.27}$$

The properly quantized flux, that is the global lift of the universal flux for odd N, is then given by

$$\begin{aligned} G_{\text{spectral}} &= \frac{1}{2}(2n+1)\left(N\mathcal{S}_{\sigma_{\text{SC}}} - \mathcal{S}_{p^*(\eta - N_b c_1(S))}\right) \\ &= \frac{1}{2}(2n+1)\left(N\mathcal{S}_{\sigma_{\text{SC}}} - \mathcal{C}_{\text{spectral}} \cdot p^*(\eta - N_b c_1(S))\right) \,. \end{aligned} \tag{4.1.28}$$

[4] In practice this amounts to setting some of the coefficients in the Tate form to 0.

This has been explicitly confirmed for $SU(5)$ in [101], and in the remainder of this chapter, we will show this proposal works also in the case for E_6, which in particular has a spectral form that differs from the standard Tate form.

4.2 Example: E_6 Singularity

The resolutions of the Tate forms for singularities (4.1.3) along the lines of section 2.3 in Calabi-Yau fourfolds in codimensions 1, 2 and 3 have been constructed for $G = SU(5)$ in [101, 133], and more generally after the paper associated to this chapter appeared in [102]. A non-trivial example to illustrate and test our proposal for the G-flux construction from spectral divisors is $G = E_6$, for which the spectral form differs from the Tate form. First we consider the resolution of the E_6 singularity, and then construct G-fluxes, both directly using surfaces in the resolved CY fourfold and by making connection to the spectral divisor construction (in particular the local limit), and show the consistency of these two approaches.

As a beneficial corollary to this we study the higher codimension structure of the elliptic fibration with an E_6 singularity and show how along the codimension 2 locus of enhanced symmetry the fibers split, realizing the matter in the **27** of E_6. Furthermore in codimension 3, the Yukawa interaction $\mathbf{27} \times \mathbf{27} \times \mathbf{27}$ is shown to be generated, as three matter divisors in the **27** become homologous. This confirms the logic put forward in [101], that although the fibers in codimension 3 may not have intersection relations governed by the Dynkin diagrams of higher rank gauge groups, this does not contradict the generation of Yukawa couplings. The existence of the latter depends on the splitting of matter divisors in such a way, that they become homologous to each other.

4.2.1 Setup

We consider the Tate form for E_6 as defined in (4.1.1, 4.1.3). As in [101, 133], we construct the resolution in the auxiliary fivefold

$$X_5 = \mathbb{P}\left(\mathcal{O} \oplus K_B^{-2} \oplus K_B^{-3}\right) , \tag{4.2.1}$$

i.e. X_5 is a $\mathbb{P}^2$ bundle over the base of the elliptic fibration, B. Divisors on X_5 consist of pullbacks of divisors on B under the projection

$$\pi_X : X_5 \to B \tag{4.2.2}$$

and a new divisor σ inherited from the hyperplane of the $\mathbb{P}^2$ fiber[5]. The projective coordinates w, x, and y on the $\mathbb{P}^2$ fiber of X_5 have the following classes in X_5

$$\begin{aligned} [w] &= \sigma\,, \qquad [x] = \sigma + 2c_1\,, \quad [y] = \sigma + 3c_1\,, \\ [z] &= S\,, \qquad [a_m] = mc_1\,, \qquad [b_m] = mc_1 - \deg(a_m)S\,. \end{aligned} \tag{4.2.3}$$

Here, z is the section that vanishes along S, which is the component of the discriminant with the singularity of type E_6. The general Tate form is

$$y^2 + a_1xy + a_3y = x^3 + a_2x^2 + a_4x + a_6\,, \tag{4.2.4}$$

which for an E_6 singularity at $z = 0$ specializes to

$$\deg(a_1) = 1\,, \qquad \deg(a_2) = 2\,, \qquad \deg(a_3) = 2\,, \qquad \deg(a_4) = 3\,, \qquad \deg(a_6) = 5\,, \tag{4.2.5}$$

i.e. inside X_5 in homogeneous coordinates this is

$$y^2w + b_1zxyw + b_3z^2yw^2 = x^3 + b_2z^2x^2w + b_4z^3xw^2 + b_6z^5w^3\,. \tag{4.2.6}$$

The discriminant has the following expansion in z

$$\begin{aligned} \Delta = &-27b_3^4z^8 \\ &+ \left((b_1b_3 + 2b_4)\left(\left(b_1^2 + 36b_2\right)b_3^2 - 32b_1b_4b_3 - 32b_4^2\right) - 216b_3^2b_6\right)z^9 + O\left(z^{10}\right)\,. \end{aligned} \tag{4.2.7}$$

In codimension 2, i.e. the first subleading order in z, the only locus of symmetry enhancement (corresponding to the matter curve in the local description) is

$$b_3 = 0\,. \tag{4.2.8}$$

The codimension 3 locus of enhanced symmetry, i.e. the Yukawa interaction, arises at

$$b_3 = b_4 = 0\,. \tag{4.2.9}$$

[5]Note that σ differs of course from the divisor σ_{SC} which we introduced in section 4.1.2. The same applies to c_1, a shorthand for $\pi_X^*(c_1(B))$ we use in the following that differs from $c_1(S)$ used in sections 4.1.2 and 4.1.3.

4.2.2 Resolution of the E_6 Singularity

We will resolve the singularity in the Tate form. As will be made clear in the discussion of G-fluxes, the resolution can be easily obtained from this for the spectral form of section 4.1. The resolution in the spectral form of section 4.1 proceeds in exactly the same way and can be recovered from the following by setting $b_1 = b_2 = 0$. Most importantly, all homological relations between the various divisors, which are crucial for the construction of G-fluxes, carry over unaltered.

4.2.2.1 Resolution in codimension 1

First resolve the geometry in codimension 1. The geometry is singular along

$$x = y = z = 0\,, \tag{4.2.10}$$

along which we blow up by introducing a $\mathbb{P}^2$ with projective coordinates $[x_1, y_1, z_1]$, which are related to the original coordinates by

$$\text{Blow-up 1:} \quad x = \zeta_1 x_1\,, \qquad y = \zeta_1 y_1\,, \qquad z = \zeta_1 z_1\,, \tag{4.2.11}$$

where $\zeta_1 = 0$ gives rise to an exceptional divisor E_1. We repeat this process along all the codimension 1 singular loci

$$\begin{aligned}
&\text{Blow-up 2:} \quad x_1 = x_2\zeta_2\,, \qquad y_1 = y_2\zeta_2\,, \qquad \zeta_1 = \zeta_{12}\zeta_2 \\
&\text{Blow-up 3:} \quad y_2 = y_3\zeta_3\,, \qquad \zeta_2 = \zeta_{123}\zeta_3\,, \qquad \zeta_2 = \zeta_{23}\zeta_3 \\
&\text{Blow-up 4:} \quad y_3 = y_4\zeta_4\,, \qquad \zeta_{123} = \zeta_{1234}\zeta_4\,, \qquad \zeta_3 = \zeta_{34}\zeta_4\,,
\end{aligned} \tag{4.2.12}$$

where each blow-up gives rise to an exceptional divisor E_i specified by $\zeta_i = 0$. After proper transforming the resulting equation, the fourfold, which is now resolved in codimension 1, takes the form

$$\begin{aligned}
0 = &-\zeta_{23}^2\zeta_{34}x_2^3\zeta_{1234} + w\left[y_4^2 + y_4 z_1(\zeta_{23}b_1\zeta_{34}\zeta_4 x_2 + b_3 w z_1)\zeta_{1234}\right] \\
&- w\left[\zeta_{23}\zeta_{34}\zeta_4 z_1^2\zeta_{1234}^2(\zeta_{23}b_2\zeta_{34}\zeta_4 x_2^2 + b_4 w x_2 z_1 + b_6\zeta_{34}\zeta_4^2 w^2 z_1^3\zeta_{1234})\right]\,.
\end{aligned} \tag{4.2.13}$$

This is now a smooth fibration in codimension 1.[6]

[6] One can check explicitly that this is non-singular: every combination of three of the seven sections x_2, y_4, z_1, ζ_{23}, ζ_{34}, ζ_{1234}, ζ_4 either violates one of the projectivity relations or the Tate form has a non-vanishing derivative with respect to it.

4.2.2.2 Resolution in higher codimension

The space (4.2.13) is still singular in higher codimension: setting $b_3 = 0$, the geometry exhibits singularities at the loci $y_4 = \zeta = 0$, where ζ is one of the exceptional sections of the blow-ups. We follow [102] to do the small resolutions, where each small resolution results in a new $\mathbb{P}^1$, characterized by a section δ_i

$$\begin{aligned} y_4 &= \delta_5 y_5\,, & \zeta_{23} &= \delta_5 \zeta_{235}\,, \\ y_5 &= \delta_6 y_6\,, & \zeta_{34} &= \delta_6 \zeta_{346}\,, \\ y_6 &= \delta_7 y_7\,, & \zeta_{1234} &= \delta_7 \zeta_{12347}\,. \end{aligned} \tag{4.2.14}$$

The three new exceptional divisors corresponding to δ_5, δ_6 and δ_7, are denoted by E_5, E_6 and E_7. The fourfold, which is now fully resolved in all codimensions, is then

$$\begin{aligned} & w y_7 \left(\delta_5\delta_6\delta_7 y_7 + \delta_7 z_1 \zeta_{12347}\left(b_1\delta_5\delta_6\zeta_4 x_2 \zeta_{235}\zeta_{346} + b_3 z_1 w\right)\right) \\ &\quad = -\zeta_{235}\zeta_{346}\zeta_{12347}\left(b_6\zeta_{346}\zeta_4^3\delta_6\zeta_{12347}^2\delta_7^2 w^3 z_1^5 + b_4\delta_7\zeta_4 z_1^3 x_2 \zeta_{12347} w^2\right. \\ &\qquad\qquad \left. + b_2\delta_5\delta_6\delta_7\zeta_4^2 z_1^2 x_2^2 \zeta_{235}\zeta_{346}\zeta_{12347} w + \delta_5 x_2^3 \zeta_{235}\right)\,. \end{aligned} \tag{4.2.15}$$

Note that $\zeta_{12347} = 0$ and $\delta_7 = 0$ define the same object in $\tilde{Y}_4$, as one can see from (4.2.15). Hence, not all exceptional divisors are linearly independent anymore in $\tilde{Y}_4$, but there now is an equivalence relation

$$E_1 - E_2 - E_3 - E_4 - E_7 \simeq_{\tilde{Y}_4} E_7\,. \tag{4.2.16}$$

The classes of the various sections are listed in (A.1.1), and the resolved fourfold is in the class

$$[\tilde{Y}_4] = 3\sigma + 6c_1 - 2E_1 - 2E_2 - 2E_3 - 2E_4 - E_5 - E_6 - E_7\,. \tag{4.2.17}$$

4.2.3 Cartan divisors

The Cartan divisors comprise the components of $z = 0$ in the resolved geometry

$$z = \zeta_{235}\zeta_{346}^2\zeta_4^3\delta_5\delta_6^2\delta_7\zeta_{12347} z_1 = 0\,. \tag{4.2.18}$$

We now identify these with negative simple roots of E_6 as well as the root $-\alpha_0$ corresponding to the extended node of the affine E_6 Dynkin diagram. The classes are[7]

Defining Section	Locus in $\tilde{Y}_4$	Class in $\tilde{Y}_4$	Label
$z_1 = 0$	$\delta_7 y_7^2 - \zeta_{235}^2 \zeta_{346} \zeta_{12347} x_2^3 = 0$	$S - E_1$	$\mathcal{D}_{-\alpha_0}$
$\delta_5 = 0$	$-b_6 \delta_6 \zeta_{235} \zeta_{346}^2 - b_4 \zeta_{235} \zeta_{346} x_2 + b_3 y_7 = 0$	E_5	$\mathcal{D}_{-\alpha_1}$
$\delta_6 = 0$	$-b_4 \zeta_4 \zeta_{346} + b_3 y_7 - \delta_5 \zeta_{346} = 0$	E_6	$\mathcal{D}_{-\alpha_2}$
$\zeta_4 = 0$	$b_3 \delta_7 \zeta_{12347} y_7 - \zeta_{346} \zeta_{12347} x_2^3 + \delta_6 \delta_7 y_7^2 = 0$	E_4	$\mathcal{D}_{-\alpha_3}$
$\zeta_{346} = 0$	$b_3 \zeta_{12347} + \delta_5 \delta_6 = 0$	$E_3 - E_4 - E_6$	$\mathcal{D}_{-\alpha_4}$
$\zeta_{235} = 0$	$\delta_5 + b_3 \zeta_{12347} = 0$	$E_2 - E_3 - E_5$	$\mathcal{D}_{-\alpha_5}$
$\zeta_{12347} = 0$	$\delta_7 = 0$	E_7	$\mathcal{D}_{-\alpha_6}$

(4.2.19)

The labeling is consistent with the standard ordering of roots of E_6. The intersection of the Cartan divisors reproduces indeed the extended Cartan matrix of E_6, with $z_1 = 0$ playing the role of the affine root, and the intersections are diagramatically depicted below:

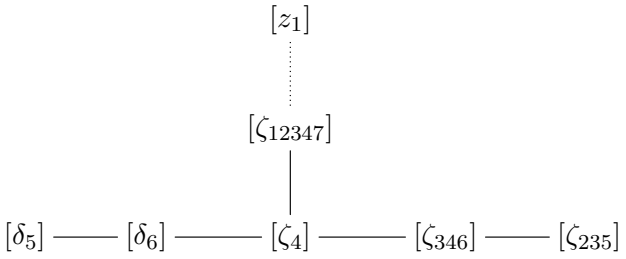

4.2.4 Matter surfaces

Along the codimension 2 subspace $b_3 = 0$ the singularity type enhances further. From the gauge theory point of view matter is generated at these loci. The intersections $\Gamma_i = [b_3] \cdot \mathcal{D}_{-\alpha_i}$ characterize the matter surfaces in X_5, and we expect these to split further such that an additional irreducible component appears in the fiber along $b_3 = 0$. Indeed, as is clear from the equations for the Cartan divisors (4.2.19) the following divisors split

- $\mathcal{D}_{-\alpha_4}$ splits into two components

$$\begin{aligned} \Gamma_{\zeta_{346}\delta_5} : &\quad b_3 = \delta_5 = \zeta_{346} = 0 \\ \Gamma_{\zeta_{346}\delta_6} : &\quad b_3 = \delta_6 = \zeta_{346} = 0\,. \end{aligned} \tag{4.2.20}$$

[7] In writing the locus of the Cartan divisors in $\tilde{Y}_4$ we used the projectivity relations of the blow-ups listed in (A.1.3) to set various sections that cannot vanish to 1.

- $\mathcal{D}_{-\alpha_1}$ splits into three components

$$\begin{aligned} \Gamma_{\zeta_{346}\delta_5}: &\quad b_3 = \delta_5 = \zeta_{346} = 0 \\ \Gamma_{-\alpha_5}: &\quad b_3 = \delta_5 = \zeta_{235} = 0 \\ \Gamma_{\delta_5 b_4}: &\quad b_3 = \delta_5 = b_4 x_2 + b_6\delta_6 = 0\,. \end{aligned} \tag{4.2.21}$$

- $\mathcal{D}_{-\alpha_2}$ splits into two components

$$\begin{aligned} \Gamma_{\zeta_{346}\delta_6}: &\quad b_3 = \delta_6 = \zeta_{346} = 0 \\ \Gamma_{\delta_6 b_4}: &\quad b_3 = \delta_6 = b_4\zeta_4 + \delta_5 = 0\,. \end{aligned} \tag{4.2.22}$$

With $[b_3] = 3c_1 - 2S$, we can now determine the holomogical classes and Cartan charges of the matter divisors. The reducible Cartan divisors split into irreducible components that correspond to weights of the **27** representation of E_6. Indeed, this was observed in [101] and has been explained in generality in [102]. In detail, the charges of the irreducible matter surfaces and their identification in terms of weights of the **27** as listed in Appendix A.2 are

Label	Cartan charges	E_6 Weight
Γ_0	$(0,0,0,0,0,1)$	$-\alpha_0$
Γ_5	$(0,0,0,1,-2,0)$	$-\alpha_5$
Γ_3	$(0,1,-2,1,0,1)$	$-\alpha_3$
Γ_6	$(0,0,1,0,0,-2)$	$-\alpha_6$
$\Gamma_{\zeta_{346}\delta_5}$	$(-1,1,0,-1,1,0)$	$-(\mu_{\mathbf{27}} - \alpha_1 - 2\alpha_2 - 2\alpha_3 - \alpha_4 - \alpha_5 - \alpha_6)$
$\Gamma_{\zeta_{346}\delta_6}$	$(1,-1,1,-1,0,0)$	$\mu_{\mathbf{27}} - \alpha_1 - 2\alpha_2 - 2\alpha_3 - 2\alpha_4 - \alpha_5 - \alpha_6$
$\Gamma_{\delta_6 b_4}$	$(0,-1,0,1,0,0)$	$-(\mu_{\mathbf{27}} - \alpha_1 - \alpha_2 - 2\alpha_3 - 2\alpha_4 - \alpha_5 - \alpha_6)$
$\Gamma_{\delta_5 b_4}$	$(-1,0,0,0,1,0)$	$\mu_{\mathbf{27}} - 2\alpha_1 - 2\alpha_2 - 2\alpha_3 - \alpha_4 - \alpha_6$

(4.2.23)

Adding all the weights in (4.2.23) together – including multiplicities – yields

$$-\alpha_0 - \alpha_1 - 2\alpha_2 - 3\alpha_3 - 2\alpha_4 - \alpha_5 - 2\alpha_6, \tag{4.2.24}$$

which is just the weight of the singular fiber $z = 0$, as expected.

In summary we find that along $b_3 = 0$ the Cartan divisors corresponding to the six roots of E_6 split into three roots and four weights of the **27** (or $\overline{\mathbf{27}}$) representation of E_6. Explicitly, the divisors associated to the roots $-\alpha_0$, $-\alpha_3$, $-\alpha_5$ and $-\alpha_6$ remain irreducible, while

$-\alpha_1$, $-\alpha_2$ and $-\alpha_4$ split according to

$$\begin{aligned}
-\alpha_1 \to & -\alpha_5 + (\mu_{\mathbf{27}} - 2\alpha_1 - 2\alpha_2 - 2\alpha_3 - \alpha_4 - \alpha_6) \\
& - (\mu_{\mathbf{27}} - \alpha_1 - 2\alpha_2 - 2\alpha_3 - \alpha_4 - \alpha_5 - \alpha_6) \\
-\alpha_2 \to & -(\mu_{\mathbf{27}} - \alpha_1 - \alpha_2 - 2\alpha_3 - 2\alpha_4 - \alpha_5 - \alpha_6) \\
& + (\mu_{\mathbf{27}} - \alpha_1 - 2\alpha_2 - 2\alpha_3 - 2\alpha_4 - \alpha_5 - \alpha_6) \\
-\alpha_4 \to & -(\mu_{\mathbf{27}} - \alpha_1 - 2\alpha_2 - 2\alpha_3 - \alpha_4 - \alpha_5 - \alpha_6) \\
& + (\mu_{\mathbf{27}} - \alpha_1 - 2\alpha_2 - 2\alpha_3 - 2\alpha_4 - \alpha_5 - \alpha_6)\,.
\end{aligned} \tag{4.2.25}$$

We made a specific choice when resolving the higher codimension singularities, and there is in fact a network of small resolutions, connected as in [133] by flop transitions. In particular, for each of these the fiber in codimension 2 will split into different sets of weights of the **27** [102].

4.2.5 Yukawa interactions

The codimension 3 locus of enhanced symmetry is characterized by $z = b_3 = b_4 = 0$, along which the fourfold equation reduces to

$$\begin{aligned}
0 = & \delta_5\delta_6\delta_7 y_7^2 - \delta_5\zeta_{235}^2\zeta_{346}\zeta_{12347}x_2^3 + b_1\delta_5\delta_6\delta_7\zeta_{47}\zeta_{235}\zeta_{346}\zeta_{12347}\zeta_{01}x_2y_7 \\
& - b_2\delta_5\delta_6\delta_7\zeta_{47}^2\zeta_{235}^2\zeta_{346}^2\zeta_{12347}^2\zeta_{01}^2x_2^2 - b_6\delta_6\delta_7^2\zeta_{47}^3\zeta_{235}\zeta_{346}^2\zeta_{12347}^3\zeta_{01}^5\,.
\end{aligned} \tag{4.2.26}$$

All matter surfaces remain irreducible except for

$$\Gamma_{\delta_5 b_4}: \qquad \delta_5 = b_4x_2 + b_6\delta_6\zeta_{346} = 0\,, \tag{4.2.27}$$

which splits into two components in the classes

$$([b_4]-[\delta_6])\cdot[\delta_5]\cdot([b_3]-[\zeta_{235}]-[\zeta_{346}]) \qquad \text{and} \qquad [\delta_6]\cdot[\delta_5]\cdot([b_3]-[\zeta_{235}]-[\zeta_{346}])\,. \tag{4.2.28}$$

Their respective Cartan charges are

$$(-1,1,0,-1,1,0) \qquad \text{and} \qquad (0,-1,0,1,0,0)\,, \tag{4.2.29}$$

which are Cartan charges of other matter divisors, adding up to the Cartan charge of the corresponding matter surface $(-1,0,0,0,1,0)$. Thus at the locus $b_3 = b_4 = 0$, three

matter surfaces become homologous, corresponding to the Yukawa interaction

$$\begin{aligned} (-1,0,0,0,1,0) \quad &\to \quad (-1,1,0,-1,1,0)+(0,-1,0,1,0,0) \\ \mu_{\mathbf{27}}-2\alpha_1-2\alpha_2-3\alpha_3-\alpha_4-\alpha_6 \quad &\to \quad -(\mu_{\mathbf{27}}-\alpha_1-2\alpha_2-2\alpha_3-\alpha_4-\alpha_5-\alpha_6) \\ &\quad\ -(\mu_{\mathbf{27}}-\alpha_1-\alpha_2-2\alpha_3-2\alpha_4-\alpha_5-\alpha_6) \end{aligned} \tag{4.2.30}$$

This exactly amounts to the generation of a $\mathbf{27}\times\mathbf{27}\times\mathbf{27}$ Yukawa coupling at the $b_3 = b_4 = 0$ locus.

4.2.6 Chern classes of the resolved Fourfold

We are interested eventually in the construction of G-flux satisfying the quantization condition

$$G+\frac{1}{2}c_2(\tilde{Y}_4)\in H^4(\tilde{Y}_4,\mathbb{Z})\,, \tag{4.2.31}$$

for which we require the second Chern class of the resolved fourfold. A complementary approach to calculating Chern classes for $SU(N)$ and $Sp(N)$ fibrations can be found in [139]. We start by working out the Chern classes of the singular fourfold Y_4: The total Chern class of the whole space X_5 is

$$c(X_5)=c(B)(1+\sigma)(1+\sigma+2c_1)(1+\sigma+3c_1)\,. \tag{4.2.32}$$

The total Chern class of Y_4 (and especially $c_2(Y_4)$) then follows by adjunction

$$c(Y_4)=\left.\frac{c(X_5)}{1+3\sigma+6c_1}\right|_{Y_4}=1+c_2+11c_1^2+4c_1\sigma+c_3(Y_4)+c_4(Y_4)\,. \tag{4.2.33}$$

Here, $c_i := \pi_X^* c_i(B)$ and we used (A.1.2) and $\sigma\cdot_{Y_4}(\sigma+3c_1)=0$, the latter being a consequence of one of the formulae in the former.

To calculate the Chern classes of the resolved fourfold, we proceed by first calculating the Chern classes of $\tilde{X}_5$, using a general result from [140]: If one blows up a nonsingular subvariety A which is the complete intersection of d hypersurfaces $Z_1,\ldots,Z_d$ of a nonsingular variety X to a new subvariety E obtaining a blown-up $\tilde{X}$, and defines the following commutative diagram

$$\begin{array}{ccc} E & \xhookrightarrow{j} & \tilde{X} \\ \downarrow{\scriptstyle g} & & \downarrow{\scriptstyle f} \\ A & \xhookrightarrow{i} & X \end{array}$$

then

$$c(\tilde{X}) = \frac{(1+[E])(1+f^*[Z_1]-[E])\cdots(1+f^*[Z_d]-[E])}{(1+f^*[Z_1])\cdots(1+f^*[Z_d])}\cdot f^*c(X)\,. \tag{4.2.34}$$

As all our blow-ups and small resolutions occur along loci described by the simultaneous vanishing of several sections, we can apply this formula, with the $[Z_i]$ being the classes of these sections. The requirement that the varieties A and X be nonsingular does not pose a problem, since we can think of blowing up (regular) hypersurfaces in X_5 and passing on to $\tilde{Y}_4$ only after having done all the resolutions. With this, we compute the total Chern class of $\tilde{X}_5$ and then, with the adjunction formula, the total Chern class of $\tilde{Y}_4$. We obtain $c_1(\tilde{Y}_4) = 0$, as required, and

$$\begin{aligned} c_2(\tilde{Y}_4) =& c_2 + 11c_1^2 + 13c_1\sigma + 3\sigma^2 \\ &- 4c_1E_1 - E_1^2 - 7c_1E_2 + 2E_1E_2 - 12c_1E_3 + 4E_1E_3 + 4E_2E_3 + E_3^2 \\ &- 15c_1E_4 + 5E_1E_4 + 4E_2E_4 + 6E_3E_4 + 2E_4^2 - 6c_1E_5 + E_1E_5 + 3E_2E_5 \\ &+ 2E_3E_5 + 4E_4E_5 - 6c_1E_6 + E_1E_6 + 3E_2E_6 + 3E_3E_6 + 3E_4E_6 + E_5E_6 \\ &- 6c_1E_7 + 2E_1E_7 + 2E_2E_7 + 2E_3E_7 + 2E_4E_7 + E_5E_7 + E_6E_7 + E_1S\,, \end{aligned} \tag{4.2.35}$$

where all E_i-independent terms located in the first line correspond to $c_2(Y_4)$.

We also find the Euler character $\chi(\tilde{Y}_4)$ by computing the top chern class. Nicely, the result can be written as the sum of the Euler character of the singular manifold $\chi(Y_4)$ and an intersection on S

$$\begin{aligned} \chi(\tilde{Y}_4) &= 3\int_B \left(120c_1^3 + 4c_1c_2 - 258c_1^2S + 183c_1S^2 - 42S^3\right) \\ &= \chi(Y_4) - 9\int_S \left(86c_1^2 - 61c_1S + 14S^2\right). \end{aligned} \tag{4.2.36}$$

This confirms by direct computation the result conjectured in [118] from heterotic/F-theory duality for an E_6 singularity.

4.3 G-flux for E_6

We are now in the position to construct G-fluxes for the E_6 singularity, both directly in terms of linear combination of holomorphic surfaces in $\tilde{Y}_4$, as well as using the proposal in terms of the spectral divisor and local fluxes made in section 4.1.

4.3.1 Direct construction in $\tilde{Y}_4$

4.3.1.1 General conditions on G

In constructing G-flux directly from holomorphic surfaces, we will restrict to fluxes that arise from intersections only. There are various conditions on the surfaces that comprise a consistent G-flux. In particular, they have to satisfy orthogonality with respect to surfaces that are pull-backs from horizontal or vertical surfaces in Y_4. Therefore, if D, D_1 and D_2 are pullbacks of divisors in B, we require

$$\sigma \cdot_{\tilde{Y}_4} D \cdot_{\tilde{Y}_4} G = D_1 \cdot_{\tilde{Y}_4} D_2 \cdot_{\tilde{Y}_4} G = 0\,. \tag{4.3.1}$$

This restricts us to two building blocks for G, namely intersections of exceptional divisors with divisors inherited from B (Cartan fluxes), i.e. $E_i \cdot_{\tilde{Y}_4} D$, and intersections of exceptional divisors with other exceptional divisors $E_i \cdot_{\tilde{Y}_4} E_j$. We furthermore want to require that the flux does not break the E_6 gauge symmetry, and thus has to satisfy

$$G \cdot_{\tilde{Y}_4} \mathcal{D}_{-\alpha_i} \cdot_{\tilde{Y}_4} D = 0\,. \tag{4.3.2}$$

Both the Cartan fluxes and the pairwise intersections will intersect the Cartan divisors nontrivially and break the E_6 symmetry. The question is then to find linear combinations with vanishing intersections. One can check that the pairwise intersections $E_i \cdot_{\tilde{Y}_4} E_j$ always intersect Cartan surfaces proportional to linear combinations of

$$S \cdot_{\tilde{Y}_4} D \cdot_{\tilde{Y}_4} S \qquad \text{and} \qquad S \cdot_{\tilde{Y}_4} D \cdot_{\tilde{Y}_4} c_1\,. \tag{4.3.3}$$

Hence, the only Cartan fluxes that can be cancelled by pairwise intersection fluxes are of the form

$$E_i \cdot_{\tilde{Y}_4} c_1 \qquad \text{or} \qquad E_i \cdot_{\tilde{Y}_4} S\,. \tag{4.3.4}$$

This gives us an a priori 42-dimensional space. As worked out in detail in Appendix A.1, there are 26 divisor relations on this space. Thus, it can be parametrized with a 16-dimensional basis of surfaces. We will use the 16 surfaces

$$\{E_i \cdot c_1\,,\ E_i \cdot S\,,\ E_3 \cdot E_5\,,\ E_3 \cdot E_6\}\,. \tag{4.3.5}$$

4.3.1.2 Quantization of G

Before evaluating the constraint (4.3.2), we check quantization of the G-flux (3.5.1) with the second Chern class of the resolved manifold (4.2.35). The class $c_2(\tilde{Y}_4)$ can be rewritten by means of (A.1.8, A.1.9, A.1.10) so that it only contains $c_2(Y_4)$ and the 16 basis surfaces

$$\begin{aligned} c_2(\tilde{Y}_4) =& c_2(Y_4) + S\cdot(3E_1 - E_2 - E_3 - E_4 + 3(E_5+E_6) - 4E_7) \\ & - c_1\cdot(10E_1 + E_2 - E_4 + 6E_5 + 4E_6 - 6E_7) + E_2\cdot E_5 - E_3\cdot E_6\,. \end{aligned} \tag{4.3.6}$$

Since $c_2(Y_4)$ is an even class, as was shown in [141], we deduce that

$$c_2(\tilde{Y}_4) = S\cdot(E_1+E_2+E_3+E_4+E_5+E_6)+c_1\cdot(E_2+E_4)+E_2\cdot E_5+E_3\cdot E_6+\text{even}\,. \tag{4.3.7}$$

So a quantized general G-flux can be described by integers a_i, b_i, p, q with

$$\begin{aligned} G =& \frac{1}{2}\left(S\cdot(E_1+E_2+E_3+E_4+E_5) + c_1\cdot(E_2+E_4) + E_2\cdot E_5 + E_5\cdot E_6\right) \\ & + \sum_{i=1}^{7} E_i\cdot(a_i c_1 + b_i S) + pE_3\cdot E_5 + qE_3\cdot E_6\,. \end{aligned} \tag{4.3.8}$$

Though sufficient, this is not a necessary condition and can sometimes be relaxed [139], e.g. for special cases of c_1 or S.

4.3.1.3 E_6-invariance of G and chirality

With this form of the flux, the condition of unbroken E_6 gauge symmetry (4.3.2) can now be evaluated and the resulting solution space has three integral parameters (a_1, b_1, N)

$$\begin{aligned}
a_2 &= 3N - a_1 + 1 & b_2 &= -2(1+N) - b_1 \\
a_3 &= -3 - 6N - a_1 & b_3 &= 1 + 4N - b_1 \\
a_4 &= 1 + 3N - a_1 & b_4 &= -2(1+N) - b_1 \\
a_5 &= -3 - 6N & b_5 &= 3 + 7N \\
a_6 &= 0 & b_6 &= -1 - N \\
a_7 &= -2a_1 & b_7 &= -1 - 2b_1 \\
p &= -2 - 3N & q &= 1 + 3N\,.
\end{aligned} \tag{4.3.9}$$

This results in the E_6-invariant G-flux

$$\begin{aligned}
G = \frac{1}{2}\,[&3(1+2N)(c_1\cdot(E_2 - 2E_3 + E_4 - 2E_5) - E_2\cdot E_5 + E_3\cdot E_6) \\
&- S\cdot(-E_1 + 3E_2 - 3E_3 + 3E_4 - 7E_5 + E_6 + 2E_7 \\
&\quad +2(2E_2 - 4E_3 + 2E_4 - 7E_5 + E_6)N)] \\
&+ (E_1 - E_2 - E_3 - E_4 - 2E_7)\cdot(a_1 c_1 + b_1 S)\,.
\end{aligned} \tag{4.3.10}$$

Note that since $\zeta_{12347} = 0$ and $\delta_7 = 0$ describe the same locus in the resolved geometry, the class of the last term in (4.3.10) which is $[\zeta_{12347}] - [\delta_7]$, is equivalent to zero. Thus, a_1 and b_1 do not have any physical relevance and will cancel out of all further computations. Finally, subtracting the (homologically zero) term $\frac{1}{2}S\cdot(E_1 - E_2 - E_3 - E_4 - 2E_7)$ from (4.3.10), the final expression for the G-flux is

$$\begin{aligned}
G = \frac{1}{2}\,(1+2N)\,[&3c_1\cdot(E_2 - 2E_3 + E_4 - 2E_5) - 3E_2\cdot E_5 + 3E_3\cdot E_6 \\
&- S\cdot(2E_2 - 4E_3 + 2E_4 - 7E_5 + E_6)]\,.
\end{aligned} \tag{4.3.11}$$

As an application, we compute the chirality induced by this G-flux, which is the intersection of G with the **27** matter surface $\mathcal{S}_{\mathbf{27}}$ from (4.3.30)

$$G \cdot_{\tilde{Y}_4} \mathcal{S}_{\mathbf{27}} = -\frac{1}{2}(1+2N)S \cdot_B (6c_1 - 5S) \cdot_B (3c_1 - 2S)\,. \tag{4.3.12}$$

Not only can this be written as an intersection in S, it also matches the result that one finds when computing the induced chirality in local models (cf. 4.3.2.3)

$$G \cdot_{\tilde{Y}_4} \mathcal{S}_{\mathbf{27}} = -\frac{1}{2}(1+2n)\eta \cdot_S (\eta - 3c_1(S))\,. \tag{4.3.13}$$

The same goes for the induced D3-tadpole. For the G-flux in the resolved geometry, we find

$$n_{\text{D3,induced}} = \frac{1}{2}G \cdot_{\tilde{Y}_4} G = \frac{3}{8}(1+2N)^2\, S \cdot_B (6c_1 - 5S) \cdot_B (3c_1 - 2S)\,, \tag{4.3.14}$$

where the local computation (see section 4.3.2.3) yields

$$n_{\text{D3,induced}} = \frac{3}{8}(1+2n)^2\, \eta \cdot_S (\eta - 3c_1(S))\,. \tag{4.3.15}$$

Again, the two results match.

4.3.2 Local Limit and Spectral Divisor

In this section, we relate our global description of the fourfold with local spectral cover models, and demonstrate how to use the spectral divisor formulation explained in section 4.1.

4.3.2.1 The Spectral Divisor in the resolved Fourfold

The spectral divisor (4.1.14) in the resolved fourfold naively reads

$$w^2 z_1^2 \delta_7 \zeta_{12347} \left(-b_3 y_7 + \zeta_4 z_1 \zeta_{235}\zeta_{346}\zeta_{12347}\left(b_4 x_2 + b_6 w \zeta_4^2 z_1^2 \zeta_{346}\delta_6\delta_7\zeta_{12347}\right)\right). \tag{4.3.16}$$

As we explained earlier, the actual spectral divisor is the irreducible component of this. The above divisor has a component $(\delta_5 = 0)|_{\tilde{Y}_4}$, as one can see from (4.2.15), and subtracting this results in the spectral divisor

$$\mathcal{C}_{\text{spectral}}: \qquad [-b_3 y_7 + \zeta_4 z_1 \zeta_{235}\zeta_{346}\zeta_{12347}\left(b_4 x_2 + b_6 w \zeta_4^2 z_1^2 \zeta_{346}\delta_6\delta_7\zeta_{12347}\right)]|_{\tilde{Y}_4} - [\delta_5]|_{\tilde{Y}_4} \tag{4.3.17}$$

which is in the class

$$[\mathcal{C}_{\text{spectral}}] = \sigma + 6c_1 - E_1 - E_2 - E_3 - E_4 - 2E_5 - E_6 - E_7 - 2S\,. \tag{4.3.18}$$

For an N-fold spectral cover model, the spectral divisor should intersect with the Cartan divisors in N times the weight corresponding to the representation, that in the local limit corresponds to the highest weight of a single sheet. In the case of E_6 this is three times the highest weight of the **27**. Indeed, intersecting the spectral divisor with the Cartan divisors yields

$$(3, 0, 0, 0, 0, 0) = 3\mu_{\mathbf{27}}\,. \tag{4.3.19}$$

4.3.2.2 Local limit and $\mathcal{C}_{\mathbf{SC}}$

From the singular form of the spectral divisor it is clear (by construction) that the Higgs bundle spectral cover emerges from the divisor (4.3.17). In the resolved geometry this is less clear. To demonstrate this we first need to establish what the local limit corresponds to in $\tilde{Y}_4$ and then apply this to the spectral divisor (4.3.17).

To identify the local limit, recall first that

$$\begin{aligned} x &= \zeta_{235}^2\zeta_{346}^3\zeta_4^4\delta_5^2\delta_6^3\delta_7^2 x_2 \\ y &= \zeta_{235}^2\zeta_{346}^4\zeta_4^6\delta_5^3\delta_6^5\delta_7^3 y_7 \\ z &= \zeta_{235}\zeta_{346}^2\zeta_4^3\delta_5\delta_6^2\delta_7^2 z_1\,, \end{aligned} \tag{4.3.20}$$

where we replaced ζ_{12347} by δ_7, as they describe the same locus in $\tilde{Y}_4$. The local limit parameters are then

$$\begin{aligned} t &= \frac{y}{x} = \frac{y_7\zeta_{346}\zeta_4^2\delta_5\delta_6^2\delta_7}{x_2} \\ s &= \frac{zx}{y} = \frac{z_1 x_2 \zeta_{235}\zeta_{346}\zeta_4\delta_7}{y_7}\,, \end{aligned} \tag{4.3.21}$$

so that the limit $t, z \to 0$ with $s = z/t$ fixed, corresponds to

$$\delta_5 \delta_6 \to 0\,. \tag{4.3.22}$$

In fact (as we show later in this section), the proper local limit for the spectral divisor — i.e. the one yielding the full spectral cover equation — in the resolved geometry is $\delta_5 \to 0$. The limit $\delta_6 \to 0$ on the other hand only reproduces the spectral cover equation in the patch $\delta_6 = 0$.

With this insight, we now apply the local limit to the spectral divisor (4.3.17). In particular we will show that the restriction of the spectral divisor to $\delta_5 = 0$ yields the spectral cover

$$\mathcal{C}_{\text{SC}} = \mathcal{C}_{\text{spectral}} \cdot_{\tilde{Y}_4} [\delta_5]\,. \tag{4.3.23}$$

The blow-up relations (A.1.3), with δ_5 set to zero, imply that the equations for the spectral divisor and the Calabi-Yau fourfold can be reduced to

$$\begin{aligned} 0 &= \delta_5 \\ 0 &= b_3 y_7 - \zeta_{235}\zeta_{346}\left(b_6 \zeta_{346}\delta_6 + b_4 x_2\right)\,. \end{aligned} \tag{4.3.24}$$

Note that $\zeta_{235} = 0$ would imply $\delta_6 y_7 = 0$, which violates the blow-up relations, so that one can set $\zeta_{235} = 1$. Finally, recall that the spectral divisor equation is $x^3 = y^2$. Going into the $x_2 \neq 0$ patch and plugging the spectral divisor equation, which reduces to $y_7^2 = \zeta_{346}$, into the Calabi-Yau condition, we obtain

$$0 = y_7\left(-b_3 + b_4\delta_6 y_7 + b_6 \delta_6^2 y_7^3\right)\,, \tag{4.3.25}$$

which in the $\delta_6 \neq 0$ patch, after removing a factor of y_7, is precisely the local equation for the SC

$$\mathcal{C}_{\text{SC}}: \qquad 0 = -b_3 + b_4 y_7 + b_6 y_7^3\,. \tag{4.3.26}$$

For $\delta_6 = 0$, (4.3.25) simply gives

$$0 = -b_3 y_7\,. \tag{4.3.27}$$

This should describe the spectral cover in the $\delta_6 = 0$ patch. We now check that this is consistent with restricting the spectral divisor in the resolved geometry to $\delta_6 = 0$. Again using the blow-up relations where $\delta_6 = 0$ reduces the spectral divisor equation and the Calabi-Yau equation simplify to

$$0 = \delta_6 = b_3 y_7 - b_4 \zeta_{346}\zeta_4 = b_3 y_7 - b_4\zeta_{346}\zeta_4 - \zeta_{346}\delta_5\,. \tag{4.3.28}$$

The difference of the last two equations thus implies $\zeta_{346} = 0$ or $\delta_5 = 0$. While the latter will be a special case of having just $\delta_5 = 0$, which we discussed above, the former simply yields for the spectral divisor

$$0 = b_3 y_7 \,. \tag{4.3.29}$$

This is in fact the equation for the spectral cover we expected from (4.3.27). Note that the **27** matter surface, which can be characterized by

$$\mathcal{S}_{\mathbf{27}} = E_6 \cdot (E_3 - E_4 - E_6) \,, \tag{4.3.30}$$

meets $\mathcal{C}_{\rm SC}$ exactly along the curve

$$y_7 = b_3 = 0 \,. \tag{4.3.31}$$

4.3.2.3 Spectral Cover flux in local E_6 models

We first construct the universal spectral cover flux for the E_6 model and in the next section use the spectral divisor to obtain its global version.

Spectral cover fluxes, as summarized in section 4.1, are constructed from line bundles over the spectral cover. The commutant of E_6 in E_8 is $SU(3)$, so that we are considering $SU(3)$ gauge bundles, that are obtained from push-forwards of line bundles L on the spectral cover. Starting with the tracelessness condition (4.1.18), we consider a divisor γ satisfying $p_*(\gamma) = 0$ and write

$$c_1(L) = \frac{1}{2} r + \gamma \,. \tag{4.3.32}$$

Generically, γ is a one-parameter family of divisors, given by (4.1.21) (for E_6, see also [116, 142])

$$\gamma = \alpha \left(3\sigma_{\rm SC} - \pi^*(\eta - 3c_1(S))\right) \,. \tag{4.3.33}$$

This flux needs to then be properly quantized. Indeed, to have $\gamma + \frac{1}{2} r$ integral, we require $\alpha = \frac{1}{2}(2n+1)$ with an integer n and thus

$$\gamma = \frac{1}{2}(2n+1) \left(3\sigma_{\rm SC} - \pi^*(\eta - 3c_1(S))\right) \,. \tag{4.3.34}$$

For completeness we compute some of the flux-related local data. The D3-brane charge induced by this flux is, as we already quoted above,

$$n_{\rm D3,induced} = -\frac{1}{2}\gamma \cdot_{\mathcal{C}_{\rm SC}} \gamma = \frac{3}{8}(2n+1)^2 \eta \cdot_S (\eta - 3c_1(S)) \,. \tag{4.3.35}$$

Furthermore, the chirality induced on the matter curve

$$[\Sigma_{\mathbf{27}}] = \mathcal{C}_{\rm SC} \cdot \sigma_{\rm SC} = (3\sigma_{\rm SC} + \pi^*\eta) \cdot \sigma_{\rm SC} \tag{4.3.36}$$

is the intersection with the flux γ

$$n_{\mathbf{27}} - n_{\overline{\mathbf{27}}} = \gamma \cdot [\Sigma_{\mathbf{27}}] = -\frac{1}{2}(2n+1)\ \eta \cdot_S (\eta - 3c_1(S))\,. \tag{4.3.37}$$

4.3.2.4 Spectral divisor flux

We are now ready to construct the spectral divisor fluxes, as outlined in section 4.1. First construct surfaces that correspond to curves inside $\mathcal{C}_{\rm SC}$, following the procedure outlined in [101,131]. There are two types of surfaces, given in (4.1.25): one arises from intersecting $\mathcal{C}_{\rm spectral}$ with σ, the other corresponds to p^*D, where D intersects S in a curve Σ (which as explained in the last subsection, can be used to engineer spectral cover fluxes) and p is the projection map

$$p: \quad \mathcal{C}_{\rm SC} \ \to\ S\,. \tag{4.3.38}$$

Subtractions have to be made from the fluxes in (4.1.25) in order to make them orthogonal to all horizontal and vertical divisors. Solving this condition results in

$$\begin{aligned} \mathcal{S}_{p^*D} &= \mathcal{C}_{\rm spectral} \cdot D - (\sigma + 6c_1 - 2S) \cdot D \\ &= -(E_1 + E_2 + E_3 + E_4 + 2E_5 + E_6 + E_7) \cdot D\,. \end{aligned} \tag{4.3.39}$$

Next, consider $\mathcal{S}_{\sigma_{\rm SC}}$. This should be a surface that contains (4.3.31) inside $\delta_5 = 0$. Such an object is $\delta_6 = \zeta_{346} = 0$. This, though, has non-zero intersections with Cartan surfaces $\mathcal{D}_{-\alpha_i} \cdot D$ other than α_1, hence its Cartan charge differs from $\mu_{\mathbf{27}}$. We are able to correct this using other Cartan fluxes though, so the surface class which we identify with $\mathcal{S}_{\sigma_{\rm SC}}$ is

$$\begin{aligned} \mathcal{S}_{\sigma_{\rm SC}} &= [\delta_6] \cdot_{\tilde{Y}_4} [\zeta_{346}] + [b_3] \cdot_{\tilde{Y}_4} (E_2 + E_3 + E_7) \\ &= (E_3 - E_4 - E_6) \cdot_{\tilde{Y}_4} E_6 + (3c_1 - 2S) \cdot_{\tilde{Y}_4} (E_2 + E_3 + E_7)\,. \end{aligned} \tag{4.3.40}$$

In fact, the correction is exactly the homological class of the Cartan roots $-(\alpha_1 + 2\alpha_2 + 2\alpha_3 + 2\alpha_4 + \alpha_5 + \alpha_6)$ which precisely amounts for the deviation of the Cartan charges of the matter surface $\Gamma_{\zeta_{346}\delta_6}$ in (4.2.23) from $\mu_{\mathbf{27}}$. Using (4.3.39) and (4.3.40), the traceless G-flux with

$$D = p^*(\eta - 3c_1(S)) = p^*(3c_1 - 2S) \tag{4.3.41}$$

that corresponds to the universal flux γ obtained in section 4.3.2.3 is

$$\begin{aligned} G_{\text{spectral}} &= \frac{1}{2}(2n+1)\left(3\mathcal{S}_{\sigma_{\text{SC}}} - \mathcal{S}_{p^*(3c_1-2S)}\right) \\ &= \frac{1}{2}(2n+1)(3E_2\cdot E_5 - 3E_3\cdot E_6 + 3c_1\cdot(E_1 - 2E_2 + E_3 - E_4 + 2E_5 - 2E_7) \\ &\qquad + S\cdot(-2E_1 + 4E_2 - 2E_3 + 4E_4 - 7E_5 + E_6 - 4E_7))\,, \end{aligned} \tag{4.3.42}$$

where (A.1.8, A.1.9, A.1.10) were used in the last step. Finally, subtracting the trivial class $[b_3]\cdot([\zeta_{12347}] - [\delta_7])$ results in

$$\begin{aligned} G_{\text{spectral}} = \frac{1}{2}(2n+1)(3E_2\cdot E_5 - 3E_3\cdot E_6 - 3c_1\cdot(E_2 - 2E_3 + E_4 - 2E_5) \\ + S\cdot(2E_2 - 4E_3 + 2E_4 - 7E_5 + E_6))\,. \end{aligned} \tag{4.3.43}$$

This spectral divisor flux therefore precisely matches the result for the global G-flux that we constructed directly from linear combinations of surfaces in (4.3.11).

Chapter 5

Tate Trees for Elliptic Fibrations with Rank one Mordell-Weil Group

Section 3.6 has discussed the phenomenological relevance of a systematic understanding of F-theory compactifications with additional abelian gauge factors. There are several models with abelian gauge groups in the literature, from the factored spectral cover models of [104–106] and their lifts to models in $\mathbb{P}_{[1,2,3]}$ [80, 107], to models based on the top construction of toric geometry [111] with both a single [2, 108–110] and multiple extra $U(1)$s [2, 79, 109, 143–146]. While these references provide an abundance of examples for elliptic fibrations with $SU(5) \times U(1)^k$ gauge groups, they do not attempt to classify all possible F-theory compactifications with additional $U(1)$s, and therefore cannot pose efficient constraints on phenomenological models in F-theory.

Finding all F-theory compactifications with additional abelian gauge factors can be translated into classifying singular elliptic fibrations with non-trivial, non-torsion Mordell-Weil group, as was seen in section 3.4. The classification of all singular elliptic fibrations with a trivial Mordell-Weil group has been given in section 2.4, using Tate's algorithm to give an explicit construction of all such fibrations as sextic hypersurfaces in $\mathbb{P}_{[1,2,3]}$. In this chapter, we apply a variant of Tate's algorithm to quartic hypersurfaces in $\mathbb{P}_{[1,1,2]}$, in order to classify all singular fibrations with rank one Mordell-Weil group.

Thereby, we find all possible realizations of F-theory models with a single extra $U(1)$. We also explicitly construct the list of allowed $U(1)$ charges for models with non-abelian

gauge factor $SU(5)$, which are of relevance for GUT model building in string theory. This chapter is based on [67].

5.1 Elliptic Fibrations with extra sections and Tate Trees

The purpose of this section is to collect general structural properties of Tate's algorithm for elliptic fibrations with rank one Mordell-Weil group. Such fibrations can be realized as quartics in $\mathbb{P}_{[1,1,2]}$, which we will review in section 5.1.1. The singular fibers are characterized by their Kodaira type as well as the separation of the two rational sections in the singular fiber. The resulting enhancement structure is tree-like and we collect general properties of this Tate tree in sections 5.1.2 and 5.1.3. In the remaining sections 5.1.4, 5.1.5 and 5.1.6 we determine the starting points of the algorithm, which are I_1 and I_2 fibers with different section separation, and discuss symmetries (lops) which map quartics, which describe the same fiber type, but have different vanishing orders, into each other. We give a summary of the results of each section at the start, allowing the reader to skip the rather technical proofs. Section 5.1.7 summarizes the resolution of the singular fibrations, which are used throughout the algorithm in order to determine the fiber types.

5.1.1 Rank one Mordell-Weil group

An elliptic curve with rank one Mordell-Weil group can be realized in terms of homogeneous quartic polynomials in the weighted projective space $\mathbb{P}_{[1,1,2]}$, as shown in section 2.2, or alternatively in $\mathrm{Bl}_{[0,1,0]}\mathbb{P}_{[1,1,2]}$, which is the blow-up at $[0,1,0]$ of $\mathbb{P}_{[1,1,2]}$ [112]. More precisely, let $[\tilde{w} : x : \tilde{y}]$ be the coordinates of the weighted projective space $\mathbb{P}_{[1,1,2]}$. Blowing this up at $\tilde{w} = \tilde{y} = 0$ yields an exceptional divisor $s = 0$ and new coordinates $\tilde{w} = sw$, $\tilde{y} = sy$. The projective relation from this new divisor is $[w : y]$, as well as the relation $[sw : x : sy]$. Consider the homogeneous polynomial of degree four in $\mathrm{Bl}_{[0,1,0]}\mathbb{P}_{[1,1,2]}$

$$\mathcal{Q}: \qquad \mathfrak{c}_0 w^4 s^3 + \mathfrak{c}_1 w^3 s^2 x + \mathfrak{c}_2 w^2 s x^2 + \mathfrak{c}_3 w x^3 = y^2 s + \mathfrak{b}_0 x^2 y + \mathfrak{b}_1 y w s x + \mathfrak{b}_2 w^2 s^2 y\,. \quad (5.1.1)$$

We consider singular elliptic fibrations, where the fiber is realized in terms of the quartic (5.1.1). In this case, the $\mathfrak{b}_i$, $\mathfrak{c}_i$ are sections of suitable line bundles on the base B of the fibration, described in more detail in section 5.1.7. The goal of this paper is to determine conditions on the coefficients $\mathfrak{b}_i$ and $\mathfrak{c}_i$ for them to realize Kodaira singular fibers above a codimension one locus $z = 0$.

By shifting and scaling the y coordinate, the quartic can be put into the form

$$\mathfrak{c}_0 w^4 s^3 + \mathfrak{c}_1 w^3 s^2 x + \mathfrak{c}_2 w^2 s x^2 + \mathfrak{c}_3 w x^3 = s y^2 + \mathfrak{b}_0 x^2 y\,, \tag{5.1.2}$$

possibly with new $\mathfrak{b}_i$ and $\mathfrak{c}_i$. The rational points $\sigma_0 = [0:1:0]$ and $\sigma_1 = [0:1:-\mathfrak{b}_0]$ of this elliptic curve in the blow-up are

$$\begin{aligned} \sigma_0 :&\qquad s = 0,\ x = 1,\ y = \mathfrak{c}_3,\ w = \mathfrak{b}_0 \\ \sigma_1 :&\qquad w = 0,\ y = 1,\ s = -\mathfrak{b}_0 x^2\,. \end{aligned} \tag{5.1.3}$$

The elliptic curve (5.1.2) has a representation in terms of a Weierstrass model, for instance with respect to the zero-section σ_0 the Weierstrass form is given by [112]

$$\hat{y}^2 = \hat{x}^3 + \left(\mathfrak{c}_1\mathfrak{c}_3 - \mathfrak{b}_0^2\mathfrak{c}_0 - \frac{\mathfrak{c}_2^2}{3}\right)\hat{x}\hat{w}^4 + \left(\mathfrak{c}_0\mathfrak{c}_3^2 - \frac{1}{3}\mathfrak{c}_1\mathfrak{c}_2\mathfrak{c}_3 + \frac{2}{27}\mathfrak{c}_2^3 - \frac{2}{3}\mathfrak{b}_0^2\mathfrak{c}_0\mathfrak{c}_2 + \frac{\mathfrak{b}_0^2\mathfrak{c}_1^2}{4}\right)\hat{w}^6\,. \tag{5.1.4}$$

The singular loci of the elliptic curve (5.1.2) are characterized by the vanishing of the discriminant

$$\begin{aligned} \Delta = 256\big(&64\mathfrak{b}_0^6\mathfrak{c}_0^3 - 16\mathfrak{c}_0^2\left(8\mathfrak{b}_0^4\mathfrak{c}_2^2 + 12\mathfrak{b}_0^4\mathfrak{c}_1\mathfrak{c}_3 - 36\mathfrak{b}_0^2\mathfrak{c}_2\mathfrak{c}_3^2 + 27\mathfrak{c}_3^4\right) + \\ &+ 8\mathfrak{c}_0\left(8\mathfrak{c}_2^3\left(\mathfrak{b}_0^2\mathfrak{c}_2 - \mathfrak{c}_3^2\right) + 4\mathfrak{c}_1\mathfrak{c}_2\mathfrak{c}_3\left(9\mathfrak{c}_3^2 - 10\mathfrak{b}_0^2\mathfrak{c}_2\right) + 3\mathfrak{c}_1^2\left(6\mathfrak{b}_0^4\mathfrak{c}_2 - \mathfrak{b}_0^2\mathfrak{c}_3^2\right)\right) + \\ &+ \mathfrak{c}_1^2\left(-27\mathfrak{b}_0^4\mathfrak{c}_1^2 + 16\mathfrak{c}_2^2\left(\mathfrak{c}_3^2 - \mathfrak{b}_0^2\mathfrak{c}_2\right) + 8\mathfrak{c}_1\left(9\mathfrak{b}_0^2\mathfrak{c}_2\mathfrak{c}_3 - 8\mathfrak{c}_3^3\right)\right)\big)\,. \end{aligned} \tag{5.1.5}$$

The Tate forms that we determine for models with extra section have $\mathfrak{b}_1$ and $\mathfrak{b}_2$ coefficients, and so in order to map back to Weierstrass by (5.1.4), one has to shift those away first to reach the form (5.1.2). This is useful when determining the simple Kodaira type of the fiber, without for instance resolving the singularity first. The shift that maps (5.1.1) back to (5.1.2) is

$$y \quad\to\quad y - \frac{1}{2}\mathfrak{b}_1 w x - \frac{1}{2}\mathfrak{b}_2 s w^2\,, \tag{5.1.6}$$

which leads to the new coefficients

$$\begin{aligned}
\mathfrak{c}_0 &\to \mathfrak{c}_0 + \frac{1}{4}\mathfrak{b}_2^2 \\
\mathfrak{c}_1 &\to \mathfrak{c}_1 + \frac{1}{2}\mathfrak{b}_1\mathfrak{b}_2 \\
\mathfrak{c}_2 &\to \mathfrak{c}_2 + \frac{1}{4}\mathfrak{b}_1^2 + \frac{1}{2}\mathfrak{b}_0\mathfrak{b}_2 \\
\mathfrak{c}_3 &\to \mathfrak{c}_3 + \frac{1}{2}\mathfrak{b}_0\mathfrak{b}_1 \\
\mathfrak{b}_0 &\to \mathfrak{b}_0 \\
\mathfrak{b}_1 &\to 0 \\
\mathfrak{b}_2 &\to 0\,.
\end{aligned} \tag{5.1.7}$$

The coefficients f and g in the Weierstrass form $y^2 = x^3 + fx + g$ after this shift are then

$$\begin{aligned}
f =& -\mathfrak{b}_0^2\mathfrak{c}_0 - \frac{1}{48}(\mathfrak{b}_1^2 + 2\mathfrak{b}_0\mathfrak{b}_2 + 4\mathfrak{c}_2)^2 \\
&+ \frac{1}{4}(\mathfrak{b}_1\mathfrak{b}_2 + 2\mathfrak{c}_1)(\mathfrak{b}_0\mathfrak{b}_1 + 2\mathfrak{c}_3) - \frac{\mathfrak{b}_2^2\mathfrak{b}_0^2}{4} \\
g =& \frac{1}{864}\left(\mathfrak{b}_1^2 + 2\mathfrak{b}_0\mathfrak{b}_2 + 4\mathfrak{c}_2\right)^3 - \frac{1}{24}\mathfrak{b}_0^2\left(\mathfrak{b}_2^2 + 4\mathfrak{c}_0\right)\left(\mathfrak{b}_1^2 + 2\mathfrak{b}_0\mathfrak{b}_2 + 4\mathfrak{c}_2\right) \\
&- \frac{1}{48}\left(\mathfrak{b}_1\mathfrak{b}_2 + 2\mathfrak{c}_1\right)\left(\mathfrak{b}_0\mathfrak{b}_1 + 2\mathfrak{c}_3\right)\left(\mathfrak{b}_1^2 + 2\mathfrak{b}_0\mathfrak{b}_2 + 4\mathfrak{c}_2\right) \\
&+ \frac{1}{16}\mathfrak{b}_0^2\left(\mathfrak{b}_1\mathfrak{b}_2 + 2\mathfrak{c}_1\right)^2 + \frac{1}{16}\left(\mathfrak{b}_2^2 + 4\mathfrak{c}_0\right)\left(\mathfrak{b}_0\mathfrak{b}_1 + 2\mathfrak{c}_3\right)^2\,.
\end{aligned} \tag{5.1.8}$$

The lowest order term that does not vanish will always be the leading coefficient of $\mathfrak{b}_1$, which thereby determines the vanishing order of f and g [1]. From the Kodaira classification this implies that for instance that I_n fibers, which have f and g of vanishing orders 0, it is necessary that $b_{1,0} \neq 0$, whereas for I_n^*, which have $\mathrm{ord}(f) = 2$ and $\mathrm{ord}(g) = 3$, $b_{1,0} = 0$ and $b_{1,1} \neq 0$. These conditions will appear naturally in Tate tree.

5.1.2 Tate's algorithm, Trees and Canonicality

A singular elliptic fibration with a section can be realized in terms of a Weierstrass model

$$y^2 = x^3 + fxw^4 + gw^6\,, \tag{5.1.9}$$

where $[w, x, y]$ are homogenous coordinates in $\mathbb{P}_{[1,2,3]}$. Let z be a local coordinate on the base of the fibration and let $z = 0$ be a component of the discriminant of the Weierstrass

[1] As will be explained in the next section in codimension 1 any vanishing order in $\mathfrak{b}_0$ can be shifted or 'lopped' away, so that this always has a zeroeth order term.

model $\Delta = 4f^3 + 27g^2$. We will assume throughout that the divisor $z = 0$ in the base is smooth. The possible singular fibers in codimension one in the base were classified by Kodaira and Néron [84–86][2]. For a given singular Weierstrass model in $\mathbb{P}_{[1,2,3]}$ Tate's algorithm [1,88,89] allows a systematic determination of the singular fibers in codimension one in the base of the fibration. The algorithm is based upon successively determining the conditions for the vanishing of the discriminant in the coordinate z in the base. The coordinate ring in a sufficiently small neighborhood on the divisor $z = 0$ in the base is a unique factorization domain (UFD) [147]. Tate's algorithm proceeds then by solving the conditions $\Delta = 0$ order by order in an expansion in z over a UFD. In the process the Weierstrass form can be brought into the so-called Tate form

$$y^2 + b_1xy + b_3y = x^3 + b_2x^2 + b_4x + b_6\,, \tag{5.1.10}$$

where the coefficients b_i are sections of suitable line bundles, and have an expansion in powers of z that characterize the singular fibers. We will refer to a Tate form as *canonical*, if it is characterized solely by the vanishing orders of the coefficients b_i. As was shown in [1], most Weierstrass forms in $\mathbb{P}_{[1,2,3]}$ can be locally put into (canonical) Tate forms, albeit there exist outliner cases, which cannot be reached without allowing for divisions, in which case only generalized Tate forms can be achieved locally. These *non-canononical* forms are not specified solely by a vanishing order of the coefficients, but require non-trivially relation among the coeffficients b_i, which cannot be removed by well-defined coordinate changes like shifts.

The goal of this paper is to apply Tate's algorithm in the context of elliptic fibrations with a rank one Mordell-Weil group, and determine Tate-like forms for these models realized in terms of a quartic equation (5.1.2) in $\mathbb{P}_{[1,1,2]}$.

We will find, that unlike in $\mathbb{P}_{[1,2,3]}$, non-canonicality of the models is quite generic, i.e., the vanishing orders alone will not determine the complete set of forms of a given fiber type. In addition to the codimension one fiber type we also analyze the possible enhancements in codimension two and three, which will depend on the position of the two sections on the fiber in codimension one. The fibers will be characterized by the following data:

- Kodaira fiber type in codimension one
- Location of sections σ_0 and σ_1 on the fiber
- Singular fiber type in codimension two

[2]This is under the assumption that the classification for surfaces obtained by Kodaira and Néron carries over to codimension one in a higher-dimensional elliptic fibration.

For each Kodaira fiber type there is an additional choice of position of the sections σ_i. This leads to a tree-like structure of the algorithm even when truncating it to one type of Kodaira fiber e.g. I_n. We will refer to these as *Tate trees*, and the first few branches for $\mathbb{P}_{[1,1,2]}$ are shown in figure 5.1.

To keep track the sections, it is useful to characterize the fibers by their Kodaira type with an additional superscript that encodes the separation of the two sections σ_i : I_n fibers (i.e. $\mathbb{P}^1$s intersecting in an affine A-type Dynkin diagram) will be labeled by $I_n^{(0||\cdots||1)}$with k separations | between 0 and 1 corresponding to σ_0 and σ_1 intersecting $\mathbb{P}^1$s which are separated by $k-1$ $\mathbb{P}^1$s, e.g. $I_n^{(0|1)}$ if the sections intersect nearest neighbor $\mathbb{P}^1$s or $I_n^{(0||1)}$ for next to nearest neighbors. Subscripts nc denote non-canonical forms.

We will show in section 5.1.3, that the sections σ_i can only intersect components of Kodaira fibers in codimension one, with multiplicity one. The location of the sections for I_n^* fiber, which has the structure of a D type affine Dynkin diagram, the sections can only be on the four end-nodes (which are the only fiber components with multiplicity one), and modulo symmetries of the diagram, there are three distinct types of fibers $I_n^{*(01)}$, $I_n^{*(0|1)}$, and $I_n^{*(0||1)}$, shown in figure 5.12. Similar restrictions apply for the type II^*, III^*, IV^* fibers.

Note that the codimension two fibers also have an interpretation in terms of representations of the associated Lie algebra of the codimension one fiber, and the distribution of the sections correspond in this context to different $U(1)$ charge assigements to the representation. This will play a key role in the application to F-theory model building. The existence of additional sections also plays a key role in the possible topologically inequivalent resolutions of the singular fibers in higher codimension as discussed in [99].

Tate's algorithm applied to the quartic in $\mathbb{P}_{[1,1,2]}$ will result in multiple Tate-type forms for each fiber type. For canonical models, i.e. those characterized in terms of simple vanishing orders of the sections $\mathfrak{c}_i$ and $\mathfrak{b}_j$ in the local coordinate z in the base, which characterizes a component of the discriminant, it is useful to write the power series expansion

$$\mathfrak{b}_i = \sum_j b_{i,j} z^j \,, \qquad \mathfrak{c}_i = \sum_j c_{i,j} z^j \,, \tag{5.1.11}$$

which for canonical models with certain higher vanishing orders in z will be specialized to

$$\mathfrak{c}_{i,j} z^j = \sum_{k=j}^{\infty} c_{i,k} z^k = c_{i,j} z^j + c_{i,j+1} z^{j+1} + \cdots \,, \tag{5.1.12}$$

i.e., a truncated power series, starting with the terms z^j, and $\mathfrak{c}_{i,j} = c_{i,j} + zc_{i,j+1} + \cdots$. For models that are characterized in terms of vanishing orders alone, i.e. models that we refer to as *canonical models*, we will use the shorthand notation

$$\begin{aligned}\mathcal{Q}(i_1,i_2,i_3,i_4,i_5,i_6,i_7): \qquad & \mathfrak{c}_{0,i_1}z^{i_1}w^4s^3 + \mathfrak{c}_{1,i_2}z^{i_2}w^3s^2x + \mathfrak{c}_{2,i_3}z^{i_3}w^2sx^2 + \mathfrak{c}_{3,i_4}z^{i_4}wx^3 \\ & = y^2s + \mathfrak{b}_{0,i_5}z^{i_5}yx^2 + \mathfrak{b}_{1,i_6}z^{i_6}ywsx + \mathfrak{b}_{2,i_7}z^{i_7}yw^2s^2\,.\end{aligned} \tag{5.1.13}$$

In many instances, Tate's algorithm will run into local obstruction in reaching a canonical form[3], so-called *non-canonical models*, in which case there are relations among the leading-order coefficients. Such relations between coefficients are typically described by the vanishing of a polynomial P in these coefficients, and we will therefore denote the corresponding non-canonical form as $\mathcal{Q}(i_1,i_2,i_3,i_4,i_5,i_6,i_7)|_P$. A vanishing order of ∞ indicates that the term is completely absent from the fibration.

5.1.3 Constraints on Sections

The sections σ_i can only intersect the multiplicity one components of the Kodaira fibers. To see this, first note that in the quartic in $\mathbb{P}_{[1,1,2]}$, the sections are on equal footing, and only by mapping to a Weierstrass model, do we single out one of the sections as the origin of the elliptic curve, e.g. σ_0 in (5.1.4). There is a symmetry that exchanges the two sections, and we can construct a Weierstrass model, with origin given by σ_1: blow-down $s = 0$, after which there is a holomorphic coordinate shift that exchanges the sections

$$\sigma_0 \leftrightarrow \sigma_1 \qquad \Longleftrightarrow \qquad y \to y \pm \mathfrak{b}_0 x^2\,. \tag{5.1.14}$$

Then σ_1 now has projective coordinates $[0:1:0]$, and will be mapped to the zero section under (5.1.4). If the fibration under consideration is singular, one can find a birational map between its desingularization and a smooth Weierstrass model with either σ_0 or σ_1 as origin by passing to the singular model, mapping to the Weierstrass model with either σ_0 or σ_1 chosen as the origin, and resolving the singular Weierstrass model.

As the intersection of the section with every fiber equals one, a section can only meet a component of the fiber that has multiplicity one [78]. In terms of the intersections of σ_i with the fiber components, this means that they can only meet the multiplicity one components of the resolved Kodaira fibers in codimension 1. These are exactly the nodes

[3]There are potentially global obstructions as pointed out in [1], which will depend on the base of the fibration. Local obstructions refer to changes of coordinates that would require divisions by sections that can vanish along $z = 0$. The type of coordinate changes that we will allow should be locally well-defined in this sense.

that are in the orbit of the affine node under an outer automorphism of the affine Dynkin diagram, which is the dual graph to the Kodaira fiber.

This considerably restricts the position of the sections for Kodaira fibers I_n^*, IV^*, III^* and II^*, which have higher multiplicity fiber components, while posing no constraint on the I_n fibers. All distributions of sections on the fibers consistent with this restriction arise in Tate's algorithm. The I_n^* fibers consistent with this restriction are shown in figure 5.12, where the sections can be distributed over the four multiplicity one fibers of the affine D_n Dynkin diagram, and figures 5.9, 5.10 and 5.11 for IV^*, III^* and II^*, respectively.

5.1.4 Starting points for Tate's algorithm

Instead of directly solving the rather complicated leading order term in the discriminant (5.1.5), we will determine where the fiber is singular, by considering the loci where the tangent space becomes degenerate to leading order in the z expansion. This will be done in local affine coordinates by covering $\mathrm{Bl}_{[0,1,0]}\mathbb{P}_{[1,1,2]}$ with open patches.

This analysis is rather technical, so we first summarize the result: There are three distinct starting point fibrations

$$\begin{aligned} I_1^{(01)}: &\quad \mathcal{Q}(1,1,0,0,0,0,1) \\ \left[I_2^{(01)}: &\quad \mathcal{Q}(0,0,1,1,1,0,0)\right] \\ I_2^{(0|1)}: &\quad \mathcal{Q}(1,1,1,1,0,0,0)\,. \end{aligned} \tag{5.1.15}$$

Of these $I_1^{(01)}$ and $I_2^{(01)}$ are contained within a single affine patch, whereas $I_2^{(0|1)}$ is not. In the next section we will show that the two fibers with zero separation between the sections $I_1^{(01)}$ and $I_2^{(01)}$ are in fact related, so that effectively there are only two starting points $I_1^{(01)}$, which gives rise to the Tate tree for I_n and I_n^*, and $I_2^{(0|1)}$, which generates the $I_{2m}^{ns(0|1)}$ part of the tree.

We will now derive these results. A complete set of patches for $\mathrm{Bl}_{[0,1,0]}\mathbb{P}_{[1,1,2]}$ is given by [4]:

Coordinate patch	Affine coordinates
$w = s = 1$	x, y
$w = x = 1$	s, y
$y = s = 1$	w, x
$y = x = 1$	s, w

(5.1.16)

First consider the patch $w = s = 1$. Assume the elliptic fiber over $z = 0$ admits a singularity in this patch at a point (x_0, y_0). Then the equations describing the quartic and its derivatives with respect to x and y have to vanish. Explicitly,

$$\begin{aligned} 0 = \quad & \mathcal{Q}|_{z=0} = -c_{0,0} + y_0^2 + x_0^2 y_0 b_{0,0} + x_0 y_0 b_{1,0} + y_0 b_{2,0} - x_0 c_{1,0} - x_0^2 c_{2,0} - x_0^3 c_{3,0} \\ 0 = & \, \partial_x \mathcal{Q}|_{z=0} = -c_{1,0} + 2x_0 y_0 b_{0,0} + y_0 b_{1,0} - 2x_0 c_{2,0} - 3x_0^2 c_{3,0} \\ 0 = & \, \partial_y \mathcal{Q}|_{z=0} = b_{2,0} + 2y_0 + x_0^2 b_{0,0} + x_0 b_{1,0} \, . \end{aligned} \tag{5.1.17}$$

Solving these equations for $c_{0,0}$, $c_{1,0}$ and $b_{2,0}$ indeed yields a discriminant vanishing to $O(z)$. Furthermore, one can perform a coordinate shift

$$\begin{pmatrix} x \\ y \end{pmatrix} \to \begin{pmatrix} x - x_0 s w \\ y - y_0 s w^2 \end{pmatrix} , \tag{5.1.18}$$

to put the singularity at the origin of the $w = s = 1$ patch. There, the quartic and its derivatives read

$$\begin{aligned} \mathcal{Q}|_{x=y=z=0} &= -c_{0,0} \\ \partial_x \mathcal{Q}|_{x=y=z=0} &= -c_{1,0} \\ \partial_y \mathcal{Q}|_{x=y=z=0} &= b_{2,0} \, . \end{aligned} \tag{5.1.19}$$

Thus, having a singularity in the fiber over $z = 0$ in $w = s = 1$ is, after a coordinate shift, equivalent to having a fiber with $c_{0,0} = c_{1,0} = b_{2,0} = 0$ that is otherwise generic. These conditions also solve the zeroth-order term of the discriminant. The canonical form for such an I_1 fiber is

$$\mathcal{Q}_{I_1} : \quad \mathfrak{c}_{0,1} z w^4 s^3 + \mathfrak{c}_{1,1} z w^3 s^2 x + \mathfrak{c}_2 w^2 s x^2 + \mathfrak{c}_3 w x^3 = s y^2 + \mathfrak{b}_0 x^2 y + \mathfrak{b}_1 s w x y + \mathfrak{b}_{2,1} s^2 w^2 y \, , \tag{5.1.20}$$

[4] The patches are characterized by the non-vanishing of certain coordinates, which we then locally set to one.

or equivalently

$$I_1^{(01)}: \qquad \mathcal{Q}(1,1,0,0,0,0,1)\,. \tag{5.1.21}$$

Its discriminant at leading order reads

$$\Delta_{I_1} = c_{0,1}\left(b_{1,0}^2+4c_{2,0}\right)^3\left(b_{0,0}^2c_{2,0}-b_{0,0}b_{1,0}c_{3,0}-c_{3,0}^2\right)z+O(z^2)\,. \tag{5.1.22}$$

Next consider the patch $w=x=1$, and assume a singularity at (s_0,y_0). The equations for the quartic and its s- and y-derivatives are

$$\begin{aligned}
0 = \quad & \mathcal{Q}|_{z=0} = s_0y_0^2+y_0b_{0,0}+s_0y_0b_{1,0}+s_0^2y_0b_{2,0}-s_0^3c_{0,0}-s_0^2c_{1,0}-s_0c_{2,0}-c_{3,0}\\
0 = & \,\partial_s\mathcal{Q}|_{z=0} = y_0^2+y_0b_{1,0}+2s_0y_0b_{2,0}-3s_0^2c_{0,0}-2s_0c_{1,0}-c_{2,0}\\
0 = & \,\partial_y\mathcal{Q}|_{z=0} = 2s_0y_0+b_{0,0}+s_0b_{1,0}+s_0^2b_{2,0}\,.
\end{aligned} \tag{5.1.23}$$

Solving for $b_{0,0}$, $c_{2,0}$ and $c_{3,0}$ and inserting into the discriminant, one finds a vanishing at leading order. Note that any singularity in this patch will also be in the patch $w=s=1$, unless it also is on $s=0$, i.e., it has inhomogeneous coordinates $(s,y)=(0,y_0)$. By the coordinate shift $y\to y-y_0wx$ any such singularity is moved to the origin of the $w=x=1$ patch. There, the derivative conditions read

$$\begin{aligned}
\mathcal{Q}|_{s=y=z=0} &= -c_{3,0}\\
\partial_s\mathcal{Q}|_{s=y=z=0} &= -c_{2,0}\\
\partial_y\mathcal{Q}|_{s=y=z=0} &= b_{0,0}\,.
\end{aligned} \tag{5.1.24}$$

Any singular fibration in this patch that is not also in the $s=w=1$ patch can therefore be brought into the form

$$I_2^{(01)}: \qquad \mathcal{Q}(0,0,1,1,1,0,0)\,. \tag{5.1.25}$$

Note furthermore that over the locus $z=0$, this fiber splits into two components:

$$\mathcal{Q}(0,0,1,1,1,0,0)|_{z=0} = s\left(y^2+b_{1,0}wxy+b_{2,0}sw^2y-c_{0,0}s^2w^4-c_{1,0}sw^3x\right)\,. \tag{5.1.26}$$

Since they intersect in the two points $s=y=0$ and $s=y+b_{1,0}wx=0$, the Kodaira fiber type of this model is I_2. After a blow-up of the form $(s,z;\zeta_1)$ in the notation of [102], see also section 5.1.7, one finds that the two components are given by $z=0$ and $\zeta_1=0$ in the proper transform of $\mathcal{Q}(0,0,1,1,1,0,0)$, respectively. Both sections σ_0 and σ_1 intersect the same fiber component $\zeta_1=0$, so that the fiber type is $I_2^{(01)}$. The leading-order

discriminant of this model is order z^2

$$\Delta_{I_2^{(01)}} = b_{1,0}^4 c_{3,1} \left(c_{3,1} + b_{1,0} b_{0,1}\right) \left(b_{1,0}^2 c_{0,0} - b_{1,0} b_{2,0} c_{1,0} - c_{1,0}^2\right) z^2 + O(z^3)\,. \tag{5.1.27}$$

In the third coordinate patch $y = s = 1$, the conditions on the quartic and its derivatives for an assumed singularity at (w_0, x_0) are

$$\begin{aligned} 0 = \quad & \mathcal{Q}|_{z=0} = 1 + x_0^2 b_{0,0} + w_0 x_0 b_{1,0} + w_0^2 b_{2,0} - w_0^4 c_{0,0} - w_0^3 x_0 c_{1,0} - w_0^2 x_0^2 c_{2,0} - w_0 x_0^3 c_{3,0} \\ 0 = \partial_w \mathcal{Q}|_{z=0} = {} & x_0 b_{1,0} + 2 w_0 b_{2,0} - 4 w_0^3 c_{0,0} - 3 w_0^2 x_0 c_{1,0} - 2 w_0 x_0^2 c_{2,0} - x_0^3 c_{3,0} \\ 0 = \partial_x \mathcal{Q}|_{z=0} = {} & 2 x_0 b_{0,0} + w_0 b_{1,0} - w_0^3 c_{1,0} - 2 w_0^2 x_0 c_{2,0} - 3 w_0 x_0^2 c_{3,0}\,. \end{aligned} \tag{5.1.28}$$

There are no solutions of these equations in the coefficients $b_{i,0}$, $c_{i,0}$ that hold for any point (w_0, x_0) in this patch. However, the only locus in the third coordinate patch that is not in $w = s = 1$ is the $w = 0$ locus. Here, the x-derivative of the quartic equation is given by

$$\partial_x \mathcal{Q}|_{w=z=0} = 2 b_{0,0} x_0\,, \tag{5.1.29}$$

and a singularity at this locus hence requires $b_{0,0} x_0 = 0$. Then, however,

$$\mathcal{Q}|_{w=z=0} = s y^2 + b_{0,0} x_0^2 = s y^2 = 1\,, \tag{5.1.30}$$

and thus $\mathcal{Q}$ can never vanish there, no matter how the $\mathfrak{b}_i$ and $\mathfrak{c}_i$ are chosen. Therefore, any singularity of the fiber in the $y = s = 1$ patch is also contained in either $w = s = 1$ or $w = x = 1$, and can therefore be described by the standard forms found above.

Lastly, the only remaining locus in the $x = y = 1$ patch that is not contained in either of the patches is $(s, w) = (0, 0)$. Here, the s-derivative of $\mathcal{Q}$ cannot vanish, since

$$\partial_s \mathcal{Q}|_{s=w=z=0} = y^2 = 1\,, \tag{5.1.31}$$

and the fiber will always be regular over this point.

There is a third starting fibration not covered by the analysis performed until here, because the singularity of this fibration is not contained within a single patch of the ambient $\mathbb{P}_{[1,1,2]}$ over the entire codimension one locus $z = 0$ in the base B: Consider again the derivatives of the elliptic fibration (5.1.17) in the patch $w = s = 1$. If $c_{0,0} = c_{1,0} = c_{2,0} = c_{3,0} = 0$ and for a generic point b on the base with non-vanishing values of $b_{0,0}$ or $b_{1,0}$, there exists an $x_0(b)$ such that all derivatives vanish at $x = x_0(b)$, $y = 0$. This is not the case on any point b on B where $b_{0,0}(b) = b_{1,0}(b) = 0$. However, on such a point, the fibration is

singular in the $w = x = 1$ patch, on the locus $y = s = 0$. This can be seen explicitly from the derivatives (5.1.24) in this patch. This results in the third starting point fiber, which is an $I_2^{(0|1)}$

$$I_2^{(0|1)}: \qquad \mathcal{Q}(1,1,1,1,0,0,0)\,, \tag{5.1.32}$$

which is singular on the entire locus $z = 0$, although its singularity is not contained in a single patch over $z = 0$. This starting point will generate the infinite series of $I_{2m}^{ns(0|1)}$ fibers, as is shown in section 5.4.3.

5.1.5 Symmetries and Pruning of the Tree

In the last section we have seen that there are three starting points for Tate's algorithm in $\mathbb{P}_{[1,1,2]}$, two of which are contained in a single patch of $\mathbb{P}_{[1,1,2]}$. We will show that two of these are related

$$I_1^{(01)}: \quad \mathcal{Q}(1,1,0,0,0,0,1) \qquad \leftrightarrow \qquad I_2^{(01)}: \quad \mathcal{Q}(0,0,1,1,1,0,0)\,. \tag{5.1.33}$$

This implies that there is a single $I_1^{(01)}$ starting point for the algorithm, giving rise to the I_n and I_n^* part of the Tate tree, and a second starting point (5.1.32) with fiber type $I_2^{(0|1)}$, which enhances to the $I_{2m}^{ns(0|1)}$ part of the tree.

To show the equivalence (5.1.33), we will use the fact that there is an exchange of the two sections σ_0 and σ_1, which maps these two fibrations into each other. For this symmetry to be manifest, we blow down the divisor $s = 0$, whereby the coordinate shift $y \to y - \frac{1}{2}\mathfrak{b}_0 x^2 - \frac{1}{2}\mathfrak{b}_2 w^2$ becomes holomorphic. After applying this shift the quartic takes the form

$$\mathfrak{c}_0 w^4 + \mathfrak{c}_1 w^3 x + \mathfrak{c}_2 w^2 x^2 + \mathfrak{c}_3 w x^3 + \mathfrak{b}_0^2 x^4 = y^2 + \mathfrak{b}_1 w x y\,. \tag{5.1.34}$$

The sections are now at $[0:1:\pm\,\mathfrak{b}_0]$. One can again analyze whether this fibration is singular in the three affine coordinate patches of $\mathbb{P}_{[1,1,2]}$, given by $w = 1$, $x = 1$ and $y = 1$. Indeed one recovers the I_1 singularity in $w = 1$ with conditions $c_{0,0} = c_{1,0} = 0$. It has discriminant

$$\Delta_{I_1} = c_{0,1}\left(b_{1,0}^2 + 4c_{2,0}\right)^3\left(b_{0,0}^2 c_{2,0} - b_{0,0}b_{1,0}c_{3,0} - c_{3,0}^2\right) z + O(z^2)\,, \tag{5.1.35}$$

and setting $c_{0,1} = 0$ enhances it into an $I_2^{(01)}$ fibration, given by

$$\mathfrak{c}_{0,2} z^2 w^4 + \mathfrak{c}_{1,1} z w^3 x + \mathfrak{c}_2 w^2 x^2 + \mathfrak{c}_3 w x^3 + \mathfrak{b}_0^2 x^4 = y^2 + \mathfrak{b}_1 w x y\,. \tag{5.1.36}$$

In the $x = 1$ patch, one again finds the $I_2^{(01)}$ singularity with $c_{3,0} = b_{0,0} = 0$. Since $\mathfrak{b}_0$ appears as a square in (5.1.34), $b_{0,0} = 0$ implies that the coefficient of the x^4-term vanishes to second order in z, and one has

$$\mathfrak{c}_0 w^4 + \mathfrak{c}_1 w^3 x + \mathfrak{c}_2 w^2 x^2 + \mathfrak{c}_{3,1} z w x^3 + \mathfrak{b}_{0,1}^2 z^2 x^4 = y^2 + \mathfrak{b}_1 w x y \,. \tag{5.1.37}$$

Now, if one interchanges $x \leftrightarrow w$ in (5.1.37), one recovers (5.1.36). This symmetry thus relates the two singular fibrations. It also explains why there is no I_1 underlying (5.1.37): $\mathfrak{b}_{0,1}^2$ simply cannot vanish to linear order in z.

The quartic (5.1.36) has (full, not leading order) discriminant

$$\begin{aligned}\Delta_{(5.1.36)} = 256 z^2 \Big(& P_0^2 \left(P_0 \mathfrak{c}_{0,2} - \mathfrak{c}_{1,1}^2\right)\left(P_0 \mathfrak{b}_0^2 - \mathfrak{c}_3^2\right) \\ & - 8\mathfrak{c}_{1,1}\mathfrak{c}_3 z \left(8\mathfrak{c}_{1,1}^2\mathfrak{c}_3^2 - 9P_0\left(\mathfrak{c}_{0,2}\mathfrak{c}_3^2 + \mathfrak{b}_0^2\mathfrak{c}_{1,1}^2\right) + 10 P_0 \mathfrak{c}_{0,2}\mathfrak{b}_0^2\right) \\ & - 16 z^2 \big(27\left(\mathfrak{c}_{0,2}^2\mathfrak{c}_3^4 + \mathfrak{b}_0^4\mathfrak{c}_{1,1}^4\right) - 36\mathfrak{c}_{0,2}\mathfrak{b}_0^2 P_0\left(\mathfrak{c}_{0,2}\mathfrak{c}_3^2 - \mathfrak{c}_{1,1}^2\mathfrak{b}_0^2\right) \\ & \qquad + 2\mathfrak{c}_{0,2}\mathfrak{b}_0^2\left(3\mathfrak{c}_{1,1}^2\mathfrak{c}_3^2 + 4P_0\mathfrak{c}_{0,2}\mathfrak{b}_0^2\right)\big) \\ & - 3072 z^3 \mathfrak{c}_{0,2}^2\mathfrak{c}_{1,1}\mathfrak{c}_3\mathfrak{b}_0^4 + 4096 z^4 \mathfrak{c}_{0,2}^3\mathfrak{b}_0^6\Big)\,.\end{aligned} \tag{5.1.38}$$

with $P_0 = \mathfrak{b}_1^2 + 4\mathfrak{c}_2$. One can easily check that it is invariant under the exchange of $w \leftrightarrow x$, which amounts to the interchanges $\mathfrak{c}_{0,2} \leftrightarrow \mathfrak{b}_0^2$ and $\mathfrak{c}_{1,1} \leftrightarrow \mathfrak{c}_3$. On the other hand, the discriminant of (5.1.37) is identical to the discriminant of (5.1.36) if one replaces $\mathfrak{c}_{0,2}$ by $\mathfrak{c}_0$, $\mathfrak{c}_{1,1}$ by $\mathfrak{c}_1$, $\mathfrak{c}_3$ by $\mathfrak{c}_{3,1}$ and $\mathfrak{b}_0$ by $\mathfrak{b}_{0,1}$. The discriminants of two quartics are structurally identical, so that they have the same enhancements. It suffices therefore to consider Tate's algorithm only for enhancements of either (5.1.36) or (5.1.37).

5.1.6 Lops

With the arguments in the last section, we can concentrate on the branch of the Tate tree, that starts from the $I_1^{(01)}$ fiber in (5.1.15)[5], realized in terms of $\mathcal{Q}(1,1,0,0,0,0,1)$. In this section, we will show that there is an additional symmetries, which we call *lops or lopping transformations*[6] (in analogy to flops) that identify different branches of the tree. In summary we show that the following two I_2 models are equivalent

$$\mathcal{Q}(2,1,1,0,0,0,1) \equiv \mathcal{Q}(0,0,1,1,1,0,0)\,. \tag{5.1.39}$$

[5]The additional $I_2^{(0|1)}$ has very simple enhancements and we discuss it separately in section 5.4.3.

[6]Lops are arboricultural operations on trees. Lopping refers to the removal of large side branches (the making of vertical cuts) [Arboricultural Association].

and for non-negative vanishing orders n_i and m_i

$$\mathcal{Q}(n_0+2,n_1+1,n_2,n_3,m_0,m_1,m_2+1) \equiv \mathcal{Q}(n_0,n_1,n_2,n_3+1,m_0+1,m_1,m_2)\,, \quad (5.1.40)$$

Here equivalence here means isomorphism of the fiber, which implies that the fiber types of the two models are identical in all codimension.

We can considerably trim the Tate tree that starts at $I_1^{(01)}$ by successive application of the lops. One important implication is that without loss of generality the vanishing order of the coefficient $\mathfrak{b}_0$ can always be set to zero, i.e.

$$\mathfrak{b}_0 = b_{0,0} + b_{0,1}z + \cdots\,, \qquad b_{0,0} \neq 0\,. \quad (5.1.41)$$

This is similar to the specialization in fibrations realized in $\mathbb{P}_{[1,2,3]}$, where the coefficients of y^2 and x^3 have been set to be one. Note that the lopping operation does not restrict the branch growing out of the second starting point, the $I_2^{(0|1)}$ model $\mathcal{Q}(1,1,1,1,0,0,1)$.[7]

We will now prove that these lops are equivalences of the fibers. First consider the two $I_2^{(01)}$ models (5.1.39). Resolving the model on the left with $(x,y,z;\zeta_1)$ results, after the proper transform, in

$$z^2\mathfrak{c}_{0,2}w^4 + z\mathfrak{c}_{1,1}w^3x + z\zeta_1\mathfrak{c}_{2,1}w^2x^2 + \zeta_1\mathfrak{c}_3wx^3 = y^2 + \zeta_1\mathfrak{b}_0x^2y + \mathfrak{b}_1ywx + z\mathfrak{b}_{2,1}w^2y\,. \quad (5.1.42)$$

where in $\mathfrak{c}$ and $\mathfrak{b}$ the exansions are now in terms of $z\zeta_1$. Likewise, the resolution of the model on the right of (5.1.39) with $(w,y,\tilde{z};\tilde{\zeta}_1)$ results in

$$\tilde{\zeta}_1^2\mathfrak{c}_0w^4 + \tilde{\zeta}_1\mathfrak{c}_1w^3x + \tilde{\zeta}_1\tilde{z}\mathfrak{c}_{2,1}w^2x^2 + \tilde{z}\mathfrak{c}_{3,1}wx^3 = y^2 + \tilde{z}\mathfrak{b}_{0,1}x^2y + \mathfrak{b}_1ywx + \tilde{\zeta}_1\mathfrak{b}_2w^2y\,. \quad (5.1.43)$$

Again each of the coefficient sections are now series in $\tilde{z}\tilde{\zeta}_1$. Comparing the two resolved equations, we see that indeed, swapping

$$\tilde{z} \quad \leftrightarrow \quad \zeta_1 \qquad \text{and} \qquad \tilde{\zeta}_1 \quad \leftrightarrow \quad z \quad (5.1.44)$$

maps (5.1.42) and (5.1.43) into each other. Furthermore, from the projective relations of the blow-up $\mathcal{Q}(2,1,1,0,0,0,1)$, we see that in (5.1.42) the two sections sit on $z=0$, and in (5.1.43) on $\tilde{\zeta}_1 = 0$, which exactly are mapped into each other. The birational map

[7] Applying the same type of arguments as in the following for the $I_1^{(01)}$ branch, after the proper transform a term $y^2\zeta_1$ in introduced, and thus is already reduced.

between these two forms is thus, to first resolve as in (5.1.42), and then blow-down $z = 0$,[8] which is precisely realized in terms of the singular model $\mathcal{Q}(0,0,1,1,1,0,0)$.

More generally, consider the quartic, without the blow-up with respect to s. We will now show that there is a symmetry between models, whose vanishing orders differ by the vector $(2,1,0,-1,-1,0,1)$, i.e. the lopping transformation (5.1.40). To prove this, consider the left hand side

$$\begin{aligned}&\mathcal{Q}(n_0+2, n_1+1, n_2, n_3, m_0, m_1, m_2+1):\\ &\qquad \mathfrak{c}_{0,n_0+2} z^{n_0+2} w^4 + \mathfrak{c}_{1,n_1+1} z^{n_1+1} w^3 x + \mathfrak{c}_{2,n_2} z^{n_2} w^2 x^2 + \mathfrak{c}_{3,n_3} z^{n_3} w x^3 \\ &\qquad = y^2 + \mathfrak{b}_{0,m_0} z^{m_0} x^2 y + \mathfrak{b}_{1,m_1} z^{m_1} y w x + \mathfrak{b}_{2,m_2+1} z^{m_2+1} w^2 y\,.\end{aligned} \tag{5.1.45}$$

Then applying one big resolution

$$(x, y, z; \zeta_1) \tag{5.1.46}$$

results, after the proper transform, in

$$\begin{aligned}&z^2\, \mathfrak{c}_{0,n_0+2} (z\zeta_1)^{n_0} w^4 + z\, \mathfrak{c}_{1,n_1+1} (z\zeta_1)^{n_1} w^3 x + \mathfrak{c}_{2,n_2} (z\zeta_1)^{n_2} w^2 x^2 + \zeta_1\, \mathfrak{c}_{3,n_3} (z\zeta_1)^{n_3} w x^3 \\ &\qquad = y^2 + \zeta_1\ \mathfrak{b}_{0,m_0} (z\zeta_1)^{m_0} x^2 y + \mathfrak{b}_{1,m_1} (z\zeta_1)^{m_1} y w x + z\, \mathfrak{b}_{2,m_2+1} (z\zeta_1)^{m_2} w^2 y\,.\end{aligned} \tag{5.1.47}$$

On the other hand, resolving the right hand side of (5.1.40), denoting the component of the discriminant by $\tilde{z}$ with

$$(w, y, \tilde{z}; \tilde{\zeta}_1) \tag{5.1.48}$$

yields after the proper transform

$$\begin{aligned}&\tilde{\zeta}_1^2\, \mathfrak{c}_{0,n_0} (\tilde{z}\tilde{\zeta}_1)^{n_0} w^4 + \tilde{\zeta}_1\, \mathfrak{c}_{1,n_1} (\tilde{z}\tilde{\zeta}_1)^{n_1} w^3 x + \mathfrak{c}_{2,n_2} (\tilde{z}\tilde{\zeta}_1)^{n_2} w^2 x^2 + \tilde{z}\, \mathfrak{c}_{3,n_3+1} (\tilde{z}\tilde{\zeta}_1)^{n_3} w x^3 \\ &\qquad = y^2 + \tilde{z}\, \mathfrak{b}_{0,m_0+1} (\tilde{z}\tilde{\zeta}_1)^{m_0} x^2 y + \mathfrak{b}_{1,m_1} (\tilde{z}\tilde{\zeta}_1)^{m_1} y w x + \tilde{\zeta}_1\, \mathfrak{b}_{2,m_2} (\tilde{z}\tilde{\zeta}_1)^{m_2} w^2 y\,.\end{aligned} \tag{5.1.49}$$

Again, the lop transformation (5.1.44) applied to these partially resolved elliptic fibrations, is a symmetry, and maps the fiber component that intersects both sections, into each other.

5.1.7 Resolutions of singular elliptic fibrations

To determine each fiber type, including the separation of the two section, in the Tate tree, we need to resolve the fiber and compute intersections. In practice the computations in this paper were done using `Smooth` [83], where the algebraic resolution procedure and

[8] More detailed studies of when such blow-downs exist, will appear in [148].

intersections are implemented for singular (elliptic) fibrations. Algebraic resolutions of the singularities of elliptic fibrations, including, the higher codmension structure of the fibers, realized in $\mathbb{P}_{[1,2,3]}$ have been discussed in [101, 102, 133, 148, 149]. We consider crepant resolutions, and allow for up to codimension 3 fibers, i.e. the base of the fibration can be up to three-dimensional. The geometric setting thereby allows not only the analysis of the codimension one fibers, but also the higher codimension structure, which has an intricate pattern depending on the location of the sections in codimension one. This is mostly motivated by model building in F-theory, where the relevant geometries are elliptic Calabi-Yau fourfolds with extra section. We now summarize the data determining the fibration, in terms of sections of line bundles of the base. The elliptic fibration is realized in the ambient fivefold $X_5 = \mathrm{Bl}_{[0,1,0]}\mathbb{P}_{[1,1,2]}(\mathcal{O} \oplus \mathcal{O}(\alpha) \oplus \mathcal{O}(\beta))$ as a hypersurface

$$\mathcal{Q}: \qquad y^2 s + \mathfrak{b}_0 x^2 y + \mathfrak{b}_1 y w s x + \mathfrak{b}_2 y w^2 s^2 = \mathfrak{c}_0 w^4 s^3 + \mathfrak{c}_1 w^3 s^2 x + \mathfrak{c}_2 w^2 s x^2 + \mathfrak{c}_3 w x^3 \quad (5.1.50)$$

with

Section	Bundle
w	$\mathcal{O}(\sigma - F)$
x	$\mathcal{O}(\sigma + \alpha)$
y	$\mathcal{O}(2\sigma + \beta - F)$
s	$\mathcal{O}(F)$
z	$\mathcal{O}(S)$

(5.1.51)

Here, σ is the section of the hyperplane class of $\mathbb{P}_{[1,1,2]}$ before blowing up at the point $[0:1:0]$, and F is the section of the new exceptional $\mathbb{P}^1$ introduced by the blow-up. α and β are two sections of line bundles on the base manifold B, which are related by $\beta = \alpha + c_1$ as shown below, where $c_1 = c_1(B)$. S is the divisor class of the singular surface $z = 0$ in B. From the equation of $\mathcal{Q}$ one infers the class of the fourfold to be

$$[Y_4] = 4\sigma + 2\beta - F\,, \quad (5.1.52)$$

and the $\mathfrak{b}_i$ and $\mathfrak{c}_i$ are sections of the following bundles

Section	Bundle
$\mathfrak{b}_i$	$\mathcal{O}(c_1+(i-1)\alpha)$
$\mathfrak{c}_i$	$\mathcal{O}(2c_1+(2-i)\alpha)$
$\mathfrak{b}_{i,j}$	$\mathcal{O}(c_1+(i-1)\alpha-jS)$
$b_{i,j}$	$\mathcal{O}(c_1+(i-1)\alpha-jS)$
$\mathfrak{c}_{i,j}$	$\mathcal{O}(2c_1+(2-i)\alpha-jS)$
$c_{i,j}$	$\mathcal{O}(2c_1+(2-i)\alpha-jS)$

(5.1.53)

One then finds for the Chern class of X_5 that

$$\begin{aligned} c(X_5) &= c(B)\cdot(1+[w])\cdot(1+[x])\cdot(1+[y])\cdot(1+[s])\big|_{X_5} \\ &= 1+c_1+4\sigma+\alpha+\beta-F+\cdots\,, \end{aligned} \tag{5.1.54}$$

with the dots indicating higher-rank forms. By adjunction, the Chern class of Y_4 is given by

$$c(Y_4) = \frac{c(X_5)}{1+[Y_4]}\bigg|_{Y_4} = 1+c_1+\alpha-\beta+\cdots\,. \tag{5.1.55}$$

The Calabi-Yau condition, which we shall impose in most practical applications to F-theory, $c_1(Y_4)=0$ thus restricts the possible choices of sections of line bundles α and β by imposing the condition

$$\beta = \alpha + c_1\,. \tag{5.1.56}$$

Furthermore, the second Chern class of Y_4 is

$$c_2(Y_4) = c_2 + c_1^2 + \alpha^2 + 6\alpha\sigma + 7\sigma^2 - 2F\,(\alpha+2\sigma) + c_1\,(3\alpha+7\sigma-2F)\,. \tag{5.1.57}$$

The projective relations

$$[sw:x:sy] \qquad \text{and} \qquad [w:y] \tag{5.1.58}$$

imply the following relations in the intersection ring of X_5

$$\begin{aligned} \sigma\cdot(\sigma+\alpha)\cdot(2\sigma+\alpha+c_1) &= 0 \\ (\sigma-F)\cdot(2\sigma+\alpha+c_1-F) &= 0\,. \end{aligned} \tag{5.1.59}$$

Repeated applications of these – and similar ones for exceptional divisors introduced by blowing up singularities – allow us to compute intersections in X_5, similar to the

computations for the standard Tate models in [101, 102]. Furthermore, we will use the following notation for resolutions: a big resolution along $x = y = \zeta_0 = 0$ with the new exceptional section ζ_1 will be denoted in the notation of [102] by

$$(x, y, \zeta_0; \zeta_1)\,. \tag{5.1.60}$$

Likewise a small resolution $y = x = 0$ with δ is denoted by $(x, y; \delta)$.

Finally, we should discuss the Mordell-Weil group, and how we compute the actual $U(1)$ charges of matter representations that are engineered in codimension 2. Recall that the Mordell-Weil group, since it is a finitely generated abelian group, can be written as

$$\mathbb{Z} \oplus \cdots \oplus \mathbb{Z} \oplus T\,, \tag{5.1.61}$$

with the torsion subgroup T. Let $\{\sigma_1, \ldots, \sigma_n\}$ be a set of rational sections generating the non-torsion part of the Mordell-Weil group. In [112], it was shown that the abelian vector fields A_i of an F-theory vacuum are dual to the images $s(\sigma_i)$ of the rational sections σ_i under the so-called Shioda map. The Shioda map is a map from the Mordell-Weil group to the homology group $H^{(1,1)}(Y_4)$ of the fourfold, and has been given and discussed e.g. in [150]. The $U(1)$ charge, associated to the abelian gauge field A_i with section σ_i, of any matter coming from a rational curve C in the fiber is given by $C \cdot s(\sigma_i)$.

The Shioda map has the property that the intersection of $s(\sigma_i)$ with any Cartan divisor $D_{-\alpha_i}$ vanishes, i.e.,

$$s(\sigma_i) \cdot D_{-\alpha_i} = 0\,. \tag{5.1.62}$$

Therefore, as one would expect, no vector multiplets are charged under A_i. Further, its intersection with any horizontal divisor $\pi^*(D_H)$ pulled back from a base divisor D_H also vanishes

$$s(\sigma_i) \cdot \pi^* D_H = 0\,. \tag{5.1.63}$$

To construct $s(\sigma)$ explicitly, we use (5.1.62) and (5.1.63) as a set of constraints on the Shioda map. This set is sufficient to fully specify $s(\sigma)$ up to redefinitons of the abelian fields A_i that preserve charge minimality.

FIGURE 5.1: The Tate tree for $\mathbb{P}_{[1,1,2]}$, up until and including the $O(z^5)$ discriminant fibers. Black lines are irreducible fiber components of the singular fibers, red nodes show where the sections intersect the irreducible components. Fiber types with green corners are non-canonical models. From each of these, there is another branch of the tree sprouting off, with multiply non-canonical fiber types. Enhancements from type II, III, IV are not shown, but discussed in the text.

5.2 Summary of Results

Tate's algorithm for Weierstrass forms in $\mathbb{P}_{[1,2,3]}$ with a given Kodaira singular fiber above $z = 0$ derives generic forms of the fibration, where the vanishing order of the coefficients around $z = 0$ completely determines the fiber type. We find that for elliptic fibrations with an additional rational section, similar Tate forms exist. However there are additional forms, called non-canonical, which are not determined fully by the vanishing orders of the coefficients, but require non-trivial relations among them. In applications to F-theory these open up interesting model building options.

The starting point of our analysis is the quartic (5.1.1) in $\mathbb{P}_{[1,1,2]}$. The codimension one fibers are characterized in terms of their Kodaira type and the separation of the two sections σ_0 and σ_1. There is additional data distinguishing models in codimension two. Canonical and non-canonical models can have the same codimension one fiber, but might differ in the codimesion two fibers. Thus in terms of applications in F-theory, they have different charged matter content. E.g. canonical I_n models have a single matter curve in the antisymmetric representation, non-canonical models will have several, with different $U(1)$ charges.

Due to the additional data specifying the separation of the two sections, the enhancement structure becomes tree-like. The first few enhancements of this Tate tree are shown in figure 5.1, based on the Tate's algorithm in section 5.3. The canonical forms for the low rank are summarized in table 5.1 and for the infinite series I_n and I_n^* can be found in table 5.2. Non-canonical models are discussed in section 5.5, focusing on the low rank cases[9]. Each of the low rank non-canonical models gives rise to a new branch of the Tate tree, with multiply non-canonical enhancements.

For I_5, which is of phenomenological interest in F-theory model building, there are three fiber types: $I_5^{(01)}$, $I_5^{(0|1)}$ and $I_5^{(0||1)}$. All of these have canonical (section 5.3.6) and non-canonical realizations. There are non-canonical models for $I_5^{(0|1)}$ and $I_5^{(0||1)}$ which we analyze in 5.5.1. As shown in section 5.5.2.1, the $I_5^{(01)}$ fiber only arises as a doubly non-canonical form. Finally, one can explicitly check where the models that are already present in the literature are located within the Tate tree. For the toric models arising from tops and for the split spectral cover models this is done in appendix B.3. The $2+3$-factorized Tate model is the non-canonical $I_5^{(0|1)}$ model, the $4+1$-factorized Tate model is a special case of the non-canonical $I_5^{(0||1)}$ model.

[9] We have not studied the full structure of non-canonical enhancements of all I_n models, however most non-canonical models will have only non-minimal codimension 2 loci, as in $\mathbb{P}_{[1,2,3]}$, which usually implies that those sections can be set to one, thus allowing shifts to canonical forms.

Fiber	ord(Δ)	Group	$\mathfrak{c}_0$	$\mathfrak{c}_1$	$\mathfrak{c}_2$	$\mathfrak{c}_3$	$\mathfrak{b}_0$	$\mathfrak{b}_1$	$\mathfrak{b}_2$
I_0	0	—	0	0	0	0	0	0	0
I_1	1	—	1	1	1	0	0	0	1
$I_2^{(01)}$	2	$SU(2)$	2	1	1	0	0	0	1
$I_2^{(0\|1)}$	2	$SU(2)$	1	1	1	1	0	0	1
$I_3^{(01)}$	3	$SU(3)$	3	2	1	0	0	0	1
$I_3^{(0\|1)}$	3	$SU(3)$	2	1	1	1	0	0	1
$I_4^{(01)}$	4	$SU(4)$	4	2	1	0	0	0	2
$I_4^{(0\|1)}$	4	$SU(4)$	3	2	1	1	0	0	1
$I_4^{(0\|\|1)}$	4	$SU(4)$	2	2	2	2	0	0	1
$I_5^{(01)}$	5	$SU(5)$	5	3	1	0	0	0	2
$I_5^{(0\|1)}$	5	$SU(5)$	4	2	1	1	0	0	2
$I_5^{(0\|\|1)}$	5	$SU(5)$	3	2	2	2	0	0	1
II	2	—	1	1	1	0	0	1	1
$III^{(01)}$	3	$SU(2)$	2	1	1	0	0	1	1
$III^{(0\|1)}$	3	$SU(2)$	1	1	1	1	0	1	1
$IV^{(01)}$	4	$SU(3)$	3	2	1	0	0	1	1
$IV^{(0\|1)}$	5	$SU(3)$	2	1	1	1	0	1	1
$I_0^{*ns(01)}$	6	G_2	4	2	0	0	0	0	2
$I_0^{*ss(01)}$	6	$SO(7)$	4	2	1	0	0	1	2
$I_0^{*ss(0\|1)}$	6	$SO(7)$	2	2	1	1	0	1	1
$I_0^{*s(01)}$	6	$SO(8)$	4	2	1	0	0	1	2
$I_0^{*(0\|1)}$	6	$SO(8)$	3	2	1	1	0	1	1
$I_1^{*(01)}$	7	$SO(10)$	5	3	1	0	0	1	2
$I_1^{*(0\|1)}$	7	$SO(10)$	4	2	1	1	0	1	2
$I_1^{*(0\|\|1)}$	7	$SO(10)$	3	2	2	1	0	1	1
$IV^{*ns(01)}$	8	F_4	4	3	2	0	0	1	2
$IV^{*(01)}$	8	E_6	5	3	2	0	0	1	2
$IV^{*(0\|1)}$	8	E_6	3	2	2	1	0	1	2
$III^{*(01)}$	9	E_7	5	3	2	0	0	1	3
$III^{*(0\|1)}$	9	E_7	3	3	2	1	0	1	2
$II^{*(01)}$	10	E_8	5	4	2	0	0	1	3
non-min	12	—	6	4	2	0	0	1	3
non-min	12	—	4	3	2	1	0	1	2

TABLE 5.1: Fiber types and vanishing orders for low-rank canonical fibrations with rank-1 Mordell-Weil group, from Tate's algorithm for quartics in $\mathbb{P}_{[1,1,2]}$. Δ specifies the vanishing order of the descriminant. If not explicitly stated otherwise, models are of split-type. The monodromy condition that differentiates between the $I_0^{*ss(01)}$ fiber from $I_0^{*s(01)}$ is given in equation (5.3.38), and the additional monodromy condition for $I_0^{*ns(01)}$ in (5.3.40).

Fiber type	Vanishing order of Δ	Gauge group	Vanishing orders of coefficient sections							
			$\mathfrak{c}_0$	$\mathfrak{c}_1$	$\mathfrak{c}_2$	$\mathfrak{c}_3$	$\mathfrak{b}_0$	$\mathfrak{b}_1$	$\mathfrak{b}_2$	
$I_{2m+k}^{(01)}$	$2m$	$SU(2m)$	$2m$	m	1	0	0	0	m	
$I_{2m+k}^{(0\|^k 1)}$	$2m+k$	$SU(2m+k)$	$2m$	m	k	k	0	0	m	$1 \le k \le m$
$I_{2m}^{(0\|^m 1)}$	$2m$	$SU(2m)$	m	m	m	m	0	0	1	
$I_{2(m+k)}^{(0\|^m 1)}$	$2(m+k)$	$SU(2(m+k))$	$m+2k$	m	m	m	0	0	$2k$	$1 \le k \le \lfloor \frac{m}{2} \rfloor$
$I_{2m+1}^{(01)}$	$2m+1$	$SU(2m+1)$	$2m+1$	$m+1$	1	0	0	0	m	
$I_{2m+k+1}^{(0\|^k 1)}$	$2m+k+1$	$SU(2m+k+1)$	$2m+1$	$m+1$	k	k	0	0	m	$1 \le k \le m$
$I_{2m+1}^{(0\|^m 1)}$	$2m+1$	$SU(2m+1)$	$m+1$	m	m	m	0	0	1	
$I_{2(m+k)+1}^{(0\|^m 1)}$	$2(m+k)+1$	$SU(2(m+k)+1)$	$m+2k+1$	m	m	m	0	0	$2k+1$	$1 \le k \le \lfloor \frac{m}{2} \rfloor$
$I_{2m}^{ns(01)}$	$2m$	$Sp(m)$	$2m$	m	0	0	0	0	m	
$I_{2m}^{ns(0\|1)}$	$2m$	$Sp(m)$	m	m	m	m	0	0	0	
$I_{2m+1}^{ns(01)}$	$2m+1$	—	$1+2m$	$1+m$	0	0	0	0	$m+1$	
$I_{2m}^{*(01)}$	$2m+6$	$SO(4m+8)$	$4+2m$	$2+m$	1	0	0	1	$2+m$	
$I_{2m+1}^{*(01)}$	$2m+7$	$SO(4m+10)$	$5+2m$	$3+m$	1	0	0	1	$2+m$	
$I_{2m}^{*(0\|1)}$	$2m+6$	$SO(4m+8)$	$3+2m$	$2+m$	1	1	0	1	$1+m$	
$I_{2m+1}^{*(0\|1)}$	$2m+7$	$SO(4m+10)$	$4+2m$	$2+m$	1	1	0	1	$2+m$	
$I_{2m}^{*(0\|\|1)}$	$2m+6$	$SO(4m+8)$	$2+m$	$2+m$	$1+m$	$1+m$	0	1	1	
$I_{2m+1}^{*(0\|\|1)}$	$2m+7$	$SO(4m+10)$	$3+m$	$2+m$	$2+m$	$1+m$	0	1	1	
$I_{2m}^{*ns(01)}$	$2m+6$	$SO(4m+7)$	$3+2m$	$2+m$	1	0	0	1	$2+m$	
$I_{2m+1}^{*ns(01)}$	$2m+7$	$SO(4m+9)$	$4+2m$	$3+m$	1	0	0	1	$2+m$	
$I_{2m}^{*ns(0\|1)}$	$2m+6$	$SO(4m+7)$	$2+2m$	$2+m$	1	1	0	1	$1+m$	
$I_{2m+1}^{*ns(0\|1)}$	$2m+7$	$SO(4m+9)$	$3+2m$	$2+m$	1	1	0	1	$2+m$	

TABLE 5.2: Vanishing orders for fibrations realizing I_n, I_n^* fiber types, both split and non-split (ns) for $n \ge 1$, with two sections in canonical form, i.e., characterized entirely in terms of vanishing order of the coefficients $\mathfrak{b}_i$ and $\mathfrak{c}_j$. There are three distinct distributions of the two sections on the fibers for the split I_n^*, modulo symmetry of the affine D type Dynkin diagram, and two for the non-split case. The I_n fibers are grouped into whether n is even or odd, and whether the separation between the two sections is small or large. For I_n the forms can be put into a single, slightly more complicated form given in (5.4.6).

5.3 Tate Trees: Canonical Forms

In this section we will determine all the canonical models, i.e. those determined solely by vanishing orders with generic coefficients c_i and b_i. The non-canonical enhancements will be discussed separately in section 5.5. In this sense the present section results in the analog of the standard Tate models in $\mathbb{P}_{[1,2,3]}$ in [89], whereas the section on non-canonical forms also encondes local obstructions such as those studied for $\mathbb{P}_{123}$ in [1]. The main difference to $\mathbb{P}_{[1,2,3]}$ is that non-canonical models are much more generic in $\mathbb{P}_{[1,1,2]}$ and also arise prominently in the I_n branch. We run the algorithm in detail up until and including $O(z^5)$, i.e. in the I_5, and derive I_0^* IV^*, III^* and II^* fibers in the next wection. Finally, we give canonical forms for all I_n and I_n^* fibers, however the (multiply) non-canonical progression for the infinite series in the algorithm is left for future work.

5.3.1 Monodromy

In section 5.1.4, it was found that there is a single I_1 fibration with canonical form

$$I_1^{(01)}: \qquad \mathcal{Q}(1,1,0,0,0,0,1) \tag{5.3.1}$$

and discriminant at leading order

$$\Delta_{I_1} = c_{0,1}\left(b_{1,0}^2 + 4c_{2,0}\right)^3\left(b_{0,0}^2c_{2,0} - b_{0,0}b_{1,0}c_{3,0} - c_{3,0}^2\right)z + O(z^2)\,. \tag{5.3.2}$$

Upon performing the coordinate shift $y \to y - \frac{1}{2}b_{1,0}wx$, one obtains the quartic

$$\begin{aligned} &y^2s + \mathfrak{b}_{0,0}x^2y + \mathfrak{b}_{1,1}zywsx + \mathfrak{b}_{2,1}zw^2s^2y \\ &= \mathfrak{c}_{0,1}zw^4s^3 + \left(\mathfrak{c}_{1,1} + \frac{1}{2}b_{1,0}b_{2,1}z\right)w^3s^2x + \left(\mathfrak{c}_{2,0} + \frac{1}{4}b_{1,0}^2\right)w^2sx^2 + \left(\mathfrak{c}_{3,0} + \frac{1}{2}b_{0,0}b_{1,0}\right)wx^3\,. \end{aligned} \tag{5.3.3}$$

Defining shifted leading coefficients of the series $\mathfrak{c}_{ij}$ as $\hat{c}_{1,1} = c_{1,1} + \frac{1}{2}b_{1,0}b_{2,1}$, $\hat{c}_{2,0} = c_{2,0} + \frac{1}{4}b_{1,0}^2$, $\hat{c}_{3,0} = c_{3,0} + \frac{1}{2}b_{0,0}b_{1,0}$ and dropping the hats, the fibration above is described by the canonical form

$$\mathcal{Q}(1,1,0,0,0,1,1)\,, \tag{5.3.4}$$

with discriminant

$$\Delta = c_{0,1}c_{2,0}^3\left(b_{0,0}^2c_{2,0} - c_{3,0}^2\right)z + O(z^2)\,. \tag{5.3.5}$$

The monodromy condition for I_n, determining whether the local gauge group is given by $SU(n)$ or $Sp\left(\lfloor\frac{n}{2}\rfloor\right)$, is checked by testing whether $c_{2,0}$ of this fiber has a square root: One

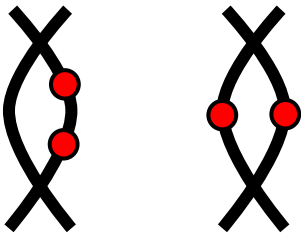

FIGURE 5.2: $I_2^{(01)}$ and $I_2^{(0|1)}$ fibers, with black lines corresponding to the two $\mathbb{P}^1$ fiber components, and the red nodes to the two sections, σ_0 and σ_1.

can always write $c_{2,0} = \mu \tilde{c}_{2,0}^2$, and choose μ such that $\mu = 1$ if μ has no zeros. Then, the local gauge group will be $SU(n)$ if $\mu = 1$, and $Sp\left(\lfloor \frac{n}{2} \rfloor\right)$ if μ has zeros. Note that $\mu = 1$ is a necessary condition for the term in brackets in the discriminant above to vanish. Further, if $\mu = 1$, one can perform the coordinate shift $y \to y - \tilde{c}_{2,0} wx$. This coordinate shift yields the canonical form

$$I_1^{(01)}: \qquad \mathcal{Q}(1,1,1,0,0,0,1)\,. \tag{5.3.6}$$

As we are interested in I_n^{split} fibers, we proceed assuming the starting I_1 singularity to be of the form (5.3.6). In the following we proceed to enhance the type of this singularity, which in the case of the quartic in $\mathbb{P}_{[1,1,2]}$ has a tree-like structure, which is characterized by the Kodaira fiber type as well as the location of the sections.

5.3.2 Discriminant at $O(z^2)$

The I_1 singularity (5.3.6) has leading-order discriminant

$$\Delta_{I_1} = c_{0,1} b_{1,0}^6 c_{3,0} \left(b_{0,0} b_{1,0} + c_{3,0}\right) z + O(z^2)\,. \tag{5.3.7}$$

The possible fiber enhancements are given by setting factors of this expression to zero.

- $c_{0,1} = 0$: $I_2^{(01)}$
  This fiber trivially has canonical form

  $$I_2^{(01)}: \qquad \mathcal{Q}(2,1,1,0,0,0,1)\,. \tag{5.3.8}$$

  Resolving the singular fiber for instance with the big resolution $(x, y, z; \zeta_1)$, using the notation of section 5.1.7, we see that the two sections intersect the same fiber component, and are thus of type $I_2^{(01)}$, and is shown on the left hand side in figure 5.2.

- $c_{3,0} = 0$: $I_2^{(0|1)}$
  The canonical form for this fiber is

$$I_2^{(0|1)}: \qquad \mathcal{Q}(1,1,1,1,0,0,1)\,. \tag{5.3.9}$$

  Here, the two sections intersect neighbouring components of the resolved fiber, i.e. of type $I_2^{(0|1)}$, shown on the right hand side in figure 5.2.

- $b_{0,0}b_{1,0} + c_{3,0} = 0$: $I_2^{(0|1)}$
  This enhancement is equivalent to setting $c_{3,0} = 0$, as can be seen as follows. Applying the coordinate shift $y \to y - b_{1,0}wx$ turns $\mathcal{Q}_{I_1}$ into a form in which the section $\tilde{c}_{3,0}$ in the new coordinates is given by $\tilde{c}_{3,0} = b_{0,0}b_{1,0} + c_{3,0}$, and all other sections are still generic. Hence, $b_{0,0}b_{1,0} + c_{3,0} = 0$ is equivalent to $\tilde{c}_{3,0} = 0$ in the new coordinates.

  During later stages of the algorithm, one encounters a few more discriminants with factors of the form $c_{3,j}\,(b_{0,j}b_{1,0} + c_{3,j})$. Let us note here that all enhancnements arising from the bracketed part of this expression are always equal to enhancements arising from $c_{3,j}$, and that there is always a coordinate shift of the form discussed here linking the two. We therefore do not treat $b_{0,j}b_{1,0} + c_{3,j}$ explicitly in the following.

- $b_{1,0} = 0$: II
  Setting $b_{1,0} = 0$ enhances the singularity in a way that leaves the I_n branch: $\mathcal{Q}_{I_1}|_{z=0}$ has a double root at $x = y = 0$, and a Taylor expansion around this double root yields

$$\mathcal{Q}_{I_1}|_{z=0,w=s=1} : y^2 + b_{1,0}xy + O(x^3, y^3) \tag{5.3.10}$$

  whose discriminant is given by $(\partial_{xy}\mathcal{Q}_{I_1})^2 - \partial_{xx}\mathcal{Q}_{I_1}\partial_{yy}\mathcal{Q}_{I_1} = b_{1,0}^2$. Vanishing of this discriminant indicates a cusp singularity with Kodaira type II.

5.3.3 Discriminant at $O(z^3)$

Each distinct I_2 fiber type opens a new branch of the algorithm, or Tate tree, yielding different enhancements. There are two I_2 fibers, where the two rational sections intersect either the same or distinct fiber components of the resolved singular fiber. Following the discriminant we now determine all the fiber types for each branch.

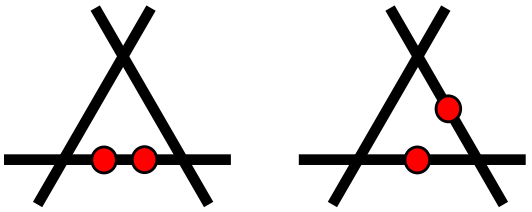

FIGURE 5.3: $I_3^{(01)}$ and $I_3^{(0|1)}$ fibers. The black lines correspond to the $\mathbb{P}^1$ fiber components, and the red nodes to the two sections, σ_0 and σ_1. Due to the symmetry of the diagram, there are only two distinct distributions of the two sections.

5.3.3.1 $I_2^{(01)}$ Branch

Consider first the branch starting from the $I_2^{(01)}$ fiber, where both sections lie on one fiber component, realized in terms of (5.3.8). The discriminant for this fibration is

$$\Delta_{I_2^{(01)}} = b_{1,0}^4 c_{3,0} \left(b_{1,0} b_{0,0} + c_{3,0}\right) P_0 z^2 + O(z^3) \tag{5.3.11}$$

with

$$P_0 = b_{1,0}^2 c_{0,2} - b_{1,0} b_{2,1} c_{1,1} - c_{1,1}^2 \,. \tag{5.3.12}$$

Each factor corresponds to an enhancement type, which we will consider in turn. The polynomials appearing in the discriminant generically give rise to non-canonical models and will be discussed later in detail. Here we will focus on the canonical branch.

- $P_0 = 0$: $I_3^{(01)}$
  The general solution to the vanishing of the polynomial (5.3.12) over a UFD is determined in appendix B.1.3 as

$$c_{1,1} = b_{1,0} \tilde{c}_{1,1} \,, \qquad c_{0,2} = b_{2,1} \tilde{c}_{1,1} + \tilde{c}_{1,1}^2 \,. \tag{5.3.13}$$

  The corresponding quartic significantly simplifies upon application of the coordinate shift $y \to y + \tilde{c}_{1,1} z s w^2$, where it takes the canonical form

$$I_3^{(01)} : \qquad \mathcal{Q}(3,2,1,0,0,0,1) \,. \tag{5.3.14}$$

  Slight variations of the polynomial P_0 will reappear at later stages of the algorithm. After applying the solution from appendix B.1.3, one can always find a coordinate shift that brings these into canonical form by enhancing the vanishing order of $\mathfrak{c}_0$ and $\mathfrak{c}_1$. The fiber type is determined by computing the intersections as described in section 5.1.7 and the fiber is depicted in figure 5.3.

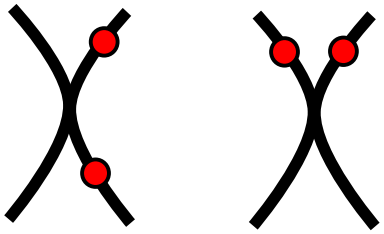

FIGURE 5.4: $III^{(01)}$ and $III^{(0|1)}$ fibers, again with black lines corresponding to the fiber components, and the red dots to the extra sections.

- $c_{3,0} = 0$: $I_3^{(0|1)}$
  The canonical form for this fiber is

$$I_3^{(0|1)}: \qquad \mathcal{Q}(2,1,1,1,0,0,1)\,. \tag{5.3.15}$$

  Here the sections are located on distinct fiber components, as shown in figure 5.3.

- $b_{1,0} = 0$: $III^{(01)}$
  This branch corresponds to a type III fiber, is shown in figure 5.4, and has canonical form

$$III^{(01)}: \qquad \mathcal{Q}(2,1,1,0,0,1,1)\,. \tag{5.3.16}$$

5.3.3.2 $I_2^{(0|1)}$ Branch

The second I_2 branch starts with $I_2^{(0|1)}$, which is realized in terms of (5.3.9). In this case the sections are on separate fiber components with the discriminant given by

$$\Delta_{I_2^{(0|1)}} = b_{1,0}^4 b_{0,0} c_{0,1} P_0 z^2 + O(z^3)\,, \tag{5.3.17}$$

with

$$P_0 = b_{0,0}^3 c_{0,1} - b_{0,0}^2 b_{1,0} c_{1,1} + b_{0,0} b_{1,0}^2 c_{2,1} - b_{1,0}^3 c_{3,1}\,. \tag{5.3.18}$$

The component $c_{0,1} = 0$ of the discriminant gives the model $I_3^{(0|1)}$ realized in terms of (5.3.15), i.e. it joins back with the branch starting from $I_2^{(01)}$.

Furthermore, the branch $b_{0,0} = 0$ has been removed by the lopping, as it is equivalent to other models, that we considered already.[10]

The other discriminant components result in the following fibers:

[10] More precisely setting $b_{0,0} = 0$ yields a (non-extremal) $I_3^{(01)}$ model, realized by $\mathcal{Q}(1,1,1,1,1,0,1)$, which is related by a lop transition to (5.3.14).

- $P_0 = 0$: $I_{3,nc}^{(0|1)}$
  P_0 is an example of the four-term polynomial discussed in appendix B.1.2, and we can directly substitute the general solution found there into $I_2^{(0|1)}$. We denote the resulting non-canonical (nc) form as

$$I_{3,nc}^{(0|1)}: \qquad \mathcal{Q}(1,1,1,1,0,0,1)|_{(5.3.18)}\,. \tag{5.3.19}$$

  Note that this gives the same fiber type as (5.3.15). However, due to the non-canonical nature of the enhancement, solving $P_0 = 0$, as in appendix B.1.2, results in the section $b_{1,0} = \sigma_1\sigma_2$ to factor. This implies that compared to the model (5.3.15), where $b_{1,0}$ is generically irreducible, the structure of the codimension 2 fibers will be different. This effect yields multiple, differently charged matter curves. We will study these models in the next section.

- $b_{1,0} = 0$: $III^{(0|1)}$
  This yields a type III fiber with canonical form

$$III^{(0|1)}: \qquad \mathcal{Q}(1,1,1,1,0,1,1)\,. \tag{5.3.20}$$

5.3.4 Discriminant at $O(z^4)$

We have seen in the last section, that at order z^3 the following fiber types occur: $I_3^{(01)}$, $I_3^{(0|1)}$, $I_{3,nc}^{(0|1)}$, as well as the type $III^{(01)}$ and $III^{(0|1)}$ fibers, each of these occured once in the algorithm. We continue here with the canonical tree growing out from $I_3^{(01)}$ and $I_3^{(0|1)}$. The enhancements of the non-canonical models will be discussed in section 5.5.

5.3.4.1 $I_3^{(01)}$ Branch

The $I_3^{(01)}$ fiber realized by $\mathcal{Q}(3,2,1,0,0,0,1)$ in (5.3.14) has discriminant

$$\Delta_{I_3^{(01)}} = b_{1,0}^3 c_{3,0}\,(b_{0,0}b_{1,0} + c_{3,0})\,P_0 z^3 + O(z^4)\,, \tag{5.3.21}$$

where the polynomial term is

$$P_0 = b_{1,0}^3 c_{0,3} - b_{1,0}^2 b_{2,1} c_{1,2} + b_{1,0} b_{2,1}^2 c_{2,1} - b_{2,1}^3 c_{3,0}\,. \tag{5.3.22}$$

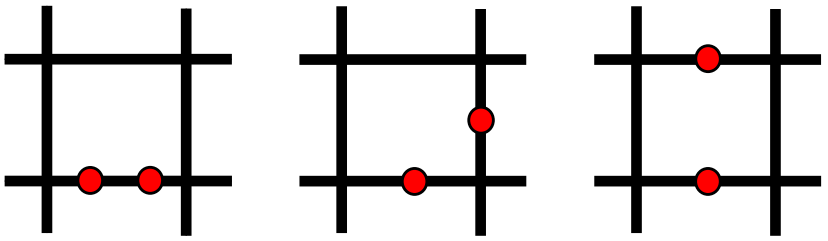

FIGURE 5.5: From left to right, showing the $I_4^{(01)}$, $I_4^{(0|1)}$ and $I_4^{(0||1)}$ fibers, respectively, with sections indicated by the red nodes.

- $c_{3,0} = 0$: $I_4^{(0|1)}$

  This enhancement splits the two sections to lie on separate, neighboring, fiber components, as shown in figure 5.5, with canonical form

$$I_4^{(0|1)}: \qquad \mathcal{Q}(3,2,1,1,0,0,1)\,. \tag{5.3.23}$$

- $P_0 = 0$: $I_4^{(01)}$ and $I_{4,nc}^{(01)}$

  Applying appendix B.1.2 to solve $P_0 = 0$, has two solutions: $b_{2,0} = c_{0,3} = 0$ or the solution given in (B.1.7). The former gives a canonical model, the latter a non-canonical one, with the same distribution of sections, however due to the non-canonicality the second one has multiple matter curves

$$I_4^{(01)}: \qquad \mathcal{Q}(4,2,1,0,0,0,2) \tag{5.3.24}$$

$$I_{4,nc}^{(01)}: \qquad \mathcal{Q}(3,2,1,0,0,0,1)|_{(5.3.22)}\,. \tag{5.3.25}$$

  The canonical model $I_4^{(01)}$ has one, whereas the non-canonical has two codimension 2 curve over $b_{1,0} = 0$. In the non-canonical fiber, there are two such loci, as $b_{1,0}$ factors into the product $\sigma_1\sigma_2$ in order to solve $P_0 = 0$.

- $b_{1,0} = 0$: $IV^{(01)}$

  As before, for the low-rank cases, the $b_{1,0} = 0$ enhancement moves us out of the I_n branch, in this case to a type IV fiber

$$IV^{(01)}: \qquad \mathcal{Q}(3,2,1,0,0,1,1)\,. \tag{5.3.26}$$

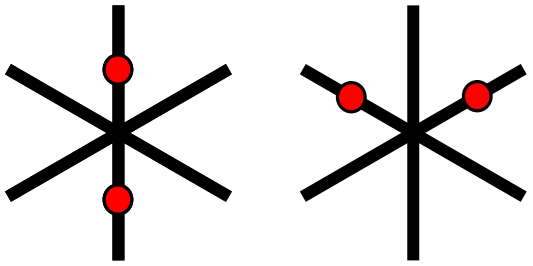

FIGURE 5.6: $IV^{(01)}$ and $IV^{(0|1)}$ fibers.

5.3.4.2 $I_3^{(0|1)}$ Branch

The second branch continues from $\mathcal{Q}(2,1,1,1,0,0,1)$ as in (5.3.15), which has leading order discriminant

$$\Delta_{I_3^{(0|1)}} = b_{1,0}^3 b_{0,0} P_0 P_1 z^3 + O(z^4)\,, \tag{5.3.27}$$

where the polynomial terms are now

$$P_0 = b_{1,0}^2 c_{0,2} - b_{1,0} b_{2,1} c_{1,1} - c_{1,1}^2\,, \tag{5.3.28}$$

$$P_1 = b_{0,0}^2 c_{1,1} - b_{0,0} b_{1,0} c_{2,1} + b_{1,0}^2 c_{3,1}\,. \tag{5.3.29}$$

The $P_0 = 0$ enhancement, which in fact after a shift is again canonical, is precisely the model that we discussed already following the other branch of the algorithm in (5.3.23), i.e. this is another instance when the branches join back together. Furthermore, $b_{0,0} = 0$ is removed by the lopping operation explained in section 5.1.6,[11] so that we are left with the following branches:

- $P_1 = 0$: $I_{4,nc}^{(0||1)}$
  P_1 can be solved along the lines of appendix B.1.3, yielding the non-canonical form, that we will discuss later, in section 5.5

  $$I_{4,nc}^{(0||1)}: \qquad \mathcal{Q}(2,1,1,1,0,0,1)|_{(5.3.29)}\,. \tag{5.3.30}$$

  This fiber is also depicted in figure 5.5, as the codimension one fiber structure does not depend on canonical versus non-canonical realization. However the codimension 2 structure will be different.

- $b_{1,0} = 0$: $IV^{(0|1)}$
  Finally, $b_{1,0} = 0$ moves us out of the I_n branch again to give another IV fiber, with

[11] Setting $b_{0,0} = 0$ here would give rise to an $I_4^{(01)}$ model, which one can check explicitly, but which moreover is expected by the lopping.

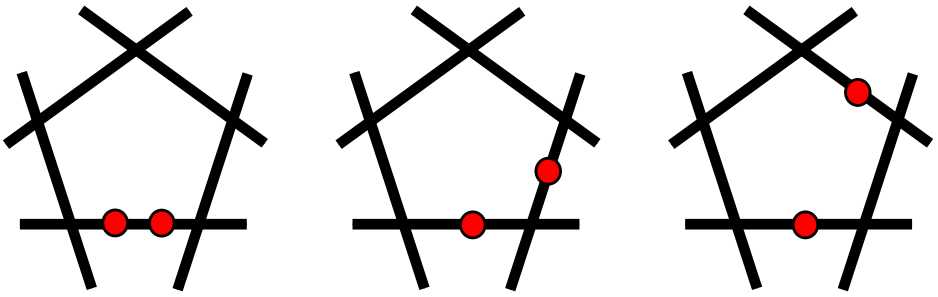

FIGURE 5.7: From left to right, showing the $I_5^{(01)}$, $I_5^{(0|1)}$ and $I_5^{(0||1)}$ fibers, respectively, with sections marked in red.

the sections located on separate fiber components

$$IV^{(0|1)}: \qquad \mathcal{Q}(2,1,1,1,0,1,1)\,. \tag{5.3.31}$$

5.3.5 Discriminant at $O(z^5)$

In the last subsection we have seen that at order z^4 in the discriminant the I_4 fiber types are $I_4^{(01)}$, $I_4^{(0|1)}$ and the non-canonical $I_{4,nc}^{(01)}$ and $I_{4,nc}^{(0||1)}$. The non-canonical models will be discussed in detail in section 5.5. Continuining with the canoncial branches in this section, we now study the enhancements starting from $I_4^{(01)}$ and $I_4^{(0|1)}$ realized by $\mathcal{Q}(4,2,1,0,0,0,2)$ and $\mathcal{Q}(3,2,1,1,0,0,1)$, respectively.

5.3.5.1 $I_4^{(01)}$ Branch

The discriminant of $I_4^{(01)}$ realized by $\mathcal{Q}(4,2,1,0,0,0,2)$ in (5.3.24) at leading order is

$$\Delta_{I_4^{(01)}} = b_{1,0}^4 c_{3,0}\,(b_{0,0}b_{1,0}+c_{3,0})\,P_0 z^4 + O(z^5)\,, \tag{5.3.32}$$

with

$$P_0 = b_{1,0}^2 c_{0,4} - b_{1,0}b_{2,2}c_{1,2} - c_{1,2}^2\,. \tag{5.3.33}$$

- $P_0 = 0$: $I_5^{(01)}$
  This polynomial term can be solved as in (5.3.13), and in fact allows for a shift to a canonical model, corresponding to $c_{0,4} = c_{1,2} = 0$. The fiber type is shown on the left of figure 5.7, and after the shift this is realized as a canonical model

$$I_5^{(01)}: \qquad \mathcal{Q}(5,3,1,0,0,0,2)\,. \tag{5.3.34}$$

Note that this model also appears from the other branch, starting with $I_4^{(0|1)}$, i.e. $\mathcal{Q}(3,2,1,1,0,0,1)$, where we set $b_{0,0} = 0$, and by the lopping we identify these models automatically.

- $c_{3,0} = 0$: $I_5^{(0|1)}$
  This enhancement yields a fiber with canonical form, shown in the middle of figure 5.7, which is realized by

$$I_5^{(0|1)}: \qquad \mathcal{Q}(4,2,1,1,0,0,2)\,. \tag{5.3.35}$$

- $b_{1,0} = 0$: $I_0^{*(01)}$
  Again $b_{1,0}$ moves out of the I_n branch, and at this order starts entering the I_n^* branch, which realizes the $SO(2n)$ gauge groups, shown in figure 5.8,

$$I_0^{*(01)}: \qquad \mathcal{Q}(4,2,1,0,0,1,2)\,. \tag{5.3.36}$$

  with the sequence (z,x,y,ζ_1), (ζ_1,y,ζ_2), $(\zeta_1,\zeta_2,\zeta_3)$, (ζ_2,x,ζ_4). After these blow-ups, the divisor $z\zeta_1 = 0$ does not intersect the elliptic fibration anymore, and the fiber components are z, ζ_2, ζ_3 and ζ_4, with all curves only intersecting ζ_4. However, $\zeta_2 = 0$ here is a doubled curve, in the sense that it has self-intersection -4 and intersects ζ_4 twice. Furthermore, the fibration over $\zeta_2 = 0$ is given by

$$c_{1,1}z^2 + c_{2,1}z\zeta_4 + c_{3,1}\zeta_4^2 = 0\,. \tag{5.3.37}$$

  This equation will factor into two parts if its discriminant is a perfect square, that is, if

$$c_{2,1}^2 - 4c_{1,1}c_{3,1} = p^2 \tag{5.3.38}$$

  for some section p. If this is the case, $\zeta_2 = 0$ splits into two fiber components, and we obtain an intersection structure like the one in figure 5.8 on the left. If the discriminant is not a perfect square, the fiber will still locally look like the one in the figure, but there will be a monodromy relating two of the multiplicity 1 fiber curves on which there is no section. The former case is denoted I_0^{*s} in the literature (with associated gauge group $SO(8)$), and the latter one I_0^{*ss} (with associated gauge group $SO(7)$).

  Although we specialized to split-type models at the beginning of this section, let us also note that Tate's algorithm yields a realization of the $I_0^{*ns(01)}$ fiber type with

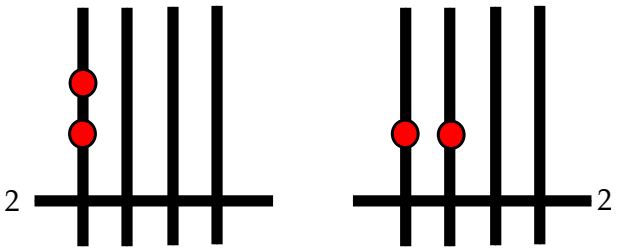

FIGURE 5.8: $I_0^{*(01)}$ and $I_0^{*(0|1)}$ fibers, where the 2 next to a black lines indicates multiplicity two of the fiber component, all other components are multiplicity one. The extra sections can only be on the multiplicity one fiber components.

associated gauge group G_2. Its equation is given by

$$I_0^{*ns(01)}: \qquad \mathcal{Q}(4,2,0,0,0,0,2)\,, \tag{5.3.39}$$

with the additional monodromy condition that

$$c_{2,0} = -b_{1,0}^2/4\,. \tag{5.3.40}$$

Note that the fiber indeed becomes $I_0^{*ss(01)}$ for $b_{1,0} = 0$.

5.3.5.2 $I_4^{(0|1)}$ Branch

The second branch at order z^4 emanates from $I_4^{(0|1)}$, realized in terms of $\mathcal{Q}(3,2,1,1,0,0,1)$ in (5.3.23), which has leading order discriminant

$$\Delta_{I_4^{(0|1)}} = b_{1,0}^4 b_{0,0} P_0 P_1 z^4 + O(z^5)\,, \tag{5.3.41}$$

with polynomial terms

$$P_0 = b_{0,0}c_{2,1} - b_{1,0}c_{3,1}\,, \tag{5.3.42}$$

$$P_1 = b_{1,0}^2 c_{0,3} - b_{1,0}b_{2,1}c_{1,2} + b_{2,1}^2 c_{2,1}\,. \tag{5.3.43}$$

The case $b_{0,0}$ already was reached in the other branch by (5.3.24), and is lopped out.

- $P_0 = 0$: $I_{5,nc}^{(0||1)}$
  Using appendix B.1.1, one can solve for $P_0 = 0$, which results in a non-canonical form with the sections located on twice removed fiber components, see the right

most fiber in figure 5.7,

$$I_{5,nc}^{(0||1)}: \qquad \mathcal{Q}(3,2,1,1,0,0,1)|_{(5.3.42)}\,. \tag{5.3.44}$$

- $P_1 = 0$: $I_5^{(0|1)}$, $I_{5,nc}^{(0|1)}$
  This fibration, too, has a non-canonical form, and solving $P_1 = 0$ using appendix B.1.3 yields the canonical model, which is exactly already reached by alternative route in (5.3.35), as well as the non-canonical

$$I_{5,nc}^{(0|1)}: \qquad \mathcal{Q}(3,2,1,1,0,0,1)|_{(5.3.43)}\,. \tag{5.3.45}$$

- $b_{1,0} = 0$: $I_0^{*(0|1)}$
  This enhancement yields a fiber with canonical form

$$I_0^{*(0|1)}: \qquad \mathcal{Q}(3,2,1,1,0,1,1)\,. \tag{5.3.46}$$

  The $I_0^{*(0|1)}$-fiber also has a semi-split version, given by the form

$$I_0^{*ss(0|1)}: \qquad \mathcal{Q}(2,2,1,1,0,1,1)\,. \tag{5.3.47}$$

  This form can be obtained e.g., as an enhancement of the $IV^{(0|1)}$ fiber (5.3.31).

5.3.6 Codimension two fibers for canonical I_5

After working through Tate's algorithm starting from the I_1 fibration of $\mathrm{Bl}_{[0,1,0]}\mathbb{P}_{[1,1,2]}$, one finds two canonical I_5 models: (5.3.34) and (5.3.35). These two models will be of particular interest for applications in F-theory model building. Therefore we will provide a few more details for these fiber types. First of all, we can determine the next order discriminant, and thereby the codimension 2 fiber types of these models. This allows computation also of the matter and corresponding $U(1)$ charges induced by the additional section, using the methods outlined in section 5.1.7. The results are given in table 5.3, and correspond to top 1 and 2 of [2], respectively. A detailed discussion of the map to tops is given in appendix B.3.

The non-canonical models will be discussed later, and go beyond the top models. We find that the codimension two fiber structure does not depend on a specific realization of a codimension one fiber type, i.e. the information about Kodaira type and location

Fiber	Model	Codim 2 locus	Representation	Codim 2 fiber
$I_5^{(01)}$	$\mathcal{Q}(5,3,1,0,0,0,2)$	$b_{1,0}$	$\mathbf{10}_0 + \overline{\mathbf{10}}_0$	$I_1^{*(01)}$
		$c_{3,0}$	$\mathbf{5}_{-1} + \overline{\mathbf{5}}_1$	$I_6^{(0\|1)}$
		$c_{3,0} + b_{0,0}b_{1,0}$	$\mathbf{5}_1 + \overline{\mathbf{5}}_{-1}$	$I_6^{(0\|1)}$
		$b_{1,0}^2 c_{0,5} - b_{1,0}b_{2,2}c_{1,3} + b_{2,2}^2 c_{2,1}$	$\mathbf{5}_0 + \overline{\mathbf{5}}_0$	$I_6^{(0\|1)}$
$I_5^{(0\|1)}$	$\mathcal{Q}(4,2,1,1,0,0,2)$	$b_{1,0}$	$\mathbf{10}_2 + \overline{\mathbf{10}}_{-2}$	$I_1^{*(0\|1)}$
		$b_{0,0}$	$\mathbf{5}_6 + \overline{\mathbf{5}}_{-6}$	$I_6^{(01)}$
		$b_{0,0}c_{2,1} - b_{1,0}c_{3,1}$	$\mathbf{5}_{-4} + \overline{\mathbf{5}}_4$	$I_6^{(0\|\|1)}$
		$b_{1,0}^2 c_{0,4} - b_{1,0}b_{2,2}c_{1,2} - c_{1,2}^2$	$\mathbf{5}_1 + \overline{\mathbf{5}}_{-1}$	$I_6^{(0\|1)}$

TABLE 5.3: There are two canonical I_5 models, for which we tabulate the vanishing order, codimension 2 enhancement loci, and the corresponding matter with $U(1)$ charges and codimension two fiber types. The models $I_5^{(01)}$ and $I_5^{(0|1)}$ agrees with the top 1 and 2, respectively, in the toric nomenclature of [2].

of the sections. Furthermore, the fiber structure in codimension one and two determines uniquely the matter and $U(1)$ charges.

Note that the fiber type in codimension two uniquely corresponds to a given matter locus, with the exception of the two loci $c_{3,0}$ and $c_{3,0} + b_{0,0}b_{1,0}$. This is not very surprising however, as the set of $U(1)$ charges in this model has a charge symmetry $q \to -q$, interchanging the charges of the two matter loci in question and leaving the other charges unchanged.

5.4 Tate tree tops and infinite branches

Despite the Tate algorithm being somewhat more involved in the present case, one can determine the remaining branches. Even with the lopping transformation taken into account to reduce the number of presentations of a given fiber type, it is still a tour de force to prove the algorithm by induction for all I_n, I_n^*. The existence of (multiply) non-canonical forms further complicate this matter. Here we determine the "tree tops", i.e. fibers realizing exceptional gauge groups models, which enhance to non-minimal models (and are thus endpoints of the algorithm). We also present canonical forms for I_n and I_n^* with any section distribution.

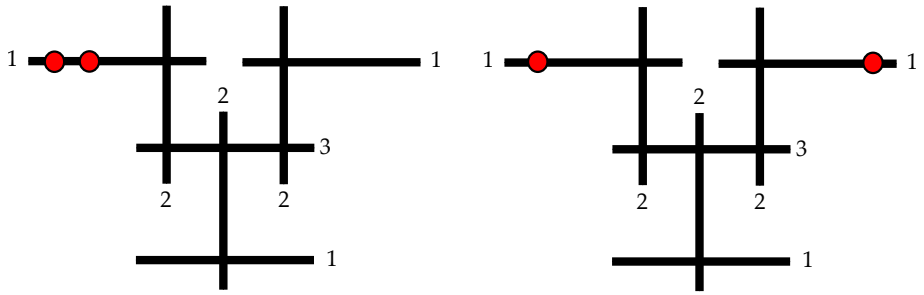

FIGURE 5.9: Modulo the $\mathbb{Z}_3$ symmetry, there are two type IV^* fibers with two sections: $IV^{*(01)}$ and $IV^{*(0|1)}$. Numerical labels indicate the multiplicity of the fiber components. The sections can again only meet the multiplicity one fiber components.

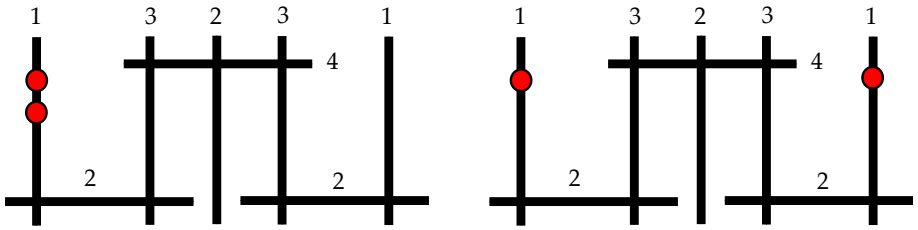

FIGURE 5.10: $III^{*(01)}$ and $III^{*(0|1)}$ fibers with the sections passing through on the two multiplicity one fiber components only. Numerical labels specify the multiplicity of the fiber components.

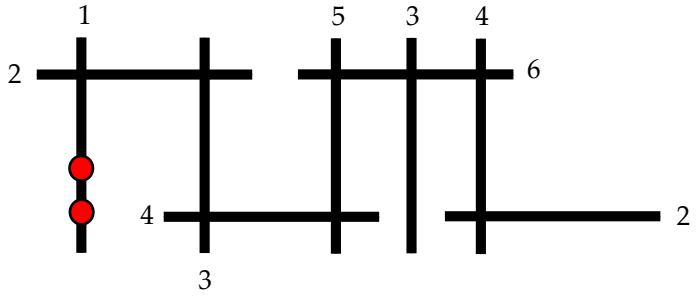

FIGURE 5.11: There is exactly one $II^{*(01)}$ fiber type, with both sections on the single multiplicity one fiber component.

5.4.1 Tate tree tops

Some branches of the Tate tree stop, as one reaches fibers with exceptional type gauge groups, such as II^*, III^*, IV^*. Further enhancement of the discriminant beyond these "tree tops" yields non-minimal models.

Fiber	Model	Codim 2 locus	Representation	Codim 2 fiber
$IV^{*(01)}$	$\mathcal{Q}(5,3,2,0,0,1,2)$	$b_{2,2}$	$\mathbf{27}_0 + \overline{\mathbf{27}}_0$	$III^{*(01)}$
		$c_{3,0}$	—	non-minimal
$IV^{*(0\|1)}$	$\mathcal{Q}(3,2,2,1,0,1,2)$	$b_{0,0}$	$\mathbf{27}_2 + \overline{\mathbf{27}}_{-2}$	$III^{*(01)}$
		$c_{1,2}$	$\mathbf{27}_{-1} + \overline{\mathbf{27}}_1$	$III^{*(0\|1)}$
$III^{*(01)}$	$\mathcal{Q}(5,3,2,0,0,1,3)$	$c_{1,3}$	$\mathbf{56}_0 + \overline{\mathbf{56}}_0$	$II^{*(01)}$
		$c_{3,0}$	—	non-minimal
$III^{*(0\|1)}$	$\mathcal{Q}(3,3,2,1,0,1,2)$	$b_{0,0}$	$\mathbf{56}_1 + \overline{\mathbf{56}}_{-1}$	$II^{*(01)}$
		$c_{0,3}$	—	non-minimal

TABLE 5.4: Codimension two fiber types and $U(1)$ charges for the IV^* and III^* models.

- The IV^* fiber types are depicted in figure 5.9. From Tate's algorithm, there are two forms, which are canonical, given by[12]

$$\begin{aligned} IV^{*(01)}: &\quad \mathcal{Q}(5,3,2,0,0,1,2) \\ IV^{*(0|1)}: &\quad \mathcal{Q}(3,2,2,1,0,1,2)\,. \end{aligned} \tag{5.4.1}$$

- There are two III^* fiber types, shown in figure 5.10. From the algorithm, these are realized by the canonical models

$$\begin{aligned} III^{*(01)}: &\quad \mathcal{Q}(5,3,2,0,0,1,3) \\ III^{*(0|1)}: &\quad \mathcal{Q}(3,3,2,1,0,1,2)\,. \end{aligned} \tag{5.4.2}$$

- There is only a single $II^{*(01)}$ fiber is given in figure 5.11, realized for instance in terms of

$$II^{*(01)}: \quad \mathcal{Q}(5,4,2,0,0,1,3)\,. \tag{5.4.3}$$

Note that all these models are such that the sections intersect the multiplicity one fiber components only, confirming our earlier general argument. There are no non-canonical forms present in the algorithm for these fiber types.[13] The codimension two enhancements and spectra of these models are summarized in table 5.4.

[12] The nomenclature for these fibers is as explained in section 5.1.2. I.e. the superscript on the standard Kodaira-Neron fiber label refers only to the multiplicity one components in the fiber, where the sections can meet.

[13] At first this is an empirical observation, i.e., the discriminant in those cases does not have non-trivial polynomial terms. This is largely due to the fact that these branches have $b_{1,0} = 0$, which turns all the non-trivial polynomials encountered in section 5.3 into simple one-term discriminant factors. This seems to be closely related to the issue that arises in codimension 2 enhancements, where a non-abelian commutant in the codimension 2 enhanced symmetry group results in monodromy, rather than multiple enhancement loci, like in [99].

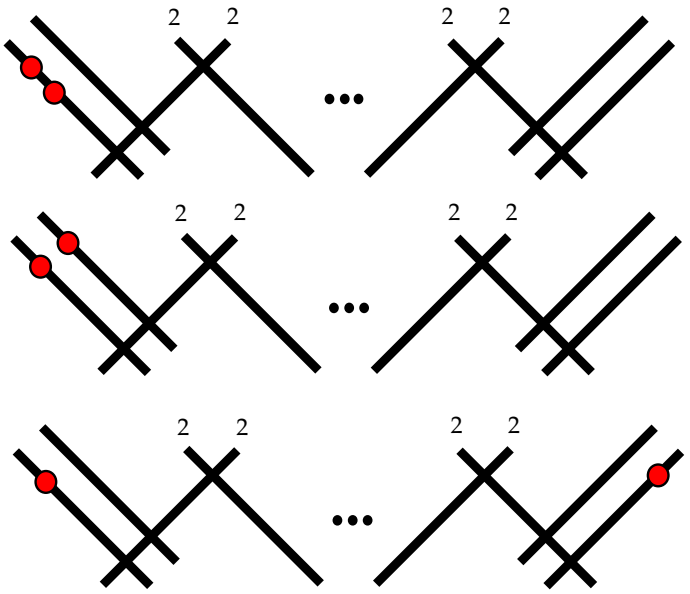

FIGURE 5.12: From top to bottom: $I_n^{*(01)}$, $I_n^{*(0|1)}$ and $I_n^{*(0||1)}$ fiber types with sections, which can intersect only the multiplicity one fiber components. Modulo the symmtries of the affine D_n Dynkin diagram, there are three distinct such distributions, all of which occur in the Tate tree.

Finally, the IV^{*ns} fiber, which realizes the group F_4, is given by

$$IV^{*ns}: \qquad \mathcal{Q}(4,3,2,0,0,1,2)\,. \tag{5.4.4}$$

This model degenerates to the split case IV^* with $c_{0,4}=0$. The vanishing of the leading order discriminant for the non-split case

$$\Delta_{IV^{*ns}} = c_{3,0}^4\left(b_{2,2}^2+4c_{0,4}\right)z^8+O(z^9)\,, \tag{5.4.5}$$

enhance either to a non-minimal model ($c_{3,0}=0$) or back to $III^{*(01)}$.

5.4.2 I_n^* Branch

The fibers of Kodaira type I_n^* only have four multiplicity one fibers components, which can intersect the sections by the argument presented in section 5.1.3. Therefore, modulo the symmetries of the affine D_n Dynkin diagram, there are three distinct fiber types, denoted $I_n^{*(01)}$, $I_n^{*(0|1)}$ and $I_n^{*(0||1)}$, respectively, which are shown in figure 5.12. We list three infinite series of realizations, which together realize all these fiber types for $n\geq 1$ in table 5.2.

Fiber	Model	Codim 2 locus	Representation	Codim 2 fiber
$I_1^{*(01)}$	$\mathcal{Q}(5,3,1,0,0,1,2)$	$c_{2,1}$	$\mathbf{16}_0 + \overline{\mathbf{16}}_0$	$IV^{*(01)}$
		$c_{3,0}$	$\mathbf{10}_1 + \mathbf{10}_{-1}$	$I_2^{*(0\|1)}$
		$b_{2,2}$	—	$I_2^{*ns(01)}$
$I_1^{*(0\|1)}$	$\mathcal{Q}(4,2,1,1,0,1,2)$	$c_{2,1}$	$\mathbf{16}_1 + \overline{\mathbf{16}}_{-1}$	$IV^{*(0\|1)}$
		$b_{0,0}$	$\mathbf{10}_{-2} + \mathbf{10}_2$	$I_2^{*(01)}$
		$c_{1,2}$	—	$I_2^{*ns(0\|1)}$
$I_1^{*(0\|\|1)}$	$\mathcal{Q}(3,2,2,1,0,1,1)$	$b_{2,1}$	$\mathbf{16}_{-1} + \overline{\mathbf{16}}_1$	$IV^{*(0\|1)}$
		$b_{0,0}$	$\mathbf{16}_3 + \overline{\mathbf{16}}_{-3}$	$IV^{*(01)}$
		$b_{0,0}c_{1,2} - b_{2,1}c_{3,1}$	$\mathbf{10}_2 + \mathbf{10}_{-2}$	$I_2^{*(0\|\|1)}$

TABLE 5.5: Codimension two fiber types and $U(1)$ charges for the I_1^* models. Note that the **10** and $\overline{\mathbf{10}}$ representations in $SO(10)$ are identical. Enhancements from split-type fibers to non-split-type fibers do not yield additional localized matter.

The two I_0^* fiber types have been described in section 5.3. In agreement with the general argument from section 5.1.3, there is no $I_n^{*ns(0||1)}$ fiber. The resolved geometries and Cartan divisors of all split-type fibrations are given in appendix B.4. For purposes of model building in F-theory, the codimension two structure and $U(1)$ charges of the I_1^* fibers are tabulated in table 5.5.

5.4.3 I_n Branch

The Kodaira I_n fibers have multiplicity one for each fiber component, and so the fibers that arise when taking into account the structure of extra sections can be characterized by the number of fiber components k, that separate the two components which intersect the sections σ_0 and σ_1. Such an $I_n^{(0|^k1)}$ fiber is realized by

$$\begin{aligned} I_{2m}^{(0|^k1)}: \quad & \mathcal{Q}\Big(2m-k, \max\left\{\left\lceil m-\frac{k}{2}\right\rceil, k\right\}, \max\{1,k\}, k, \\ & \qquad 0, 0, \min\left\{\left\lfloor m-\frac{k}{2}\right\rfloor, \max\{1, 2(m-k)\}\right\}\Big) \\ I_{2m+1}^{(0|^k1)}: \quad & \mathcal{Q}\Big(2m+1-k, \max\left\{\left\lceil m+1-\frac{k}{2}\right\rceil, k\right\}, \max\{1,k\}, k, \\ & \qquad 0, 0, \max\left\{\left\lfloor m+1-\frac{k}{2}\right\rfloor, \max\{1, 2(m-k)+1\}\right\}\Big). \end{aligned} \tag{5.4.6}$$

In both cases, we assume $m \geq 3$, with the lower cases having been given in section 5.3. The full ordered sequence of resolutions, the resolved geometries, and the Cartan divisors can again be found in appendix B.4. An alternative representation of these is given in the summary table 5.2.

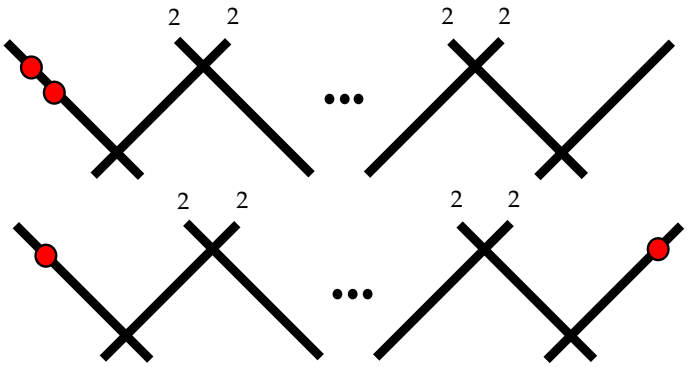

FIGURE 5.13: There are two non-split $I_n^{ns(01)}$ and $I_n^{ns(0|1)}$ fibers with two sections, which intersect the multiplicity one fiber components.

Note that these forms are only canonical. However, for I_n with $n > 9$, the general solutions to the polynomial discriminant factors of these I_n models introduce codimension two loci which the fibration enhances to a non-minimal form. Requiring the absence of such loci allows us to always find coordinate shifts that put these models into canonical form. This is similar to the situation in $\mathbb{P}^{(1,2,3)}$.

Furthermore, there are fibrations realizing the non-split fiber types $I_{2m}^{ns(01)}$, $I_{2m+1}^{ns(01)}$, and $I_{2m}^{ns(0|1)}$. They are given by

$$\begin{aligned} I_{2m}^{ns(01)}: &\quad \mathcal{Q}(2m, m, 0, 0, 0, 0, m) \\ I_{2m+1}^{ns(01)}: &\quad \mathcal{Q}(2m+1, m+1, 0, 0, 0, 0, m+1) \\ I_{2m}^{ns(0|1)}: &\quad \mathcal{Q}(m, m, m, m, 0, 0, 0,) \,, \end{aligned} \tag{5.4.7}$$

respectively. While the first two of these forms arise as enhancements of the I_1 starting point fiber, the last series is obtained by enhancing the third starting point fibration from (5.1.32), which was not contained within a single patch of the ambient space X over the entire locus $z = 0$ in the base manifold B. The fiber types are depicted in figure 5.13.

5.5 Tate Trees: Non-Canonical Forms

In the last two section we considered only the canonical enhancement patterns in the Tate tree, i.e. those that are characterized by vanishing orders of the coefficient sections alone. There are several branches which are however non-canonical: there is no shift or simple coordinate change that is locally well-defined and will put the forms into a canonical form. These arise whenever the discriminant has a factor that is a quadratic or higher degree polynomial in the sections c_i and b_j. Studying these branches amounts to finding solutions

to polynomial equations in UFD, which can be done explicitly in simple instances and is summarized in appendix B.1.

For $\mathbb{P}_{[1,2,3]}$ a similar analysis was performed for the standard Tate's algorithm in [1], where one cannot achieve the standard (i.e. canonical) Tate form in only a few outlier cases. In $\mathbb{P}_{[1,1,2]}$, the situation is quite different: non-canonical forms are very common. In fact, each non-canonical form gives rise to a new branch of the algorithm, with multiply-non-canonical forms, e.g. a canonical I_n model can enhance to a non-canonical I_{n+1} model, which in turn can have a non-trivial polynomial term in the discriminant, which yields a doubly non-canonical I_{n+2} model etc. In section 5.3 we only summarized the fiber types of these non-canonical models and will now provide details for these, as well as some studies of doubly non-canonical models. Multiply non-canonical models can be quite involved, we leave this for future work.

From the point of view of model building in F-theory, these non-canonical forms open up some exciting model building prospects. The types of codimension one fibers that can be realized in terms of non-canonical models are the same as in the canonical branch. However, the codimension two structure is very different, and allows for instance to have multiple enhancement loci from I_n to I^*_{n-4}. Concretely, for I_5 models realizing $SU(5)$ gauge theories, this means there are multiple, distinct loci with **10** matter, charged differently under the $U(1)$ that arises from the extra section. In the following we will concentrate on the non-canonical I_5 fibers, either arising from canonical I_4 or non-canonical I_4.

5.5.1 Non-canonical I_5 from canonical I_4

Starting with the canonical I_4 models, there are two non-canonical enhancements to I_5, both of which emanate from $I_4^{(0|1)}$ realized in terms of $\mathcal{Q}(3,2,1,1,0,0,1)$, and are part of the branch discussed in section 5.3.5.2: The codimension 2 fibers, and matter with $U(1)$ charge spectrum of these non-canonical I_5 models are summarized in table 5.6. Note that the fiber structure in codimension 2 follows the pattern discussed in section 5.1.3.

5.5.1.1 $I_{5,nc}^{(0||1)}$

This model arises in the algorithm in (5.3.44), as a specialization of the canonical I_4 model $\mathcal{Q}(3,2,1,1,0,0,1)$, which has a component in the discriminant given by

$$P = b_{0,0}c_{2,1} - b_{1,0}c_{3,1} = 0\,. \tag{5.5.1}$$

Fiber	Model	Codim 2 locus	Representation	Codim 2 fiber
$I_{5,nc}^{(0\|\|1)}$	$Q(3,2,1,1,0,0,1)\|_{(5.3.42)}$	σ_3	$\mathbf{10}_1+\overline{\mathbf{10}}_{-1}$	$I_1^{*(0\|\|1)}$
		σ_1	$\mathbf{10}_{-4}+\overline{\mathbf{10}}_4$	$I_1^{*(01)}$
		σ_2	$\mathbf{5}_{-7}+\overline{\mathbf{5}}_7$	$I_6^{(01)}$
		(5.5.5)	$\mathbf{5}_{-2}+\overline{\mathbf{5}}_2$	$I_6^{(0\|\|1)}$
		(5.5.6)	$\mathbf{5}_3+\overline{\mathbf{5}}_{-3}$	$I_6^{(0\|\|\|1)}$
$I_{5,nc}^{(0\|1)}$	$Q(3,2,1,1,0,0,1)\|_{(5.3.43)}$	σ_1	$\mathbf{10}_2+\overline{\mathbf{10}}_{-2}$	$I_1^{*(0\|1)}$
		σ_2	$\mathbf{10}_{-3}+\overline{\mathbf{10}}_3$	$I_1^{*(0\|\|1)}$
		$b_{0,0}$	$\mathbf{5}_6+\overline{\mathbf{5}}_{-6}$	$I_6^{(01)}$
		(5.5.11)	$\mathbf{5}_{-4}+\overline{\mathbf{5}}_4$	$I_6^{(0\|\|1)}$
		(5.5.12)	$\mathbf{5}_1+\overline{\mathbf{5}}_{-1}$	$I_6^{(0\|1)}$

TABLE 5.6: Codimension two loci, fiber types, and matter and $U(1)$ charges for non-canonical I_5 models arising from canonical I_4 models. These models generalize top 4, and tops 2 and 3 respectively.

As explained in appendix B.1.1, over a UFD, this requires the existence of new sections σ_i satisfying

$$b_{0,0}=\sigma_1\sigma_2\,,\quad c_{2,1}=\sigma_3\sigma_4\,,\quad b_{1,0}=\sigma_1\sigma_3\,,\quad c_{3,1}=\sigma_2\sigma_4\,, \tag{5.5.2}$$

with σ_2 and σ_3 coprime, which automatically solves $P=0$. The resulting model has fiber type

$$I_{5,nc}^{(0\|\|1)}:\qquad \mathcal{Q}(3,2,1,1,0,0,1)\|_{(5.3.42)}\,, \tag{5.5.3}$$

and leading order discriminant

$$\Delta_{I_5^{(0\|\|1)}}=\sigma_1^4\sigma_3^4\sigma_2P_2P_3z^5+O(z^6)\,, \tag{5.5.4}$$

where

$$P_2=\sigma_4b_{2,1}^2+\sigma_1^2\sigma_3c_{0,3}-\sigma_1b_{2,1}c_{1,2} \tag{5.5.5}$$

$$\begin{aligned}P_3=&\,\sigma_1\sigma_2^2\left(\sigma_1c_{1,2}-\sigma_4b_{2,1}\right)+\sigma_3\sigma_2\left(\sigma_4\sigma_1b_{1,1}-\sigma_1^2c_{2,2}+\sigma_4^2\right)\\&+\sigma_1\sigma_3^2\left(\sigma_1c_{3,2}-\sigma_4b_{0,1}\right)\,.\end{aligned} \tag{5.5.6}$$

Note that the standard $b_{1,0}=0$ locus is now reducible due to (5.5.2), which gives rise to two codimension two enhancements to I_1^* (or **10** matter loci), shown in figure 5.14. The spectrum is summarized in table 5.6. In appendix B.3, it is shown that if the section σ_1 never vanishes on B, one can perform a coordinate shift to obtain the canonical model $\mathcal{Q}(3,2,2,2,0,0,1)$, which is also known as top 4 in the literature. This non-canonical

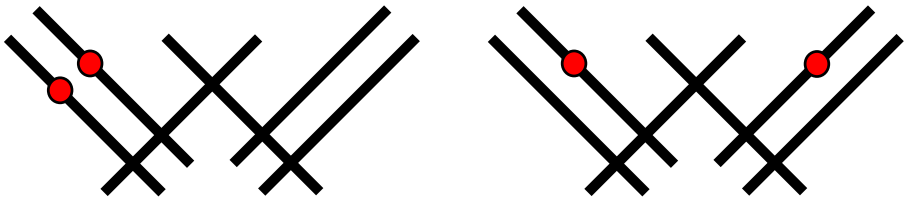

FIGURE 5.14: $I_1^{*(0|1)}$ and $I_1^{*(0||1)}$ fibers obtained in codimension two of the $I_{5,nc}^{(0|1)}$ fiber over the curves $\sigma_1 = 0$ and $\sigma_2 = 0$, respectively.

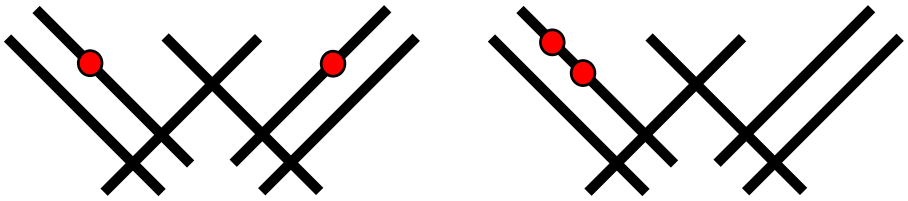

FIGURE 5.15: $I_1^{*(0||1)}$ and $I_1^{*(01)}$ fibers obtained in codimension two of the $I_{5.nc}^{(0||1)}$ fiber over the curves $\sigma_3 = 0$ and $\sigma_1 = 0$, respectively.

model is therefore a generalization of the top 4 of [2].

5.5.1.2 $I_{5,nc}^{(0|1)}$

Starting with the same canonical I_4 there is a non-canonical I_5 obtained by setting

$$P = b_{1,0}^2 c_{0,3} - b_{1,0} b_{2,1} c_{1,2} + b_{2,1}^2 c_{2,1} = 0\,, \tag{5.5.7}$$

which has a general solution obtained in appendix B.1.3, if there exist sections σ_i such that

$$b_{1,0} = \sigma_1\sigma_2\,, \quad b_{2,1} = \sigma_1\sigma_3\,, \quad c_{0,3} = \sigma_3\sigma_4\,, \quad c_{2,1} = \sigma_2\sigma_5\,, \quad c_{1,2} = \sigma_2\sigma_4 + \sigma_3\sigma_5\,, \tag{5.5.8}$$

again with σ_2 and σ_3 coprime. This model has fiber type

$$I_{5,nc}^{(0|1)}: \qquad \mathcal{Q}(3,2,1,1,0,0,1)|_{(5.3.43)} \tag{5.5.9}$$

and discriminant

$$\Delta_{I_5^{(0|1)}} = \sigma_1^4\sigma_2^4 b_{0,0} P_2 P_3 z^5 + O(z^6)\,, \tag{5.5.10}$$

where

$$P_2 = \sigma_1 c_{3,1} - \sigma_5 b_{0,0} \tag{5.5.11}$$

$$P_3 = -\sigma_2^3\left(\sigma_4\sigma_1 b_{2,2} - \sigma_1^2 c_{0,4} + \sigma_4^2\right) + \sigma_3\sigma_2^2\left(\sigma_1\left(\sigma_5 b_{2,2} - \sigma_1 c_{1,3}\right) + \sigma_4\left(\sigma_1 b_{1,1} + 2\sigma_5\right)\right)$$

$$- \sigma_3^2\sigma_2 \left(\sigma_1 \left(\sigma_4 b_{0,0} - \sigma_1 c_{2,2}\right) + \sigma_1\sigma_5 b_{1,1} + \sigma_5^2\right) + \sigma_1\sigma_3^3 \left(\sigma_5 b_{0,0} - \sigma_1 c_{3,1}\right) . \quad (5.5.12)$$

Again $b_{1,0} = \sigma_1\sigma_2$, factors and yields two codimension two loci of I_1^* type, shown in figure 5.15, and the spectrum is listed in table 5.6.

If either of the two sections σ_1, σ_2 do not vanish on the base manifold, there is a coordinate shift, explicitly given in appendix B.3, into the canonical models $\mathcal{Q}(4,3,2,1,0,0,1)$ (if σ_1 does not vanish), or $\mathcal{Q}(4,2,1,1,0,0,2)$ (if σ_2 is always nonzero). These two models are sometimes referred to in the literature as tops 3 and 2, respectively, and the non-canonical model is a generalization of these two toric models.

5.5.2 Non-canonical I_5 from non-canonical I_4

Non-canonical I_5 models can arise also from non-canonical I_4 models, which in turn are enhancements of (canonical[14]) I_3 models. Solving in full generality for these discriminant loci is quite complicated, and we will present here only example solutions for these doubly non-canonical forms. The key feature is that these models potentially allow for three enhancement loci to I_1^*. The models we present here will be special solutions to the discriminant equation for doubly non-canonical *ncnc* models, i.e. enhancements along non-trivial polynomial factors in the discriminant, which arise in non-canonical models. We will address *ncnc* type models also in section 5.6 in $\mathbb{P}_{[1,2,3]}$.

5.5.2.1 $I_{4,nc}^{(01)}$ Branch

The form $\mathcal{Q}(3,2,1,0,0,0,1)|_{(5.3.22)}$ from (5.3.25) has leading-order discriminant

$$\Delta_{I_4^{(01)}} = \sigma_1^4\sigma_2^4\sigma_5 \left(\sigma_5 + \sigma_1 b_{0,0}\right) P_2 z^4 + O(z^5) , \quad (5.5.13)$$

with

$$\begin{aligned} P_2 =& \sigma_1 \left(\sigma_4\sigma_2^2 - \sigma_3\sigma_6\sigma_2 + \sigma_3^2\sigma_5\right) \left(\sigma_2^2 b_{2,2} + \sigma_3 \left(\sigma_3 b_{0,0} - \sigma_2 b_{1,1}\right)\right) \\ &+ \sigma_2\sigma_1^2 \left(\sigma_3 \left(\sigma_3 \left(\mathrm{c31}\sigma_3 - \sigma_2 c_{2,2}\right) + \sigma_2^2 c_{1,3}\right) - \sigma_2^3 c_{0,4}\right) + \left(\sigma_4\sigma_2^2 - \sigma_3\sigma_6\sigma_2 + \sigma_3^2\sigma_5\right)^2 , \end{aligned} \quad (5.5.14)$$

and σ_2, σ_3 coprime. σ_1 and σ_2 divide $b_{1,0}$, hence the corresponding enhancements are not considered here.

[14] We consider the branch starting from a non-canonical I_3 case in the next subsection.

- $\sigma_5 = 0$: $I_5^{(0|1)}$

  σ_5 divides $c_{3,0}$. Thus, by first enhancing $c_{3,0}$ and then reconsidering the non-canonical enhancement that led to $\mathcal{Q}(3,2,1,0,0,0,1)|_{(5.3.22)}$, one arrives at the non-canonical fibration $\mathcal{Q}(3,2,1,1,0,0,1)|_{(5.3.43)}$.

- $P_2 = 0$: $I_{5,ncnc}^{(01)}$

  Solving this in full generality is rather difficult. However, the main goal here is to obtain a class of solutions, that result in three charged **10** matter loci, i.e. three loci where the fiber enhances to I_1^*.

  This enhancement yields a doubly non-canonical fibration. Note that P_2 is of schematic form

$$P_2 = \sigma_2^4 A - \sigma_2^3\sigma_3 B + \sigma_2^2\sigma_3^2 C - \sigma_2\sigma_3^3 D + \sigma_3^4(\sigma_5(\sigma_5 + \sigma_1 b_{0,0}))\,. \tag{5.5.15}$$

  As in the solutions in appendix B.1, one notes that necessary conditions for $P_2 = 0$ are $\sigma_3|\sigma_2^4 A$ and $\sigma_2|\sigma_3^4((\sigma_5(\sigma_5 + \sigma_1 b_{0,0})))$. However, $\sigma_2 = \sigma_3 = 0$ results directly in a non-minimal enhancement, and so we can discard this. Therefore we have $(\sigma_2, \sigma_3) = 1$. Then one other alternative is that $\sigma_2|\sigma_5$ (or $\sigma_2|(\sigma_5 + \sigma_1 b_{0,0})$ –we will not consider this and thereby the solution is only an example solution for this doubly non-canonical case), so that

$$\chi = (\sigma_2, \sigma_5)\,, \qquad \sigma_2 = \chi\chi_2\,, \qquad \sigma_5 = \chi\chi_5\,. \tag{5.5.16}$$

  From this $b_{1,0} = \sigma_1\sigma_2 = \sigma_1\chi\chi_2$, one expects that this twice non-canonical model therefore should have three **10** curves. Inserting this results in the polynomial, we obtain

$$P_2 = \chi(\chi\tilde{A}^2 + \tilde{B}\tilde{A}\sigma_1 + \sigma_1^2\chi_2\tilde{C})\,, \tag{5.5.17}$$

  where $\tilde{A} = \sigma_3^2\chi_5 - \sigma_3\sigma_6\chi_2 + \sigma_4\chi\chi_2^2$. At this point we specialize to the solution where we solve $\tilde{A} = 0$ and then the remaining terms to vanish. This is not the general solution, however it will exemplify the feature that this model has three **10** matter loci. Solving $\tilde{A} = 0$ by the three-term polyonimal solution in appendix B.1.3 results in

$$\sigma_2 = s_1 s_2\,, \quad \sigma_3 = s_1 s_3\,, \quad \chi\sigma_4 = s_3 s_4\,, \quad \chi_5 = s_2 s_5\,, \quad \sigma_6 = s_2 s_4 + s_3 s_5\,. \tag{5.5.18}$$

By the co-primeness of σ_1 and σ_2 we have that $s_1 = 1$. Furthermore, the middle equation implies

$$\chi = \lambda_1\lambda_2\,, \quad \sigma_4 = \sigma_3\lambda_4\,, \quad s_3 = \lambda_1\lambda_3\,, \quad s_4 = \lambda_2\lambda_4\,. \tag{5.5.19}$$

Furthermore solving $\tilde{C} = 0$ for $c_{3,1}$ results in a complete solution of $P_2 = 0$ where

$$b_{1,0} = \lambda_1\lambda_2\sigma_1 s_2\,. \tag{5.5.20}$$

The codimension two locus $\lambda_1 = 0$ is non-minimal, whereas all remaining ones give rise to I_1^* fibers. Thus, one would naively think that this is a model with three **10** matter curves. However, λ_2 and s_2 appear in the exact same pattern in the hypersurface equation of this form, and therefore behave similarly. One is thus left with only two **10** curves, namely $s_2 = 0$ and $\sigma_1 = 0$. The leading coefficients in summary are (setting $\lambda_1 = 1$ to avoid the non-minimal locus)

$$\begin{aligned}
c_{0,3} &= \lambda_3^2\lambda_4\\
c_{1,2} &= \lambda_3(s_5\lambda_3 + 2s_2\lambda_2\lambda_4)\\
c_{2,1} &= s_2\lambda_2(2s_5\lambda_3 + s_2\lambda_2\lambda_4)\\
c_{3,0} &= s_2^2 s_5\lambda_2^2\\
c_{3,1} &= \frac{1}{\lambda_3^3}\lambda_2 s_2\left(\lambda_2^2 s_2^2 c_{0,4} + \lambda_3\left(\lambda_3 c_{2,2} - \lambda_2 s_2 c_{1,3}\right)\right)\\
b_{0,0} &= b_{0,0}\\
b_{1,0} &= s_2\lambda_2\sigma_1\\
b_{2,1} &= \lambda_3\sigma_1\,.
\end{aligned} \tag{5.5.21}$$

Note that we can set $\lambda_3 = 1$ without any loss of matter loci. The discriminant of this equation is given by

$$\Delta_{I_5^{(01)}} = s_2^4 s_5\lambda_2^4\sigma_1^4\left(s_2 s_5\lambda_2 + b_{0,0}\sigma_1\right)P_3 \tag{5.5.22}$$

Fiber	Model	Codim 2 locus	Representation	Codim 2 fiber
$I^{(01)}_{5,ncnc}$	$Q(3,2,1,0,0,0,1)\vert_{(5.5.21)}$	σ_1	$\mathbf{10}_0 + \overline{\mathbf{10}}_0$	I_1^*
		s_2	$\mathbf{10}_0 + \overline{\mathbf{10}}_0$	I_1^*
		s_5	$\mathbf{5}_1 + \overline{\mathbf{5}}_{-1}$	I_6
		$s_2 s_5 \lambda_2 + b_{0,1}\sigma_1$	$\mathbf{5}_{-1} + \overline{\mathbf{5}}_1$	I_6
		(5.5.23)	$\mathbf{5}_0 + \overline{\mathbf{5}}_0$	I_6

TABLE 5.7: Codimension two loci, fiber types, and matter and $U(1)$ charges of the twice non-canonical I_5 model.

with

$$\begin{aligned} P_3 =& b_{0,0}^2 \left(-s_5 + s_2\lambda_2\lambda_4\right) \\ &+ b_{0,0} s_2 \lambda_2 \Big[2 s_5 \left(b_{1,1} - s_2\lambda_2 b_{2,2}\right) \\ &+ s_2\lambda_2 \left(-2\lambda_4 b_{1,1} + 2 s_2 \lambda_2 \lambda_4 b_{2,2} - 3 s_2 \lambda_2 \sigma_1 c_{0,4} + 2\sigma_1 c_{1,3}\right) - \sigma_1 c_{2,2} \Big] \\ &+ s_2^2 \lambda_2^2 \Big[- s_5 \left(b_{1,1} - s_2\lambda_2 b_{2,2}\right)^2 + s_2^3 \lambda_2^3 \left(\lambda_4 b_{2,2}^2 + \sigma_1 \left(-3 b_{2,2} c_{0,4} + \sigma_1 c_{0,5}\right)\right) \\ &+ s_2^2 \lambda_2^2 \left(-2\lambda_4 b_{1,1} b_{2,2} + \sigma_1 \left(3 b_{1,1} c_{0,4} + 2 b_{2,2} c_{1,3} - \sigma_1 c_{1,3}\right)\right) \\ &+ s_2 \lambda_2 \left(\lambda_4 b_{1,1}^2 + \sigma_1 \left(-2 b_{1,1} c_{1,3} - b_{2,2} c_{2,2} + \sigma_1 c_{2,3}\right) + \sigma_1 \left(b_{1,1} c_{2,2} - \sigma_1 c_{3,2}\right)\right) . \Big] \end{aligned} \tag{5.5.23}$$

The matter curves and $U(1)$ charges of this model are shown in table 5.7. Note that this is in fact a new fiber type, as there is no $I^{(01)}_{5,nc}$.

- $P_2 = 0$: (alternative solution) $I_5^{(01)}$
  An alternative way to solve for this doubly non-canonical model is to consider P_2 with the subleading $c_{i,j}$ terms set to zero

$$\begin{aligned} P_2|_{c_{i,j}=0} = & \left(\sigma_2^2\sigma_4 - \sigma_2\sigma_3\sigma_6 + \sigma_3^2\sigma_5\right) \times \\ & \times \left(\sigma_3^2(b_{0,0}\sigma_1 + \sigma_5) - \sigma_2\sigma_3(b_{1,1}\sigma_1 + \sigma_6) + \sigma_2^2(b_{2,2}\sigma_1 + \sigma_4)\right) . \end{aligned} \tag{5.5.24}$$

The first factor will not give an $SU(5)$ model, as the discriminant goes up to $O(z^7)$. However the second factor

$$\tilde{P}_2 = \sigma_3^2(b_{0,0}\sigma_1 + \sigma_5) - \sigma_2\sigma_3(b_{1,1}\sigma_1 + \sigma_6) + \sigma_2^2(b_{2,2}\sigma_1 + \sigma_4) \tag{5.5.25}$$

can be solved by

$$\begin{aligned}\sigma_4 &= \sigma_3\rho_4 - \sigma_1 b_{2,2}\\ \sigma_5 &= \sigma_2\rho_5 - \sigma_1 b_{0,0}\\ \sigma_6 &= -\sigma_1 b_{1,1} + \sigma_2\rho_4 + \sigma_3\rho_5\,.\end{aligned} \tag{5.5.26}$$

The resulting model has discriminant

$$\begin{aligned}\Delta_{\tilde{P}_2} =&\rho_5\sigma_1^4\sigma_2^4\left(\sigma_2^2 b_{2,2} + \sigma_3\left(\sigma_3 b_{0,0} - \sigma_2 b_{1,1}\right)\right)\left(\sigma_1 b_{0,0} - \rho_5\sigma_2\right)\times\\ &\times\left(\rho_4\sigma_2^3 b_{2,2} - \sigma_3\sigma_2^2\left(\rho_4 b_{1,1} + \rho_5 b_{2,2}\right) + \sigma_3^2\sigma_2\left(\rho_4 b_{0,0} + \rho_5 b_{1,1} + \sigma_1^2 b_{0,1}\right) z^5\right.\\ &\left.- \rho_5\sigma_3^3 b_{0,0}\right) + O(z^6)\,.\end{aligned} \tag{5.5.27}$$

There are three loci that result in codimension two loci $\sigma_1 = 0$ and $\sigma_3 = 0$ with I_1^* fibers, however the third factor $\sigma_2^2 b_{2,2} + \sigma_3\left(\sigma_3 b_{0,0} - \sigma_2 b_{1,1}\right) = 0$ is in fact again I_6. It would be quite exciting to solve these ncnc enhacements in generality and determine models with three distinctly charged **10** matter loci.

5.5.2.2 $I_{4,nc}^{(0||1)}$ Branch

The non-canonical fibration $\mathcal{Q}(2,1,1,1,0,0,1)|_{(5.3.29)}$ obtained from (5.3.30) has discriminant

$$\Delta_{I_4^{(0||1)}} = \sigma_1^4\sigma_2\sigma_3^4 P_2 P_3 z^4 + O(z^5) \tag{5.5.28}$$

with

$$\begin{aligned}P_2 =&\sigma_1^2 c_{0,2} - \sigma_1\sigma_4 b_{2,1} - \sigma_4^2\,,\\ P_3 =&\sigma_2^3\left(-\left(\sigma_4\sigma_1 b_{2,1} - \sigma_1^2 c_{0,2} + \sigma_4^2\right)\right) + \sigma_3\sigma_2^2\left(\sigma_1\left(\sigma_5 b_{2,1} - \sigma_1 c_{1,2}\right) + \sigma_4\left(\sigma_1 b_{1,1} + 2\sigma_5\right)\right)\\ &- \sigma_3^2\sigma_2\left(\sigma_1\left(\sigma_4 b_{0,1} - \sigma_1 c_{2,2}\right) + \sigma_1\sigma_5 b_{1,1} + \sigma_5^2\right) + \sigma_1\sigma_3^3\left(\sigma_5 b_{0,1} - \sigma_1 c_{3,2}\right)\,,\end{aligned} \tag{5.5.29}$$

and σ_2, σ_3 coprime. σ_1 and σ_3 divide $b_{1,0}$, hence their enhancements do not yield I_n singularities and are irrelevant to us here.

- $\sigma_2 = 0$: $I_5^{(0|1)}$

  Recall that σ_2 divides $b_{0,0}$. Thus, by first enhancing along this locus and then reconsidering the polynomial that led to $\mathcal{Q}(2,1,1,1,0,0,1)|_{(5.3.29)}$, one obtains the canonical fibration $\mathcal{Q}(2,1,1,2,1,0,1)$.

- $P_2 = 0$: $I_5^{(0||1)}$
  Similarly (and by a suitable coordinate shift), one finds that $P_2 = 0$ yields the non-canonical fiber $\mathcal{Q}(3,2,1,1,0,0,1)|_{(5.3.42)}$.

- $P_3 = 0$:
  $P_3 = 0$, on the other hand, produces a doubly non-canonical fiber, which can be studied along the lines of the example in section 5.5.2.1.

5.5.3 Non-canonical I_4 from non-canonical I_3

5.5.3.1 $I_3^{(0|1)}$ Branch

The discriminant of $\mathcal{Q}(1,1,1,1,0,0,1)|_{(5.3.18)}$ obtained from (5.3.19) at leading order reads

$$\Delta_{I_3^{(0|1)}} = \sigma_1^6\sigma_2\sigma_3^2\sigma_4 P_2 P_2 z^3 + O(z^4)\,, \tag{5.5.30}$$

with

$$\begin{aligned} P_2 = &-\sigma_3\sigma_4\sigma_2^4\left(\sigma_1 b_{2,1} + 2\alpha\right) + \sigma_3^2\sigma_2^3\left(\alpha\sigma_1 b_{2,1} + \sigma_4\left(\sigma_1 b_{1,1} + 2\sigma_5\right) - \sigma_1^2 c_{0,2} + \alpha^2\right) \\ &- \sigma_3^3\sigma_2^2\left(\sigma_5\left(\sigma_1 b_{2,1} + 2\alpha\right) + \sigma_1\left(\alpha b_{1,1} + \sigma_4 b_{0,1} - \sigma_1 c_{1,2}\right)\right) \\ &+ \sigma_3^4\sigma_2\left(\sigma_1\left(\alpha b_{0,1} - \sigma_1 c_{2,2}\right) + \sigma_1\sigma_5 b_{1,1} + \sigma_5^2\right) + \sigma_1\sigma_3^5\left(\sigma_1 c_{3,2} - \sigma_5 b_{0,1}\right) + \sigma_4^2\sigma_2^5\,. \end{aligned} \tag{5.5.31}$$

Again, σ_2 and σ_3 are coprime. Since σ_1 and σ_3 are divisors of $b_{1,0}$, $\sigma_1 = 0$ and $\sigma_3 = 0$ are enhancements leaving the I_n branch and are thus not considered here.

- $\sigma_2 = 0$: $I_4^{(0|1)}$
  Since σ_2 divides $b_{0,0}$, one can, instead of first considering the enhancement P_0 of the $I_2^{(0|1)}$ form leading to $\mathcal{Q}(1,1,1,1,0,0,1)|_{(5.3.18)}$, alternatively first enhance $b_{0,0} = 0$ to $\mathcal{Q}(1,1,1,1,1,0,1)$, and consider the $P_0 = 0$ enhancement with $\sigma_2 = 0$ imposed there. This imposition yields $P_0 = c_{3,1}$, hence the resulting fibration is canonical and given by
  $$\mathcal{Q}(1,1,1,2,1,0,1)\,, \tag{5.5.32}$$
  which is lop-equivalent to $\mathcal{Q}(3,2,1,1,0,0,2)$, a special case of the canonical $I_4^{(0|1)}$ fiber type discussed in section 5.3.

- $\sigma_4 = 0$: $I_4^{(0||1)}$
  This enhancement yields the non-canonical fibration $\mathcal{Q}(2,1,1,1,0,0,1)|_{(5.3.29)}$ in a similar way.

- $P_2 = 0$:
  This enhancement yields a doubly non-canonical fibration.

5.6 Non-canonical forms in $\mathbb{P}_{[1,2,3]}$

While non-canonical forms appear very commonly in the Tate tree of $\mathbb{P}_{[1,1,2]}$, they also occur in Tate's algorithm for Weierstrass forms embedded in $\mathbb{P}_{[1,2,3]}$. For most parts in $\mathbb{P}_{[1,2,3]}$ the canonical Tate forms can be reached through locally well-defined coordinate changes, i.e. those that do not require any divisions. In [1], it was already observed that a generalized ansatz is required for the fiber types I_n for $n = 2m+1$ except $n = 7, 9$. There are furthermore outlier cases, where neither the Tate form nor the new ansatz of [1] can be achieved, I_n for $n = 6, 7, 8, 9$. These models can be discussed with the same type of methods that we have used for the non-canonical models in $\mathbb{P}_{[1,1,2]}$, and we will now derive explicit forms for the non-canonical models and examples for the multiply non-canonical cases. Note that one of the key assumptions in [1] is that there are no codimension two non-minimal loci, i.e. once put into Weierstrass form, the vanishing orders of (f, g, Δ) in codimension one and two stay below $(4, 6, 12)$. This allowed shifts back to canonical forms for the infinite series I_n without monodromy. The structure of the non-canonical forms in the Tate tree of $\mathbb{P}_{[1,2,3]}$ is depicted in figure 5.16.

Recall that a generic elliptic fibration with section can be embedded into the projective space $\mathbb{P}_{[1,2,3]}$ by the hypersurface equation

$$\mathcal{P}: \qquad y^2 + \mathfrak{b}_1 yx + \mathfrak{b}_3 y = x^3 + \mathfrak{b}_2 x^2 + \mathfrak{b}_4 x + \mathfrak{b}_6\,, \tag{5.6.1}$$

where w, x and y are the coordinates of $\mathbb{P}_{[1,2,3]}$ with weights 1, 2, and 3, respectively, and we have set $w = 1$. Tate's algorithm in $\mathbb{P}_{[1,2,3]}$ then provides the vanishing orders $(i_1, i_2, i_3, i_4, i_6)$ of the sections $\mathfrak{b}_i$ of canonical Tate forms, which we will denote by

$$\begin{aligned}\mathcal{P}(i_1, i_2, i_3, i_4, i_6): \qquad & y^2 + \mathfrak{b}_{1,i_1} z^{i_1} yx + \mathfrak{b}_{3,i_3} z^{i_3} y \\ & = x^3 + \mathfrak{b}_{2,i_2} z^{i_2} x^2 + \mathfrak{b}_{4,i_4} z^{i_4} x + \mathfrak{b}_{6,i_6} z^{i_6}\,.\end{aligned} \tag{5.6.2}$$

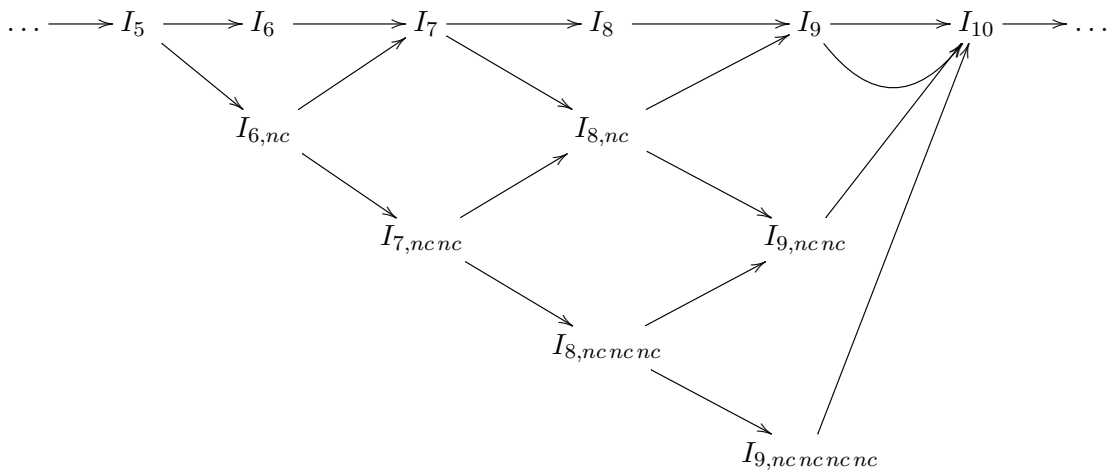

FIGURE 5.16: The schematic Tate tree for the I_n-type enhancements of the I_5 fiber in $\mathbb{P}_{[1,2,3]}$, including the non-canonical forms for I_6 to I_9. The I_9 enhancement which would normally lead to $I_{10,nc}$ can be shifted to the canonical I_{10}, and the same applies to all $I_{2m+1} \to I_{2m+2}$ enhancements that follow [1]. Below we will show explicitly that there is a multiply non-canonical enhancement, starting from I_7, which yields an I_{11} model, that can then be brought back into canonical Tate form.

5.6.1 Non-canonical I_6 from canonical I_5

The first non-canonical Tate forms in the $\mathbb{P}_{[1,2,3]}$ Tate tree arise from the enhancement of the I_5 canonical Tate form

$$\mathcal{P}(0,1,2,3,5): \qquad y^2 + \mathfrak{b}_1 yx + \mathfrak{b}_{3,2} z^2 y = x^3 + \mathfrak{b}_{2,1} z x^2 + \mathfrak{b}_{4,3} z^3 x + \mathfrak{b}_{6,5} z^5 \,, \tag{5.6.3}$$

which has discriminant

$$\Delta_{I_5}: \qquad b_{1,0}^4 \left(b_{3,2}^2 b_{2,1} - b_{3,2} b_{1,0} b_{4,3} + b_{1,0}^2 b_{6,5} \right) z^5 + O(z^6) \,. \tag{5.6.4}$$

The locus $b_{1,0} = 0$ yields an I_1^* model $\mathcal{P}(1,1,2,3,5)$.

The interesting part of the discriminant enhancements arise in the I_n branch, where $P = 0$ gives rise to a canonical I_6 and a non-canonical $I_{6,nc}$ model.The polynomial term in this discriminant is exactly of the form discussed in appendix B.1.3. The only solutions that do not also set $b_{1,0} = 0$, which is already a factor in the discriminant, are: $b_{3,2} = b_{6,5} = 0$, and the non-trivial solution from (B.1.12). The former solution indeed yields the canonical form $\mathcal{P}(0,1,3,3,6)$ of the I_6 fiber in $\mathbb{P}_{[1,2,3]}$. The latter solution, however, has not been

discussed in the literature so far, and it leads to a non-canonical I_6 Tate form, namely

$$\begin{aligned} I_{6,nc}: \quad & \mathcal{P}(0,1,2,3,5) \text{ with} \\ & b_{1,0}=\sigma_1\sigma_3,\ b_{3,2}=\sigma_1\sigma_2,\ b_{6,5}=\sigma_2\sigma_5,\ b_{2,1}=\sigma_3\sigma_4,\ b_{4,3}=\sigma_3\sigma_5+\sigma_2\sigma_4 \end{aligned} \tag{5.6.5}$$

or explicitly

$$I_{6,nc}: \quad y^2+\sigma_2^2xy+\zeta_0^2\sigma_2\sigma_3y=x^3+\zeta_0\sigma_2\sigma_5x^2+\zeta_0^3\left(\sigma_2\sigma_4+\sigma_3\sigma_5\right)x+\zeta_0^5\sigma_3\sigma_4\,. \tag{5.6.6}$$

Note that in general there are no shifts that bring this into canonical form. The discriminant of this non-canonical I_6 model is

$$\Delta_{I_{6,nc}}=\sigma_1^4\sigma_3^3P_6z^6+O(z^7) \tag{5.6.7}$$

with

$$\begin{aligned} P_6=&\,\sigma_3\left(\sigma_2\sigma_4-\sigma_3\sigma_5\right)^2+\sigma_1\sigma_3\left(\sigma_3\sigma_5-\sigma_2\sigma_4\right)\left(\sigma_3b_{3,3}-\sigma_2b_{1,1}\right) \\ &+\sigma_1^2\left(\sigma_2^3-\sigma_2^2\sigma_3b_{2,2}+\sigma_2\sigma_2^2b_{4,4}-\sigma_3^3b_{6,6}\right)\,. \end{aligned} \tag{5.6.8}$$

For this form the **15** matter locus $b_{1,0}=0$ splits into two components:

$$b_{1,0}=\sigma_1\sigma_3\,. \tag{5.6.9}$$

Setting either of σ_1 or σ_3 to zero yields an enhancement to type I_2^*. Therefore, this model has two **15** curves, plus the single **6** curve already present in the canonical model and here obtained from setting the long polynomial to zero.

In [1], there was a non-canonical I_6 model originating from [98] presented as evidence that not all I_6 singularities can be brought into canonical form. The model reads

$$y^2-\frac{9}{4}t^2xy+z^2y=x^3\,. \tag{5.6.10}$$

It is a special case of the general non-canonical I_6 model (5.6.6), which can be obtained by $\sigma_1=\sigma_2=1$, $\sigma_4=\sigma_5=0$, $\sigma_3=-9/4t^2$, and also setting all subleading terms to zero.

5.6.2 Non-canonical I_7 from non-canonical I_6

Continuing on from this $I_{6,nc}$ non-canonical model, the polynomial term P_6 in the discriminant allows for a doubly non-canonical enhancement to an $I_{7,ncnc}$ model, $I_{6,nc}|_{P_6=0}$,

i.e.

$$I_{7,ncnc}: \left(y^2+\sigma_2^2xy+\zeta_0^2\sigma_2\sigma_3y=x^3+\zeta_0\sigma_2\sigma_5x^2+\zeta_0^3\left(\sigma_2\sigma_4+\sigma_3\sigma_5\right)x+\zeta_0^5\sigma_3\sigma_4\right)|_{P_6=0} \tag{5.6.11}$$

with P_6 in (5.6.8). Solving the condition $P_6=0$ in general is rather tricky, however several subcases of solutions can be obtained. For instance (setting the subleading $b_{i,j}=0$ in P_6, as well as $\sigma_5=0$) for

$$b_{1,0}=u^5\,,\quad b_{2,0}=0\,,\quad b_{3,0}=-u^3v^2\,,\quad b_{4,0}=u^2v^3\,,\quad b_{6,0}=-v^5\,,\qquad (u,v)=1\,. \tag{5.6.12}$$

An alternative solution, again setting the higher $b_{i,j}=0$ in P_6, as well as $\sigma_4=0$ yields

$$b_{1,0}=\sigma_1^3\,,\quad b_{2,0}=\sigma_1^2\sigma_5\,,\quad b_{3,0}=-\sigma_1\sigma_5^2\,,\quad b_{4,0}=-\sigma_5^3\,,\quad b_{6,0}=0\,,\qquad (\sigma_1,\sigma_5)=1\,. \tag{5.6.13}$$

Another model from [98], presented in [1] as an outlier case, is I_7 fibration which could not be brought into canonical form:

$$y^2-54t^3xy+24tz^2y=x^3+36t^2zx^2-16z^3x\,. \tag{5.6.14}$$

This model is a special case of the doubly non-canonical I_7 model (5.6.11), and the special solution (5.6.13), which enhances the non-canonical I_6 model by solving the polynomial term in (5.6.7). One can find it by starting with the non-canonical I_6 model from (5.6.6), and setting

$$\sigma_4=0\,,\quad \sigma_5=1\,,\quad \sigma_1=-\frac{3}{4}t\,,\quad \sigma_2=36t^2\,,\quad \sigma_3=-16\,, \tag{5.6.15}$$

as well as having all subleading terms equal to zero.

5.6.3 Non-canonical I_8 from canonical I_7

Another non-canonical form, which is similar to the one above, can be obtained by starting from the canonical I_7 form $\mathcal{P}(0,1,3,4,7)$, with discriminant

$$\Delta_{I_7}: \qquad b_{1,0}^4\left(b_{3,3}^2b_{2,1}-b_{3,3}b_{1,0}b_{4,4}+b_{1,0}^2b_{6,7}\right)z^7+O(z^8)\,, \tag{5.6.16}$$

and solving the three-term polynomial. It reads

$$\begin{aligned} I_{8,nc}: \qquad & \mathcal{P}(0,1,3,4,7) \text{ with} \\ & b_{1,0} = \sigma_1\sigma_2,\ b_{3,3} = \sigma_1\sigma_3,\ b_{6,7} = \sigma_3\sigma_4,\ b_{2,1} = \sigma_2\sigma_5,\ b_{4,4} = \sigma_2\sigma_4 + \sigma_3\sigma_5\,. \end{aligned} \tag{5.6.17}$$

By the same argument as above, this model has two **28** curves (as opposed to the canonical I_8 model with a single **28** curve), plus an **8** curve. Again there is a non-canonical enhancement starting from this

$$P_8 = \sigma_2^2\left(\sigma_3\left(\sigma_3 b_{2,2} - b_{4,5}\sigma_2\right) + \sigma_2^2 b_{6,8}\right) - \left(\sigma_2\sigma_4 - \sigma_3\sigma_5\right)\sigma_2\left(\sigma_2 b_{3,4} - \sigma_3 b_{1,1}\right) - \left(\sigma_2\sigma_4 - \sigma_3\sigma_5\right)^2\,. \tag{5.6.18}$$

5.6.4 Canonical I_{11} model via non-canonical enhancements

Finally, one can enhance beyond the outlier cases, and reach vanishing orders of the discriminant that are larger than 10. In those cases, it was shown in [98] that these can be shifted back to canonical mocels, under the assumption of absence of non-minimal loci in codimension two.

In practice, we can see this in the following enhancement of the non-canonical I_8 model from the previous subsection by finding solutions to (5.6.18). While not completely general,

$$b_{1,1} = b_{2,2} = b_{3,4} = b_{4,5} = b_{6,8} = 0\,, \quad \sigma_5 = \sigma_2\alpha\,, \quad \sigma_4 = \sigma_3\alpha \tag{5.6.19}$$

solves $P_8 = 0$. Note that here we only set the subleading $b_{i,j} = 0$, not the full series. The resulting enhancement is of Kodaira type I_9 and has leading order discriminant

$$\Delta_{I_9} = \sigma_1^6\sigma_2^3\left(\sigma_2^3 b_{6,9} - \sigma_2^2\sigma_3 b_{4,6} + \sigma_2\sigma_3^2 b_{2,3} - \sigma_3^3\right) z^9 + O(z^{10})\,. \tag{5.6.20}$$

The polynomial term in the discriminant of this specialized I_9 can in turn be solved by

$$\sigma_2 = 1\,, \quad b_{6,9} = \rho_4\sigma_3\,, \quad b_{4,6} = \rho_4 + \alpha\sigma_3\,, \quad b_{2,3} = \alpha\sigma_3\,. \tag{5.6.21}$$

Also setting $\mathfrak{b}_{1,3} = \mathfrak{b}_{2,4} = \mathfrak{b}_{3,6} = \mathfrak{b}_{4,7} = \mathfrak{b}_{6,10} = 0$ yields a model of Kodaira type I_{11}, with equation

$$\begin{aligned} & y^2 + \left(\sigma_1 + z^2 b_{1,2}\right) xy + \left(\sigma_3\sigma_1 + z^2 b_{3,5}\right) z^3 y \\ & = x^3 + \left(\alpha + (\alpha + \sigma_3)\, z^2\right) zx^2 + \left(2\alpha\sigma_3 + (\alpha\sigma_3 + \rho_5)\, z^2\right) z^4 x + \left(\alpha\sigma_3^2 + z^2\sigma_3\rho_5\right) z^7 \end{aligned} \tag{5.6.22}$$

and discriminant

$$\Delta_{I_{11}} = \sigma_1^4 \left(\sigma_3 b_{1,2} - b_{3,5}\right) \left(\alpha\sigma_1\sigma_3 - \sigma_3^2\sigma_1 - \rho_5\sigma_1 - \alpha\sigma_3 b_{1,2} + \alpha b_{3,5}\right) z^{11} + O(z^{12})\,. \tag{5.6.23}$$

The locus $\sigma_1 = 0$ enhances to I_7^*, while the two polynomials give enhancements to I_{12}, but are both minimal, i.e. the corresponding Weierstrass model does not have vanishing orders $\mathrm{mult}(f, g, \Delta) \geq (4, 6, 12)$. Consistently with the result in [98], there is a coordinate change, that brings this to canonical form[15].

[15] We thank Dave Morrison and Sheldon Katz for discussions on this point.

Chapter 6

Conclusion

String phenomenology models low-energy physics within string theory, realizing two goals: On the one hand, string theory provides a UV-complete unification of gravity and gauge interactions, addressing a multitude of phenomenological problems of current theories. On the other hand, the existence of such embeddings can be used to systematically restrict the space of viable low-energy models.

The main way to achieve this is the process of compactification, which translates physical properties of the string theoretic model into geometric features of a compactification manifold. These manifolds can be studied comprehensively with powerful tools from algebraic geometry. Often, a complete classification of some geometric attribute is possible, which can then be re-translated into a complete set of allowed physical properties.

An area in string phenomenology where this approach has proven very constructive is F-theory, which itself is one of the most general classes of string compactifications. F-theory can be understood as a non-perturbative generalization of type IIB string theory, whose compactification manifolds are elliptic fibrations, which are well-studied in mathematics. In this thesis, we have applied the idea of studying elliptic fibrations to obtain insights about generic compactification geometries, with the aim to systematically constrain physical models, in two instances within F-theory.

While the interplay between local models and their global counterparts is usually thought of as occuring between the low-energy gauge theory of a compactification and its string or F-theory embedding, it also manifests itself in F-theory: if one is interested only in gauge degrees of freedom, one can perform an analysis solely on the sublocus on which they are localized. This local study then may be enhanced or constrained by global considerations.

A way to do so is given by the spectral cover formalism, which we have generalized in chapter 4 of this thesis by introducing a new object called the spectral divisor. Specifically, for loci with associated gauge group $SU(5)$ the spectral cover formalism allows for the local construction of G-flux, and thus for the local computation of chiral indices and induced D3-brane charges. The spectral divisor extends the local G-flux construction to all other gauge groups which admit a spectral cover formulation.

To exemplify this analysis we have resolved a singular fibration with associated gauge group E_6 over a generic base manifold, and constructed its G-flux both globally and locally via the spectral divisor. We have then checked that both constructions agree in the chiral indices and D3-brane charges they compute, and further confirmed that the global G-flux does not capture additional information compared to the local one in generic models. While doing so, we have also confirmed a conjecture from heterotic/F-theory duality about the Euler character of resolved elliptic fibrations with E_6-type singularities, proving a physical result using geometric methods.

Another instantiation of the interplay between low-energy physics and geometry in F-theory are abelian gauge symmetries. These are highly relevant in low-energy field theoretic model building, and described in F-theory by additional sections of the elliptic fibration. In chapter 5, we studied singular elliptic fibrations with a single extra section, and utilize Tate's algorithm to classify such fibrations and to construct standard forms for each of them. In this way we are able to obtain all fibers of the form $U(1) \times G$ with a non-abelian gauge factor G. We find that the classification extends the known Kodaira classification of singular fibers by adding information about the relative location of the two sections.

Furthermore, the analysis allowed us to obtain a complete list of allowed $U(1)$ charges for matter transforming in non-trivial representations under the non-abelian gauge groups in F-theory models. We have explicitly computed this list for the phenomenologically interesting case of $G = SU(5)$. It contains models that have so far not appeared in the literature, stressing the importance of studying such compactifications systematically, and specifically extends those obtained from local models with the spectral cover formalism.

There are two natural ways to extend this analysis in future work which are being investigated at present. Firstly, it would be interesting to extend the procedures from chapter 5 to F-theory models with more than one abelian gauge factor, corresponding to elliptic fibrations with more than two sections. For fibrations with three sections, one can apply Tate's algorithm in an at least qualitatively similar way [120]. The desired end result here is again a full list of singular fibrations, classified by their Kodaira type and the relative

locations of the sections, as well as a list of achievable $U(1)$ charges for F-theory models with gauge groups of the form $U(1) \times U(1) \times G$.

Secondly, having gained this new set of constraints from F-theory, it is interesting and in line with the general idea of finding restrictions to low-energy physics to see if and how string phenomenology models are impacted by them [121]. More specifically, one would like to see whether known applications of additional $U(1)$s in field theory model building, such as the $U(1)_{PQ}$ used to restrict proton decay and alleviate the μ-problem, can still be engineered in F-theory compactifications.

A third continuation of the work in this thesis, and another example of using a UV-complete model to constrain local physics, would be the construction of G-flux in global models with abelian gauge factors. Since we have found standard forms for all such models with a single extra $U(1)$ in chapter 5, one could apply the procedures of [101] and chapter 4 to find the most general global G-flux in such models, and compare it with local G-flux obtained from split spectral cover models which locally describe extra $U(1)$ gauge groups. It is not clear if the global flux provides one with more freedom (as global models with gauge group $U(1) \times G$ do) or not (as the global G-flux did in comparison with the spectral cover flux), and it would be interesting to see if one could find new mechanisms or constraints on F-theory models from this construction.

Finally, computations in global F-theory models often involve many calculations in algebraic geometry related to resolving singular elliptic fibrations and computing intersections between curves and divisors of them. These can be automated to a high degree, and to that end there is a Mathematica package called `Smooth` currently in development [83], which we have used to compute many of the results in this thesis and aim to finalize and release.

In conclusion, in this thesis we have fruitfully applied the paradigm of studying the geometry of compactification manifolds to systematically learn about models in string phenomenology. A better description of fluxes and a classification of abelian gauge charges provide important constraints on viable string compactifications in F-theory. Since the results we have obtained in this thesis, as well as the ones outlined as future work, are comprehensive in their nature, they tell us about what is realizable in F-theory compactifications *and what is not*.

Thus, they both enlighten and narrow down the space of realizable low-energy physics, serving as a step towards the current long-term goal of string phenomenology: a comprehensive analysis of all string theoretic scenarios including which ones are in accordance with *all* physical observations, both in particle physics and in cosmology, and emphasizing their testable predictions going beyond the ones made by models in low-energy physics. The philosophy of studying these scenarios systematically, as applied in this thesis, might ultimately prove successful at achieving this ambitious goal.

Appendix A

Appendices to Chapter 4

A.1 Details of the geometry of $\tilde{X}_5$ and $\tilde{Y}_4$

A.1.1 Blow-up and Intersection relations

The classes of the various sections after the blow-ups and small resolutions in $\tilde{X}_5$ and $\tilde{Y}_4$ are

$$\begin{aligned}
[x_2] &= \sigma + 2c_1 - E_1 - E_2 \\
[y_7] &= \sigma + 3c_1 - E_1 - E_2 - E_3 - E_4 - E_5 - E_6 - E_7 \\
[z_1] &= S - E_1 \\
[\zeta_{12347}] &= E_1 - E_2 - E_3 - E_4 - E_7 \\
[\zeta_{235}] &= E_2 - E_3 - E_5 \\
[\zeta_{346}] &= E_3 - E_4 - E_6 \\
[\zeta_4] &= E_4 \\
[\delta_i] &= E_i \qquad i = 5, 6, 7\,.
\end{aligned} \tag{A.1.1}$$

The blow-up relations in $\tilde{X}_5$ are

$$\begin{aligned}
0 &= \sigma \cdot (\sigma + 2c_1) \cdot (\sigma + 3c_1) \\
0 &= (\sigma + 2c_1 - E_1) \cdot (\sigma + 3c_1 - E_1) \cdot (S - E_1) \\
0 &= (\sigma + 2c_1 - E_1 - E_2) \cdot (\sigma + 3c_1 - E_1 - E_2) \cdot (E_1 - E_2) \\
0 &= (\sigma + 3c_1 - E_1 - E_2 - E_3) \cdot (E_1 - E_2 - E_3) \cdot (E_2 - E_3) \\
0 &= (\sigma + 3c_1 - E_1 - E_2 - E_3 - E_4) \cdot (E_1 - E_2 - E_3 - E_4) \cdot (E_3 - E_4) \\
0 &= (\sigma + 3c_1 - E_1 - E_2 - E_3 - E_4 - E_5) \cdot (E_2 - E_3 - E_5) \\
0 &= (\sigma + 3c_1 - E_1 - E_2 - E_3 - E_4 - E_5 - E_6) \cdot (E_3 - E_4 - E_6) \\
0 &= (\sigma + 3c_1 - E_1 - E_2 - E_3 - E_4 - E_5 - E_6 - E_7) \cdot (E_1 - E_2 - E_3 - E_4 - E_7)\,.
\end{aligned} \tag{A.1.2}$$

A.1.2 Holomorphic surfaces

To construct the G-flux directly, we need to determine an independent set of holomorphic surfaces in the resolved geometry. The various projectivity relations encode all the relations between the surfaces

$$\begin{array}{lrl}
\text{Original} & (x, y, z) & = \big(\zeta_{235}^2\zeta_{346}^3\zeta_4^4\zeta_{12347}\delta_7\delta_5^2\delta_6^3 x_2, \zeta_{235}^2\zeta_{346}^4\zeta_4^6\zeta_{12347}\delta_5^3\delta_6^5\delta_7^2 y_7, \\
 & & \quad \zeta_{235}\zeta_{346}^2\zeta_4^3\zeta_{12347}\delta_5\delta_6^2\delta_7 z_1\big) \\
\text{Blow-up 1} & [x_1, y_1, z_1] & = [x_2\zeta_{235}\delta_5\zeta_4\delta_6\zeta_{346}, y_7\zeta_{235}\zeta_{346}^2\zeta_4^3\delta_5^2\delta_6^3\delta_7, z_1] \\
\text{Blow-up 2} & [x_2, y_2, \zeta_2] & = [x_2, y_7\delta_5\delta_6^2\delta_7\zeta_4^2\zeta_{346}, \zeta_{12347}\delta_7\zeta_{346}\delta_6\zeta_4^2] \\
\text{Blow-up 3} & [y_3, \zeta_{123}, \zeta_{23}] & = [y_7\delta_5\delta_6\delta_7\zeta_4, \zeta_{12347}\delta_7\zeta_4, \zeta_{235}\delta_5] \\
\text{Blow-up 4} & [y_4, \zeta_{1234}, \zeta_{34}] & = [y_7\delta_5\delta_6\delta_7, \zeta_{12347}\delta_7, \zeta_{346}\delta_6] \\
\text{Blow-up 5} & [y_5, \zeta_{235}] & = [y_7\delta_6\delta_7, \zeta_{235}] \\
\text{Blow-up 6} & [y_6, \zeta_{346}] & = [y_7\delta_7, \zeta_{346}] \\
\text{Blow-up 7} & [y_7, \zeta_{12347}] &
\end{array} \tag{A.1.3}$$

In particular, the following sets of equations do not admit solutions:

$$\begin{gathered}
z_1 = \delta_5 = 0\,, \qquad z_1 = \delta_6 = 0\,, \qquad z_1 = \zeta_4 = 0\,, \qquad z_1 = \zeta_{346} = 0\,, \qquad z_1 = \zeta_{235} = 0\,, \\
x_2 = \delta_6 = 0\,, \qquad x_2 = \zeta_4 = 0\,, \qquad x_2 = \zeta_{346} = 0\,, \qquad x_2 = \delta_7 = 0\,, \\
\delta_7 = \zeta_{235}\,, \qquad \delta_7 = \zeta_{346}\,, \qquad \delta_7 = \delta_5\,, \qquad \delta_7 = \delta_6 = 0\,, \qquad \zeta_4 = \delta_5 = 0
\end{gathered} \tag{A.1.4}$$

$$\zeta_4 = \zeta_{235} = 0\,, \qquad \zeta_{235} = \delta_6 = 0\,, \qquad \delta_5 = \zeta_{12347} = 0\,, \qquad \delta_6 = \zeta_{12347} = 0\,.$$

Using that $\sigma \cdot E_i = 0$, this gives us a total of 19 relations (the last one being described below) on the space spanned by

$$E_i \cdot E_j \,(i \neq j)\,, \qquad E_i \cdot c_1\,, \qquad E_i \cdot S\,. \tag{A.1.5}$$

As this space is 35-dimensional, it can be described by a 16-dimensional basis, which we can parametrize using the 14 intersections

$$E_i \cdot c_1\,, \qquad E_i \cdot S\,, \tag{A.1.6}$$

and two of the form $E_i \cdot E_j$ that are not linear combinations of (A.1.6). A convenient choice for the latter is

$$E_2 \cdot E_5\,, \qquad E_3 \cdot E_6\,, \tag{A.1.7}$$

From these, we can now derive all other intersections and obtain the following tables (we give an expression for $E_1 \cdot E_7$ below):

$\cdot$	E_1	E_2	E_3	E_4
E_1	$---$	$S \cdot E_2$	$S \cdot E_3$	$S \cdot E_4$
E_2	$S \cdot E_2$	$---$	$(2c_1 - S) \cdot E_3$	$(2c_1 - S) \cdot E_4$
E_3	$S \cdot E_3$	$(2c_1 - S) \cdot E_3$	$---$	$(2c_1 - S) \cdot E_4$
E_4	$S \cdot E_4$	$(2c_1 - S) \cdot E_4$	$(2c_1 - S) \cdot E_4$	$---$
E_5	$S \cdot E_5$	$E_2 \cdot E_5$	$(S - E_2) \cdot E_5$	0
E_6	$S \cdot E_6$	$(2c_1 - S) \cdot E_6$	$E_3 \cdot E_6$	$(2(S - c_1) - E_3) \cdot E_6$
E_7	$E_1 \cdot E_7$	$(2c_1 - E_1) \cdot E_7$	$(2c_1 - E_1) \cdot E_7$	$(2c_1 - E_1) \cdot E_7$

(A.1.8)

$\cdot$	E_5	E_6	E_7
E_1	$S \cdot E_5$	$S \cdot E_6$	$E_1 \cdot E_7$
E_2	$E_2 \cdot E_5$	$(2c_1 - S) \cdot E_6$	$(2c_1 - E_1) \cdot E_7$
E_3	$(S - E_2) \cdot E_5$	$E_3 \cdot E_6$	$(2c_1 - E_1) \cdot E_7$
E_4	0	$(2(S - c_1) - E_3) \cdot E_6$	$(2c_1 - E_1) \cdot E_7$
E_5	$---$	$(2c_1 - S - E_3) \cdot E_6$	0
E_6	$(2c_1 - S - E_3) \cdot E_6$	$---$	0
E_7	0	0	$---$

(A.1.9)

We can also write the diagonal entries of the tables as functions of our basis. To do this, we have to use the last three relations of (A.1.2) as well as four new relations. These new relations are all found along the same lines (and only valid within $\tilde{Y}_4$): When one puts both of the variables in the first column of the table below to zero and evaluates the Tate equation (4.2.15), one finds that the Tate equation becomes a product whose factors are such that the vanishing of any of them would violate the blow-up relation (A.1.3) in the second column.

Non-vanishing pair of sections in $\tilde{Y}_4$	Blow-up relation	Relation in homology
$z_1,\ y_7$	1	$(S-E_1)\cdot\left(\sigma+3c_1-\sum_{i=1}^{7}E_i\right)=0$
$z_1,\ x_2$	1	$(S-E_1)\cdot(\sigma+2c_1-E_1-E_2)=0$
$x_2,\ \zeta_{12347}$	2	$(\sigma+2c_1-E_1-E_2)\cdot(E_1-E_2-E_3-E_4-E_7)=0$
$\zeta_{235},\ \zeta_{12347}$	3	$(E_2-E_3-E_5)\cdot(E_1-E_2-E_3-E_4-E_7)=0$
$\zeta_{346},\ \zeta_{12347}$	4	$(E_3-E_4-E_6)\cdot(E_1-E_2-E_3-E_4-E_7)=0$

(A.1.10)

Since the first of these homological relations involves $S\cdot\sigma$, which is not in our vector space, we find an alternative relation. We note that on the surface obtained by restricting $z_1=\zeta_{12347}=0$ in $\tilde{Y}_4$, necessarily $\delta_7=0$ follows. Vice versa, if one considers $z_1=\delta_7=0$ in $\tilde{Y}_4$, one automatically has $\zeta_{12347}=0$. This establishes

$$(S-E_1)\cdot E_7=(S-E_1)\cdot(E_1-E_2-E_3-E_4-E_7) \tag{A.1.11}$$

or

$$(S-E_1)\cdot(E_1-E_2-E_3-E_4-2E_7)=0\,. \tag{A.1.12}$$

Since it does not involve $\sigma\cdot S$, we will work with this relation. We now have all the necessary information to rewrite the surfaces $E_i\cdot E_i$ in terms of our basis surfaces (A.1.6)

and (A.1.7):

$$
\begin{aligned}
E_1 \cdot E_1 &= S \cdot (E_1 - 2E_7) + 2E_1 \cdot E_7 \,, \\
E_2 \cdot E_2 &= 2c_1 \cdot (E_2 - E_1) + S \cdot (E_1 - 2E_7) + 2E_1 \cdot E_7 \,, \\
E_3 \cdot E_3 &= 2c_1 \cdot (E_2 - E_1) + S \cdot (E_1 - E_2 + E_3 - 2E_7) + 2E_1 \cdot E_7 \,, \\
E_4 \cdot E_4 &= 2c_1 \cdot (E_2 - E_1 + E_3 - E_4) + S \cdot (E_1 - E_2 - E_3 + 2E_4 - 2E_7) + 2E_1 \cdot E_7 \,, \\
E_5 \cdot E_5 &= -3c_1 \cdot (E_2 - E_3 - E_5) + S \cdot (2E_2 - 2E_3 - 3E_5) + 2E_2 \cdot E_5 \,, \\
E_6 \cdot E_6 &= -3c_1 \cdot (E_3 - E_4 - E_6) + S \cdot (2E_3 - 2E_4 + E_5 - 3E_6) - E_2 \cdot E_5 + 3E_3 \cdot E_6 \,, \\
E_7 \cdot E_7 &= 3c_1 \cdot (E_1 - E_2 - E_3 - E_4 - 3E_7) \\
&\quad + S \cdot (-2E_1 + 2E_2 + 2E_3 + 2E_4 + 4E_7) + 2E_1 \cdot E_7 \,,
\end{aligned}
\tag{A.1.13}
$$

Finally, we can use the difference of the first two relations of (A.1.10) to write

$$
\begin{aligned}
0 = (S - E_1) \cdot (c_1 - E_3 - E_4 - E_5 - E_6 - E_7) &\overset{\text{A.1.8}}{=} (S - E_1) \cdot (c_1 - E_7) \\
\Rightarrow E_1 \cdot E_7 &= S \cdot E_7 + c_1 \cdot E_1 - c_1 \cdot S \,.
\end{aligned}
\tag{A.1.14}
$$

A.2 E_6 weights and roots

As a useful reference, we list the simple roots and the weights of the **27** representation of E_6.

Root vectors	Simple roots
$(2,-1,0,0,0,0)$	α_1
$(-1,2,-1,0,0,0)$	α_2
$(0,-1,2,-1,0,-1)$	α_3
$(0,0,-1,2,-1,0)$	α_4
$(0,0,0,-1,2,0)$	α_5
$(0,0,-1,0,0,2)$	α_6

(A.2.1)

Weight vectors in the **27**	Weights
$(1,0,0,0,0,0)$	$\mu_{\mathbf{27}}$
$(-1,1,0,0,0,0)$	$\mu_{\mathbf{27}}-\alpha_1$
$(0,-1,1,0,0,0)$	$\mu_{\mathbf{27}}-\alpha_1-\alpha_2$
$(0,0,-1,1,0,1)$	$\mu_{\mathbf{27}}-\alpha_1-\alpha_2-\alpha_3$
$(0,0,0,-1,1,1)$	$\mu_{\mathbf{27}}-\alpha_1-\alpha_2-\alpha_3-\alpha_4$
$(0,0,0,1,0,-1)$	$\mu_{\mathbf{27}}-\alpha_1-\alpha_2-\alpha_3-\alpha_6$
$(0,0,0,0,-1,1)$	$\mu_{\mathbf{27}}-\alpha_1-\alpha_2-\alpha_3-\alpha_4-\alpha_5$
$(0,0,1,-1,1,-1)$	$\mu_{\mathbf{27}}-\alpha_1-\alpha_2-\alpha_3-\alpha_4-\alpha_6$
$(0,0,1,0,-1,-1)$	$\mu_{\mathbf{27}}-\alpha_1-\alpha_2-\alpha_3-\alpha_4-\alpha_5-\alpha_6$
$(0,1,-1,0,1,0)$	$\mu_{\mathbf{27}}-\alpha_1-\alpha_2-2\alpha_3-\alpha_4-\alpha_6$
$(0,1,-1,1,-1,0)$	$\mu_{\mathbf{27}}-\alpha_1-\alpha_2-2\alpha_3-\alpha_4-\alpha_5-\alpha_6$
$(1,-1,0,0,1,0)$	$\mu_{\mathbf{27}}-\alpha_1-2\alpha_2-2\alpha_3-\alpha_4-\alpha_6$
$(0,1,0,-1,0,0)$	$\mu_{\mathbf{27}}-\alpha_1-\alpha_2-2\alpha_3-2\alpha_4-\alpha_5-\alpha_6$
$(1,-1,0,1,-1,0)$	$\mu_{\mathbf{27}}-\alpha_1-2\alpha_2-2\alpha_3-\alpha_4-\alpha_5-\alpha_6$
$(-1,0,0,0,1,0)$	$\mu_{\mathbf{27}}-2\alpha_1-2\alpha_2-2\alpha_3-\alpha_4-\alpha_6$
$(1,-1,1,-1,0,0)$	$\mu_{\mathbf{27}}-\alpha_1-2\alpha_2-2\alpha_3-2\alpha_4-\alpha_5-\alpha_6$
$(-1,0,0,1,-1,0)$	$\mu_{\mathbf{27}}-2\alpha_1-2\alpha_2-2\alpha_3-\alpha_4-\alpha_5-\alpha_6$
$(1,0,-1,0,0,1)$	$\mu_{\mathbf{27}}-\alpha_1-2\alpha_2-3\alpha_3-2\alpha_4-\alpha_5-\alpha_6$
$(-1,0,1,-1,0,0)$	$\mu_{\mathbf{27}}-2\alpha_1-2\alpha_2-2\alpha_3-2\alpha_4-\alpha_5-\alpha_6$
$(1,0,0,0,0,-1)$	$\mu_{\mathbf{27}}-\alpha_1-2\alpha_2-3\alpha_3-2\alpha_4-\alpha_5-2\alpha_6$
$(-1,1,-1,0,0,1)$	$\mu_{\mathbf{27}}-2\alpha_1-2\alpha_2-3\alpha_3-2\alpha_4-\alpha_5-\alpha_6$
$(-1,1,0,0,0,-1)$	$\mu_{\mathbf{27}}-2\alpha_1-2\alpha_2-3\alpha_3-2\alpha_4-\alpha_5-2\alpha_6$
$(0,-1,0,0,0,1)$	$\mu_{\mathbf{27}}-2\alpha_1-3\alpha_2-3\alpha_3-2\alpha_4-\alpha_5-\alpha_6$
$(0,-1,1,0,0,-1)$	$\mu_{\mathbf{27}}-2\alpha_1-3\alpha_2-3\alpha_3-2\alpha_4-\alpha_5-2\alpha_6$
$(0,0,-1,1,0,0)$	$\mu_{\mathbf{27}}-2\alpha_1-3\alpha_2-4\alpha_3-2\alpha_4-\alpha_5-2\alpha_6$
$(0,0,0,-1,1,0)$	$\mu_{\mathbf{27}}-2\alpha_1-3\alpha_2-4\alpha_3-3\alpha_4-\alpha_5-2\alpha_6$
$(0,0,0,0,-1,0)$	$\mu_{\mathbf{27}}-2\alpha_1-3\alpha_2-4\alpha_3-3\alpha_4-2\alpha_5-2\alpha_6$

(A.2.2)

Appendix B

Appendices to Chapter 5

B.1 Polynomial equations in UFDs

In this appendix, we summarize how to solve polynomial equations over unique factorization domain (UFD), which appear recurrently in the discriminant. The sections b_i and c_j of the quartic equation realizing the elliptic curve with two sections, take values in a UFD, given by the ring of local functions on the base of the fibration [147]. Similar methods were used for $\mathbb{P}^{(1,2,3)}$ in [1] for the Tate's algorithm.

B.1.1 Two-term Polynomial

The first such recurring polynomial is given by

$$P = s_\alpha s_\beta - s_\gamma s_\delta \,. \tag{B.1.1}$$

The condition $P = 0$ then amounts to the fact that $s_\alpha s_\beta$ and $s_\gamma s_\delta$ have identical factorizations into irreducibles. Therefore, the most general Ansatz compatible with $P = 0$ is

$$\begin{aligned} s_\alpha &= \sigma_1\sigma_2 \,, \qquad & s_\beta &= \sigma_3\sigma_4 \,, \\ s_\gamma &= \sigma_1\sigma_3 \,, \qquad & s_\delta &= \sigma_2\sigma_4 \,. \end{aligned} \tag{B.1.2}$$

Furthermore, with (a, b) denoting the greatest common divisor of a and b, it is possible to choose these sections such that $\sigma_1 = (s_\alpha, s_\gamma)$ and $\sigma_4 = (s_\beta, s_\delta)$, thereby making the pairs $\{\sigma_2, \sigma_3\}$ and $\{\sigma_1, \sigma_4\}$ coprime.

B.1.2 Four-term Polynomial

A second recurring four-term polynomial in the discriminants of the fiber is of the form

$$P = b_i^3 c_0 - b_i^2 b_j c_1 + b_i b_j^2 c_2 - b_j^3 c_3 \,. \tag{B.1.3}$$

To solve $P = 0$, first note, that b_j divides the last three terms, it also has to divide the first, hence $b_j | b_i^3 c_0$. Analogously, $b_i | b_j^3 c_3$.

Next, decompose $b_i = \sigma_1 \sigma_2$ and $b_j = \sigma_1 \sigma_3$, where $\sigma_1 = (b_i, b_j)$. σ_1 being the greatest common divisor implies that all irreducibles in σ_2 do not divide σ_3 and vice versa – any such irreducibles would be subsumed within σ_1. Then, one can rewrite the polynomial

$$P = \sigma_1^3 \left(\sigma_2^3 c_0 - \sigma_2^2 \sigma_3 c_1 + \sigma_2 \sigma_3^2 c_2 - \sigma_3^3 c_3 \right) \,. \tag{B.1.4}$$

Now one has $\sigma_2 | \sigma_3^3 c_3$. But since σ_2 and σ_3 do not share any irreducibles, this condition amounts to $\sigma_2 | c_3$. Thus $c_3 = \sigma_2 \sigma_5$. By a similar argument $c_0 = \sigma_3 \sigma_4$. Applying these decompositions, the polynomial reads

$$P = \sigma_1^3 \sigma_2 \sigma_3 \left(\sigma_2 \left(\sigma_2 \sigma_4 - c_1 \right) + \sigma_3 \left(c_2 - \sigma_3 \sigma_5 \right) \right) \,. \tag{B.1.5}$$

The factors $\sigma_1^3 \sigma_2 \sigma_3$ can at times give rise to new canonical enhancements, which have not appeared elsewhere in the algorithm and therefore have to be always checked as well. So these solutions are

$$\begin{aligned} \sigma_1 = 0 : &\qquad b_i = b_j = 0 \\ \sigma_2 = 0 : &\qquad b_i = c_3 = 0 \\ \sigma_3 = 0 : &\qquad b_j = c_0 = 0 \end{aligned} \tag{B.1.6}$$

and correspond to canonical enhancements.

The other solutions are characterized in the tems of the vanishing of the remaining factor in P. Define $\tilde{\alpha} = \sigma_2 \sigma_4 - c_1$ and $\tilde{\beta} = c_2 - \sigma_3 \sigma_5$. As again σ_2 and σ_3 do not share any irreducibles, one has $\sigma_3 | \tilde{\alpha}$ and $\sigma_2 | \tilde{\beta}$, hence there are decompositions $\tilde{\alpha} = \sigma_3 \alpha$ and $\tilde{\beta} = \sigma_2 \beta$. With the non-vanishing of b_i and b_j, $P = 0$ is now reduced to $\alpha = -\beta$. Solving for the

coefficients, one obtains

$$\begin{aligned} c_0 &= \sigma_3\sigma_4 \\ c_1 &= \sigma_2\sigma_4 + \sigma_3\alpha \\ c_2 &= \sigma_3\sigma_5 + \sigma_2\alpha \\ c_3 &= \sigma_2\sigma_5 \\ b_i &= \sigma_1\sigma_2 \\ b_j &= \sigma_1\sigma_3 \end{aligned} \tag{B.1.7}$$

as the final solution set to $P = 0$ with six free functions σ_1, σ_2, σ_3, σ_4, σ_5 and α, with σ_2 and σ_3 coprime.

There are in summary four branches of the solution set to $P = 0$: (B.1.6) and (B.1.7).

B.1.3 Three-term Polynomials

Another recurring polynomial with three terms is given by

$$P = b_i^2 c_\alpha - b_i b_j c_\beta + b_j^2 c_\gamma \,. \tag{B.1.8}$$

In the same vein as above, one can use the divisibility conditions to find the general Ansatz

$$\begin{aligned} b_i &= \sigma_1\sigma_2 \\ b_j &= \sigma_1\sigma_3 \\ c_\alpha &= \sigma_3\sigma_4 \\ c_\gamma &= \sigma_2\sigma_5 \,. \end{aligned} \tag{B.1.9}$$

Then, the polynomial equation reduces to

$$P = \sigma_1^2\sigma_2\sigma_3(\sigma_2\sigma_4 + \sigma_3\sigma_5 - c_\beta) \tag{B.1.10}$$

This has solutions

$$\begin{aligned} \sigma_1 = 0: &\qquad b_i = b_j = 0 \\ \sigma_2 = 0: &\qquad b_i = c_\gamma = 0 \\ \sigma_3 = 0: &\qquad b_j = c_\alpha = 0 \,. \end{aligned} \tag{B.1.11}$$

as well as the solution where $b_i, b_j \neq 0$

$$\begin{aligned} b_i &= \sigma_1\sigma_2 \\ b_j &= \sigma_1\sigma_3 \\ c_\alpha &= \sigma_3\sigma_4 \\ c_\gamma &= \sigma_2\sigma_5 \\ c_\beta &= \sigma_2\sigma_4 + \sigma_3\sigma_5 \,. \end{aligned} \tag{B.1.12}$$

The most general solution to the three-term polynomial thus has five free functions σ_1, σ_2, σ_3, σ_4 and σ_5, and the two functions σ_2, σ_3 are coprime. In summary, there are four solution sets to (B.1.10): (B.1.11) and (B.1.12).

Another three-term polynomial that one encounters while working through the algorithm is

$$P = b_1^2 c_0 - b_1 b_2 c_1 - c_1^2 \,. \tag{B.1.13}$$

Since b_1 divides the first two terms, one has $b_1 | c_1^2$, the most general ansatz compatible with which is $b_1 = \alpha^2\beta$, $c_1 = \alpha\beta\gamma$. Let furthermore $\delta = (\alpha, \gamma)$, and $\alpha = \delta\tilde{\alpha}$, $\gamma = \delta\tilde{c}_1$. Then, $(\tilde{\alpha}, \tilde{c}_1) = 1$, and one has

$$\begin{aligned} b_1 &= \tilde{\alpha}^2\delta^2\beta \,, \\ c_1 &= \delta^2\tilde{\alpha}\beta\tilde{c}_1 \,. \end{aligned} \tag{B.1.14}$$

The polynomial is now given by

$$P = \tilde{\alpha}^2\delta^4\beta^2 \left(\tilde{\alpha}^2 c_0 - \tilde{\alpha} b_2 \tilde{c}_1 - \tilde{c}_1^2\right) \,. \tag{B.1.15}$$

Immediately there is the solution, which gives rise to a canonical model

$$b_1 = c_1 = 0 \,. \tag{B.1.16}$$

The remaining polynomial term gives another solution: as $\tilde{\alpha}$ divides the first two terms in the bracket, $\tilde{\alpha} | \tilde{c}_1^2$ holds. However, since also $(\tilde{\alpha}, \tilde{c}_1) = 1$, it follows that $\tilde{\alpha} = 1$. Therefore, $b_1 = \delta^2\beta$ and the second solution to $P = 0$ is given by

$$\begin{aligned} b_1 &= \delta^2\beta \\ c_1 &= \delta^2\beta\tilde{c}_1 = b_1\tilde{c}_1 \\ c_0 &= b_2\tilde{c}_1 + \tilde{c}_1^2 \,. \end{aligned} \tag{B.1.17}$$

B.2 Alternative forms for I_5

In this section, the matter content and $U(1)$ charges of all canonical and singly non-canonical I_5 models is summarized. We have already seen that there are multiple, equivalent ways of realizing I_5 fibers with two sections, and at times it might be useful to have all the realizations. Our focus on I_5 is purely motivated from its application in F-theory model building, but similar forms can be obtained in the algorithm for any I_n following our results in section 5.4.3 for the I_n and the symmetries in section 5.1.5 and the lop transformations in 5.1.6. The forms presented in the main part of the paper, are a minimal set, realizing each fiber type, as well as being equivalent to the ones in this appendix by the arguments in sections 5.1.5 and 5.1.6.

In table B.2 the following definitions were used:

$$P_0 = b_{0,1}c_{2,1} - b_{1,0}c_{3,2} \tag{B.2.1}$$

$$P_1 = b_{1,0}^2 c_{0,1} - b_{1,0}b_{2,0}c_{1,1} + b_{2,0}^2 c_{2,1} \tag{B.2.2}$$

$$P_2 = \sigma_4 b_{2,0}^2 + \sigma_1^2\sigma_3 c_{0,1} - \sigma_1 b_{2,0}c_{1,1} \tag{B.2.3}$$

$$\begin{aligned} P_3 = {} & \sigma_1\sigma_2^2\left(\sigma_1 c_{1,1} - \sigma_4 b_{2,0}\right) + \sigma_3\sigma_2\left(\sigma_4\sigma_1 b_{1,1} - \sigma_1^2 c_{2,2} + \sigma_4^2\right) \\ & + \sigma_1\sigma_3^2\left(\sigma_1 c_{3,3} - \sigma_4 b_{0,2}\right) \end{aligned} \tag{B.2.4}$$

$$P_4 = \sigma_1 c_{3,2} - \sigma_5 b_{0,1} \tag{B.2.5}$$

$$\begin{aligned} P_5 = {} & -\sigma_2^3\left(\sigma_4\sigma_1 b_{2,1} - \sigma_1^2 c_{0,2} + \sigma_4^2\right) + \sigma_3\sigma_2^2\left(\sigma_1\left(\sigma_5 b_{2,1} - \sigma_1 c_{1,2}\right) + \sigma_4\left(\sigma_1 b_{1,1} + 2\sigma_5\right)\right) \\ & - \sigma_3^2\sigma_2\left(\sigma_1\left(\sigma_4 b_{0,1} - \sigma_1 c_{2,2}\right) + \sigma_1\sigma_5 b_{1,1} + \sigma_5^2\right) + \sigma_1\sigma_3^3\left(\sigma_5 b_{0,1} - \sigma_1 c_{3,2}\right) . \end{aligned} \tag{B.2.6}$$

B.3 Relation to Top Models and Spectral Covers

Previously models with extra sections were constructed based on toric tops [2, 109–111]. Furthermore, there are models in the standard $\mathbb{P}^{(1,2,3)}$ that realize extra sections [80, 107], and were constructed inspired by and are related to factored spectral cover models [104–106]. We should finally comment on the relation of the Tate models found here to these top models.

The short summary is: all top models feature in the tree, in terms of canonical models. However the tree gives rise to more models, namely, the non-canonical models. The non-canonical models have the same fiber types as canonical ones, however their codimension

Model	Matter locus	Representation	Fiber type
$\mathcal{Q}(5,3,1,0,0,2)$	$b_{1,0}$	$\mathbf{10}_0 + \overline{\mathbf{10}}_{-0}$	$I_5^{(01)}$
	$c_{3,1}$	$\mathbf{5}_{-1} + \overline{\mathbf{5}}_1$	
	$c_{3,1} + b_{0,0}b_{1,0}$	$\mathbf{5}_1 + \overline{\mathbf{5}}_{-1}$	
	$b_{1,0}^2 c_{0,5} - b_{1,0}b_{2,2}c_{1,3} + b_{2,2}^2 c_{2,1}$	$\mathbf{5}_0 + \overline{\mathbf{5}}_0$	
$\mathcal{Q}(4,2,1,1,0,0,2)$	$b_{1,0}$	$\mathbf{10}_2 + \overline{\mathbf{10}}_{-2}$	$I_5^{(0\|1)}$
	$b_{0,0}$	$\mathbf{5}_6 + \overline{\mathbf{5}}_{-6}$	
	$b_{0,0}c_{2,1} - b_{1,0}c_{3,1}$	$\mathbf{5}_{-4} + \overline{\mathbf{5}}_4$	
	$b_{1,0}^2 c_{0,4} - b_{1,0}b_{2,2}c_{1,2} - c_{1,2}^2$	$\mathbf{5}_1 + \overline{\mathbf{5}}_{-1}$	
$\mathcal{Q}(4,3,2,1,0,0,1)$	$b_{1,0}$	$\mathbf{10}_{-3} + \overline{\mathbf{10}}_3$	$I_5^{(0\|1)}$
	$b_{0,0}$	$\mathbf{5}_6 + \overline{\mathbf{5}}_{-6}$	
	$c_{3,1}$	$\mathbf{5}_{-4} + \overline{\mathbf{5}}_4$	
	$b_{1,0}^3 c_{0,4} - b_{1,0}^2 b_{2,1}c_{1,3} + b_{1,0}b_{2,1}^2 c_{2,2} - b_{2,1}^3 c_{3,1}$	$\mathbf{5}_1 + \overline{\mathbf{5}}_{-1}$	
$\mathcal{Q}(3,2,2,2,0,0,1)$	$b_{1,0}$	$\mathbf{10}_1 + \overline{\mathbf{10}}_{-1}$	$I_5^{(0\|\|1)}$
	$b_{0,0}$	$\mathbf{5}_{-7} + \overline{\mathbf{5}}_7$	
	$b_{1,0}c_{0,3} - b_{2,1}c_{1,2}$	$\mathbf{5}_{-2} + \overline{\mathbf{5}}_2$	
	$b_{0,0}^2 c_{1,2} - b_{0,0}b_{1,0}c_{2,2} + b_{1,0}^2 c_{3,2}$	$\mathbf{5}_3 + \overline{\mathbf{5}}_{-3}$	
$\mathcal{Q}(3,2,1,1,1,0,1)$	$b_{1,0}$	$\mathbf{10}_0 + \overline{\mathbf{10}}_0$	$I_5^{(01)}$
	$c_{3,1}$	$\mathbf{5}_{-1} + \overline{\mathbf{5}}_1$	
	$c_{3,1} + b_{0,1}b_{1,0}$	$\mathbf{5}_1 + \overline{\mathbf{5}}_{-1}$	
	$b_{1,0}^2 c_{0,3} - b_{1,0}b_{2,1}c_{1,2} + b_{2,1}^2 c_{2,1}$	$\mathbf{5}_0 + \overline{\mathbf{5}}_0$	
$\mathcal{Q}(2,1,1,2,1,0,1)$	$b_{1,0}$	$\mathbf{10}_2 + \overline{\mathbf{10}}_{-2}$	$I_5^{(0\|1)}$
	$b_{0,1}$	$\mathbf{5}_6 + \overline{\mathbf{5}}_{-6}$	
	$b_{1,0}^2 c_{0,2} - c_{1,1}^2$	$\mathbf{5}_1 + \overline{\mathbf{5}}_{-1}$	
	$b_{0,1}c_{2,1} - b_{1,0}c_{3,2}$	$\mathbf{5}_{-4} + \overline{\mathbf{5}}_4$	
$\mathcal{Q}(0,0,1,3,2,0,0)$	$b_{1,0}$	$\mathbf{10}_2 + \overline{\mathbf{10}}_{-2}$	$I_5^{(0\|1)}$
	$b_{0,2}$	$\mathbf{5}_6 + \overline{\mathbf{5}}_{-6}$	
	$b_{1,0}^2 c_{0,0} - b_{1,0}b_{2,0}c_{1,0} - c_{1,0}^2$	$\mathbf{5}_1 + \overline{\mathbf{5}}_{-1}$	
	$b_{0,2}c_{2,1} - b_{1,0}c_{3,3}$	$\mathbf{5}_{-4} + \overline{\mathbf{5}}_4$	
$\mathcal{Q}(1,1,1,2,2,0,0)$	$b_{1,0}$	$\mathbf{10}_0 + \overline{\mathbf{10}}_0$	$I_5^{(01)}$
	$b_{1,0}^2 c_{0,1} - b_{1,0}b_{2,0}c_{1,1} + b_{2,0}^2 c_{2,1}$	$\mathbf{5}_0 + \overline{\mathbf{5}}_0$	
	$c_{3,2}$	$\mathbf{5}_1 + \overline{\mathbf{5}}_{-1}$	
	$c_{3,2} + b_{0,2}b_{1,0}$	$\mathbf{5}_{-1} + \overline{\mathbf{5}}_1$	
$\mathcal{Q}(2,2,2,2,1,0,0)$	$b_{1,0}$	$\mathbf{10}_{-3} + \overline{\mathbf{10}}_3$	$I_5^{(0\|1)}$
	$b_{0,1}$	$\mathbf{5}_6 + \overline{\mathbf{5}}_{-6}$	
	$c_{3,2}$	$\mathbf{5}_{-4} + \overline{\mathbf{5}}_4$	
	$b_{1,0}^3 c_{0,2} - b_{1,0}^2 b_{2,0}c_{1,2} + b_{1,0}b_{2,0}^2 c_{2,2} - b_{2,0}^3 c_{3,2}$	$\mathbf{5}_1 + \overline{\mathbf{5}}_{-1}$	
$\mathcal{Q}(1,1,2,3,1,0,0)$	$b_{1,0}$	$\mathbf{10}_1 + \overline{\mathbf{10}}_{-1}$	$I_5^{(0\|\|1)}$
	$b_{0,1}$	$\mathbf{5}_{-7} + \overline{\mathbf{5}}_7$	
	$b_{1,0}c_{0,1} - b_{2,0}c_{1,1}$	$\mathbf{5}_{-2} + \overline{\mathbf{5}}_2$	
	$b_{0,1}^2 c_{1,1} - b_{0,1}b_{1,0}c_{2,2} + b_{1,0}^2 c_{3,3}$	$\mathbf{5}_3 + \overline{\mathbf{5}}_{-3}$	

TABLE B.1: Matter curves and $U(1)$ charges for canonical I_5 models.

2 structure is different: in particular the canonical models, and thus the tops, have only one type of codimension 2 locus that is of type I_1^*, i.e. gives rise to **10** matter.

The top models were already mentioned, in particular, top 1 and 2 (in the labeling of [2]) are exactly the two canonical I_5 models, obtained in section 5.3.6.

The other tops are obtained from non-canonical forms as specializations. Consider the non-canonical I_5 model, $\mathcal{Q}(3,2,1,1,0,0,1)|_{(5.3.43)}$, and specialize by assuming that σ_2 never vanishes. This has two effects: The matter curve above $\sigma_2 = 0$ will not be present in the spectrum anymore, and $b_{1,0}|b_{2,1}$. Therefore, an expression of the form $\frac{b_{2,1}}{b_{1,0}} = \frac{\sigma_3}{\sigma_2}$ is

Model	Matter locus	Representation	Fiber type
$Q(1,1,1,2,1,0,0)\vert_{(B.2.1)}$	σ_3	$\mathbf{10}_1 + \overline{\mathbf{10}}_{-1}$	$I_5^{(0\vert\vert 1)}$
	σ_1	$\mathbf{10}_{-4} + \overline{\mathbf{10}}_4$	
	σ_2	$\mathbf{5}_{-7} + \overline{\mathbf{5}}_7$	
	(B.2.3)	$\mathbf{5}_{-2} + \overline{\mathbf{5}}_2$	
	(B.2.4)	$\mathbf{5}_3 + \overline{\mathbf{5}}_{-3}$	
$Q(1,1,1,2,1,0,0)\vert_{(B.2.2)}$	σ_1	$\mathbf{10}_2 + \overline{\mathbf{10}}_{-2}$	$I_5^{(0\vert 1)}$
	σ_2	$\mathbf{10}_{-3} + \overline{\mathbf{10}}_3$	
	$b_{0,1}$	$\mathbf{5}_6 + \overline{\mathbf{5}}_{-6}$	
	(B.2.5)	$\mathbf{5}_{-4} + \overline{\mathbf{5}}_4$	
	(B.2.6)	$\mathbf{5}_1 + \overline{\mathbf{5}}_{-1}$	

TABLE B.2: Matter curves and $U(1)$ charges for non-canonical I_5 models arising from canonical I_4 models through Tate's algorithm, which are related to those in section 5.5 under lopping transformation.

now well-defined over the whole base manifold. Then apply the coordinate shift

$$\begin{pmatrix} x \\ y \end{pmatrix} \to \begin{pmatrix} x - \frac{\sigma_3}{\sigma_2} zsw \\ y \end{pmatrix}, \tag{B.3.1}$$

which gives a new fibration that has canonical form

$$\mathcal{Q}(4,2,1,0,0,0,2) \tag{B.3.2}$$

and is known in the literature as Top 2. Similarly, if $\sigma_1 = 1$, then $b_{1,0}|c_{2,1}$ and $b_{2,1}|c_{0,3}$, and the now well-defined shift

$$y \quad \to \quad y + \frac{\sigma_4}{\sigma_1} z^2 s w^2 + \frac{\sigma_5}{\sigma_1} zwx \tag{B.3.3}$$

produces the canonical form

$$\mathcal{Q}(4,3,2,1,0,0,1)\,, \tag{B.3.4}$$

also known as Top 3.

Next, the noncanonical form $\mathcal{Q}(3,2,1,1,0,0,1)\vert_{(5.3.42)}$ has a canonical subform for $\sigma_1 = 1$, which is reachable by shifting

$$y \quad \to \quad y + \frac{\sigma_4}{\sigma_1} zwx \tag{B.3.5}$$

and given by

$$\mathcal{Q}(3,2,2,2,0,0,1) \tag{B.3.6}$$

or Top 4.

Furthermore, there is an identification between the non-canonical $I_5^{(0|1)}$ and $I_5^{(0||1)}$ models and the ones arising from mapping a factorised Tate form in $\mathbb{P}_{[1,2,3]}$ to $\mathrm{Bl}_{[0,1,0]}\mathbb{P}_{[1,1,2]}$ that have been discussed in [80]. There, the model corresponding to a $4+1$-factorized Tate model was found to be given by

$$sy^2 + \mathfrak{b}_0 x^2 y = \mathfrak{c}_{0,2} s^3 w^4 + \mathfrak{c}_{1,1} s^2 w^3 x + \mathfrak{c}_{2,0} s w^2 x^2 + \mathfrak{c}_{3,0} w x^3 \,, \tag{B.3.7}$$

with coefficient specializations

$$\begin{aligned} c_{0,2} &= \frac{1}{4} b_{2,1}^2 \\ c_{1,1} &= -\frac{1}{2} \sigma_1 b_{2,1} \sigma_3 \\ c_{2,0} &= \frac{1}{4} \sigma_1^2 \sigma_3^2 \\ c_{2,1} &= \sigma_4 \sigma_3 - \frac{1}{2} \sigma_1 b_{2,1} \\ c_{3,0} &= \frac{1}{2} \sigma_1^2 \sigma_3 \\ c_{3,1} &= \sigma_4 \,. \end{aligned} \tag{B.3.8}$$

After the coordinate shift

$$y \quad \to \quad y - \frac{1}{2} b_{2,1} z s w^2 + \frac{1}{2} \sigma_1 \sigma_3 w x \,, \tag{B.3.9}$$

this model turns out to be identical to the non-canonical fibration $Q(3,2,1,1,0,0,1)|_{(5.3.42)}$, specialized with $\sigma_2 = 1$.

The $3+2$-factorized Tate model reads

$$sy^2 + \mathfrak{b}_0 x^2 y = \mathfrak{c}_{0,2} s^3 w^4 + \mathfrak{c}_{1,1} s^2 w^3 x + \mathfrak{c}_{2,0} s w^2 x^2 + \mathfrak{c}_{3,0} w x^3 \,, \tag{B.3.10}$$

with coefficient specializations

$$\begin{aligned} c_{0,2} &= \frac{1}{4}\sigma_1^2\sigma_3^2 \\ c_{0,3} &= \sigma_3\sigma_4 \\ c_{1,1} &= \frac{1}{2}\sigma_2\sigma_1^2\sigma_3 \\ c_{1,2} &= \sigma_5\sigma_3 + \sigma_2\sigma_4 \\ c_{2,0} &= \frac{1}{4}\sigma_2^2\sigma_1^2 \\ c_{2,1} &= \sigma_2\sigma_5 - \frac{1}{2}\sigma_1\sigma_3 b_{0,0} \\ c_{3,0} &= -\frac{1}{2}\sigma_2\sigma_1 b_{0,0}\,. \end{aligned} \tag{B.3.11}$$

Here, the coordinate shift

$$y \quad \to \quad y - \frac{1}{2}\sigma_1\sigma_3 zsw^2 - \frac{1}{2}\sigma_1\sigma_2 wx \tag{B.3.12}$$

identifies this fibration with the non-canonical model $Q(3,2,1,1,0,0,1)|_{(5.3.43)}$.

B.4 Resolutions for I_n^* and I_n fibers

In this appendix, we present the resolved geometries and Cartan divisors for the fibrations with fiber types $I_n^{*(01)}$, $I_n^{*(0|1)}$, $I_n^{*(0||1)}$ and $I_n^{(0|^k 1)}$ given in section 5.4. All resolutions were implemented in mathematica using [83].

B.4.1 $I_n^{*(01)}$

The ordered set of resolutions that resolves the $I_n^{*(01)}$ fibration in all codimensions is given by

$$\begin{aligned} &(z,x,y;\zeta_1), \qquad (\zeta_1,y;\epsilon_0), \qquad (\zeta_1,\epsilon_0;\delta_0), \\ &(\epsilon_0,x;\epsilon_1), \qquad (\epsilon_0,\epsilon_1;\delta_1), \qquad (\epsilon_1,y;\epsilon_2), \\ &\qquad (\epsilon_{k-1},\epsilon_k;\delta_k), \qquad (\epsilon_k,x;\epsilon_{k+1}) \qquad k \text{ even} \\ &\qquad (\epsilon_{k-1},\epsilon_k;\delta_k), \qquad (\epsilon_k,y;\epsilon_{k+1}) \qquad k \text{ odd}\,. \end{aligned} \tag{B.4.1}$$

for $k = 2, \ldots, n$. For n odd, the fully resolved geometry is given by

$$\begin{aligned}
&y^2 s\left(\epsilon_0\epsilon_2\epsilon_4\cdots\epsilon_{n+1}\right) + \mathfrak{b}_0 x^2 y\zeta_1\left(\delta_0\delta_1^2\delta_2^3\cdots\delta_n^{n+1}\right)\\
&+ \mathfrak{b}_{1,1} swxyz\zeta_1\left(\delta_0\cdots\delta_n\right)\left(\epsilon_0\cdots\epsilon_{n+1}\right) + \mathfrak{b}_{2,2+\frac{n-1}{2}} y s^2 w^2 z^{2+\frac{n-1}{2}}\zeta_1^{1+\frac{n-1}{2}}\left(\delta_0^n\delta_1^{n-1}\cdots\delta_{n-1}\right)\\
=&\,\mathfrak{c}_{0,n+4} w^4 s^3 z^{4+n}\zeta_1^{2+n}\left(\delta_0^{2n+2}\delta_1^{2n}\cdots\delta_n^2\right)\left(\epsilon_0^{n+1}\epsilon_1^n\cdots\epsilon_n\right)\\
&+ \mathfrak{c}_{1,2+\frac{n+1}{2}} w^3 s^2 xz^{2+\frac{n+1}{2}}\zeta_1^{1+\frac{n+1}{2}}\left(\delta_0^{2n+2}\delta_1^{2n}\cdots\delta_n^2\right)\left(\left(\epsilon_0\epsilon_1\right)^{\frac{n+1}{2}}\left(\epsilon_2\epsilon_3\right)^{\frac{n-1}{2}}\cdots\left(\epsilon_{n-1}\epsilon_n\right)\right)\\
&+ \mathfrak{c}_{2,1} sw^2x^2z\zeta_1\left(\epsilon_1\epsilon_3\epsilon_5\cdots\epsilon_n\right)\\
&+ \mathfrak{c}_3 wx^3\zeta_1\left(\delta_1\delta_2^2\cdots\delta_n^n\right)\left(\left(\epsilon_1\epsilon_2\right)\left(\epsilon_3\epsilon_4\right)^2\cdots\left(\epsilon_n\epsilon_{n+1}\right)^{\frac{n+1}{2}}\right)\left(\epsilon_1\epsilon_3\cdots\epsilon_n\right).
\end{aligned} \tag{B.4.2}$$

The irreducible Cartan divisors are

Section	Equation in Y_4
z	$-c_{3,0}wx^3\zeta_1 + y\epsilon_0\left(sy + b_{0,0}x^2\zeta_1\delta_0\right)$
ϵ_0	$c_{2,1}z + c_{3,0}\delta_1$
δ_0	$\epsilon_0 - x^2\zeta_1\epsilon_1\left(c_{2,1}z + c_{3,0}x\delta_1\epsilon_1\right)$
$\delta_{0<i<n}$, i odd	$c_{2,1}\epsilon_i - y^2\epsilon_{i-1}\epsilon_{i+1}$
$\delta_{0<i<n}$, i even	$\epsilon_i - c_{2,1}x^2\epsilon_{i-1}\epsilon_{i+1}$
ϵ_n	$b_{2,2+\frac{n-1}{2}}\delta_{n-1} + \epsilon_{n+1}$
ϵ_{n+1}	$b_{2,2+\frac{n-1}{2}}y - \epsilon_n\left(c_{2,1}x^2 + \delta_n\left(c_{1,2+\frac{n+1}{2}}x + c_{0,n+4}\delta_n\right)\right)$
δ_n	$c_{2,1}\epsilon_n - y\epsilon_{n-1}\left(y\epsilon_{n+1} + b_{2,2+\frac{n-1}{2}}\delta_{n-1}\right)$

(B.4.3)

The intersections follow from the projective relations induced by the blow-ups, can be computed as outlined in section 5.1.7. They reproduce the affine D_{n+4} Dynkin diagram if the divisors are ordered as $(z, \epsilon_0, \delta_0, \delta_1, \ldots, \delta_n, \epsilon_n, \epsilon_{n+1})$. Both σ_0 and σ_1 intersect $z = 0$.

For even n, the fully resolved geometry reads

$$\begin{aligned}
&y^2 s\left(\epsilon_0\epsilon_2\epsilon_4\cdots\epsilon_n\right) + \mathfrak{b}_0 x^2 y\zeta_1\left(\delta_0\delta_1^2\delta_2^3\cdots\delta_n^{n+1}\right)\\
&+ \mathfrak{b}_{1,1} swxyz\zeta_1\left(\delta_0\cdots\delta_n\right)\left(\epsilon_0\cdots\epsilon_{n+1}\right) + \mathfrak{b}_{2,2+\frac{n}{2}} y s^2 w^2 z^{2+\frac{n}{2}}\zeta_1^{1+\frac{n}{2}}\left(\delta_0^{n+1}\delta_1^n\cdots\delta_n\right)\\
=&\,\mathfrak{c}_{0,n+4} w^4 s^3 z^{4+n}\zeta_1^{2+n}\left(\delta_0^{2n+2}\delta_1^{2n}\cdots\delta_n^2\right)\left(\epsilon_0^{n+1}\epsilon_1^n\cdots\epsilon_n\right)\\
&+ \mathfrak{c}_{1,2+\frac{n}{2}} w^3 s^2 xz^{2+\frac{n}{2}}\zeta_1^{1+\frac{n}{2}}\left(\delta_0^n\delta_1^{n-1}\cdots\delta_{n-1}\right)\left(\left(\epsilon_0\epsilon_1\right)^{\frac{n}{2}}\left(\epsilon_2\epsilon_3\right)^{\frac{n}{2}-1}\cdots\left(\epsilon_{n-2}\epsilon_{n-1}\right)\right)\\
&+ \mathfrak{c}_{2,1} sw^2x^2z\zeta_1\left(\epsilon_1\epsilon_3\epsilon_5\cdots\epsilon_{n+1}\right)\\
&+ \mathfrak{c}_3 wx^3\zeta_1\left(\delta_1\delta_2^2\cdots\delta_n^n\right)\left(\left(\epsilon_1\epsilon_2\right)\left(\epsilon_3\epsilon_4\right)^2\cdots\left(\epsilon_{n-1}\epsilon_n\right)^{\frac{n}{2}}\right)\left(\epsilon_1\epsilon_3\cdots\epsilon_{n-1}\right)\epsilon_{n+1}^{2+\frac{n}{2}},
\end{aligned} \tag{B.4.4}$$

and the irreducible Cartan divisors are

Section	Equation in Y_4
z	$-c_{3,0}wx^3\zeta_1 + y\epsilon_0\left(sy + b_{0,0}x^2\zeta_1\delta_0\right)$
ϵ_0	$c_{2,1}z + c_{3,0}\delta_1$
δ_0	$\epsilon_0 - x^2\zeta_1\epsilon_1\left(c_{2,1}z + c_{3,0}x\delta_1\epsilon_1\right)$
$\delta_{0<i<n}$, i odd	$c_{2,1}\epsilon_i - y^2\epsilon_{i-1}\epsilon_{i+1}$
$\delta_{0<i<n}$, i even	$\epsilon_i - c_{2,1}x^2\epsilon_{i-1}\epsilon_{i+1}$
ϵ_n	$c_{1,2+\frac{n}{2}}\delta_{n-1} + c_{2,1}\epsilon_{n+1}$
ϵ_{n+1}	$c_{1,2+\frac{n}{2}}x - \epsilon_n\left(y^2 + b_{2,2+\frac{n}{2}}y\delta_n - c_{0,4+n}\delta_n^2\right)$
δ_n	$\epsilon_n - x\epsilon_{n-1}\left(c_{2,1}x\epsilon_{n+1} + c_{1,2+\frac{n}{2}}\delta_{n-1}\right)$

(B.4.5)

Again and with the same ordering as above, one finds that the intersections yield the affine D_{n+4} Dynkin diagram, with σ_0 and σ_1 being located on $z = 0$.

B.4.2 $I_n^{*(0|1)}$

The ordered set of resolutions that resolves the $I_n^{*(0|1)}$ fibration in all codimensions is given by

$$\begin{aligned}
&(z,x,y;\zeta_1), \qquad (z,y;\epsilon_0), \qquad (\zeta_1,y;\epsilon_1),\\
&(\epsilon_0,\zeta_1,\delta_0), \qquad (\zeta_1,\epsilon_1;\delta_1), \qquad (\epsilon_1,x;\epsilon_2),\\
&\qquad\qquad (\epsilon_{k-1},\epsilon_k;\delta_k), \qquad (\epsilon_k,y;\epsilon_{k+1}) \qquad k \text{ even}\\
&\qquad\qquad (\epsilon_{k-1},\epsilon_k;\delta_k), \qquad (\epsilon_k,x;\epsilon_{k+1}) \qquad k \text{ odd}\,.
\end{aligned} \tag{B.4.6}$$

for $k = 2,\ldots,n$. The resolved geometry for odd n reads

$$\begin{aligned}
&y^2 s\epsilon_0\left(\epsilon_1\epsilon_3\cdots\epsilon_n\right) + \mathfrak{b}_0 x^2 y\zeta_1\left(\delta_1\delta_2^2\cdots\delta_n^n\right)\epsilon_1\left((\epsilon_2\epsilon_3)^2(\epsilon_4\epsilon_5)^3\cdots(\epsilon_{n-1}\epsilon_n)^{\frac{n+1}{2}}\right)\epsilon_{n+1}^{\frac{n+3}{2}}\\
&\quad + \mathfrak{b}_{1,1}swxyz\zeta_1\left(\delta_0\delta_1\cdots\delta_n\right)\left(\epsilon_0\epsilon_1\cdots\epsilon_{n+1}\right)\\
&\quad + \mathfrak{b}_{2,1+\frac{n+1}{2}}ys^2w^2z^{1+\frac{n+1}{2}}\zeta_1^{\frac{n+1}{2}}\left(\delta_0^{n+1}\delta_1^n\cdots\delta_n\right)\epsilon_0^{1+\frac{n+1}{2}}\epsilon_1^{\frac{n+1}{2}}\left((\epsilon_2\epsilon_3)^{\frac{n-1}{2}}(\epsilon_4\epsilon_5)^{\frac{n-3}{2}}\cdots(\epsilon_{n-1}\epsilon_n)\right)\\
&= \mathfrak{c}_{0,3+n}w^4s^3z^{3+n}\zeta_1^{1+n}\left(\delta_0^{2+2n}\delta_1^{2n}\cdots\delta_n^2\right)\epsilon_0^{n+2}\left(\epsilon_1^n\epsilon_2^{n-1}\cdots\epsilon_n\right)\\
&\quad + \mathfrak{c}_{1,2+\frac{n-1}{2}}w^3s^2xz^{2+\frac{n-1}{2}}\zeta_1^{1+\frac{n-1}{2}}\left(\delta_0^n\delta_1^{n-1}\cdots\delta_{n-1}\right)\epsilon_0^{\frac{n+1}{2}}\left((\epsilon_1\epsilon_2)^{\frac{n-1}{2}}(\epsilon_3\epsilon_4)^{\frac{n-3}{2}}\cdots(\epsilon_{n-2}\epsilon_{n-1})\right)\\
&\quad + \mathfrak{c}_{2,1}sw^2x^2z\zeta_1\left(\epsilon_2\epsilon_4\cdots\epsilon_{n+1}\right)\\
&\quad + \mathfrak{c}_{3,1}wx^3z\zeta_1^2\left(\delta_0\delta_1^2\cdots\delta_n^{n+1}\right)\epsilon_1\left((\epsilon_2\epsilon_3)^2(\epsilon_4\epsilon_5)^3\cdots(\epsilon_{n-1}\epsilon_n)^{\frac{n+1}{2}}\right)\left(\epsilon_2\epsilon_4\cdots\epsilon_{n-1}\right)\epsilon_{n+1}^{\frac{n+3}{2}}\,.
\end{aligned} \tag{B.4.7}$$

The irreducible Cartan divisors are given by

Section	Equation in Y_4
z	$b_{0,0}x^2\zeta_1 + s\epsilon_0$
ϵ_0	$b_{0,0}y\epsilon_1 - z\left(c_{2,1}s + c_{3,1}\delta_0\epsilon_1\right)$
δ_0	$c_{2,1}z\zeta_1 - \epsilon_1\left(\epsilon_0 + b_{0,0}\zeta_1\delta_1\right)$
$\delta_{0<i<n}$, i odd	$\epsilon_i - c_{2,1}x^2\epsilon_{i-1}\epsilon_{i+1}$
$\delta_{0<i<n}$, i even	$c_{2,1}\epsilon_i - y^2\epsilon_{i-1}\epsilon_{i+1}$
ϵ_n	$c_{1,2+\frac{n-1}{2}}\delta_{n-1} + c_{2,1}\epsilon_{n+1}$
ϵ_{n+1}	$c_{1,2+\frac{n-1}{2}}x + \epsilon_n\left(y^2 + b_{2,1+\frac{n+1}{2}}y\delta_n - c_{0,3+n}\delta_n^2\right)$
δ_n	$\epsilon_n - x\epsilon_{n-1}\left(c_{1,2+\frac{n-1}{2}}\delta_{n-1} + c_{2,1}x\epsilon_{n+1}\right)$

(B.4.8)

Ordering the cartan divisors as $(z, \epsilon_0, \delta_0, \delta_1, \ldots, \delta_n, \epsilon_n, \epsilon_{n+1})$, one reproduces the affine D_{n+4} Dynkin diagram, with $w = 0$ intersecting z, and $s = 0$ intersecting ϵ_0.

For even n, the geometry is

$$
\begin{aligned}
&y^2 s\epsilon_0\left(\epsilon_1\epsilon_3\cdots\epsilon_{n+1}\right) + \mathfrak{b}_0 x^2 y\zeta_1\left(\delta_1\delta_2^2\cdots\delta_n^n\right)\epsilon_1\left((\epsilon_2\epsilon_3)^2(\epsilon_4\epsilon_5)^3\cdots(\epsilon_n\epsilon_{n+1})^{\frac{n+2}{2}}\right)\\
&\quad + \mathfrak{b}_{1,1}swxyz\zeta_1\left(\delta_0\delta_1\cdots\delta_n\right)\left(\epsilon_0\epsilon_1\cdots\epsilon_{n+1}\right)\\
&\quad + \mathfrak{b}_{2,1+\frac{n}{2}}ys^2w^2z^{1+\frac{n}{2}}\zeta_1^{\frac{n}{2}}\left(\delta_0^n\delta_1^{n-1}\cdots\delta_{n-1}\right)\epsilon_0^{1+\frac{n}{2}}\epsilon_1^{\frac{n}{2}}\left((\epsilon_2\epsilon_3)^{\frac{n-2}{2}}(\epsilon_4\epsilon_5)^{\frac{n-4}{2}}\cdots(\epsilon_{n-2}\epsilon_{n-1})\right)\\
&= \mathfrak{c}_{0,3+n}w^4s^3z^{3+n}\zeta_1^{1+n}\left(\delta_0^{2+2n}\delta_1^{2n}\cdots\delta_n^2\right)\epsilon_0^{n+2}\left(\epsilon_1^n\epsilon_2^{n-1}\cdots\epsilon_n\right)\\
&\quad + \mathfrak{c}_{1,2+\frac{n}{2}}w^3s^2xz^{2+\frac{n}{2}}\zeta_1^{1+\frac{n}{2}}\left(\delta_0^{n+1}\delta_1^n\cdots\delta_n\right)\epsilon_0^{\frac{n+2}{2}}\left((\epsilon_1\epsilon_2)^{\frac{n}{2}}(\epsilon_3\epsilon_4)^{\frac{n-2}{2}}\cdots(\epsilon_{n-1}\epsilon_n)\right)\\
&\quad + \mathfrak{c}_{2,1}sw^2x^2z\zeta_1\left(\epsilon_2\epsilon_4\cdots\epsilon_n\right)\\
&\quad + \mathfrak{c}_{3,1}wx^3z\zeta_1^2\left(\delta_0\delta_1^2\cdots\delta_n^{n+1}\right)\epsilon_1\left((\epsilon_2\epsilon_3)^2(\epsilon_4\epsilon_5)^3\cdots(\epsilon_n\epsilon_{n+1})^{\frac{n+1}{2}}\right)\left(\epsilon_2\epsilon_4\cdots\epsilon_n\right)\,.
\end{aligned}
\tag{B.4.9}
$$

and the Cartan divisors are

Section	Equation in Y_4
z	$b_{0,0}x^2\zeta_1 + s\epsilon_0$
ϵ_0	$b_{0,0}y\epsilon_1 - z\left(c_{2,1}s + c_{3,1}\delta_0\epsilon_1\right)$
δ_0	$c_{2,1}z\zeta_1 - \epsilon_1\left(\epsilon_0 + b_{0,0}\zeta_1\delta_1\right)$
$\delta_{0<i<n}$, i odd	$\epsilon_i - c_{2,1}x^2\epsilon_{i-1}\epsilon_{i+1}$
$\delta_{0<i<n}$, i even	$c_{2,1}\epsilon_i - y^2\epsilon_{i-1}\epsilon_{i+1}$
ϵ_n	$b_{2,1+\frac{n}{2}}\delta_{n-1} + \epsilon_{n+1}$
ϵ_{n+1}	$b_{2,1+\frac{n}{2}}y - \epsilon_n\left(c_{2,1}x^2 + c_{1,2+\frac{n}{2}}x\delta_n + c_{0,3+n}\delta_n^2\right)$
δ_n	$c_{2,1}\epsilon_n - y\epsilon_{n-1}\left(b_{2,1+\frac{n}{2}}\delta_{n-1} + y\epsilon_{n+1}\right)$

(B.4.10)

The ordering of the Cartan divisors and intersection structure is equivalent to the odd case.

B.4.3 $I_n^{*(0||1)}$

The ordered set of resolutions to desingularize the $I_n^{*(0||1)}$ fibration is

$$\begin{aligned}(z,x,y;\zeta_1),\ (z,y;\zeta_2),\ (\zeta_1,y;\zeta_3),\\ (\zeta_1,\zeta_2;\zeta_4),\ (\zeta_2,\zeta_3;\delta_1),\\ (\delta_{k-1},y;\delta_k)\qquad k=2,\dots,n\,.\end{aligned} \tag{B.4.11}$$

The resolved geometry reads, for odd n,

$$\begin{aligned}&y^2s + \mathfrak{b}_0x^2y\zeta_2\zeta_3\left(\delta_1\delta_2^2\cdots\delta_n^n\right)\\ &+ \mathfrak{b}_{1,1}swxyz\zeta_0\zeta_1\zeta_2\zeta_3\zeta_4\left(\delta_1\cdots\delta_n\right) + \mathfrak{b}_{2,1}ys^2w^2z\zeta_2\\ =\,&\mathfrak{c}_{0,2+\frac{n+1}{2}}w^4s^3z^{2+\frac{n+1}{2}}\zeta_1^{\frac{n+1}{2}}\zeta_2^{1+\frac{n+1}{2}}\zeta_3^{\frac{n-1}{2}}\zeta_4^{n+1}\left(\delta_1^n\delta_2^{n-1}\cdots\delta_n\right)\\ &+ \mathfrak{c}_{1,2+\frac{n-1}{2}}w^3s^2xz^{2+\frac{n-1}{2}}\zeta_1^{1+\frac{n-1}{2}}\zeta_2^{1+\frac{n-1}{2}}\zeta_3^{\frac{n-1}{2}}\zeta_4^{n}\left(\delta_1^{n-1}\delta_2^{n-2}\cdots\delta_{n-1}\right)\\ &+ \mathfrak{c}_{2,1+\frac{n+1}{2}}sw^2x^2z^{1+\frac{n+1}{2}}\zeta_1^{1+\frac{n+1}{2}}\zeta_2^{\frac{n+1}{2}}\zeta_3^{\frac{n+1}{2}}\zeta_4^{n+1}\left(\delta_1^n\delta_2^{n-1}\cdots\delta_n\right)\\ &+ \mathfrak{c}_{3,1+\frac{n-1}{2}}wx^3z^{1+\frac{n-1}{2}}\zeta_1^{2+\frac{n-1}{2}}\zeta_2^{\frac{n-1}{2}}\zeta_3^{1+\frac{n-1}{2}}\zeta_4^{n}\left(\delta_1^{n-1}\delta_2^{n}\cdots\delta_{n-1}\right)\,.\end{aligned} \tag{B.4.12}$$

and the corresponding irreducible Cartan divisors are

Section	Equation in Y_4
z	$b_{0,0}x^2\zeta_1 + s\zeta_2$
ζ_1	$b_{2,1}z + \zeta_3$
ζ_2	$b_{0,0}y$
ζ_3	$b_{2,1}y$
ζ_4	$b_{2,1}z\zeta_2 + b_{0,0}\zeta_1\zeta_3 + \zeta_2\zeta_3\delta_1$
$\delta_i < n$	$b_{2,1}\zeta_2 + b_{0,0}\zeta_3$
δ_n	$b_{2,1}y\zeta_2 + b_{0,0}y\zeta_3 - \zeta_2^{\frac{n-1}{2}}\zeta_3^{\frac{n-1}{2}}\delta_{n-1}\left(c_{2,1+\frac{n+1}{2}}\zeta_2 + c_{3,1+\frac{n-1}{2}}\zeta_3\right)$

(B.4.13)

Again, the intersections reproduce the affine D_{n+4} Dynkin diagram. The required ordering is $(z, \zeta_1, \zeta_4, \delta_1, \delta_2, \ldots, \delta_n, \zeta_2, \zeta_3)$. Here, the section $w = 0$ intersects z, and $s = 0$ intersects ζ_2.

For even n, the geometry is

$$\begin{aligned}
&y^2 s + \mathfrak{b}_0 x^2 y\zeta_2\zeta_3\left(\delta_1\delta_2^2\cdots\delta_n^n\right)\\
&+ \mathfrak{b}_{1,1}swxyz\zeta_0\zeta_1\zeta_2\zeta_3\zeta_4\left(\delta_1\cdots\delta_n\right) + \mathfrak{b}_{2,1}ys^2w^2z\zeta_2\\
=&\,\mathfrak{c}_{0,2+\frac{n}{2}}w^4s^3z^{2+\frac{n}{2}}\zeta_1^{\frac{n}{2}}\zeta_2^{1+\frac{n}{2}}\zeta_3^{-1+\frac{n}{2}}\zeta_4^n\left(\delta_1^{n-1}\delta_2^{n-2}\cdots\delta_{n-1}\right)\\
&+ \mathfrak{c}_{1,2+\frac{n}{2}}w^3s^2xz^{2+\frac{n}{2}}\zeta_1^{1+\frac{n}{2}}\zeta_2^{1+\frac{n}{2}}\zeta_3^{\frac{n}{2}}\zeta_4^{1+n}\left(\delta_1^n\delta_2^{n-1}\cdots\delta_n\right)\\
&+ \mathfrak{c}_{2,1+\frac{n}{2}}sw^2x^2z^{1+\frac{n}{2}}\zeta_1^{1+\frac{n}{2}}\zeta_2^{\frac{n}{2}}\zeta_3^{\frac{n}{2}}\zeta_4^n\left(\delta_1^{n-1}\delta_2^{n-2}\cdots\delta_{n-1}\right)\\
&+ \mathfrak{c}_{3,1+\frac{n}{2}}wx^3z^{1+\frac{n}{2}}\zeta_1^{2+\frac{n}{2}}\zeta_2^{\frac{n}{2}}\zeta_3^{1+\frac{n}{2}}\zeta_4^{1+n}\left(\delta_1^n\delta_2^{n-1}\cdots\delta_n\right).
\end{aligned} \tag{B.4.14}$$

The irreducible Cartan divisors read

Section	Equation in Y_4
z	$b_{0,0}x^2\zeta_1 + s\zeta_2$
ζ_1	$b_{2,1}z + \zeta_3$
ζ_2	$b_{0,0}y$
ζ_3	$b_{2,1}y$
ζ_4	$b_{2,1}z\zeta_2 + b_{0,0}\zeta_1\zeta_3 + \zeta_2\zeta_3\delta_1$
$\delta_{i<n}$	$b_{2,1}\zeta_2 + b_{0,0}\zeta_3$
δ_n	$b_{2,1}y\zeta_2 + b_{0,0}y\zeta_3 - \zeta_2^{\frac{n}{2}}\zeta_3^{\frac{n-2}{2}}\delta_{n-1}\left(c_{0,2+\frac{n}{2}}\zeta_2 + c_{2,1+\frac{n}{2}}\zeta_3\right)$

(B.4.15)

The intersection structure is equivalent to the odd case.

B.4.4 $I^{(0|^k1)}_{2m+k}$

For this fiber type, the resolution sequence reads (with $z = \zeta_0$)

$$\begin{aligned} (\zeta_i, x, y, \zeta_{i+1}) \qquad & i = 0, \dots, m-1, \\ (\zeta_i, y, \delta_i) \qquad & i = 1, \dots, m-1, \\ (z, y, \epsilon_1) \qquad & \text{if } k > 0, \\ (\epsilon_i, y, \epsilon_{i+1}) \qquad & i = 1, \dots, k-1\,. \end{aligned} \tag{B.4.16}$$

The resolved geometry is

$$\begin{aligned} & y^2 s \left(\delta_1 \delta_2 \cdots \delta_{m-1} \left(\left(\epsilon_1 \epsilon_2^2 \cdots \epsilon_k^k\right)\right.\right. \\ & + \mathfrak{b}_0 x^2 y \left(\delta_1 \delta_2^2 \cdots \delta_{m-1}^{m-1}\right) \left(\zeta_1 \zeta_2^2 \cdots \zeta_m^m\right) \\ & + \mathfrak{b}_1 swxyz + \mathfrak{b}_{2,m} y s^2 w^2 z^m \left(\delta_1^{m-1} \delta_2^{m-2} \cdots \delta_{m-1}\right) \left(\epsilon_1^m \epsilon_2^m \cdots \epsilon_k^m\right) \left(\zeta_1^{m-1} \zeta_2^{m-2} \cdots \zeta_{m-1}\right) \\ = & \mathfrak{c}_{0,2m} w^4 s^3 z^{2m} \left(\zeta_1^{2(m-1)} \zeta_2^{2(m-2)} \cdots \zeta_{m-1}^2\right) \left(\delta_1^{2m-3} \delta_2^{2m-5} \cdots \delta_{m-1}\right) \times \\ & \times \left(\epsilon_1^{2m-1} \epsilon_2^{2m-3} \cdots \epsilon_k^{2(m-k)-1}\right) \\ & + \mathfrak{c}_{1,m} w^3 s^2 x z^m \left(\zeta_1^{m-1} \zeta_2^{m-2} \cdots \zeta_{m-1}\right) \left(\delta_1^{m-2} \delta_2^{m-3} \cdots \delta_{m-2}\right) \left(\epsilon_1^{m-1} \epsilon_2^{m-2} \cdots \epsilon_k^{m-k}\right) \\ & + \mathfrak{c}_{2,k} s w^2 x^2 z^k \left(\zeta_1^k \zeta_2^k \cdots \zeta_m^k\right) \left(\delta_1^{k-1} \delta_2^{k-1} \cdots \delta_{m-1}^{k-1}\right) \left(\epsilon_1^{k-1} \epsilon_2^{k-2} \cdots \epsilon_{k-1}\right) \\ & \left.\left. + \mathfrak{c}_{3,k} w x^3 z^k \left(\zeta_1^{k+1} \zeta_2^{k+2} \cdots \zeta_m^{k+m}\right) \left(\delta_1^k \delta_2^{k+1} \cdots \delta_{m-1}^{m+k-2}\right) \left(\epsilon_1^{k-1} \epsilon_2^{k-1} \cdots \epsilon_{k-1}\right) \right)\right. . \end{aligned} \tag{B.4.17}$$

The Cartan divisors are

Section	Equation in Y_4
z	$b_{1,0} swx + \delta_1 \left(s\epsilon_1 + b_{0,0} x^2 \zeta_1\right)$
ζ_1	$b_{1,0} x + \delta_1$
$\zeta_{2 \le j \le m-1}$	$b_{1,0} x + \delta_{j-1} \delta_j$
ζ_m	$b_{1,0} xy - c_{1,m} x \zeta_{m-1} + \delta_{m-1} \left(y^2 + b_{2,m} y \zeta_{m-1} - c_{0,2m} \zeta_{m-1}^2\right)$
$\delta_{j \le m-2}$	$b_{1,0} y$
δ_{m-1}	$b_{1,0} y - c_{1,m} \delta_{m-1} \zeta_m$
$\epsilon_{j \le k-1}$	$b_{1,0} s + b_{0,0} \delta_1$
ϵ_k	$b_{1,0} sy + b_{0,0} y \delta_1 - \delta_1^{k-1} \epsilon_{k-1} \left(c_{2,k} s + c_{3,k} \delta_1\right)$

(B.4.18)

If one orders the Cartan divisors as $(z, \zeta_1, \ldots, \zeta_m, \delta_{m-1}, \delta_{m-2}, \ldots, \delta_1, \epsilon_k, \epsilon_{k-1}, \ldots, \epsilon_1)$, then each Cartan divisor intersects exactly its neighbours, and ζ_0 also intersects ϵ_1. This replicates the affine A_{2m+k-1} Dynkin diagram.

B.4.5 $I^{(0|^k 1)}_{2m+k+1}$

The resolution sequence here is (with $z = \zeta_0$)

$$\begin{aligned}
(\zeta_i, x, y, \zeta_{i+1}) \qquad & i = 0, \ldots, m-1, \\
(\zeta_i, y, \delta_i) \qquad & i = 1, \ldots, m-1, \\
(z, y, \epsilon_1) \qquad & \text{if } k > 0, \\
(\epsilon_i, y, \epsilon_{i+1}) \qquad & i = 1, \ldots, k-1, \\
(\zeta_m, y, \zeta_{m+1})\,. &
\end{aligned} \tag{B.4.19}$$

The resolved geometry is given by

$$\begin{aligned}
& y^2 s \left(\delta_1 \delta_2 \cdots \delta_{m-1} \left(\left(\epsilon_1 \epsilon_2^2 \cdots \epsilon_k^k\right) \zeta_{m+1}\right.\right. \\
& \quad + \mathfrak{b}_0 x^2 y \left(\delta_1 \delta_2^2 \cdots \delta_{m-1}^{m-1}\right) \left(\zeta_1 \zeta_2^2 \cdots \zeta_m^m\right) \zeta_{m+1}^m \\
& \quad \left.\left. + \mathfrak{b}_1 s w x y z + \mathfrak{b}_{2,m} y s^2 w^2 z^m \left(\delta_1^{m-1} \delta_2^{m-2} \cdots \delta_{m-1}\right) \left(\epsilon_1^m \epsilon_2^m \cdots \epsilon_k^m\right) \left(\zeta_1^{m-1} \zeta_2^{m-2} \cdots \zeta_{m-1}\right)\right.\right. \\
& = \mathfrak{c}_{0,2m} w^4 s^3 z^{2m} \left(\zeta_1^{2(m-1)} \zeta_2^{2(m-2)} \cdots \zeta_{m-1}^2\right) \left(\delta_1^{2m-3} \delta_2^{2m-5} \cdots \delta_{m-1}\right) \times \\
& \quad \times \left(\epsilon_1^{2m-1} \epsilon_2^{2m-3} \cdots \epsilon_k^{2(m-k)-1}\right) \\
& \quad + \mathfrak{c}_{1,m} w^3 s^2 x z^m \left(\zeta_1^{m-1} \zeta_2^{m-2} \cdots \zeta_{m-1}\right) \left(\delta_1^{m-2} \delta_2^{m-3} \cdots \delta_{m-2}\right) \left(\epsilon_1^{m-1} \epsilon_2^{m-2} \cdots \epsilon_k^{m-k}\right) \\
& \quad + \mathfrak{c}_{2,k} s w^2 x^2 z^k \left(\zeta_1^k \zeta_2^k \cdots \zeta_m^k \zeta_{m+1}^k\right) \left(\delta_1^{k-1} \delta_2^{k-1} \cdots \delta_{m-1}^{k-1}\right) \left(\epsilon_1^{k-1} \epsilon_2^{k-2} \cdots \epsilon_{k-1}\right) \\
& \quad + \mathfrak{c}_{3,k} w x^3 z^k \left(\zeta_1^{k+1} \zeta_2^{k+2} \cdots \zeta_m^{k+m}\right) \left(\delta_1^k \delta_2^{k+1} \cdots \delta_{m-1}^{m+k-2}\right) \left(\epsilon_1^{k-1} \epsilon_2^{k-1} \cdots \epsilon_{k-1}\right) \zeta_{m+1}^{k+m-1}\,.
\end{aligned} \tag{B.4.20}$$

The Cartan divisors read

Section	Equation in Y_4
z	$b_{1,0}swx + \delta_1\left(s\epsilon_1 + b_{0,0}x^2\zeta_1\right)$
ζ_1	$b_{1,0}x + \delta_1$
$\zeta_{2\leq j\leq m-1}$	$b_{1,0}x + \delta_{j-1}\delta_j$
ζ_m	$b_{1,0}xy + \delta_{m-1}\left(b_{2,m}\zeta_{m-1} + \zeta_{m+1}\right)$
ζ_{m+1}	$b_{1,0}xy + \delta_{m-1}\left(b_{2,m}y - \zeta_m\left(c_{1,m+1}x + c_{0,2m+1}\delta_{m-1}\right)\right)$
$\delta_{j\leq m-2}$	$b_{1,0}y$
δ_{m-1}	$b_{1,0}y - c_{1,m}\delta_{m-1}\zeta_m$
$\epsilon_{j\leq k-1}$	$b_{1,0}s + b_{0,0}\delta_1$
ϵ_k	$b_{1,0}sy + b_{0,0}y\delta_1 - \delta_1^{k-1}\epsilon_{k-1}\left(c_{2,k}s + c_{3,k}\delta_1\right)$

(B.4.21)

Ordering the Cartan divisors as $(z, \zeta_1, \ldots, \zeta_m, \zeta_{m+1}, \delta_{m-1}, \delta_{m-2}, \ldots, \delta_1, \epsilon_k, \epsilon_{k-1}, \ldots, \epsilon_1)$ yields the affine A_{2m+k} Dynkin diagram.

B.4.6 $I^{(0|^m 1)}_{2(m+k)}$

In this case, the resolution sequence is, after identifying $z = \zeta_0$,

$$\begin{aligned} &(\zeta_i, y, \zeta_{i+1}) && i = 0, \ldots, m-1, \\ &(\zeta_i, x, \delta_i) && i = 1, \ldots, m-1, \\ &(\zeta_i, x, \zeta_{i+1}) && i = m, \ldots, m+2k-1\,. \end{aligned} \tag{B.4.22}$$

The resolved geometry is

$$
\begin{aligned}
& y^2 s \left(\delta_2 \delta_3^2 \cdots \delta_{m-1}^{m-2}\right) \left(\zeta_1 \zeta_2^2 \cdots \zeta_m^m\right) \left(\zeta_{m+1}^{m-1} \zeta_{m+2}^{m-2} \cdots \zeta_{m+2k}^{m-2k}\right) \\
& + \mathfrak{b}_0 x^2 y \left(\delta_1 \delta_2 \cdots \delta_{m-1}\right) \left(\zeta_{m+1} \zeta_{m+2}^2 \cdots \zeta_{m+2k}^{2k}\right) \\
& + \mathfrak{b}_1 s w x y z \\
& + \mathfrak{b}_{2,2k} y s^2 w^2 z^{2k} \left(\delta_1^{2k-1} \delta_2^{2k-1} \cdots \delta_{m-1}^{2k-1}\right) \left(\zeta_1^{2k} \zeta_2^{2k} \cdots \zeta_m^{2k}\right) \left(\zeta_{m+1}^{2k-1} \zeta_{m+2}^{2k-2} \cdots \zeta_{m+2k-1}\right) \\
= & \mathfrak{c}_{0,m+2k} w^4 s^3 z^{m+2k} \left(\zeta_1^{m+2k-1} \zeta_2^{m+2k-2} \cdots \zeta_{m+2k-1}\right) \left(\delta_1^{m+2k-2} \delta_2^{m+2k-3} \cdots \delta_{m-1}^{2k}\right) \\
& + \mathfrak{c}_{1,m} w^3 s^2 x z^m \left(\delta_1^{m-1} \delta_2^{m-2} \cdots \delta_{m-1}\right) \left(\zeta_1^{m-1} \zeta_2^{m-2} \cdots \zeta_{m-1}\right) \\
& + \mathfrak{c}_{2,m} s w^2 x^2 z^m \left(\delta_1^m \delta_2^{m-1} \cdots \delta_{m-1}^2\right) \left(\zeta_1^{m-1} \zeta_2^{m-2} \cdots \zeta_{m-1}\right) \left(\zeta_{m+1} \zeta_{m+2}^2 \cdots \zeta_{m+2k}^{2k}\right) \\
& + \mathfrak{c}_{3,m} w x^3 z^m \left(\delta_1^{m+1} \delta_2^m \cdots \delta_{m-1}^3\right) \left(\zeta_1^{m-1} \zeta_2^{m-2} \cdots \zeta_{m-1}\right) \left(\zeta_{m+1}^2 \zeta_{m+2}^4 \cdots \zeta_{m+2k}^{4k}\right) .
\end{aligned}
\tag{B.4.23}
$$

and the irreducible Cartan Divisors are

Section	Equation in Y_4
z	$b_{1,0} s w x + b_{0,0} x^2 \delta_1 + s \zeta_1$
ζ_1	$b_{1,0} s + b_{0,0} \delta_1$
$\zeta_{2 \le j \le m-1}$	$b_{1,0} s + b_{0,0} \delta_{j-1} \delta_k$
ζ_m	$b_{1,0} s y - \delta_{m-1} \times$
	$\times \left(c_{1,m} s^2 \zeta_{m-1} + \zeta_{m+1} \left(-b_{0,0} y + \delta_{m-1} \zeta_{m-1} \left(c_{2,m} s + c_{3,m} \delta_{m-1} \zeta_{m+1}\right)\right)\right)$
$\zeta_{m+1 \le j \le m+2k-1}$	$b_{1,0} y - c_{1,m} \delta_{m-1}$
ζ_{m+2k}	$b_{1,0} x y - c_{1,m} x \delta_{m-1} + \delta_{m-1}^{2k-1} \zeta_{m+2k-1} \left(b_{2,2k} y - c_{0,m+2k} \delta_{m-1}\right)$
δ_1	$b_{1,0} x + \delta_2 \zeta_1 \zeta_2^2$
$\delta_{2 \le j \le m-1}$	$b_{1,0} x$

(B.4.24)

With the ordering $(z, \zeta_1, \ldots, \zeta_{m+2k}, \delta_{m-1}, \delta_{m-2}, \ldots, \delta_1)$, the affine $A_{2(m+k)-1}$ Dynkin diagram is reproduced.

B.4.7 $I^{(0|^m 1)}_{2(m+k)+1}$

Here, the resolution sequence reads, after identifying $z = \zeta_0$,

$$
\begin{aligned}
(\zeta_i, y, \zeta_{i+1}) \qquad & i = 0, \ldots, m-1, \\
(\zeta_i, x, \delta_i) \qquad & i = 1, \ldots, m-1, \\
(\zeta_i, x, \zeta_{i+1}) \qquad & i = m, \ldots, m+2k .
\end{aligned}
\tag{B.4.25}
$$

The resolved geometry is given by

$$\begin{aligned}
&y^2 s\left(\delta_2\delta_3^2\cdots\delta_{m-1}^{m-2}\right)\left(\zeta_1\zeta_2^2\cdots\zeta_m^m\right)\left(\zeta_{m+1}^{m-1}\zeta_{m+2}^{m-2}\cdots\zeta_{m+2k+1}^{m-2k-1}\right)\\
&+\mathfrak{b}_0 x^2 y\left(\delta_1\delta_2\cdots\delta_{m-1}\right)\left(\zeta_{m+1}\zeta_{m+2}^2\cdots\zeta_{m+2k+1}^{2k+1}\right)\\
&+\mathfrak{b}_1 swxyz\\
&+\mathfrak{b}_{2,2k+1} y s^2 w^2 z^{2k+1}\left(\delta_1^{2k}\delta_2^{2k}\cdots\delta_{m-1}^{2k}\right)\left(\zeta_1^{2k+1}\zeta_2^{2k+1}\cdots\zeta_m^{2k+1}\right)\left(\zeta_{m+1}^{2k}\zeta_{m+2}^{2k-1}\cdots\zeta_{m+2k}\right)\\
=&\,\mathfrak{c}_{0,m+2k+1} w^4 s^3 z^{m+2k+1}\left(\zeta_1^{m+2k}\zeta_2^{m+2k-1}\cdots\zeta_{m+2k}\right)\left(\delta_1^{m+2k-1}\delta_2^{m+2k-2}\cdots\delta_{m-1}^{2k+1}\right)\\
&+\mathfrak{c}_{1,m} w^3 s^2 x z^m\left(\delta_1^{m-1}\delta_2^{m-2}\cdots\delta_{m-1}\right)\left(\zeta_1^{m-1}\zeta_2^{m-2}\cdots\zeta_{m-1}\right)\\
&+\mathfrak{c}_{2,m} s w^2 x^2 z^m\left(\delta_1^m\delta_2^{m-1}\cdots\delta_{m-1}^2\right)\left(\zeta_1^{m-1}\zeta_2^{m-2}\cdots\zeta_{m-1}\right)\left(\zeta_{m+1}\zeta_{m+2}^2\cdots\zeta_{m+2k+1}^{2k+1}\right)\\
&+\mathfrak{c}_{3,m} w x^3 z^m\left(\delta_1^{m+1}\delta_2^m\cdots\delta_{m-1}^3\right)\left(\zeta_1^{m-1}\zeta_2^{m-2}\cdots\zeta_{m-1}\right)\left(\zeta_{m+1}^2\zeta_{m+2}^4\cdots\zeta_{m+2k+1}^{4k+2}\right).
\end{aligned} \tag{B.4.26}$$

and the irreducible Cartan divisors by

Section	Equation in Y_4
z	$b_{1,0}swx + b_{0,0}x^2\delta_1 + s\zeta_1$
ζ_1	$b_{1,0}s + b_{0,0}\delta_1$
$\zeta_{2\le j\le m-1}$	$b_{1,0}s + b_{0,0}\delta_{j-1}\delta_k$
ζ_m	$b_{1,0}sy - \delta_{m-1}\times$
	$\times\left(c_{1,m}s^2\zeta_{m-1} + \zeta_{m+1}\left(-b_{0,0}y + \delta_{m-1}\zeta_{m-1}\left(c_{2,m}s + c_{3,m}\delta_{m-1}\zeta_{m+1}\right)\right)\right)$
$\zeta_{m+1\le j\le m+2k}$	$b_{1,0}y - c_{1,m}\delta_{m-1}$
ζ_{m+2k+1}	$b_{1,0}xy - c_{1,m}x\delta_{m-1} + \delta_{m-1}^{2k}\zeta_{m+2k}\left(b_{2,2k+1}y - c_{0,m+2k+1}\delta_{m-1}\right)$
δ_1	$b_{1,0}x + \delta_2\zeta_1\zeta_2^2$
$\delta_{2\le j\le m-1}$	$b_{1,0}x$

(B.4.27)

The divisor ordering $(z, \zeta_1, \ldots, \zeta_{m+2k+1}, \delta_{m-1}, \delta_{m-2}, \ldots, \delta_1)$ reproduces the affine $A_{2(m+k)}$ Dynkin diagram.

B.4.8 $I_n^{ns(01)}$

For the non-split-type fibers in the I_n series, one again distinguishes between even $n = 2m$ and odd $n = 2m+1$. In both cases, the ordered resolution sequence is given by

$$\begin{aligned}
&(z, x, y; \zeta_1),\\
&(\zeta_i, x, y; \zeta_{i+1}), \qquad i = 1, \ldots, m-1 \quad .
\end{aligned} \tag{B.4.28}$$

For n even, the geometry is given by

$$\begin{aligned} & y^2 s + \mathfrak{b}_0 x^2 y \left(\zeta_1 \zeta_2^2 \cdots \zeta_m^m\right) + \mathfrak{b}_1 s w x y + \mathfrak{b}_{2,m} s^2 w^2 y z^m \left(\zeta_1^{m-1} \zeta_2^{m-2} \cdots \zeta_{m-1}\right) \\ = & \, \mathfrak{c}_{0,2m} s^3 w^4 z^{2m} \left(\zeta_1^{2(m-1)} \zeta_2^{2(m-2)} \cdots \zeta_{m-1}\right) \\ & + \mathfrak{c}_{1,m} s^2 w^3 x z^m \left(\zeta_1^{m-1} \zeta_2^{m-2} \cdots \zeta_{m-1}\right) + \mathfrak{c}_2 s w^2 x^2 + \mathfrak{c}_3 w x^3 \left(\zeta_1 \zeta_2^2 \cdots \zeta_m^m\right) , \end{aligned} \tag{B.4.29}$$

and the irreducible Cartan divisors are

Section	Equation in Y_4
z	$-c_{2,0} s w^2 x^2 + s y \left(b_{1,0} w x + y\right) + x^2 \zeta_1 \left(b_{0,0} y - c_{3,0} w x\right)$
$\zeta_{1 \leq i < m}$	$-c_{2,0} x^2 + y \left(b_{1,0} x + y\right)$
ζ_m	$-c_{2,0} x^2 + b_{1,0} x y + y^2 - c_{1,m} x \zeta_{m-1} + b_{2,m} y \zeta_{m-1} - c_{0,2m} \zeta_{m-2}^2$

(B.4.30)

For odd n, the geometry reads

$$\begin{aligned} & y^2 s + \mathfrak{b}_0 x^2 y \left(\zeta_1 \zeta_2^2 \cdots \zeta_m^m\right) + \mathfrak{b}_1 s w x y + \mathfrak{b}_{2,m+1} s^2 w^2 y z^{m+1} \left(\zeta_1^m \zeta_2^{m-1} \cdots \zeta_m\right) \\ = & \, \mathfrak{c}_{0,2m+1} s^3 w^4 z^{2m+1} \left(\zeta_1^{2m-1} \zeta_2^{2m-3} \cdots \zeta_m\right) + \mathfrak{c}_{1,m+1} s^2 w^3 x z^{m+1} \left(\zeta_1^m \zeta_2^{m-1} \cdots \zeta_m\right) \\ & + \mathfrak{c}_2 s w^2 x^2 + \mathfrak{c}_3 w x^3 \left(\zeta_1 \zeta_2^2 \cdots \zeta_m^m\right) , \end{aligned} \tag{B.4.31}$$

and the Cartan divisors are

Section	Equation in Y_4
z	$-c_{2,0} s w^2 x^2 + s y \left(b_{1,0} w x + y\right) + x^2 \zeta_1 \left(b_{0,0} y - c_{3,0} w x\right)$
$\zeta_{1 \leq i \leq m}$	$-c_{2,0} x^2 + y \left(b_{1,0} x + y\right)$

(B.4.32)

For even n, the Cartan matrix one obtains from the ordering $(z, \zeta_1, \ldots, \zeta_n)$ reproduces the C_n-type Dynkin diagrams, as expected.

Bibliography

[1] S. Katz, D. R. Morrison, S. Schafer-Nameki, and J. Sully, *Tate's algorithm and F-theory*, *JHEP* **1108** (2011) 094, [1106.3854]. 3, 4, 2.4, 2.3, 2.4, 2.4, 4, 4.1.1, 5.1.2, 5.1.2, 3, 5.3, 5.5, 5.6, 5.16, 5.6.1, 5.6.2, B.1

[2] J. Borchmann, C. Mayrhofer, E. Palti, and T. Weigand, *Elliptic fibrations for SU(5) x U(1) x U(1) F-theory vacua*, *Phys.Rev.* **D88** (2013) 046005, [1303.5054]. 3, 3.4, 5, 5.3.6, 5.3, 5.5.1.1, B.3

[3] **Particle Data Group** Collaboration, C. Amsler *et. al.*, *Review of particle physics*, *Phys. Lett.* **B667** (2008) 1. 4, 1.2

[4] **Particle Data Group** Collaboration, J. Beringer *et. al.*, *Review of Particle Physics (RPP)*, *Phys.Rev.* **D86** (2012) 010001. 1, 1.1

[5] **ATLAS** Collaboration, G. Aad *et. al.*, *Observation of a new particle in the search for the Standard Model Higgs boson with the ATLAS detector at the LHC*, *Phys.Lett.* **B716** (2012) 1–29, [1207.7214]. 1, 1.1

[6] **CMS** Collaboration, S. Chatrchyan *et. al.*, *Observation of a new boson at a mass of 125 GeV with the CMS experiment at the LHC*, *Phys.Lett.* **B716** (2012) 30–61, [1207.7235]. 1, 1.1

[7] M. Green, J. Schwarz, and E. Witten, *Superstring Theory: Volume 1, Introduction*. Cambridge Monographs on Mathematical Physics. Cambridge University Press, 1988. 1

[8] M. Green, J. Schwarz, and E. Witten, *Superstring Theory: Volume 2, Loop Amplitudes, Anomalies and Phenomenology*. Cambridge Monographs on Mathematical Physics. Cambridge University Press, 1987. 1

[9] J. Polchinski, *String Theory: Volume 1, An Introduction to the Bosonic String*. Cambridge Monographs on Mathematical Physics. Cambridge University Press, 1998. 1

[10] J. Polchinski, *String Theory: Volume 2, Superstring Theory and Beyond*. Cambridge Monographs on Mathematical Physics. Cambridge University Press, 1998. 1, 3.1, 3.1

[11] L. Ibáñez and A. Uranga, *String Theory and Particle Physics: An Introduction to String Phenomenology*. Cambridge University Press, 2012. 1

[12] K. Becker, M. Becker, and J. Schwarz, *String Theory and M-Theory: A Modern Introduction*. Cambridge University Press, 2006. 1

[13] S. Weinberg, *A Model of Leptons*, *Phys.Rev.Lett.* **19** (1967) 1264–1266. 1.1

[14] S. Weinberg, *Cosmology*. Cosmology. OUP Oxford, 2008. 1.1

[15] **ALEPH Collaboration, CDF Collaboration, D0 Collaboration, DELPHI Collaboration, L3 Collaboration, OPAL Collaboration, SLD Collaboration, LEP Electroweak Working Group, Tevatron Electroweak Working Group, SLD Electroweak and Heavy Flavour Groups** Collaboration, *Precision Electroweak Measurements and Constraints on the Standard Model*, 1012.2367. 1.1

[16] G. Feldman, J. Hartnell, and T. Kobayashi, *Long-baseline neutrino oscillation experiments*, *Adv.High Energy Phys.* **2013** (2013) 475749, [1210.1778]. 1.1

[17] Y. Sofue and V. Rubin, *Rotation curves of spiral galaxies*, *Ann.Rev.Astron.Astrophys.* **39** (2001) 137–174, [astro-ph/0010594]. 1.1

[18] P. Schneider, J. Ehlers, and E. Falco, *Gravitational Lenses*. Astronomy and Astrophysics Library. Springer, 1999. 1.1

[19] **Supernova Cosmology Project** Collaboration, A. J. Conley *et. al.*, *Measurement of Omega(m), Omega(lambda) from a blind analysis of Type Ia supernovae with CMAGIC: Using color information to verify the acceleration of the Universe*, *Astrophys.J.* **644** (2006) 1–20, [astro-ph/0602411]. 1.1

[20] **Planck** Collaboration, P. Ade *et. al.*, *Planck 2013 results. I. Overview of products and scientific results*, 1303.5062. 1.1

[21] **WMAP** Collaboration, G. Hinshaw *et. al.*, *Nine-Year Wilkinson Microwave Anisotropy Probe (WMAP) Observations: Cosmological Parameter Results*, *Astrophys.J.Suppl.* **208** (2013) 19, [1212.5226]. 1.1

[22] S. P. Martin, *A Supersymmetry primer*, hep-ph/9709356. 1.2, 1.2

[23] J. Terning, *Modern Supersymmetry: Dynamics and Duality*. International Series of Monographs on Physics. OUP Oxford, 2006. 1.2

[24] H. Baer and X. Tata, *Weak Scale Supersymmetry: From Superfields to Scattering Events*. Cambridge University Press, 2006. 1.2

[25] Y. Golfand and E. Likhtman, *Extension of the Algebra of Poincare Group Generators and Violation of p Invariance*, *JETP Lett.* **13** (1971) 323–326. 1.2

[26] S. Dimopoulos and H. Georgi, *Softly Broken Supersymmetry and SU(5)*, *Nucl.Phys.* **B193** (1981) 150. 1.2

[27] L. O'Raifeartaigh, *Spontaneous Symmetry Breaking for Chiral Scalar Superfields*, *Nucl.Phys.* **B96** (1975) 331. 1.2

[28] P. Fayet and J. Iliopoulos, *Spontaneously Broken Supergauge Symmetries and Goldstone Spinors*, *Phys.Lett.* **B51** (1974) 461–464. 1.2

[29] R. Barbieri and A. Strumia, *The 'LEP paradox'*, hep-ph/0007265. 1

[30] S. Dimopoulos and D. W. Sutter, *The Supersymmetric flavor problem*, *Nucl.Phys.* **B452** (1995) 496–512, [hep-ph/9504415]. 1.2

[31] J. R. Ellis and D. V. Nanopoulos, *Flavor Changing Neutral Interactions in Broken Supersymmetric Theories*, *Phys.Lett.* **B110** (1982) 44. 1.2

[32] M. Dine and A. E. Nelson, *Dynamical supersymmetry breaking at low-energies*, *Phys.Rev.* **D48** (1993) 1277–1287, [hep-ph/9303230]. 1.2

[33] M. Dine, A. E. Nelson, and Y. Shirman, *Low-energy dynamical supersymmetry breaking simplified*, *Phys.Rev.* **D51** (1995) 1362–1370, [hep-ph/9408384]. 1.2

[34] M. Dine, A. E. Nelson, Y. Nir, and Y. Shirman, *New tools for low-energy dynamical supersymmetry breaking*, *Phys.Rev.* **D53** (1996) 2658–2669, [hep-ph/9507378]. 1.2

[35] A. E. Nelson and N. Seiberg, *R symmetry breaking versus supersymmetry breaking*, *Nucl.Phys.* **B416** (1994) 46–62, [hep-ph/9309299]. 1.2

[36] S. Raby, *Grand Unified Theories*, hep-ph/0608183. 1.3

[37] H. Georgi, *Lie Algebras in Particle Physics: From Isospin to Unified Theories*. Frontiers in Physics Series. Westview Press, 1999. 1.3

[38] R. Slansky, *Group theory for unified model building*, *Physics Reports* **79** (1981), no. 1 1–128. 1.3

[39] J. C. Pati and A. Salam, *Lepton Number as the Fourth Color*, *Phys.Rev.* **D10** (1974) 275–289. 1.3

[40] H. Georgi and S. L. Glashow, *Unity of all elementary-particle forces*, *Physical Review Letters* **32** (1974) 438–441. 1.3, 1.3

[41] R. D. Peccei and H. R. Quinn, *Cp conservation in the presence of pseudoparticles*, *Phys. Rev. Lett.* **38** (Jun, 1977) 1440–1443. 1.3

[42] R. D. Peccei and H. R. Quinn, *Constraints imposed by* CP *conservation in the presence of pseudoparticles*, *Phys. Rev. D* **16** (Sep, 1977) 1791–1797. 1.3

[43] J. M. Maldacena, *The Large N limit of superconformal field theories and supergravity*, *Adv.Theor.Math.Phys.* **2** (1998) 231–252, [hep-th/9711200]. 1.4

[44] O. Aharony, S. S. Gubser, J. M. Maldacena, H. Ooguri, and Y. Oz, *Large N field theories, string theory and gravity*, *Phys.Rept.* **323** (2000) 183–386, [hep-th/9905111]. 1.4

[45] S. A. Hartnoll, *Lectures on holographic methods for condensed matter physics*, *Class.Quant.Grav.* **26** (2009) 224002, [0903.3246]. 1.4

[46] K. Hori, S. Katz, A. Klemm, R. Pandharipande, R. Thomas, C. Vafa, R. Vakil, and E. Zaslow, *Mirror Symmetry*. Clay mathematics monographs. American Mathematical Society, 2003. 1.4, 1

[47] J. H. Conway and S. P. Norton, *Monstrous moonshine*, *Bull. London Math. Soc.* **11** (1979). 1.4

[48] R. E. Borcherds, *Monstrous moonshine and monstrous Lie superalgebras*, *Invent. Math.* **109** (1992), no. 2 405–444. 1.4

[49] L. Randall and R. Sundrum, *A Large mass hierarchy from a small extra dimension*, *Phys.Rev.Lett.* **83** (1999) 3370–3373, [hep-ph/9905221]. 1.4, 1.5

[50] L. Randall and R. Sundrum, *Out of this world supersymmetry breaking*, *Nucl.Phys.* **B557** (1999) 79–118, [hep-th/9810155]. 1.4

[51] S. Kachru, R. Kallosh, A. D. Linde, and S. P. Trivedi, *De Sitter vacua in string theory*, *Phys.Rev.* **D68** (2003) 046005, [hep-th/0301240]. 1.4

[52] C. Burgess, R. Kallosh, and F. Quevedo, *De Sitter string vacua from supersymmetric D terms*, *JHEP* **0310** (2003) 056, [hep-th/0309187]. 1.4

[53] M. Rummel and A. Westphal, *A sufficient condition for de Sitter vacua in type IIB string theory*, *JHEP* **1201** (2012) 020, [1107.2115]. 1.4

[54] A. H. Guth, *Inflationary universe: A possible solution to the horizon and flatness problems*, *Phys. Rev. D* **23** (Jan, 1981) 347–356. 1.4, 1.5

[55] A. Linde, *A new inflationary universe scenario: A possible solution of the horizon, flatness, homogeneity, isotropy and primordial monopole problems*, *Physics Letters B* **108** (1982), no. 6 389 – 393. 1.4, 1.5

[56] S. Kachru, R. Kallosh, A. D. Linde, J. M. Maldacena, L. P. McAllister, *et. al.*, *Towards inflation in string theory*, *JCAP* **0310** (2003) 013, [hep-th/0308055]. 1.4

[57] D. Baumann and L. McAllister, *Inflation and String Theory*, 1404.2601. 1.4, 1.5

[58] T. Kaluza, *Zum unitaetsproblem in der physik*, *Sitzungsber. Preuss. Akad. Wiss.* (1921) 966–972. 1.5

[59] O. Klein, *Quantentheorie und fuenfdimensionale relativitaetstheorie*, *Zeitschrift fur Physik* **37** (dec, 1926) 895–906. 1.5

[60] V. Rubakov and M. Shaposhnikov, *Do we live inside a domain wall?*, *Physics Letters B* **125** (1983), no. 23 136 – 138. 1.5

[61] N. Arkani-Hamed, S. Dimopoulos, and G. Dvali, *The Hierarchy problem and new dimensions at a millimeter*, *Phys.Lett.* **B429** (1998) 263–272, [hep-ph/9803315]. 1.5

[62] I. Antoniadis, N. Arkani-Hamed, S. Dimopoulos, and G. Dvali, *New dimensions at a millimeter to a Fermi and superstrings at a TeV*, *Phys.Lett.* **B436** (1998) 257–263, [hep-ph/9804398]. 1.5

[63] R. Blumenhagen, M. Cvetic, P. Langacker, and G. Shiu, *Toward realistic intersecting D-brane models*, *Ann.Rev.Nucl.Part.Sci.* **55** (2005) 71–139, [hep-th/0502005]. 1.5

[64] H. P. Nilles, S. Ramos-Sanchez, M. Ratz, and P. K. Vaudrevange, *From strings to the MSSM*, *Eur.Phys.J.* **C59** (2009) 249–267, [0806.3905]. 1.5

[65] C. Vafa, *Evidence for F-Theory*, *Nucl. Phys.* **B469** (1996) 403–418, [hep-th/9602022]. 1.5, 2, 3.1

[66] M. Kuntzler and S. Schafer-Nameki, *G-flux and Spectral Divisors*, *JHEP* **1211** (2012) 025, [1205.5688]. 1.7, 4

[67] M. Kuntzler and S. Schafer-Nameki, *Tate Trees for Elliptic Fibrations with Rank one Mordell-Weil group*, 1406.5174. 1.7, 3.6, 4.1.1, 5

[68] S.-T. Yau, *On the ricci curvature of a compact khler manifold and the complex monge-ampre equation, i*, *Communications on Pure and Applied Mathematics* **31** (1978), no. 3 339–411. 2

[69] E. Witten, *Nonperturbative superpotentials in string theory*, *Nucl.Phys.* **B474** (1996) 343–360, [hep-th/9604030]. 2, 3.2

[70] P. Griffiths and J. Harris, *Principles of Algebraic Geometry*. Wiley Classics Library. Wiley, 2011. 1

[71] P. Deligne, *Courbes elliptiques: formulaire d'apres J. Tate (Proc. Internat. Summer School, Univ. Antwerp, Antwerp, 1972)*, *Lecture Notes in Math.* **476** (1975) 53–73. 2.1

[72] J. Silverman, *The Arithmetic of Elliptic Curves*. Graduate Texts in Mathematics. Springer, 2009. 2.1

[73] G. Roch, *Ueber die anzahl der willkuerlichen constanten in algebraischen functionen*, *Crelle J. Math.* **64** (1865) 372–376. 2.1

[74] L. J. Mordell, *On the rational solutions of indeterminate equations of the third and fourth degree*, *Proc. Cambridge Philos. Soc.* **21** (1922) 179–192. 2.2

[75] A. Weil, *L'arithmétique sur les courbes algébriques*, *Acta Mathematica* **52** (1929), no. 1 281–315. 2.2

[76] J. Silverman and J. Tate, *Rational Points on Elliptic Curves*. Springer Undergraduate Texts in Mathematics and Technology. Springer, 1992. 2.2

[77] S. Lang, *Algebra*. Graduate Texts in Mathematics. Springer New York, 2002. 2.2

[78] R. Miranda, *The basic theory of elliptic surfaces*. Dottorato di Ricerca in Matematica. [Doctorate in Mathematical Research]. ETS Editrice, Pisa, 1989. 2.2, 5.1.3

[79] M. Cvetic, D. Klevers, and H. Piragua, *F-Theory Compactifications with Multiple U(1)-Factors: Constructing Elliptic Fibrations with Rational Sections*, *JHEP* **1306** (2013) 067, [1303.6970]. 2.2, 5

[80] C. Mayrhofer, E. Palti, and T. Weigand, *U(1) symmetries in F-theory GUTs with multiple sections*, *JHEP* **1303** (2013) 098, [1211.6742]. 2.2, 3.4, 5, B.3, B.3

[81] R. Hartshorne, *Algebraic Geometry*. Graduate Texts in Mathematics. Springer, 1977. 2.3

[82] E. A. Bartolo and J. Ortigas-Galindo, *Q-resolutions and intersection numbers*, *Monografias des Seminario Matematico Garcia de Galdeano* (2011). 2.3

[83] M. Kuntzler and C. Lawrie, `Smooth`*: A Mathematica package for studying resolutions of singular fibrations, Version 0.4*, . 2.3, 5.1.7, 6, B.4

[84] K. Kodaira, *On the structure of compact complex analytic surfaces. i.*, *Am. J. Math.* **86** (1964) 751–798. 2.4, 2.4, 5.1.2

[85] K. Kodaira, *On the structure of compact complex analytic surfaces. ii, iii.*, *Am. J. Math.* **88** (1966) 682–721. 2.4, 2.4, 5.1.2

[86] A. Néron, *Modèles minimaux des variétés abéliennes sur les corps locaux et globaux*, *Inst. Hautes Études Sci. Publ.Math. No.* **21** (1964) 128. 2.4, 2.4, 5.1.2

[87] D. R. Morrison and C. Vafa, *Compactifications of F-Theory on Calabi–Yau Threefolds – II*, *Nucl. Phys.* **B476** (1996) 437–469, [hep-th/9603161]. 5, 3.1, 3.4

[88] J. Tate, *Algorithm for determining the type of a singular fiber in an elliptic pencil*, *Modular functions of one variable, IV (Proc. Internat. Summer School, Univ. Antwerp, Antwerp, 1972), Lecture Notes in Math.* **476** (1975) 33–52. 2.4, 5.1.2

[89] M. Bershadsky, K. A. Intriligator, S. Kachru, D. R. Morrison, V. Sadov, *et. al.*, *Geometric singularities and enhanced gauge symmetries*, *Nucl.Phys.* **B481** (1996) 215–252, [hep-th/9605200]. 2.4, 2.4, 4, 4.1.1, 5.1.2, 5.3

[90] T. Weigand, *Lectures on F-theory compactifications and model building*, *Class.Quant.Grav.* **27** (2010) 214004, [1009.3497]. 1

[91] A. Maharana and E. Palti, *Models of Particle Physics from Type IIB String Theory and F-theory: A Review*, *Int.J.Mod.Phys.* **A28** (2013) 1330005, [1212.0555]. 1

[92] D. R. Morrison and C. Vafa, *Compactifications of F-Theory on Calabi–Yau Threefolds – I*, *Nucl. Phys.* **B473** (1996) 74–92, [hep-th/9602114]. 3.1

[93] V. Braun and D. R. Morrison, *F-theory on Genus-One Fibrations*, 1401.7844. 2

[94] D. R. Morrison and W. Taylor, *Sections, multisections, and U(1) fields in F-theory*, 1404.1527. 2

[95] C. Mayrhofer, D. R. Morrison, O. Till, and T. Weigand, *Mordell-Weil Torsion and the Global Structure of Gauge Groups in F-theory*, 1405.3656. 2, 4

[96] T. W. Grimm, *The N=1 effective action of F-theory compactifications*, *Nucl.Phys.* **B845** (2011) 48–92, [1008.4133]. 3.2

[97] F. Denef, *Les Houches Lectures on Constructing String Vacua*, 0803.1194. 3.2

[98] S. H. Katz and C. Vafa, *Matter from geometry*, *Nucl.Phys.* **B497** (1997) 146–154, [hep-th/9606086]. 3.3, 5.6.1, 5.6.2, 5.6.4, 5.6.4

[99] H. Hayashi, C. Lawrie, D. R. Morrison, and S. Schafer-Nameki, *Box Graphs and Singular Fibers*, *JHEP* **1405** (2014) 048, [1402.2653]. 3.3, 5.1.2, 13

[100] S. Katz and D. R. Morrison, *Gorenstein threefold singularities with small resolutions via invariant theory for weyl groups*, *J. Algebraic Geom.* **1** (1992) 449–530, [alg-geom/9202002]. 3.3

[101] J. Marsano and S. Schafer-Nameki, *Yukawas, G-flux, and Spectral Covers from Resolved Calabi-Yau's*, *JHEP* **1111** (2011) 098, [1108.1794]. 3.3, 3.3, 3.3, 3.5, 3.5, 4, 4.1.1, 4.1.2, 4.1.3, 4.1.3, 4.1.3, 4.2, 4.2.1, 4.2.4, 4.3.2.4, 5.1.7, 5.1.7, 6

[102] C. Lawrie and S. Schafer-Nameki, *The Tate Form on Steroids: Resolution and Higher Codimension Fibers*, 1212.2949. 3.3, 4.1.3, 4.2, 4.2.2.2, 4.2.4, 4.2.4, 5.1.4, 5.1.7, 5.1.7

[103] C. Beasley, J. J. Heckman, and C. Vafa, *GUTs and Exceptional Branes in F-theory - I*, *JHEP* **01** (2009) 058, [0802.3391]. 3, 3.6, 3.7

[104] J. Marsano, N. Saulina, and S. Schafer-Nameki, *Monodromies, Fluxes, and Compact Three-Generation F-theory GUTs*, *JHEP* **08** (2009) 046, [0906.4672]. 3.4, 4, 4.1.1, 4.1.2, 5, B.3

[105] J. Marsano, N. Saulina, and S. Schafer-Nameki, *Compact F-theory GUTs with $U(1)_{PQ}$*, *JHEP* **04** (2010) 095, [0912.0272]. 3.4, 4.1.1, 4.1.2, 5, B.3

[106] M. J. Dolan, J. Marsano, N. Saulina, and S. Schafer-Nameki, *F-theory GUTs with U(1) Symmetries: Generalities and Survey*, 1102.0290. 3.4, 3.7, 4.1.1, 5, B.3

[107] T. W. Grimm and T. Weigand, *On Abelian Gauge Symmetries and Proton Decay in Global F-theory GUTs*, *Phys.Rev.* **D82** (2010) 086009, [1006.0226]. 3.4, 4.1.1, 4.1.1, 5, B.3

[108] V. Braun, T. W. Grimm, and J. Keitel, *New Global F-theory GUTs with U(1) symmetries*, *JHEP* **1309** (2013) 154, [1302.1854]. 3.4, 5

[109] J. Borchmann, C. Mayrhofer, E. Palti, and T. Weigand, *SU(5) Tops with Multiple U(1)s in F-theory*, 1307.2902. 3.4, 5, B.3

[110] V. Braun, T. W. Grimm, and J. Keitel, *Geometric Engineering in Toric F-Theory and GUTs with U(1) Gauge Factors*, *JHEP* **1312** (2013) 069, [1306.0577]. 3.4, 5, B.3

[111] P. Candelas, A. Constantin, and H. Skarke, *An Abundance of K3 Fibrations from Polyhedra with Interchangeable Parts*, *Commun. Math. Phys.* **324** (2013) 937–959, [1207.4792]. 3.4, 5, B.3

[112] D. R. Morrison and D. S. Park, *F-Theory and the Mordell-Weil Group of Elliptically-Fibered Calabi-Yau Threefolds*, *JHEP* **1210** (2012) 128, [1208.2695]. 3.4, 5.1.1, 5.1.1, 5.1.7

[113] M. Bies, C. Mayrhofer, C. Pehle, and T. Weigand, *Chow groups, Deligne cohomology and massless matter in F-theory*, 1402.5144. 5

[114] L. B. Anderson, J. J. Heckman, and S. Katz, *T-Branes and Geometry*, *JHEP* **1405** (2014) 080, [1310.1931]. 5, 6

[115] E. Witten, *On flux quantization in M-theory and the effective action*, *J. Geom. Phys.* **22** (1997) 1–13, [hep-th/9609122]. 3.5, 4.1.3

[116] R. Donagi and M. Wijnholt, *Higgs Bundles and UV Completion in F-Theory*, 0904.1218. 3.5, 3.7, 4, 4.1.1, 4.1.2, 4.1.2, 4.3.2.3

[117] S. Sethi, C. Vafa, and E. Witten, *Constraints on low-dimensional string compactifications*, *Nucl. Phys.* **B480** (1996) 213–224, [hep-th/9606122]. 3.5

[118] R. Blumenhagen, T. W. Grimm, B. Jurke, and T. Weigand, *Global F-theory GUTs*, *Nucl.Phys.* **B829** (2010) 325–369, [0908.1784]. 3.5, 4.2.6

[119] R. Donagi and M. Wijnholt, *Breaking GUT Groups in F-Theory*, 0808.2223. 3.6

[120] C. Lawrie, D. Sacco, and S. Schafer-Nameki, *To appear*, . 3.6, 6

[121] S. Schafer-Nameki and J. Wong, *Work in Progress*, . 3.6, 6

[122] C. Beasley, J. J. Heckman, and C. Vafa, *GUTs and Exceptional Branes in F-theory - II: Experimental Predictions*, *JHEP* **01** (2009) 059, [0806.0102]. 3.7

[123] R. Donagi and M. Wijnholt, *Model Building with F-Theory*, 0802.2969. 3.7

[124] R. Friedman, J. Morgan, and E. Witten, *Vector bundles and F theory*, *Commun.Math.Phys.* **187** (1997) 679–743, [hep-th/9701162]. 3.7, 4, 4.1.1, 4.1.1

[125] H. Hayashi, R. Tatar, Y. Toda, T. Watari, and M. Yamazaki, *New Aspects of Heterotic–F Theory Duality*, *Nucl. Phys.* **B806** (2009) 224–299, [0805.1057]. 3.7

[126] R. Donagi and M. Wijnholt, *Gluing Branes, I*, 1104.2610. 6

[127] R. Donagi and M. Wijnholt, *Gluing Branes II: Flavour Physics and String Duality*, 1112.4854. 6

[128] S. Cecotti, C. Cordova, J. J. Heckman, and C. Vafa, *T-Branes and Monodromy*, 1010.5780. 6

[129] J. Marsano, N. Saulina, and S. Schfer-Nameki, *Global Gluing and G-flux*, *JHEP* **1308** (2013) 001, [1211.1097]. 6

[130] C.-C. Chiou, A. E. Faraggi, R. Tatar, and W. Walters, *T-branes and Yukawa Couplings*, *JHEP* **1105** (2011) 023, [1101.2455]. 6

[131] J. Marsano, N. Saulina, and S. Schafer-Nameki, *On G-flux, M5 instantons, and U(1)s in F-theory*, 1107.1718. 3.7, 4, 4.1.1, 3, 4.1.3, 4.3.2.4

[132] J. Marsano, N. Saulina, and S. Schafer-Nameki, *F-theory Compactifications for Supersymmetric GUTs*, *JHEP* **08** (2009) 030, [0904.3932]. 4

[133] M. Esole and S.-T. Yau, *Small resolutions of SU(5)-models in F-theory*, 1107.0733. 4, 4.2, 4.2.1, 4.2.4, 5.1.7

[134] J. Marsano, N. Saulina, and S. Schafer-Nameki, *A Note on G-Fluxes for F-theory Model Building*, *JHEP* **11** (2010) 088, [1006.0483]. 4, 4.1.1, 3, 4.1.3

[135] R. Tatar, Y. Tsuchiya, and T. Watari, *Right-handed Neutrinos in F-theory Compactifications*, *Nucl.Phys.* **B823** (2009) 1–46, [0905.2289]. 4.1.1

[136] S. Krause, C. Mayrhofer, and T. Weigand, *G_4 flux, chiral matter and singularity resolution in F-theory compactifications*, *Nucl.Phys.* **B858** (2012) 1–47, [1109.3454]. 53 pages, 2 figures. 4.1.1

[137] A. P. Braun, A. Collinucci, and R. Valandro, *G-flux in F-theory and algebraic cycles*, *Nucl.Phys.* **B856** (2012) 129–179, [1107.5337]. 55 pages, 1 figure/ added refs, corrected typos. 4.1.1

[138] M. Esole and S.-T. Yau, *Small resolutions of SU(5)-models in F-theory*, 1107.0733. 4.1.3

[139] A. Collinucci and R. Savelli, *On Flux Quantization in F-Theory II: Unitary and Symplectic Gauge Groups*, *JHEP* **1208** (2012) 094, [1203.4542]. 4.2.6, 4.3.1.2

[140] P. Aluffi, *Chern classes of blow-ups*, *Math. Proc. Cambridge Philos. Soc.* (2008) [0809.2425]. 4.2.6

[141] A. Collinucci and R. Savelli, *On Flux Quantization in F-Theory*, 1011.6388. 4.3.1.2

[142] C.-M. Chen and Y.-C. Chung, *On F-theory E_6 GUTs*, *JHEP* **1103** (2011) 129, [1010.5536]. 4.3.2.3

[143] M. Cvetic, A. Grassi, D. Klevers, and H. Piragua, *Chiral Four-Dimensional F-Theory Compactifications With SU(5) and Multiple U(1)-Factors*, 1306.3987. 5

[144] M. Cvetic, D. Klevers, and H. Piragua, *F-Theory Compactifications with Multiple U(1)-Factors: Addendum*, *JHEP* **1312** (2013) 056, [1307.6425]. 5

[145] M. Cvetic, D. Klevers, H. Piragua, and P. Song, *Elliptic Fibrations with Rank Three Mordell-Weil Group: F-theory with U(1) x U(1) x U(1) Gauge Symmetry*, 1310.0463. 5

[146] S. Krippendorf, D. K. Mayorga Pena, P.-K. Oehlmann, and F. Ruehle, *Rational F-Theory GUTs without exotics*, *JHEP* **1407** (2014) 013, [1401.5084]. 5

[147] M. Auslander and D. A. Buchsbaum, *Unique factorization in regular local rings*, *Proc. Nat. Acad. Sci. U.S.A.* **45** (1959) 733–734. 5.1.2, B.1

[148] A. P. Braun and S. Schafer-Nameki, *Box Graphs and Resolutions I*, 1407.3520. 8, 5.1.7

[149] H. Hayashi, C. Lawrie, and S. Schafer-Nameki, *Phases, Flops and F-theory: SU(5) Gauge Theories*, *JHEP* **1310** (2013) 046, [1304.1678]. 5.1.7

[150] D. S. Park, *Anomaly Equations and Intersection Theory*, *JHEP* **1201** (2012) 093, [1111.2351]. 29 pages + appendices, 8 figures/ v2: minor corrections, references added. 5.1.7